School of Engineering
Department of Chemical Engineering

The Role of Impurities and Additives in the Crystallisation of Gypsum

Stefanus Muryanto

This thesis is presented for the Degree of
DOCTOR of PHILOSOPHY
of Curtin University of Technology

December 2002

Declaration

This thesis contains no material which has been accepted for the award of any other degree or diploma in any university.

To the best of my knowledge and belief this thesis contains no material previously published by any other person except where due acknowledgment has been made.

Signature: .....

Date: 15 SEPTEMBER 2003

Acknowledgments

I would like to thank a number of people for their help during the course of this study. I am particularly grateful to my supervisors: Associate Professor H M Ang and Professor G M Parkinson, for their guidance, help and encouragement throughout all stages of this research. My appreciation also goes to:

1. The Analytical Laboratory staff at the Department of Chemical Engineering, especially Mr John Lauridsen and Mr John Murray for their help.

2. The staff of the workshop at the School of Engineering, particularly Mr Derrick Oxley and Mr Peter Bruce for their high standard of work for the scale formation experimental rig.

3. The staff and postgraduates at the School of Engineering for their help and friendship.

4. The staff at the School of Applied Chemistry, Curtin University of Technology, and in particular, Drs Andrew Rohl and Franca Jones for their critical comments on the literature review. Special thanks are due to Ms Claire Hitchen, personal assistant to Professor G M Parkinson, for her organising our regular discussion on the research progress.

5. The staff at the School of Applied Physics, Curtin University of Technology, particularly Ms Elaine Miller, for helping me with the use of SEM facilities.

6. The staff at the Particle Size Analysis Division of CSIRO Minerals, Perth, Western Australia, especially Mr Phan Tung Khanh, for the opportunity to learn and use the particle size analyser.

7. The staff at the Centre for Educational Advancement, Curtin University of Technology, especially Ms Jenny Lalor for her support in using the software package for the analysis of the experimental data. Special thanks are due to Mr Desmond Thornton for his help with the long document handling.

8. The staff at NewSouth Global Pty Ltd, the University of New South Wales, in particular, Mrs Cynthia Grant, the project manager, for managing my scholarship as well as for funding some of my conferences relevant to the project.

9. The Department of Chemical Engineering for supporting one of my conferences, relevant to the thesis.

10. The Department of National Education, the Republic of Indonesia, for providing the scholarship for the PhD studies.

11. The staff at T L Robertson Library, Curtin University of Technology, especially those in charge with the Inter Library Loan service.

Finally, I would like to thank my family for their unconditional love, patience and understanding during my being away, to complete my studies in Australia.

Publications from the present study: 2001 to 2002

The full manuscripts are presented in **Appendix F**.

1. G.Headley, **S.Muryanto** and, H.M.Ang. (2001), "Effects of Additives on the Crystallisation Rate of Calcium Sulphate Dihydrate", the 6th World Congress of Chemical Engineering, Melbourne, Australia.

2. **S.Muryanto**, and H.M.Ang. (2001), "A Continuous Laboratory Crystalliser for Final Year Chemical Engineering Undergraduate Projects", ASEAN Regional Symposium on Chemical Engineering 2001, Bandung, Indonesia.

3. **S.Muryanto**, H.M.Ang, and G.M.Parkinson. (2002), "Crystallisation Kinetics of Calcium Sulphate Dihydrate in the Presence of Additives", World Engineering Congress 2002, Sarawak, Malaysia.

4. **S.Muryanto**, H.M.Ang, E. Santoso, and G.M.Parkinson. (2002) "Gypsum scaling in isothermal flow systems", ASEAN Regional Symposium on Chemical Engineering 2002, Kuala Lumpur, Malaysia.

5. **S.Muryanto**, H.M.Ang, E.Santoso, and G.M.Parkinson. (2002), "Morphology of Gypsum Scale Formed in Pipes under Isothermal Conditions. A Once-Through Pipe Flow Experiment", Chemical Engineering Congress 2002, Manila, The Philippines. (accepted)

6. **S.Muryanto**, H.M.Ang, and E.Santoso. (2002), "A Typical Final Year Chemical Engineering Undergraduate Laboratory Project: Scaling", Journal of Chemical Engineering Education. (submitted)

7. **S.Muryanto**, H.M.Ang, and G.M.Parkinson. (2002), "Review of Gypsum Scaling Research: Effect of Admixtures on Gypsum Crystallisation Kinetics", ASEAN Journal of Chemical Engineering. (submitted)

Abstract

Scale formation is one of the persistent problems in mineral processing and related industries. One of the main components of the scale is frequently gypsum or calcium sulphate dihydrate (= $CaSO_4.2H_2O$). Gypsum is formed through the process of crystallisation, and it is well known that crystallisation process is significantly affected by the presence of admixtures. Industrially, scale formation occurs in an environment which is very rarely free from the presence of admixtures. In a typical mineral processing industry, certain types of admixtures are present, which may include metallic ions (e.g. originated from corrosion products) and certain types of the flotation agents used.

The effect of admixtures on crystallisation kinetics and cyclical morphology can be very significant, even if they are present in trace amounts. It is important to emphasise that the effects are generally specific, that there is no unified theory that applies to all and every situation.

The present study has investigated the effect of certain admixtures on gypsum crystallisation, and was accomplished in three phases of experiments: (1) seeded batch crystallisation; (2) seeded continuous crystallisation, and (3) once through flow system under isothermal condition. The three phases of the work used equimolar solutions of $CaCl_2$ and Na_2SO_4 to produce $CaSO_4$ which is the precipitating species.

The seeded batch crystallisation experiment explored the effect of two flotation agents commonly used in mineral processing plants: (1) sodium isopropyl xanthate (= SIPX) and, (2) isopropyl thionocarbamate. The experiments were performed at 25, 35, and 45^0C, respectively. The initial concentration of the crystallising solution was 2,000 ppm of Ca^{2+} and it reached the equilibrium concentration values of between 1,000 and 8,00 ppm of Ca^{2+} in 90 minutes. The effect of the two selected admixtures on crystallisation was measured by continuous monitoring of the desupersaturation of the crystallising solution with time, which subsequently resulted in the determination of the crystallisation rate constant. The results are as follows. Firstly, the admixtures selected (either individually or in combination) were able to retard the growth rate of gypsum.

In the absence of any admixture, the second order rate constant was between 1,405 x 10^{-6} and 1,561 x 10^{-6} ppm^{-1} min^{-1}. Addition of SIPX at a typical plant dosing level (= 0.200 g/L) reduced the rate constant to 475 x 10^{-6} ppm^{-1} min^{-1}, while isopropyl thionocarbamate at a typical plant dosing level (= 0.070 g/L) decreased the rate constant to 254 x 10^{-6} ppm^{-1} min^{-1}. However, addition of a combination of the two admixtures, each at a typical plant concentration level, reduced the rate constant to 244 x 10^{-6} ppm^{-1} min^{-1}, which was only slightly below that in the presence of isopropyl thionocarbamate. Thus, in these batch crystallisation studies, isopropyl thionocarbamate seemed to be dominant over SIPX.

Secondly, the batch crystallisation system in the current work did not show any induction time. It was concluded that the seeds added into the batch system could be capable of eliminating the induction time. Thirdly, the reduced growth rate of the gypsum crystals as affected by the admixtures was probably caused by the adsorption of admixtures onto the crystal surface.

The second phase of the project involved a seeded continuous (MSMPR) crystalliser. Some parameters used in this experiment (mean residence time, agitation speed and type of one admixture) were taken from the batch experiment carried out in the first phase of the project. Three admixtures were chosen for the seeded continuous crystallisation: (1) SIPX, (2) Fe^{3+}, (3) Zn^{2+}, and they were used either individually on in combination with each other. SIPX was chosen as it is one of the most common flotation agents used in mineral processing. Metallic ions: Fe^{3+} and Zn^{2+} were selected, since they were found in substantial amounts in both scale samples and process water in certain minerals processing industries. In general, the admixtures tested were found to be able to inhibit the crystal growth rates, but to enhance the nucleation rates. In addition, the growth rate was found to be dependent on crystal size, and hence, a correlation between these two parameters and the admixture concentration was formulated.

For a fixed level of concentration (± 700 ppm of Ca^{2+} at steady state) and crystal surface area, it was proved that for each crystallisation temperature: 25 and 40^0C, the correlation function can be represented as

$$G = k L^{\alpha} (1+C)^{\beta}$$

where:

G = linear growth rate, micron/hour

k, **α**,and **β** = dimensionless constants

L = (sphere equivalent) crystal size, micron

C = concentration of the admixtures used, ppm.

For both the crystallisation temperatures used, the correlation function shows that the growth rate is significantly dependent on crystal size, but a weak function of admixture concentrations. The mechanism of crystal growth inhibition was assumed to be that of adsorption of admixtures onto the active growth sites, thereby decreasing or stopping the growth. Similar to the first phase of the present study, this seeded continuous crystallisation also showed no induction time.

The third phase of the project investigated the gypsum scale formation in a once-through pipe flow system under isothermal condition and in the presence of admixtures. Four types of pipe materials were tested: PVC, brass, copper and stainless steel. Two admixtures were selected: SIPX and Fe^{3+}. The behaviour of the gypsum scale formation was measured as the mass of the gypsum scale deposited on the substrate per unit area of the pipe surface.

Within the range of the experimental conditions applied in this scale formation study, the following results were obtained. Firstly, the mass of the gypsum scale increased with concentration (in the range: 2,000 to 6,000 ppm of Ca^{2+}) and that the correlation between the mass and the concentration can be represented by quadratic functions. Secondly, the mass of the gypsum scale decreased with increasing concentration of the admixtures used. Thirdly, the flow rate of the scaling solutions (in the range: 0.4 to 1.3 cm/sec) did not significantly affect the mass of the gypsum scale. PVC

produced the highest mass of gypsum scale, followed by brass, copper, and stainless steel, respectively.

Fourthly, the presence of admixtures caused the surface of the scale deposit to become rougher than was the case in a pure system, and longer scaling experimental times resulted in denser scale deposits. In this scale formation project, the induction time was investigated. In contrast with the first and the second phase of the projects, the induction time in the scale gypsum formation experiment was significant. At a concentration of 2,000 ppm of Ca^{2+}, pure gypsum solutions had induction times of about 105 minutes at 18.3^0C and 97 minutes at 20.3^0C. In the presence of 10 ppm of SIPX, the scaling solution at 2,000 ppm of Ca^{2+} and 19.2^0C had an induction time of 1,400 minutes.

The present study produced three important findings. Firstly, the presence of Fe^{3+} or sodium isopropyl xanthate (SIPX) reduced the growth rate of gypsum crystallised either in a vessel (= a continuous crystalliser) or in a pipe flow system. Secondly, the rate of growth of gypsum crystals was found to be consistently higher in the vessel than in the pipe flow system. The rate of growth of the pure gypsum in the crystalliser at 25^0C was 0.0389 kg/m^2 hour while those in the pipe flow system were between 0.0289 and 0.0202 kg/m^2 hour, depending on the pipe material and the scaling solution flow rate. Thirdly, with respect to gypsum scaling, PVC was the least favourable material, followed by brass and copper, while the most favourable was stainless steel.

It is believed that the present study has significantly contributed to the understanding of the effect of admixtures on crystallisation of gypsum, especially in relation to the scale formation.

TABLE of CONTENTS

LIST of FIGURES

LIST of TABLES

CHAPTER 1 INTRODUCTION

1. Background of the Study

Effect of admixtures on the crystallisation of gypsum has been widely studied, and significant advances have been made. The motivation for this field of research is mainly driven by the need to develop methods to control scale formation, which is one of the persistent problems faced by many industrial processes. Research has shown that one of the major constituents of many industrial scales is calcium sulphate dihydrate (= $CaSO_4.2H_2O$) or gypsum. In industrial practice, gypsum generally forms or crystallises out of impure solutions, which contain many different admixtures. One of the most frequently employed methods of studying the crystallisation of gypsum is, therefore, the use of admixtures to influence the crystallisation process (Adams and Papangelakis 2000; Amjad 1985; Amjad 1988; Amjad and Hooley 1986; Amjad and Masler 1985; He *et al.* 1994; Jamialahmadi and Muller-Steinhagen 2000; Klepetsanis and Koutsoukos 1998; Liu and Nancollas 1973; Tadros and Mayes 1979; van Rosmalen *et al.* 1982; Weijnen and van Rosmalen 1984; Weijnen and van Rosmalen 1985; Witkamp *et al.* 1990). It is evident from all these previous investigations that the presence of admixtures in a solution can have a considerable effect on crystallisation kinetics, even if they are present in minute amounts. The effect is mostly dependent on the particular solvent-solute systems and the characteristics of the crystal surface.

Research aimed at preventing or controlling gypsum scale formation could be divided into two categories. First, earlier studies by Hasson and Zahavi (Hasson and Zahavi 1970), Liu and Nancollas (Liu and Nancollas 1973) and many others (about 20 research works dating back to as early as 1958), mainly focused on the kinetics of scale formation. Second, most of the later studies (Bansal and Muller-Steinhagen 1993; Bansal *et al.* 1997; Bansal *et al.* 2000; Bott 1995; Chamra and Webb 1994; Li and Webb 2000; Linnikov 1999; Middis *et al.* 1998; Mori *et al.* 1996; Sudmalis and Sheikholeslami 2000), on the other hand, have put emphasis on the external factors influencing the deposition of the scale. These factors include hydrodynamics of the scale forming solutions, the characteristics of the solid surface, the configuration of the heat transfer equipment, etc.

Most previous laboratory scale research on the effect of admixtures on the crystallisation of gypsum was conducted in batch type crystallisers (see 20 references tabulated in **Tables 4.1** and **4.8**, respectively, in **Chapter 4**), apparently for the ease of operation and the economy of materials required. Only a few researchers conducted continuous crystallisation of gypsum (Adams and Papangelakis 2000; Jamialahmadi and Muller-Steinhagen 2000). The work of Adams and Papangelakis (Adams and Papangelakis 2000), although using a continuous mode crystallisation, laid emphasis on the formation of scale and its morphology, and not on the growth rate of crystals within the crystalliser. The present study is aimed at investigating the effects of admixtures on crystallisation kinetics of gypsum in vessels (both in batch and continuous crystallisers), as well as in a flowing system. This investigation involved three phases of experimental work as detailed in the next section.

2. Outline of the Thesis

The present study comprises three phases of experimental work as follows:

Phase 1: batch crystallisation
Phase 2: continuous crystallisation
Phase 3: scaling experiments.

This thesis contains nine chapters, in which the three phases of the experimental work are consecutively presented in **Chapters 4** to **7**. Each chapter begins with an introduction to outline its content and closes with a summary highlighting the main points. In addition, references are placed after each chapter where appropriate. The description of each chapter is given in the following paragraphs.

Chapter 1 introduces the reader to the background and purpose of the present study, the contribution of the previous researchers in this area of research, the present state of knowledge about the study topic, and the sequence of approach taken for the present study. It closes with a detailed outline of the chapters in the thesis.

Chapter 2 reviews the literature pertinent to crystallisation of gypsum. It starts with a review of basic crystallisation theory. Then, it discusses the extensive research that has been done, and advances that have been made in the area of gypsum crystallisation. Next, discussion on the available techniques for the calculation of crystallisation kinetics, which will be adopted in this study, is presented. The chapter closes with the justification on the use of an MSMPR crystalliser for the second phase of the experimental work in this study and the selection of admixtures.

Chapter 3 presents the literature review relevant to gypsum scale formation and inhibition. It shows that earlier research on scaling, mainly focused on the kinetics of scale formation and the effects of the presence of admixtures. In addition to the effect of admixtures, most of the later studies have emphasised the effects of external factors, such as the hydrodynamics of the system, the surface topography of the solid surface where the scale may form, and the geometry of the equipment where scaling usually occurs.

Chapter 4 discusses the first phase of the present study, which is the batch crystallisation of gypsum in the presence of selected admixtures. Using a batch crystallisation method, it was discovered that the two admixtures selected, that is, sodium isopropyl xanthate (SIPX) and isopropyl thionocarbamate, were able to reduce the growth rate. The calculation of growth rate was performed, by measuring the reduction of the cation (= Ca^{2+}) concentration in the crystallising solution as the crystallisation process proceeded. Some parameters that were used in this batch crystallisation experiment were applied in the subsequent experiments conducted in a continuous mode. These parameters are: the mean residence time, the agitation speed and one of the admixtures (SIPX). The continuous crystallisation experiment is detailed in **Chapter 6**.

Chapter 5 elaborates the materials and methods that were used in the continuous crystallisation experiments, which is the second phase of the project. Firstly, the mass balance calculations were carried out to determine the quantities of raw materials needed and the amounts of the crystals that would be produced, as well as the stream flow rates and their compositions.

Secondly, the present chapter elaborates the detailed description of the crystalliser (a mixed suspension mixed product removal, or MSMPR), and its performance. Thirdly, a section is devoted to explain the preparation of the crystallising solutions ($CaCl_2$ and Na_2SO_4), followed by an explanation on the preparation of the gypsum crystals as seeds. Fourthly, sampling and measurements to extract the experimental data are presented. These data include solution concentration with respect to Ca^{2+}, slurry density and crystal size distribution (= CSD). Finally, a discussion on the experimental design selected for this experiment is given. Three factors were examined: (1) type of admixtures, (2) concentration of admixtures, (3) crystallisation temperatures. However, some alterations were later made to the implementation of the experimental design, and these alterations are discussed in **Appendix C**.

Chapter 6 discusses the continuous crystallisation of gypsum in the presence of admixtures, that is, the second phase of the study. It was found that the experimental runs reasonably satisfied the conditions of an ideal MSMPR. The crystallisation kinetics: nucleation and growth rates were calculated from the crystal size distribution (CSD) using the Population Balance Equation (PBE). The growth rate was observed to be dependent on crystal size. In almost all cases and within the concentration range tested, higher admixture concentrations induced higher reduction on the growth rates, but enhanced the nucleation rates. Since the growth rate was found to be size dependent, an attempt was made to correlate the growth rate with crystal size and concentration of the admixtures.

Chapter 7 describes the last or the third phase of the project, i.e. gypsum scaling experiments, where scale formation of gypsum on pipe walls was studied in a once through flow system under isothermal conditions. The parameters investigated were: the concentration level, the flow rate, the type and concentration of admixtures, and the type of the piping materials. The effects of these parameters on the scale formation were measured as the amount of the mass of the scale deposited on the surface of the pipe walls. Furthermore, the scale deposits were morphologically studied using scanning electron microscopy (SEM), in order to reveal information about the growth of the scale. The experimental rig and its performance are detailed in this chapter.

The experimental conditions were maintained so that effects caused by foreign particle deposition and removal of scale by shear forces were minimised. An attempt to correlate the results from phase two and phase three of the experimental work is also detailed in this chapter.

Chapter 8 describes the conclusions of the present study and recommendations for future work.

Chapter 9 compiles all the chapter summaries, with the intention to provide a more detailed summary than that given in the abstract at the beginning of the thesis.

CHAPTER 2 LITERATURE REVIEW – PART 1: CRYSTALLISATION OF GYPSUM IN THE PRESENCE OF ADMIXTURES

2.1. Introduction

This thesis involves three phases of experiments on gypsum crystallisation in the presence of admixtures: (1) batch crystallisation, (2) continuous crystallisation, and (3) scaling experiments. The first and second phases were performed in batch and continuous crystallisers, respectively, whereas for the third phase, a pipe flow system was used. Hence, it was considered necessary to construct a review of literature that appropriately fits these three experimental phases.

In this chapter, part 1 of the literature review, crystallisation of gypsum in the presence of admixtures (related to the first two phases of the project) is discussed. The second part of the literature review deals with the phenomenon of gypsum scale formation and inhibition, and is presented as a separate chapter, that is in **Chapter 3**.

2.2. Kinetics of Crystallisation

Crystallisation is one of the oldest separation processes. It serves both as a separation as well as a purification technique to obtain crystalline products using relatively less energy than other separation methods. It is traditional to refer to crystallisation as a process involving only liquid solutions, although in some cases it occurs out of melt or gaseous phases.

Crystallisation process consists of two basic steps namely nucleation and growth. Nucleation is the formation of crystal nuclei or stable crystalline phase in the crystallising system. The crystalline solids subsequently grow to visible size. The rates of nucleation and growth determine the characteristics of the ultimate product crystals. In addition, agglomeration phenomenon i.e. the process where two or more crystals collide and stick together to form a single crystalline entity, can have a significant effect on crystal growth.

Nucleation or the birth of new crystals is the formation of a solid phase from a liquid (which can be either a solution or melt). The newly born crystals then grow larger. Nucleation and growth of crystals are both rate processes and are defined as crystallisation kinetics. The two processes are only possible if the solution is either supersaturated or undercooled which is actually also one of the ways to obtain a supersaturated condition. The crystallisation kinetics is, therefore, essentially governed by the level of supersaturation. In order to understand the crystallisation process, especially its kinetics, the knowledge of supersaturation is important and will be discussed in the following section on **Supersaturation and metastability**.

2.2.1. Supersaturation and metastability

With respect to crystallisation behaviour, a solution can be described as either undersaturated, saturated or supersaturated. Supersaturated solutions are thermodynamically unstable, which means that out of such solutions, the occurrence of nucleation and crystal growth are theoretically possible. Nucleation and growth are in fact the crystallisation steps to relieve the solutions from their unstable conditions back to equilibrium. However, up to a certain supersaturation level, a solution may appear to be stable and its properties do not change. This condition is described as the metastability. Briefly, supersaturated solutions can be classified as being in the labile or metastable region.

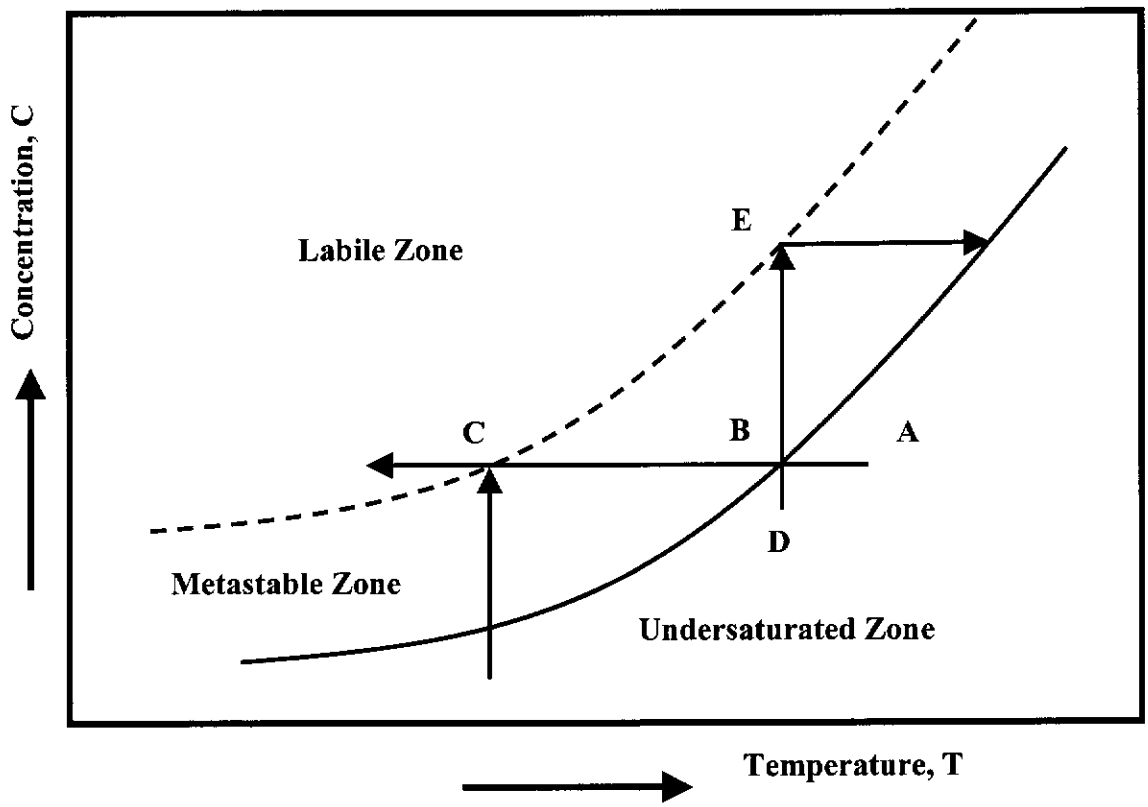

Figure 2.1 A typical supersaturation and metastability diagram

Figure 2.1 shows a typical diagram, which is normally used to explain the phenomenon of a crystallisation process in terms of supersaturation. A solution at point **A** is undersaturated. Such a solution is not able to crystallise because the solubility product of the solute has not reached a certain value where the solute will no longer be able to dissolve in it. Thus, if crystals of the solute are added into such a solution, they will start to dissolve. Lowering the temperature of the undersaturated solution at **A**, for example up to point **B**, will result in the solution being saturated. The solid curve is termed the saturation curve, which means that the solution at or along that line is no longer able to dissolve more solute and is, therefore, thermodynamically stable. Solute crystals added into such a solution will remain intact. The thermodynamic equilibrium state of the solution prevents the crystals from either growing or dissolving in the solution. Further cooling causes the solution to enter into the metastable zone where crystals might start to grow. Further away from the saturation curve or nearer the supersolubility curve (= the dashed line curve), the possibility of the rate of growth increases.

If the solution has been cooled past the point **C**, it will be in the labile zone. In this zone, the crystallisation process may take place rapidly in order to relieve the highly supersaturated condition and push back to its equilibrium. As can be seen from **Figure 2.1**, the higher the concentration the more labile the solution and thus, the easier for the nucleation to occur. At very high supersaturations, therefore, the nucleation rate can no longer be controlled which leads to a condition called spontaneous nucleation. All the conditions above, however, apply to homogeneous nucleation, where no solute crystals are present in the solution. Adding solute crystals to a supersaturated solution, however low the supersaturation level might be, will result in the growth of the crystals at the expense of the solute concentration and the growth will cease as soon as the solution has again achieved its equilibrium or its saturated condition. It is also clear from **Figure 2.1**, that the width of a metastable zone can be expressed by either the difference in cooling temperature or the difference in concentration of the solution. Thus, metastable limit can be achieved in two ways. Firstly, by cooling the solution while keeping the concentration of the solute at a constant value. Secondly, by increasing the concentration of the solution without changing the solution temperature, thus, using an isothermal process. This second method is usually carried out by evaporation of the solvent at constant temperature. Referring to **Figure 2.1** the second method will follow the path: **D - B - E** as follows.

An undersaturated solution is evaporated at a constant temperature until a saturated condition, that is point **B** is reached. Further evaporation will cause an increase in the solute content along the line **B - E**. When point **E** is reached the solution has arrived at its metastability limit. On further evaporation the solution will enter the labile zone, where nucleation or the formation of a solid phase called nucleus, takes place very rapidly and that the higher the concentration (= supersaturation) the higher the likelihood of nucleation occurring.

2.2.2. Nucleation

Nuclei formation takes place in several different ways. The formation may originate from attrition, which is especially true for large crystals. The formation of nuclei by crystal attrition is regarded as the one that occurs under macroscopic condition

because the result of the attrition can visually be detected (Jancic and Grootscholten 1984; Larson 1984). With large crystals, the attrition effect can be seen, as the crystals become rounded especially at the corners (Myerson 1993). On the other hand, the formation of nuclei can also proceed in sub-microscopic range, such as in the process of homogeneous nucleation. The currently available equipment for nucleation process detection, particularly in sub-microscopic range, is usually not adequate, hence assumptions are sometimes necessary. As an example, detecting zero size nuclei is impossible, thus it is actually only an assumption that nuclei have zero sizes (Jancic and Grootscholten 1984). Furthermore, the collected data from analytical equipment have to be statistically treated and then interpreted. For example, laser diffraction equipment to analyse crystal or particle size distribution assumes that the particles are spherical in shape. For non-spherical particles, therefore, a characteristic equivalent shape should be used.

Crystallisation is a process by which a change of phase occurs to obtain crystalline product from a solution. A solution in the crystallisation term usually refers to a liquid solution, although it can be solids (= melt) or a gaseous phase. A solution is a mixture that consists of two or more species that form a homogeneous phase. One of those species is termed the solvent and the other is the solute(s). A solution is formed when the solute is dissolved in the solvent. Adding more solutes to the solvent continuously will cause the solution to reach a certain level of concentration of solute that is called the saturation level. When the saturation level has been attained the solution can no longer dissolve more solute. The maximum amount of solute that can be dissolved in a solvent is temperature dependent. Thus, the saturation level is influenced by temperature. A solution with a solute concentration at saturation level is in equilibrium. In order for the crystallisation process to occur the solution concentration has to be raised above its equilibrium level. The difference between the equilibrium concentration and that above the equilibrium is known as the supersaturation level. In a case where supersaturation is not too high, the solution is said to be in a metastable region. In this region, formation of stable crystalline solids is possible but usually the rate is very slow or negligible. If the supersaturated solution contains crystals, for example by adding a certain amount of them, then the added crystals will grow. The level of supersaturation can be raised until the maximum boundary of the metastable region is reached. This boundary is

shown in **Figure 2.1** (section **2.2.1. Supersaturation and metastability**) as the dashed line curve called the supersolubility curve. As crystallisation is a concentration-driven process, raising the level of supersaturation will result in an increase in the rate of nuclei formation. If the maximum boundary is exceeded, for example by raising the supersaturation level, then the nucleation rate will also increase. Control of nucleation rate in a situation where metastable region has been exceeded is difficult. Nucleation rate increases sharply once a certain supersaturation level has been exceeded. Crystallisation process should aim at maintaining the crystallising solution in the metastable region in order to control the nucleation rate. Controlling the nucleation rate means determining the amount or the number of crystals produced and consequently also controlling the distribution of crystals with regard to size, which is known as crystal size distribution (**CSD**), the explanation of which is given in section **2.6**.

The following diagram shows the mechanism, by which nucleation occurs.

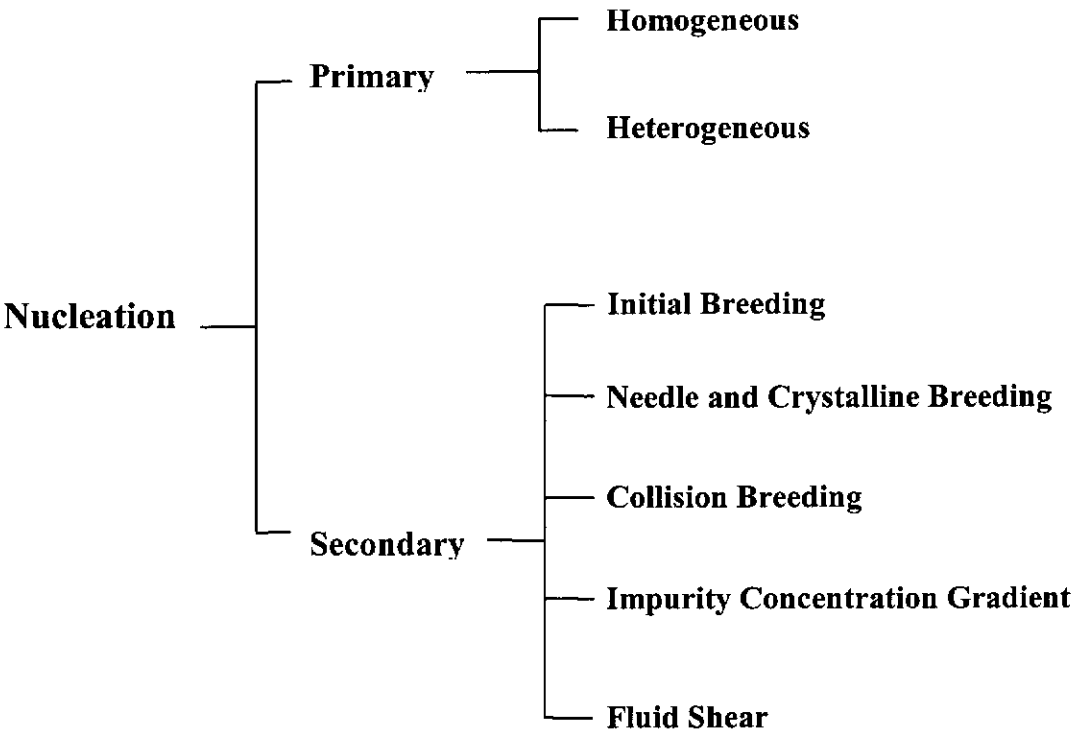

Figure 2.2 Schematic representation of nucleation mechanism (Jancic and Grootscholten 1984)

2.2.2.1. Primary nucleation

Primary nucleation occurs in a crystallising solution in the absence of solute crystals and usually takes place at relatively very high supersaturations. Primary nucleation is generally subdivided into two categories: homogeneous and heterogeneous nucleation.

2.2.2.1.a. Homogeneous nucleation

As a supersaturated solution is not in equilibrium, there are fluctuations in local concentrations which give rise to the formation of small and unstable molecular aggregates called clusters and that these clusters are continuously forming and falling apart. In a homogeneous nucleation mechanism there is no foreign surface present in the crystallising solution on which nucleation can start. Instead, the new phase formation takes place by statistical fluctuations of solute entities, which form clusters. It is assumed that clusters are formed by an addition mechanism of growth units. As addition continues the cluster grows until a critical size is reached. The attainment of critical size, however, is subject to the level of saturation of the crystallising liquid. In undersaturated or just-saturated solutions the clusters will never reach a critical size because the system is stable, hence, the number of clusters formed is equal to the number of clusters decayed away. Clusters of a critical size can be formed in supersaturated solutions where the size is inversely dependent on the level of supersaturation. The higher the supersaturation the smaller the critical size of the clusters, that is why higher supersaturated solutions are less stable than those of lower ones (Myerson 1993).

Nucleus size

Thermodynamically, in homogeneous nucleation the free energy change for the formation of nucleus, that is the Gibbs free energy, ΔG, is the sum of two opposing terms.

The free energy change for the phase transformation per unit volume (= solute molecules attached and incorporated into a cluster), ΔG_{volume}, is negative and equal to

$$\Delta G_{volume} = -\frac{k_v L^3}{V_m}\Delta\mu \tag{2.1}$$

where,

k_v = volume shape factor, dimensionless

L = size of cluster, μm

V_m = molecular volume, μm^3

$\Delta\mu$ = chemical potential difference per solute molecule.

On the other hand, the free energy change for the formation of the nucleus surface, $\Delta G_{surface}$, is positive and is equal to

$$\Delta G_{surface} = k_a L^2 \gamma \tag{2.2}$$

where,

k_a = surface shape factor, dimensionless

L = size of cluster, μm

γ = interfacial free energy, erg/particle.

Since clusters are minute bodies, the assumption of a cluster as a sphere is justified and **Eq. (2.1)** becomes

$$\Delta G = -\frac{4\pi r^3}{3V_m}\Delta\mu + 4\pi r^2\gamma \tag{2.3}$$

where r = radius of cluster, μm.

The critical radius of the cluster, **r***, can be calculated by minimising the free energy equation above with respect to radius:

$$\frac{d(\Delta G)}{dr} = -\frac{4\pi r^2}{V_m}\Delta\mu + 8\pi r\gamma = 0 \tag{2.4}$$

or

$$r^* = \frac{2\gamma V_m}{\Delta\mu}$$

and

$$n^* = \frac{4}{3}\frac{\pi r^{*3}}{V_m}$$

Therefore, the solute particle numbers required to form a nucleus, **n***, is

$$n^* = \left(\frac{2a\gamma}{3\Delta\mu}\right)^3$$

where "**a**" = surface area of a solute entity in the cluster surface.

The corresponding critical Gibbs free energy is then,

$$\Delta G^* = \frac{1}{3}4\pi r^{*}\gamma$$

or

$$\Delta G^* = \frac{16\pi\gamma^3 V_m^2}{3\Delta\mu^2}$$

or

$$\Delta G^* = \frac{16\pi\gamma^3 V_m^2}{3k^2T^2(\ln S)^2}$$

The nucleation rate can now be calculated using the Arrhenius type equation,

$$B_0 = A\exp\left(-\frac{\Delta G}{kT}\right)$$

In this case, ΔG is chosen as $\Delta G_{critical} = \Delta G^*$. Therefore,

$$B_0 = A\exp\left(-\frac{16\pi\gamma^3 V_m^2}{3k^3T^3(\ln S)^2}\right) \tag{2.5}$$

It is obvious from **Eq. (2.5)** that nucleation rate is a function of supersaturation, temperature and surface energy. The rate of nucleation will increase with increasing supersaturation and temperature. On the other hand, it will decrease if the surface energy is increasing. The Gibbs free energy, **ΔG**, is usually plotted versus the cluster radius as shown in **Figure 2.3**. As can be seen in **Figure 2.3**, a cluster radius greater than the critical size, $\mathbf{r_C}$, is associated with decreasing free energy and therefore the nuclei will survive to grow.

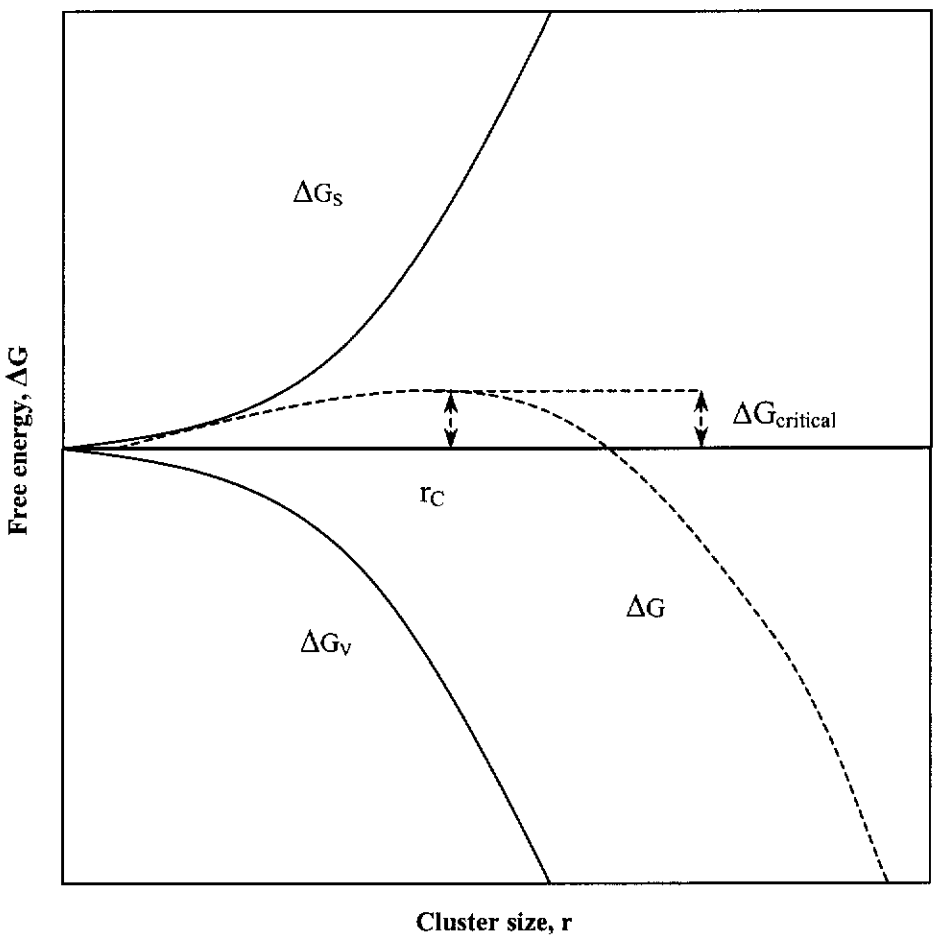

Figure 2.3 Gibbs free energy diagram for homogeneous nucleation showing free energy change versus cluster size

2.2.2.1.b. Heterogeneous nucleation

As homogeneous nucleation requires a very high level of supersaturation, the occurrence of it is practically rare and in most situations heterogeneous nucleation takes place before reaching conditions suitable for homogeneous nucleation. Under heterogeneous conditions, which mean that the crystallising solution is not homogeneous due to the presence of foreign bodies, the formation of nuclei calls for less energy than that under homogeneous conditions. It has been postulated that the difference in energy requirement for both the two situations is related to the wetting angle, θ, between the foreign surface and the nucleus. The relationship is formulated in **Eq.(2.6)**.

$$\Delta G_{homogeneous} = \frac{(2+\cos\theta)(1-\cos\theta)^2}{4}\Delta G_{heterogeneous} \qquad (2.6)$$

Equation (2.6) implies that under condition of complete wetting, that is θ = 0, the energy required for homogeneous nucleation is zero, which means that spontaneous nucleation could take place.

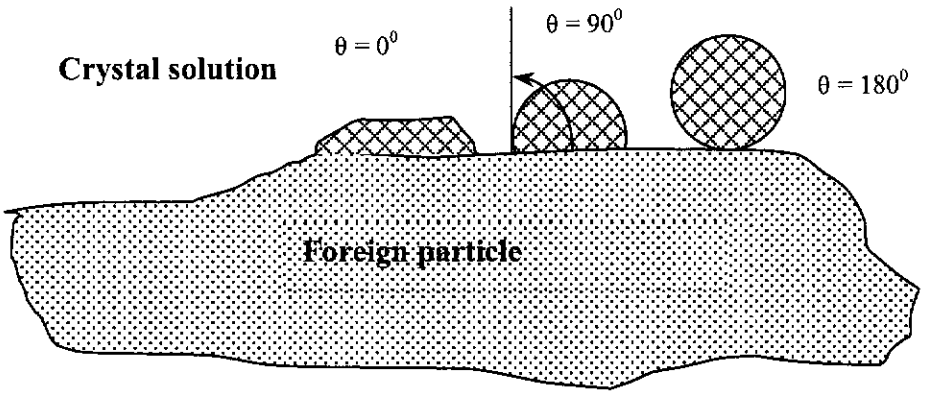

Figure 2.4 Nucleation on a foreign particle for different wetting angles

2.2.2.2. Secondary nucleation

Secondary nucleation is the mechanism of formation of nuclei under the influence of crystals or solid matter found in a supersaturated solution. In this study secondary nucleation is considered to be the main nucleation mechanism as is evident from the

roughness of the seed crystal surfaces (Nyvlt 1985). In a stirred crystalliser especially when supersaturation level is not high, secondary nucleation is the most important source of nuclei. The extent of secondary nucleation is partly dictated by the area and roughness of the crystal surface. When the surface is rough which implies that there are a large number of dislocation points, the number of nuclei formed is high. Similarly, the larger the area the more dislocation points will be found (assuming that the density of dislocation points is constant), hence more nuclei will be born. This also implies that size dependent growth of crystals is dependent on the surface roughness. Large crystals have large surface areas and thus have more dislocation points. Practically, it is sufficient to assume that secondary nucleation must be dominant in stirred crystallisers. One reason is that crystal surfaces will always be rough. Even smooth surfaces of a crystal are actually microscopically rough, hence, the possibility of secondary nucleation always exists. Another reason is that detachment of tiny fragments from the crystal surface is always induced by agitation or stirring in the crystalliser. The nucleation process is classified and explained in the following section.

2.2.2.2.a. Initial breeding

If a crystal is put into a supersaturated solution, a number of small crystalline particles (= nuclei) is usually formed (Jancic and Grootscholten 1984; Myerson 1993; Rousseau *et al.* 1976). This phenomenon happens even if the level of supersaturation is relatively low. The appearance of these nuclei can be caused by crystallite fragments that are detached from the surface of the "parent crystals" added into the supersaturated solution. The crystallite fragments might be formed during storage or when the crystal drying process takes place quickly. As the phenomenon occurs only at the time when the crystals are first put into the solution, the mechanism is called initial breeding (Jancic and Grootscholten 1984). Initial breeding is also called dust breeding due to the source of nuclei or crystallite fragments, which are likened to "dust" attached to the parent crystals (Myerson 1993). It is obvious that the mechanism of initial breeding is not significantly affected by stirring because the detachment of the small crystallites from the parent crystals is relatively easy . In addition, level of supersaturation does not influence

the initial breeding strongly due to the larger size of the detached crystals relative to that of clusters, and thus it is very unlikely that the detached crystals will disintegrate. If there is no disintegration, then all crystallites will grow to become crystals. Assuming that the same size of surface area of added crystals was attached by the same number of crystallites, it might be possible to relate nucleation rate with the surface area of the added crystals. The occurrence of initial breeding can be prevented or lessened by pretreating the parent crystals, such as by elutriation or washing. Initial breeding can be categorised as "apparent" secondary nucleation because there is no formation of completely new nuclei (Nyvlt 1985).

2.2.2.2.b. Needle breeding and polycrystalline breeding

In a solution with higher level of supersaturation, abnormal growth of crystals is often found. This abnormal growth appears as needles and is attached at the ends of parent crystals causing the roughening of crystal surfaces. Mixing or agitating the solution causes these needle-like fragments to break away and detach from the parent crystals. If the level of supersaturation is even higher the needle-like fragments might grow and attach to each other forming aggregates or "polycrystals". This form too can be broken and detached from the parent crystals and hence the name polycrystalline breeding. The detachment will occur due to lowering of supersaturation or abrasion. If crystals were well-formed, polycrystalline breeding can be neglected (Desai *et al.* 1974). This type of breeding is also termed apparent secondary nucleation, for the same reason as the initial breeding (Nyvlt 1985).

2.2.2.2.c. Collision breeding

Collision breeding takes place in a crystallisation process, which involves agitation where crystals collide among themselves and/or with crystalliser internals. Because the main cause is collision, the collision breeding can occur even if the supersaturation level is low and the crystals have regular shape (Jancic and Grootscholten 1984). Collision breeding is an important phenomenon for crystallisation process which involves high slurry density. If slurry density is low and the crystals are of small sizes the collision breeding can be neglected because

small crystals tend to follow the liquid streams and therefore do not collide either among themselves and/or with the stirrer or the crystalliser internals.

Collision breeding is generally differentiated into two types (Jancic and Grootscholten 1984). First, attrition type, in which new crystals are formed from the fragments generated by the collision or impact. The process of attrition breeding will leave visible defects on the surface of the parent crystals and in some cases the parent crystals will become rounded. Attrition breeding is usually found in a system with intense agitation. Second, contact nucleation, in which the mechanism does not leave macroscopic defects on the surface of the parent crystals. The formation of nuclei in this process can either be caused by micro abrasion or from the adsorbed solute layer, which has not been crystallised.

Contact nucleation is probably the most important type of secondary nucleation in crystallisation for the following reasons. Firstly, for initial breeding to occur the crystals must have tiny fragments. Thus, initial breeding does not always take place. Secondly, crystallisation will not produce needle breeding unless the level of supersaturation is reasonably high. Thirdly, in order for the attrition to happen, agitation in the crystalliser should be such as to cause strong collision among the suspended crystals and between the crystals and the crystalliser internals. Moreover, the suspension or slurry density should also be reasonably high. In a situation where the concentration is low contact nucleation well occurs but attrition is not likely to take place.

2.2.2.2.d. Nucleation caused by impurity concentration gradient

This type of nucleation occurs when the process of crystallisation proceeds in the presence of impurities (Jancic and Grootscholten 1984; Myerson 1993). If seed crystals are present in the crystallising solution, a boundary layer will form between the solution and the surface of the crystals. Impurities in the solution may be incorporated in the lattice or onto the surface of the growing crystals, thus creating a gradient of impurity concentration inside and along the width of the boundary layer.

Further away from the crystal surface, the concentration gradient will be lower and this condition enhances the possibility of spontaneous nucleation.

2.2.2.2.e. Nucleation caused by fluid shear

The term fluid shear indicates that nucleation occurs in a non-stagnant crystallising system (Jancic and Grootscholten 1984; Myerson 1993). Shearing flow caused by agitation or movement of solution inside a crystalliser is responsible for the breeding of nuclei. There are two sources of the nuclei, namely the dendritic crystallites and the boundary layer. In a crystallising solution with high supersaturation, on the surface of crystals may develop dendritic growth which due to shearing action within the solution will be broken and grow as nuclei . The second source of the nuclei is the boundary layer, which is removed by the shearing action of the fluid (Tai and Wu 1992). In this case the removed layer will act as growth units.

In summary the mechanism of nucleation can be stated as follows.

Nuclei-forming components in the form of solute entities that exist in a crystallising solution interact randomly to form stable nuclei centres known as clusters which subsequently grow to become nuclei.

Nuclei-forming components interact with foreign substances found in the crystallising solution to become nuclei.

Crystals inoculated into the crystallising solution might bring the nuclei-forming components with them. These components might break away from the inoculated crystals and grow to become nuclei.

Inoculated crystals interact with the crystallising solution to produce nuclei.

Inoculated crystals collide among themselves and/or with crystalliser internals to produce nuclei.

The origin of the nuclei-forming components can be twofold:

1. The components may already exist in the crystallising solution.

2. The components are brought into the crystallising solution by the added crystals.

Once nuclei are formed, they subsequently grow to become crystals, which can be detected visually. The growth of crystals is discussed in the next section.

2.2.3. Growth of crystals

After nucleation or the birth of new crystals, the subsequent crystallisation step is crystal growth where nuclei grow larger by the deposition of solute molecules or growth units, which break whatever bonds they have with the crystallising or supersaturated solution and make new bonds with the crystals. Crystal growth theories have evolved over the past century and it appears that the development leads to the molecular or an atomic level identification, which involves not only the crystals but also the environment wherein the crystals grow. The growth of crystals means a regular addition of solute molecules or growth units from a supersaturated solution onto the crystal faces. Therefore, the solution concentration is depleting while the size and weight of the crystals increase. The growth of crystals is determined by the rate of increase in the size of the surfaces. Different faces may grow at different rates and this condition dictates the final shape of crystals. The fastest growing faces will disappear while the slowest ones will remain, leaving the crystal bounded by the slowest growing faces.

There are several ways to describe the crystal growth rate. First, the growth rate is measured as a change in some dimensions with time, and this is known as the linear growth rate (Nyvlt 1992; Sohnel and Garside 1992). As crystals have more than one face, the linear growth rate must be specific to a particular face. It is usually meant to be the growth rate of a certain face in the direction normal to that face. This can

be a difficult decision because different faces of a crystal might grow at different rates, so that from one particular crystal several different growth rates may be obtained. This situation can be useful for the fundamental study of crystal growth such as a crystallographic study where growth of different faces of a crystal needs to be compared.

Second, the crystal growth rate can also be measured by observing the change in the characteristic dimension with time. As is well known each type of crystal has its own characteristic dimension, such as spherical, plate-like, needle-like etc. For example, if the crystal is spherical in shape the characteristic dimension is its diameter. Thus the growth rate can be determined as the change in diameter over a certain length of time (Nyvlt 1985).

Third, the crystal growth rate can also be determined as the overall growth of the crystal. In this case, the usual method to be used is to determine the change of the crystal mass per unit time (Nyvlt 1985). The book written by Nyvlt *et al.* (Nyvlt 1985) gives a comprehensive review of the theories of crystal growth, wherein as many as ten theories and models are discussed. The discussion was adopted here to elaborate the development of crystal growth theories. The theories are classified into two groups, that is, based on either thermodynamic or kinetic properties, as explained in the following section.

2.2.3.1. Theories based on thermodynamic properties

2.2.3.1.a. Theory of limiting faces

This is considered to be the oldest theory of crystal growth since its inception was started in the 19th century (Curie, 1885, as quoted by (Nyvlt 1985)). It explains the relationship between the shape of a crystal and the surface energies of its individual planes. The growth of individual planes or faces of a crystal depends on the capability of the crystallisation system to proceed towards a more stable equilibrium state. Specifically, the growth of individual planes depends on the specific surface

energies of those planes. The Wulff theorem is generally used to calculate the specific surface energies as follows.

$$\sigma_1/h_1 = \sigma_2/h_2 = \ldots\ldots = \sigma_i/h_i = \ldots\ldots = \sigma_n/h_n = \text{constant} \quad (2.7)$$

where

σ_i = the specific energy of the *i*-th plane, erg/particle

h_i = the distance of the *i*-th plane from the centre of the crystal, μm.

If a certain face releases a large amount of energy it will experience the fastest growth and vice versa. Hence, the face will either grow bigger or disappear. The face with the slowest linear growth rate determines the final shape of the crystal.

2.2.3.1.b. Theory of Kossel and Stransky

Kossel and Stransky (Mullin 1972; Myerson 1993; Nyvlt 1985; Ohara and Reid 1973) suggested that crystals grow by a repetitive process of incorporation of growth units onto a plane. Because a plane is the least energetically favourable site, the incorporation of a growth unit onto it is the least expected. However, once an initial species or growth unit has incorporated onto the plane, many other growth units will rapidly cover the plane and eventually form a completely new plane layer on top of the previous plane. Then, the slow process of finding an initial growth unit to attach to the newly formed plane follows and the same process repeats. Thus, there is fluctuation of growth. The theory also assumes that crystals have no imperfection on their surfaces and that their shapes are regular. Kossel and Stransky proposed that the amount of energy liberated during the incorporation of a growth unit, e.g. an ionic species, onto a crystal plane depends on its position relative to the plane. Four equations were formulated.

$$E_H = 0.8738\ e^2/r \quad (2.8)$$

$$E_R = 0.2470\ e^2/r \quad (2.9)$$

$$E_K = 0.0903\ e^2/r \quad (2.10)$$

$$E_P = 0.0660\ e^2/r \quad (2.11)$$

where, **E** refers to the amount of energy liberated, **e** is the elementary charge and **r** the ion distance. The subscripts **H**, **R**, **K**, and **P** refer to the position of the growth unit relative to the crystal plane as follows:

H = "half-central" position

R = the unit is located in a corner of a completed plane

K = the unit is added at the edge of a completed plane

P = the unit is added in the centre of a completed plane.

2.2.3.1.c. The solid on solid (SOS) model

The SOS Model (Nyvlt 1985) explains that crystal growth mechanism is dependent on the roughness of the crystal surface. The rougher the surface the easier the growth units attach themselves to the surface. In this regard the similarity between the SOS Model and the Kossel and Stransky Theory is evident. Furthermore, in both theories a crystal is seen to consist of regularly structured repetitive units. During growth process, the solid species in the boundary layer are in contact with the liquid phase. The SOS model assumes that during crystal growth, the liquid phase in contact with the surface of the crystal could become solid particles. The total number of particles in the phase layer, **N**, is then calculated using the following equation:

$$\mathbf{N} = \mathbf{N_{ns}} + \mathbf{N_{nf}} \qquad (2.12)$$

where $\mathbf{N_{ns}}$ and $\mathbf{N_{nf}}$ are the total number of the solid species and the liquid species respectively.

2.2.3.2. Theories based on kinetic properties

2.2.3.2.a. Boundary layer theory

This theory is advanced by Volmer (Nyvlt 1985) and is an important breakthrough of crystal growth based on kinetic theory. As opposed to previous theories, Volmer considered the existence of a boundary layer, which strongly adheres to the crystal surface. **Figure 2.5** shows the layout of the boundary layer.

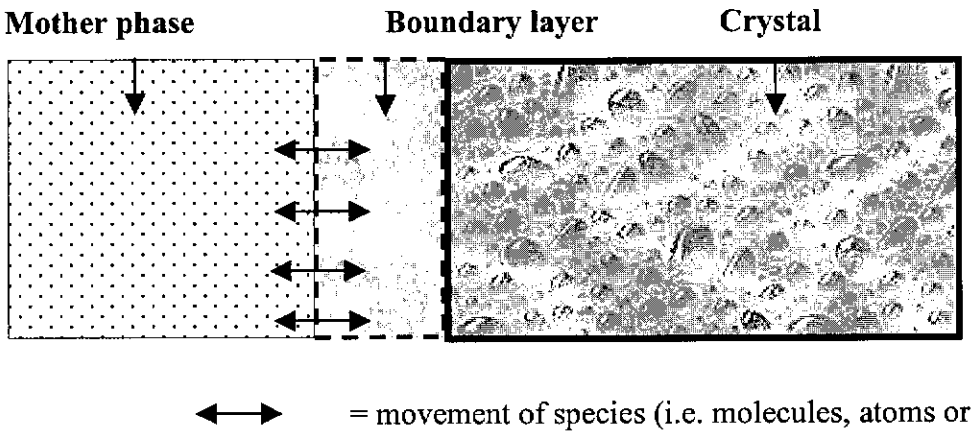

Figure 2.5 Schematic representation of the Boundary Layer Theory

Depending on its energy level, a growth unit can either move back to the mother phase, stay in the boundary layer, or be adsorbed onto the crystal surface. Thus, it is predicted that unless the growth unit or species has a high energy, it will stay in the boundary layer or be adsorbed onto the surface of the crystal. The rate at which the species moves is determined by the coefficient of surface self-diffusion of the species, **D**, as follows:

$$\mathbf{D = d^2/4t} \qquad (2.13)$$

where,

d = average distance between adsorbed species in the boundary layer, (μm)

t = mean time period spent by the particle in the position corresponding to the potential valley (= possible rest positions of the adsorbed particles), (sec).

2.2.3.2.b. Surface diffusion model (BCF Model)

This surface diffusion model was developed by Burton, Cabrera and Frank; hence the name of the theory is also shortened as the BCF Model (Myerson 1993; Nyvlt 1985; Ohara and Reid 1973). The Surface Diffusion Model does not recognise the existence of the boundary layer, instead it explains that the species of growth moves directly from the bulk of the solution to the crystal surface (Ohara and Reid 1973). It then moves over the surface and attaches itself to the most energetically favourable growth sites. In terms of energy level there are three regions, as depicted in the following figure (**Figure 2.6**).

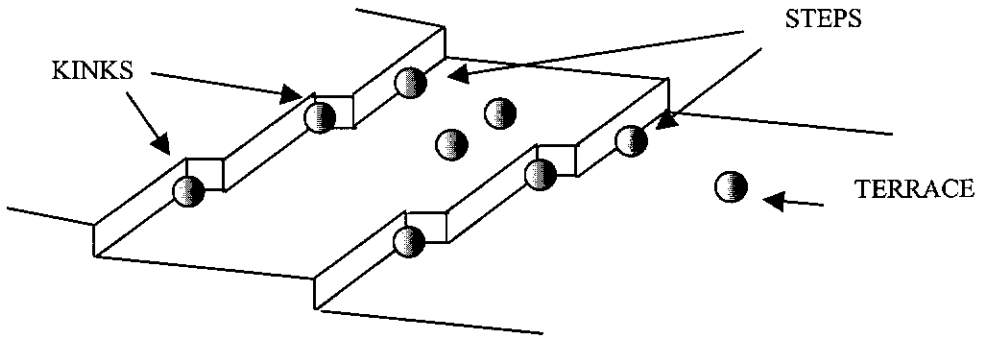

Figure 2.6 Schematic representation of the Surface Diffusion Model

The rate of crystal growth is significantly dependent on its surface structure. As a growth site, the crystal surface is generally classified into three regions as depicted in **Figure 2.6**. The first region is the terrace that appears as a flat surface. This region is atomically smooth and has a low energy. As can be seen from **Figure 2.6**, an atom, a molecule or a growth unit has only one side to attach on the surface. Therefore, a terrace is an unfavourable site for a growth unit attachment. The second region is the step that separates flat terraces. A growth unit attached onto this region has two-side attachment. One side is attached to the terrace; the other is attached to the step. Thus, the probability of attachment is greater than that on the terrace. If a particular step cannot grow completely along the terrace, it gives rise to yet another region called a kink. It can be seen that a kink is the most favourable site for attachment due to the three sides that belong to it. Kinks have the highest bonding energy and offer the most favourable sites for unit growth or particle integration. Thus, consistency can be seen among all models so far discussed, in that the face of a crystal is the most difficult surface onto which a growth unit can stick itself. This theory, however, did not explain how kinks, steps or terraces are formed. The growth rate equation of the BCF model is represented as follows:

$$\mathbf{R = A\ \sigma^2\ tanh\ (B/\ \sigma)} \qquad (2.14)$$

where,

R = crystal growth rate, g/sec

σ = supersaturation

= S – 1, where S = c/c*, dimensionless

A, B = temperature dependent constants.

2.2.3.2.c. Bulk diffusion model

The Surface Diffusion Model is more suitable for a crystallisation from vapour phase where the concentration gradient is usually small and negligible (Nyvlt 1985). For a solution crystallisation where the concentration gradient in the solution phase is greater than that in the vapour phase crystallisation, it seems logical to assume that the bulk diffusion can be a controlling factor. In order to adsorb onto the crystal surface, the growth units need to move from the bulk of the solution through a layer, which adheres to the crystal surface. Hence, the thickness of the layer plays an important role. Consequently, all factors that affect the thickness of such layer must be considered. A relationship for the linear growth rate, **l**, is formulated as follows:

$$l = \frac{s.B.k.T.c_{eq}.\Omega}{4\gamma}.b.\frac{1}{\left[1+\frac{B.a}{D}\ln\frac{c.\delta}{b.a}\sinh\frac{b}{c}\right]} \qquad (2.15)$$

where,

l = linear rate of face growth perpendicular to the surface, (μm/sec)

s = number of cooperating spirals on the surface, dimensionless

B = a complex factor characterising the rate of incorporation of the growth particle into the step

k = Boltzmann constant, (erg/particle.^{0}K)

T = absolute temperature, ^{0}K

c_{eq} = equilibrium concentration of a saturated solution, (particles/ml)

Ω = volume of the growth particle in the crystal, ml

γ = surface free energy of a particle incorporated into the step, (erg/particle)

a = mean distance between growth units in the crystal, μm

D = diffusion coefficient, (cm^2/sec)

c = a factor which equals to (4 γ a)/(skTδ)

δ = thickness of the diffusion (unstirred) layer on the crystal surface, μm

2.2.3.2.d. Combined bulk-surface diffusion

This theory considers all the factors that exist in both bulk and surface diffusion theories (Nyvlt 1985). It explains that all these factors exert resistance to the incorporation of species of growth onto the crystal surface and that the resistance dictates the growth rate. The mathematical model of the combined bulk-surface diffusion is so complicated (Nyvlt 1985) that it lies outside the scope of this work.

2.2.3.2.e. The kinematic theory

In the surface diffusion model, the growth sites, whether they are surfaces, steps or kinks, are considered as composed of regular distribution of mono-atomic steps. In the kinematic theory, these growth sites are considered as irregular, thus there is no crystal surface that is absolutely smooth (Nyvlt 1985). The surface roughness affects crystal growth by affecting the layer movement. The step velocity, **u**, which governs the rate of the layer movement, and hence, the rate of the crystal growth, is formulated as follows:

$$\mathbf{u} = \mathbf{q}/\mathbf{n} \tag{2.16}$$

where,

u = step velocity, (length/time)

q = step flux
= number of steps passing a given point per unit time

n = step density
= number of steps per unit length in a given area.

The kinematic theory considers both lattice defects and surface roughness as the controlling factors for crystal growth.

2.2.3.2.f. The diffusion layer model

The Diffusion Layer Model describes the crystal growth mechanism as consisting of two consecutive steps, that is, diffusion of growth units towards the crystal surface

followed by integration or adsorption onto that surface (Mullin 1972; Myerson 1993; Nyvlt 1985).

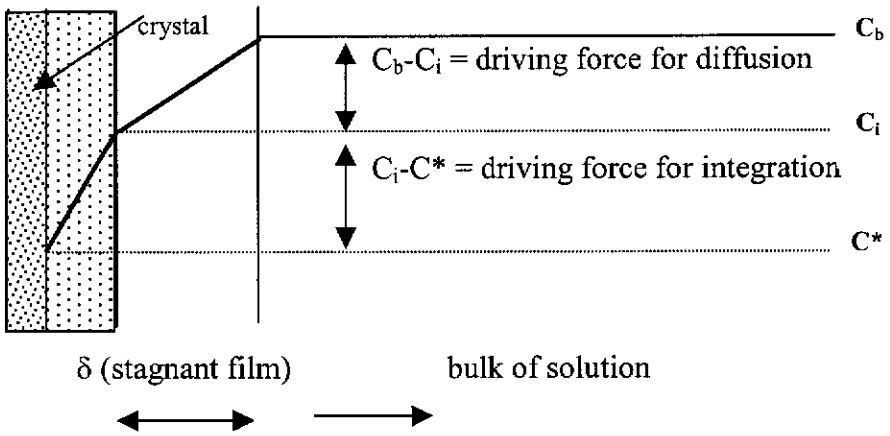

Figure 2.7 Schematic representation of the Diffusion Layer Model

Figure 2.7 shows the layout of the diffusion layer model, where the notations are defined as follows:

C_b = concentration in the bulk of the solution, g/L

C_i = concentration at the interface, g/L

C^* = concentration at saturated condition, g/L.

The diffusion rate of a growth unit into the crystal surface can usually be represented by the following equation:

$$\frac{dm}{dt} = D\,A\,\frac{C_b - C_i}{\delta} \qquad (2.17)$$

where,

dm/dt = diffusion rate, (g/sec)

D = diffusion coefficient, cm^2/sec

A = surface area of crystal, cm^2.

Further discussion on the use of the previous equation in this work, is given in section **4.4** in **Chapter 4**.

2.2.3.2.g. The nuclei above nuclei (NAN) model

In the NAN Model (Myerson 1993; Nyvlt 1985; Ohara and Reid 1973) a nucleus is thought to have circular shape and thus of two dimension on a flat surface. The NAN Model is also known as the Two Dimensional Growth Theory (Myerson 1993; Ohara and Reid 1973). This theory assumes that a crystallising solution has a constant supersaturation; hence bulk diffusion does not occur. The two dimensional nuclei form on the crystal surface and then they grow sideways. However, this theory is somewhat ambiguous in describing the growth rate of nuclei, and three models are advanced:

- Mono Nuclear Model
- Poly Nuclear Model
- Birth and Spread Model.

Mono Nuclear Model explains that the rate of growth of nuclei is extremely fast. The rate of crystal growth, **G**, is defined simply as:

$$\mathbf{G = h.\ A.\ I} \qquad (2.18)$$

where,

h = step height, μm

A = crystal surface area, μm^2

I = rate of formation of a critical nucleus per unit surface area per unit time.

Poly Nuclear Model, however, assumes exactly the opposite of that of the Mono Nuclear Model, that is the rate of growth is zero or that the two dimensional nuclei once formed do not grow at all. In other words, there have to be a large number of nuclei, which sit next to each other until they cover the entire layer. The rate of crystal growth is represented by the following equation:

$$\mathbf{G = J.\ \pi.\ h.\ r_c^2} \qquad (2.19)$$

where,

J = a constant factor

$\mathbf{r_c}$ = the radius of the critical nucleus, μm.

Between the two extreme of Mono Nuclear and Poly Nuclear Models there is the Birth and Spread (B/S) Model. The B/S Model has a finite constant rate and is independent of size. In reality, the Mono Nuclear Model is not adequate because it contradicts the experimental data (Myerson 1993). According to the Mono Nuclear Model large faces grow faster than small faces which in reality the opposite occurs. The Poly Nuclear Model is not adequate either, because it expects that at a certain supersaturation level, the growth rate, **G**, will achieve a maximum and decline afterwards, the condition, which has not been experimentally observed. In reality, **G** always increases with supersaturation. In the B/S Model, **G** increases with both supersaturation and temperature. It can be assumed that the spread of the nuclei on the crystal surface could be dependent on the level of supersaturation as well as on the temperature.

The crystal growth according to the B/S Model is expressed as follows:

$$\mathbf{G = h.\ J^{1/3}.\ (v^*)^{2/3}} \qquad (2.20)$$

where,

$\mathbf{v^*}$ = the rate of the spread of the nucleus.

All the three models have disadvantages, which make them difficult to be considered as adequate models. The following reasons can be put forward. First, in all of the three models, the growth process is assumed to be a non-continuous. Second, at a low supersaturation, the calculated growth rates obtained are much lower than that of the experimental data.

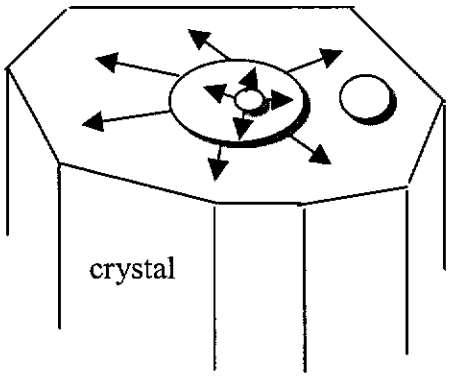

Figure 2.8 Birth and Spread Model

The Two Dimensional Model is not widely accepted due to the fact that dislocation-free crystals are very rare. Instead, the "spiral mechanism" theory dominates. However, the Two Dimensional Model (which is sometimes called the Two Dimensional Nucleation-mediated Growth Theory) is sometimes still used, for example by van der Leeden *et al.* (van der Leeden *et al.* 1993) to explain the retardation of growth of $BaSO_4$ by certain organic additives in an unseeded precipitation. They assumed that the surfaces of $BaSO_4$ crystals obtained from the experiment were screw dislocation-free and atomically smooth. The assumption could be questioned because the supersaturation ratio used was rather high, i.e about 9.00, which normally would enhance rough crystal surfaces (Myerson 1993). It could be argued that for Two Dimensional Theory to apply, the crystals should be carefully grown so as to obtain growth sites with low dislocation density.

The previous discussion about theories of crystal growth could be summed up in a few sentences as the following:

It appears that at the beginning, the theory of crystal growth focused on the growth of the crystal per se without considering the existence of the environment surrounding the crystals, such as the mother phase. Furthermore, the crystals were considered as ideal substances, regular in shape and had no defects. The growth was also ideal in that the deposition of the growth units proceeded in a regular manner with the growth units themselves regular in shape. Later developments considered crystals more realistically, i.e. that the surfaces of the crystals were not smooth and had imperfections or defects. Defects were seen as the ideal growth

sites. Subsequent development focused not only on the crystals and their nature but also on the environment in which the crystals grow. The nature of the crystallising solution was seen as having significant effects on the growth of crystals. Based on this proposition several theories were advanced.

It is interesting to note, however, that whenever one theory failed to explain a certain crystallisation condition, another theory seems to be able to shed light on it. As an example, the layer by layer mechanism as proposed in the Birth and Spread Model, is difficult to explain considering the fact that crystal faces can grow at a very low supersaturation (as low as 0.1 %) which indicates that the number of nuclei might not be enough to cover the entire layer (de Jong 1984). *However, using the Surface Diffusion Model, it can be assumed that most probably the number of nuclei still manage to cover the kink sites in a continuous manner, hence the growth process is still possible* (Nancollas 1979).

Like any other particulate processes, crystallisation and especially precipitation is almost always subject to agglomeration. Through agglomeration phenomenon, the CSD as well as the shape of crystals in a crystallisation system may change, hence, product quality as well as down stream processing may also be affected.

2.2.4. Solubility

Solutions are formed, by mixing two or more components, such as adding and dissolving a solid substance in a liquid substance. The solid component is termed the solid solute and the liquid component, the solvent. The amount of solute that can dissolve in a given amount of solvent is temperature dependent. In most cases, increasing the temperature of the solvent will result in dissolving more solute. A few cases, however, show the opposite. As more solute dissolves in the solvent, the resulting solution becomes increasingly "concentrated" and eventually a condition will be reached where no more solute can dissolve. In other words, the amount of solute that can dissolve has reached the maximum. The maximum amount of solute

that can dissolve in a solvent at a given temperature is called the solute solubility. Solubility is, therefore, temperature dependent.

Buds *et al.* (Budz *et al.* 1986), investigating the effect of some admixtures on a continuous precipitation of gypsum found that Al^{3+}, maleate and fumarate ions at concentrations between 10 – 200, 120 – 800, and 120 – 300 ppm respectively, had no effect on gypsum solubility. The solubility data of the substance to be crystallised is especially important in cases where the crystallisation processes are to be carried out in multi-component systems. However, the availability of such data is also subject to specific systems. In some multi-component systems, trace amounts of foreign substances can have significant effects on crystallisation kinetics. In some other systems, for example, in the crystallisation of sodium chloride in the presence of sodium sulphate, the presence of Na^+ and SO_4^{2-} as much as 1,620 and 3,380 ppm respectively, had little influence on crystallisation kinetics (page 100, Mullin 1979).

A solvent can be regarded as an impurity in the crystallisation from solution. It can interact with solute to influence the solvation of ions and molecules. The adsorbed layer as well as the active growth sites on a growing crystal can also be influenced by the solvent (page 98 Mullin 1979). The effects of solvent, however, have not been extensively studied, at least not as much as that for the effects of impurities. Studies on solvent effect are usually carried out to examine the solubility values of solutes or impurities, which dissolve in such a solvent. In certain cases, the interfacial tension between crystal and solution was examined to verify the solubility of the crystal. The results appear to be dependent on the crystallisation system. For one system, the decrease in interfacial tension resulted in a decrease in crystal solubility (page 98 Mullin 1979). This is the case of the crystallisation of KCl in water-ethanol solvent. For another system, increasing the interfacial tension results in a solubility decrease (page 98 Mullin 1979). This was found in the crystallisation of cyclonite in water-acetone solution. The interfacial tension in both cases was invariably changed by changing the proportion or ratio of the organic components (ethanol or acetone) making up the solvent. Kitamura *et al.* maintain that the influence of solvent is more evident for crystallisation of organic materials (page 111, Ohtaki 1998). They have also found that a certain type of crystal can assume different polymorphism if it was crystallised in different type of solvents. Based on the data of Marshall and Slusher

as cited by Hodgson and Jordan (Hodgson and Jordan 1976), it has been shown that the solubility of calcium sulphate dihydrate (calcium sulphate dihydrate) in normal seawater is practically constant at temperatures between 20^0C and 50^0C. It appears therefore, that organic solvents have much more influence on the crystallisation process than do inorganic solvents.

In this study the stability of the supersaturated solutions was verified by the constancy of the total calcium ions in the solution for at least two hours with stirring at 125 rpm, using Ca Ion Selective Electrode (Nancollas *et al.* 1979b).

2.3. Effects of Admixtures on Kinetics of Crystallisation

During a crystallisation process, nucleation, crystal growth and crystal morphology can significantly be affected by the presence of small amounts of impurities. They affect the purity and shape of the crystals in the crystallising system. Impurities and additives are collectively known as admixtures. Impurities are substances, which are present in the crystallising system as unwanted components. They originate from various sources such as raw materials, minute particles detached from crystallisation equipment, reaction among the crystallising components and so on. Additives on the other hand, are chemical substances, which are intentionally added into the crystallising solution to help the crystallisation process by altering the crystallisation parameters. Admixtures can either enhance or restrain the crystallisation kinetics, i.e. nucleation and growth of crystals.

Additives are widely used in the crystallisation process. They are usually added to the process to promote the crystallisation efficiency such as filtration. Adding additives to the process is sometimes also carried out to improve the crystal product performance such as flowability so that handling of the product (= storage, transportation etc.) is more convenient. These two previous examples show that the added additives affect the shape, i.e. the habit and/or morphology of the crystals.

The surface of a newly formed crystal may adsorb the admixtures and subsequently a change in surface characteristic follows, which influences the crystal growth, the tendency for agglomeration, the dispersion characteristic etc. If there is different

growth rate among different faces of a crystal, the crystal will finally appear with different shapes. Thus the morphology of the crystal has changed. The mechanism of the effect of admixtures on crystallisation is specific. There is no consistent theory available as yet with regard to the influence of admixtures on crystallisation process. In general, however, the effect of admixtures on crystallisation process can be summed up as follows.

1. *Admixtures influence the solution or the interface between solution and crystals by changing their properties, and thus changing the crystal surface characteristics.*

2. *Admixtures are incorporated into the crystal lattice and thus change the habit and morphology of the crystals.*

3. *Admixtures react chemically with other component(s) in the solution, and hence, influence the crystallisation process.*

4. *Admixtures are adsorbed onto the crystal face and thus, the growth of the face is retarded.*

For each and individual crystallisation system, however, the influence of admixtures is specific. In other words, it cannot be predicted beforehand which one of the possible mechanisms will operate. They will only be found after studying the particular crystallisation system in question. Moreover, it is very likely that one or more mechanisms will work at the same time.

Shor and Larson (Shor and Larson 1971) investigated the effect of metallic ions and surface-active agents on nucleation and growth rate of KNO_3 crystals in a continuous

cooling crystalliser. It was found that the metallic ions Co^{2+} and Cr^{3+} both reduced the nucleation rate. The reduction was due to an adsorption of the charged cations (Co^{2+} and/or Cr^{3+}) on the nucleation sites present on the crystal surface. Higher concentration of charged cations results in more nucleation sites being blocked and hence further reduction in nucleation rate. It was also proposed that the reduction in nucleation rate could be due to the collision between ions in the solution. As the +2 or +3 charged ions adsorbed on the crystal surface, the chance that positive and negative ions colliding on or near the crystal surface is reduced. Consequently, the formation of clusters of ions, which leads to the birth of nuclei, is also reduced.

The reverse phenomenon, however, was observed when surface active agents were used. In fact, Shor and Larson (Shor and Larson 1971) found that increasing the concentration of the surface-active agents increased the nucleation rate. It seemed that the surface-active agents would have lowered the surface tension of the solutions and consequently the contact angles of clusters with the crystal surfaces in the solution decreased. As contact angle decreases the critical free energy of formation of clusters also decreases causing an increase in nuclei formation.

Mechanism of the effect of admixtures on the growth rate of crystals could be classified into four categories (Moyers and Rousseau 1987). Firstly, the admixtures might be adsorbed onto the crystal surface. Thus, they form a barrier to ward off transfer of growth units from the solution to the crystal surface. Secondly, the admixtures might be adsorbed and occupy active growth sites, such as kinks, rendering the sites unavailable for attachment of solutes or growth units to the crystal surface. Thirdly, instead of affecting the crystal surface, admixtures might influence the formation of solute clusters, which then results in affecting the growth. Finally, the admixtures might integrate into the crystal structure.

The growth of crystals can be disrupted by the presence of admixtures in one of the following mechanisms. Firstly, the admixtures change the solution properties. Secondly, the admixtures alter properties of the solid-liquid interface in the crystallising solution. Thirdly, the admixtures selectively adsorb on the various crystal faces. Selective adsorption causes the disruption of the growth of crystal faces and changing the surface energies. For example, low concentrations of certain

dyes can cause dendritic growth of $KClO_3$ crystals. The opposite is also true. A trace amount of pectic acid can stop the dendritic growth of NH_4Cl crystals. Not only is the growth stopped but also the shape, the direction and the degree of branching are altered. Adsorption of inhibitor onto the crystal surface may induce crystal tendency to disperse or agglomerate (van der Leeden and van Rosmalen 1987). This occurs if the adsorption process is such that the composition and charge of the electrical double layer surrounding the crystals are altered.

During a crystal growth process admixtures will first be adsorbed into the interface and then incorporated onto the crystal surface. However, not all parts of the crystal surface are able to receive the oncoming admixtures. There seems to be preselected or favourable parts into which the admixtures can readily be incorporated (van der Leeden and van Rosmalen 1987). As explained by Mullin, a crystal face, which is entirely covered by kinks, will experience the fastest growth (Mullin 1972). Once the admixtures have been built on the surface layer, they will inhibit the regular deposition of oncoming growth layer. The inhibition will cause the perpendicular growth of that particular face to slow down relative to other faces resulting in the widening of the face, and therefore, the morphology of the crystal will also change (Lahav and Leiserowitz 1990).

It is often overlooked, however, that there is the adverse effect of admixtures, that is, an increase in admixture concentration will increase the crystal growth. The adverse effect prevails whenever one of the growth parameters is extremely affected so that other interrelated parameters are abruptly influenced in the opposite direction (van der Leeden and van Rosmalen 1987). These two authors proposed two conditions for this adverse effect. First, the phenomenon of an opposing effect, which is most likely found in a continuous crystallisation process. If an admixture is a very strong inhibitor for nucleation and growth, there will be an accumulation of supersaturation up to a point where an "outburst" of nuclei occurs which is then followed by desupersaturation. Second, at low concentrations, adsorption of a very strong inhibitive admixture onto the surface of crystals and nuclei will be observable. However, the crystallisation process itself will only start after being simulated by the presence of higher admixture levels where the admixture act as template for nucleation. Besides gypsum crystallisation system as investigated by van der Leeden and van Rosmalen (van der Leeden and van Rosmalen 1987), other systems which

are known to undergo adverse effect are the crystallisation of lead nitrate in the presence of methylene blue (Blitznakov, 1965, as quoted in Industrial Crystallization and Precipitation Workshop, Curtin University of Technology, Perth, Australia, 1998), and calcium oxalate monohydrate in the presence of L-glutamic acid (DeLong and Briedis 1985).

2.4. Previous Studies on the Effects of Admixtures on Gypsum Crystallisation

Klepetsanis and Koutsoukos (Klepetsanis and Koutsoukos 1998) in their study on the effect of organophosphorus compounds on the kinetics of gypsum crystallisation showed that the effectiveness of inhibitors in suppressing crystal growth can be related to the morphology of the crystals. They found that the intensity of adsorption of inhibitors on different faces of a crystal varies, thus resulting in a change of the crystal morphology. This finding indicates that preferential poisoning of active growth sites on crystal surface by ionised organophosphorus compounds must have occurred.

An investigation of the factors which affect the growth rates of the habit faces of gypsum revealed that the phenomenon of preferential adsorption can be interpreted with reference to the charge of the ions forming the crystal lattice (Edinger 1973). As an example, the (111) face of gypsum crystals consists of Ca^{2+}, and hence, should offer favourable sites for anionic species. Accordingly, if the face consists of both anionic and cationic species, the adsorption phenomenon will be dictated by the competition of the strength of the two species.

Sarig *et al.* found that PGA (= polyglutamic acid) strongly retarded gypsum precipitation from seawater (Sarig *et al.* 1975). Moreover, the habit of gypsum was also significantly changed. One of the main factors to evaluate the retardation efficiency of an inhibitor is by looking at the relationship between the lattice of the crystals and the molecular structure of the admixtures or inhibitors (Davey 1979). Sarig *et al.* (Sarig *et al.* 1975) also found that the effect of PVS (= polyvinyl sulfonate) on the crystallisation of gypsum was less significant than that of PGA.

The PVS only coarsened the faces of the crystals but was unable to change the morphology. The difference in effect between the PVS and PGA on gypsum is caused by the difference in their molecular structures or their functional groups. The sulfonic groups in PVS are closer to each other than that of the carboxylic groups in PGA. In addition the distance between the carboxylic groups in PGA, i.e. 8 Å is almost the same as the distance between Ca ions in $CaSO_4.2H_2O$, which is 8.1 Å. Therefore, the effect is mainly caused by the structural compatibility between PGA and $CaSO_4.2H_2O$. In other words, if inhibitors are structurally well fitted to the crystal lattice of the precipitating crystals, those inhibitors can be the most efficient growth retarders.

The effect of low molecular weight polyacrylates (molecular weight between 710 and 12,800) on growth of gypsum was studied by Amjad and Masler using the highly reproducible seeded growth technique (Amjad and Masler 1985). The result of their study showed that increasing the amount of seeds will result in the proportional increase of crystallisation rate indicating that the crystallisation process proceeded without the occurrence of secondary nucleation or spontaneous precipitation. The slurry density in the crystalliser they used, however, was not mentioned so that it cannot be ascertained whether attrition of crystals had occurred to influence the crystallisation rate. Their study did not include characterisation of the crystals so that the effect of the admixtures on the crystal habit or CSD was not known. In fact, they only studied the effect of the admixtures on crystal growth by comparing the length of induction period relative to the amount of the admixtures used. Molecular weight (MW) and concentrations of polyacrylates within the range used in their study (MW: 710 – 12,800, concentrations: 0.00 – 0.25 ppm) did not affect the crystallisation rate but only affected the induction period. The higher the concentration of polyacrylates the longer the induction period, which suggested that the polyacrylates incorporated into the growing gypsum crystals.

Hamdona *et al.* (Hamdona *et al.* 1993) in their recent work on unseeded crystallisation of gypsum compared the inhibitory performance of organophosphorus compounds and metal ions. It was discovered that the organophosphorus compounds were able to completely stop the growth of the crystals while for the metallic ions a complete inhibition was not possible. Although the specific type of the

organophosphorus species was not mentioned, it could be postulated in this case that the organic chains had acted as a "fence" so that the advancing growth of the crystals was more effectively blocked. These researchers also discussed the effectiveness of exceedingly low concentrations of admixtures on crystal growth. It was found that even traces of ion-exchange resins used to prepare the de-ionised water for the crystallising solution hindered the crystal growth, which pointed to the preferential blocking of active growth sites on the crystal surface. It was also interesting to note, however, that agitation speed, which they applied up to 300 rpm, did not have any effect on the crystallisation rate. It can be postulated therefore that their unseeded growth experiment was not a diffusion controlled crystallisation system.

Al-Sabbagh *et al.* (Al-Sabbagh *et al.* 1996) studied the effect of different defoaming agents on the habit and filterability of gypsum crystals. The habit of gypsum was observed to change from needle-like to compact. The study showed that habit modification was influenced by the functional groups adsorbed on specific surface of crystals. The concentrations of the admixtures used were relatively high: 100 ppm. It was found that esterified citric acid was successful to be used as admixtures. This is due to the carboxylate groups (COO-), which have distances of 3.5 Å which is very similar to the distance between Ca ions in (111) face of gypsum. Face (111) experienced a reduction in growth rate. The experiment was done in an unseeded batch crystalliser with level of concentration of about 1,600 ppm of Ca^{2+}. The batch crystallisation experiment exhibited no induction period. It was found that the functional group COO- was the active functional group. This was shown by an increase in the filtration time when citric acid was used instead of esterified citric acid. As is known, citric acid ($(C_3H_4(OH)(CO_2H)_3$) has three COO- while esterified citric acid has only two because one group was esterified (esterified citric acid was used as defoaming agents). It was discovered that if citric acid was used, the filtration time was shorter due to the change in habit from needle-like to compact or stumpy. The habit change was also evident from a microscopic examination. At pH ≤ 2 there was no habit change due to complete protonated citric acid ($C_6H_8O_7$). At pH values between 2 and 6, higher concentration was required because citric acid was dissociated only between 20 to 50 %. At pH values ≥ 6 citric acid was an optimal agent for habit change due to complete dissociation. Fully dissociated citric

acid yields free COO- which are active as crystal modifiers by incorporation onto the crystal surface.

Weijnen and van Rosmalen (Weijnen and van Rosmalen 1985) investigated the growth kinetics of gypsum using the seeded growth technique where the seed crystals were very small in size to simulate the condition in scale formation. They studied six different polyelectrolytes at concentrations between 0.02 and 2.00 ppm. These researchers found that the effectiveness of a polyelectrolyte type growth inhibitor depends on the pH of the crystallising solution. It was concluded that the pH values must be such that a sufficiently anionic charge density exists, so as to promote a strong electrostatic interaction between the inhibitor and the crystal surface. Stronger interaction leads to stronger attachment of inhibitor to the surface of the crystals, which leads to effective growth retardation.

He, Oddo and Tomson (He *et al.* 1994) studied the growth rate of calcium sulphate dihydrate in a 500 ml jacketed pyrex glass reactor using the seeded growth technique. They found that there was no induction period preceding the growth, and that the crystals started growing, once they were added into the crystallising solution. Their work showed that the rate of growth was a linear function of seed concentration (seed concentrations used were from 0.20 to 4.00 grams per litre) indicating that the only reaction occurred was that on the surface of the seed crystals. The high activation energy found confirmed that surface reaction was indeed the rate-determining step. Their study showed that the ionic strength of the crystallising solution was an important factor for crystal growth rate.

Another work of Weijnen and van Rosmalen (Weijnen and van Rosmalen 1984) investigated the effect of Cu^{2+} and Zn^{2+} on the growth rate of gypsum where the Cu^{2+} and Zn^{2+} were derived from their sulphate salts. They observed that as much as 100 ppm of SO_4^{2-}originated from the copper and zinc sulphate salts added into the solution did not alter the ionic strength, and thus the gypsum solubility was the same as that of pure solutions. Higher charge densities of Cu^{2+} and Zn^{2+} than that of Ca^{2+} was assumed to result in the enhanced growth rate of the gypsum crystals.

Admixtures are generally preferentially adsorbed on certain crystal faces so that the growth of those faces is altered. The adsorption of admixtures upon crystal surfaces is also influenced by the charge, the steric arrangement of the admixtures molecules, the dipole moment as well as the electric field on the crystal surface. The influence of the charge of the admixtures can be shown by comparison between the rate of incorporation of Cd^{2+} and that of Al^{3+} into gypsum crystals (Witkamp and van Rosmalen 1987). Witkamp and van Rosmalen found that the uptake of Cd^{2+} takes place through an isomorphous substitution of Ca ions in the crystal structure. The process of substitution is made possible by the similarity between the ionic radii of Cd^{2+} and Ca^{2+}. These two metallic ions have very similar radii of 1.10 and 1.12 Å respectively (Lide 1999). The uptake of Al^{3+}, however, is difficult because its ionic radius is only about half that of Ca^{2+}. The difficulty in incorporation can also be explained by the fact that the charge of 3+ in Al ions needs compensation.

The influence of sodium chloride on the growth rate of gypsum is also positive, that is, the higher the NaCl concentrations the higher the growth rates (Brandse and van Rosmalen 1977). Their experimental data did not accurately fit the second order growth kinetics, which is generally used as the empirical equation for gypsum crystallisation system. The equation is of the form,

$$-\frac{dC}{dt} = kS(C - C_s)^n \qquad (2.21)$$

where,

-dC/dt = growth rate, g/min

k = growth rate constant, $(L^2)/(g)(min)$ (for n = 2)

S = number of growing sites, dimensionless

C = solution concentration, g/L

C_s = saturation concentration at particular ionic strength, g/L

n = growth order, dimensionless.

A better fit would be obtained if correction were made on factor **S**, which is the number of growing sites. As the crystals grow the total surface area increases so does the number of growing sites. Hence, correction should be made by relating **S** to

the increase in total surface area. Furthermore, the experimental data showed that the relative increase in growth rate is not directly proportional to the relative increase of calcium ions in the solution. This could be due to the interaction of the Na^+ and or Cl^- with Ca^{2+} in the solution, which results in alteration of the activities of these ions (Shinoda 1978).

Tadros and Mayes (Tadros and Mayes 1979) microscopically studied the linear growth rate of gypsum under the influence of carboxylic and phosphonic acid derivatives. They found that reaction crystallisation of calcium sulphate dihydrate from its pure components yielded crystals of varying sizes, ranging from subsieve size of about 5 μm to 200 μm and that the crystals were either needle- or plate-like. Adding admixtures to the reaction, however, caused the crystals produced to become uniform in size as well as in shape. It was thus concluded that admixtures influence the crystal habit and morphology. Tadros and Mayes also observed that inhibition of growth on different crystal faces was selective. Retardation was observed on the (111) face whereas the (110) face was enhanced. The work of Tadros and Mayes showed that crystal habit modification occurs due to the correspondence between ion spacing within certain crystal planes and configuration of the C chains of the adsorbed admixtures. For example, the distance from Ca^{2+} - to - Ca^{2+} at the (111) face = 3.7 Å whereas the distance between C atoms in carboxylic groups = 3.5 Å. Thus, the two distances are quite similar which consequently enable the carboxylic groups to replace the Ca^{2+}.

A seeded growth method was used by Amjad (Amjad 1988) to investigate the kinetics of gypsum growth in the presence of polymers as admixtures. It was found that the crystallisation rate, **k**, was directly proportional to the amount of seed crystals added initially into the crystalliser, thus it can be concluded that the growth occurred on the added seeds only. Amjad used slurry densities between 1.30 and 2.10 g/L but the stirring rate was not mentioned. It should be assumed therefore that the speed of stirring must be low enough so as not to cause crystal attrition. Amjad showed that trace amounts of polymers having carboxyl groups (-COOH) were an effective growth inhibitor. The same findings were obtained by Smith and Alexander (Smith and Alexander 1970) in their investigation on the effect of admixtures on the crystallisation process of calcium sulphate dihydrate. The

effectiveness of the carboxyl containing polymers as gypsum growth retarder was assumed to be due to the highly anionic nature of carboxyl groups, which has the ability to preferentially adsorb on the active growth sites of the crystal surfaces. Smith and Alexander made this assumption as they discovered that cationic charged polymers were not effective as inhibitors. The preferential adsorption of carboxyl groups on the crystal surface was later assumed to be due to complexation reaction with the Ca^{2+}in the crystal lattice (Weijnen and van Rosmalen 1984).

Preferential adsorption of admixtures onto the crystal surface was also found in the study of crystal growth of gypsum in the presence of phosphonates carried out by Liu and Nancollas (Liu and Nancollas 1973). Their study showed that in the presence of phosphonates, the habit of gypsum crystal was modified and that the lower the admixture concentration the more pronounced the modification. Hence it could be advanced that certain faces of gypsum crystals must have been favoured by admixture attachment. When the number of the admixture molecules in the solution increases due to higher concentration, however, all surfaces could be covered so that retardation of growth for those surfaces was the same. As a result, the morphology might be changed but the habit was retained.

It appears from the literature review that the effects of admixtures on the crystallisation of calcium sulphate dihydrate or gypsum are dependent on specific solvent-solute systems and accordingly different researchers have advanced a variety of explanations. All the explanations put forward suggest, that the effects of admixtures already materialise even if they are present in minor amount in the crystallising system. Another important aspect that has to be considered in studying the effects of admixtures is the characteristics of the crystal surface.

2.5. Batch and Continuous Crystallisation

One of the considerations in a crystallisation operation is whether the operation should be carried out in a batch or continuous mode (Jancic and Grootscholten 1984; Myerson 1993; Nyvlt 1992). In addition, there is also the operation, which is done with a mode somewhere between batch and continuous: semicontinuous. In this case

the product withdrawal is either batch wise or periodically (Nyvlt 1992). The batch mode is usually chosen for the following features.

1. Production rates are small so that a series of continuous crystallisers and other processing equipment is not economically feasible.

2. Materials to crystallise are very expensive, such as pharmaceutical or fine chemicals. Using batch mode with small production capacity enables the inventory management (material losses etc.) to be more accurate and reliable.

3. The crystallisation operation uses only simple instrumentation and operation. For some batch crystallisations, the operation can be left unattended if necessary, which is advantageous for small producers who cannot meet the high demand for labour force in terms of qualification as well as quantity.

4. The crystallising materials are prone to form scaling both on the walls of the crystallisers as well as of the related equipment. With batch crystallisers the scale can be removed after each batch cycle.

5. The crystallising materials have slow growth rate and there is no need for product classification or when a slight change in product quality, which often occurs from one batch to the next, is allowable.

6. When a relatively large plant site is available.

Briefly, the choice of conducting the crystallisation operation in either batch or continuous is mainly governed by both technical and economic considerations. All conditions contrary to the features described previously are clearly favourable for continuous operations.

Whether the operation is done in a batch or continuous mode, a precisely uniform product size is impossible to obtain. Instead, the crystals produced have range of sizes or that the crystals have size distribution. The following section discusses

characterisation of the crystalline product, which is usually carried out with respect to either size or shape.

2.6. Crystal Size Distribution (CSD)

Crystalline product obtained from a crystallisation process can be characterised with respect to size and shape and it is always found that the crystals vary in size and that no two individual crystals have perfectly identical shape. Therefore one of the main characteristics of crystalline product is the distribution of sizes or the Crystal Size Distribution (CSD). For non-crystalline or agglomerated product the CSD is termed particle size distribution or PSD. In addition, the shape of the crystals is also an important characteristic.

CSD is best presented graphically in some type of **X-Y** plot, where the **X**-axis represents the crystal size and the **Y**-axis the amount of crystals, respectively. In addition, the crystals should have unit size, which is representative of their shape. For example, if the crystals are spherical, it is logical to represent the size as the crystal diameter. For other shapes, a characteristic dimension of the crystals is used. This means that the shape of the crystals is "converted" to be equivalent to a certain shape such as a sphere. In this study the unit size of the crystals is calculated as the sphere equivalent diameter. Similarly, for the **Y** or the vertical axis which represents the "amount" of the crystals, several types of units can be used, for example, surface area, volume, number or mass.

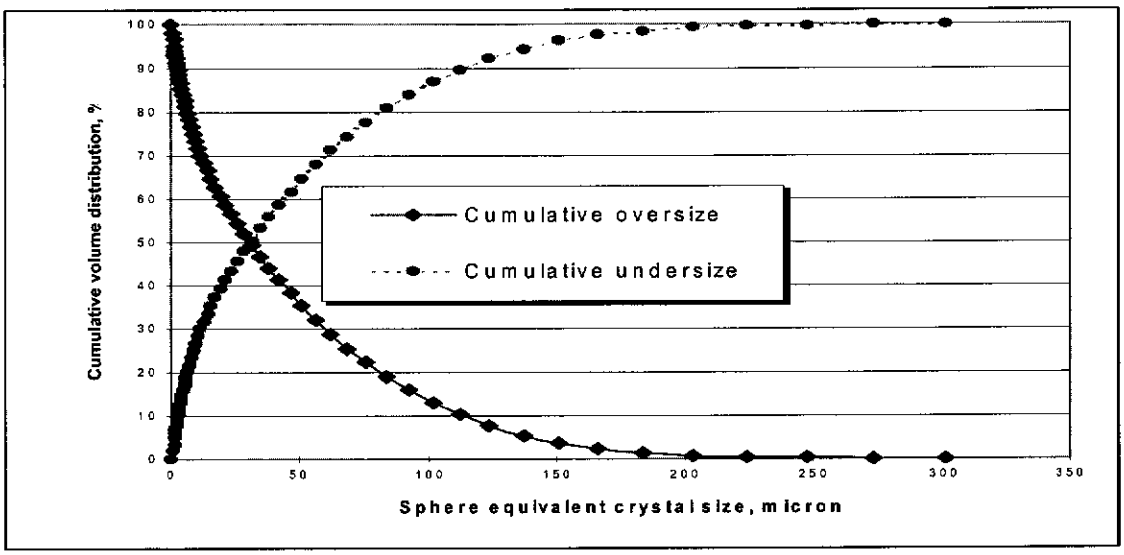

Figure 2.9 A typical cumulative distribution plot obtained from an MSMPR

There are two common types of graphs to represent the distribution: histogram and cumulative graphs. The histogram shows the number or mass of crystals which falls within each size range. The cumulative plot, on the other hand, depicts the number or mass of crystals above or below a certain size. **Figure 2.9** is an example of the cumulative plot obtained from a mixed-suspension-mixed-product-removal (= MSMPR) crystalliser. The figure shows two curves: cumulative oversize and cumulative undersize. Cumulative oversize curve shows the fractions of the crystals above or larger than a particular size. On the other hand, the cumulative undersize curve illustrates the fraction of the crystals, which is below or smaller than a particular size.

Another way of presenting the CSD is through the use of a crystal population density plot as depicted in **Figure 2.10**, which shows the number of crystals of a given size in a given volume.

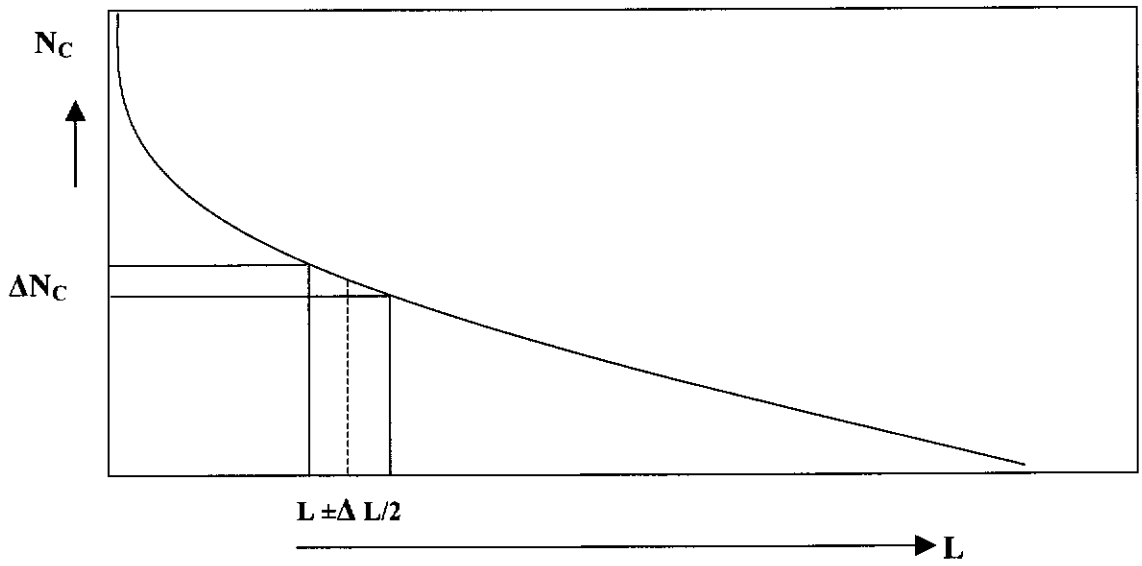

Figure 2.10 Schematic representation of CSD in a population density plot

The number of crystals in the size interval L ± ΔL/2 is equal to ΔN_c. For a sufficiently narrow interval the limit value can be applied, thus

$$\lim_{\Delta \to 0} \frac{\Delta N}{\Delta L} = n(L) \qquad (2.22)$$

where **n(L)** is the population density of crystals of size **L**. Again for a sufficiently narrow interval, the curve in **Figure 2.10** can be assumed as a straight line, thus **n(L)** equals to the slope of the line.

2.7. Population Balance Equation (PBE)

A complete crystallisation process requires three types of conservation laws. Firstly, the material balances, to calculate, for example, the yield or production rate. Secondly, the enthalpy balance to calculate energy requirement. Thirdly, the population balance to calculate the crystal size distribution (CSD). Clearly, the third balance is unique to crystallisation and other particulate processes. PBE relates how the distribution of crystals with regard to size develops over time under certain crystallisation parameters. The parameters may include supersaturation of the solution, crystallisation temperature, residence time, chemical composition of the solution etc.

Briefly, PBE serves two purposes. Firstly, if a set of crystallisation operating conditions was applied and under which an experimental CSD was obtained, then a set of parameters describing the kinetic of the crystallisation process can be estimated. Secondly, (which is the reverse of the first purpose) given a set of equations describing certain kinetics of the crystallisation process, the desired CSD can be estimated. Thus, PBE is obviously a useful tool in crystallisation process. It was developed by Randolph and Larson (Randolph and Larson 1988) and is a well-established technique to derive crystallisation kinetics and is especially useful because of its capability to determine both nucleation and growth rates simultaneously. The following section on **Continuous Crystallisers** illustrates the power of PBE in extracting the crystallisation kinetics.

2.8. Continuous Crystallisers

The concept of PBE assumes that the crystalliser feed stream contains no crystals. Thus, the concept applies to unseeded MSMPR. In this study, addition of seed crystals is necessary to enhance the crystallisation kinetics, namely the nucleation and growth rates. To accommodate the seeded conditions, a new concept based on that of Randolph and Larson was developed for the MSMPR system (Chan 1997). The concept was adopted for this work and was based on the following assumptions.

1. The system operates in a continuous steady state condition.

2. The volume of the crystalliser is constant.

3. The birth of crystals is through nucleation only; there is no effect of attrition and agglomeration.

4. Both solid and liquid phases have identical residence times.

The work of Chan (Chan 1997) for the steady state population balance for a seeded MSMPR crystalliser is given as follows.

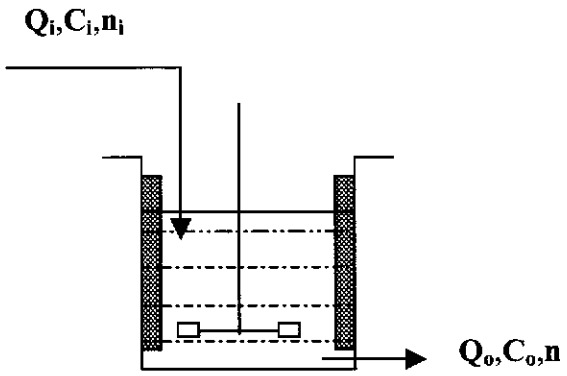

Figure 2.11 Schematic representation of a continuous (MSMPR) crystalliser

It was assumed that in a crystalliser with volume, **V**, there are crystals with arbitrary sizes of L_1 and L_2, with population density, n_1 and n_2, and with growth rates, G_1 and G_2.

The number of crystals entering the range L_1 and L_2 with incremental time Δt, because of growth is:

$$V\, n_1\, G_1\, \Delta t \tag{2.23}$$

The number of crystals exiting the system in the range L_1 and L_2 with incremental time Δt, because of growth is:

$$V\, n_2\, G_2\, \Delta t \tag{2.24}$$

Because the feed stream contains seed crystals in the range L_1 and L_2, the input into the distribution in the volume **V**, becomes,

$$Q_i\ \bar{n}_i\, \Delta L\, \Delta t \tag{2.25}$$

where,

Q_i = volumetric flow rate, L/min

$\bar{n}_i$ = average population density of the seeds in the range L_1 to L_2 in the feed,

(μm^{-1}. litre crystalliser suspension^{-1})

ΔL = $(L_1 - L_2)$, μm

Δt = time increment, min.

In the same manner, the number of crystals exiting the system is,

$$Q\ \bar{n}\ \Delta L\ \Delta t \tag{2.26}$$

where

Q = Qi = volumetric flow rate, L/min

$\bar{n}$ = average population balance of product crystals,

(μm^{-1}. litre crystalliser suspension^{-1})

At steady state condition of solid phase, it is safe to assume that the input to size range **ΔL** = the output from size range **ΔL**.

Then, by combining **Eqs.(2.23)** to **(2.26)**

$$V\ n_1\ G_1\ \Delta t + Q_i\ \bar{n}i\ \Delta L\ \Delta t = V\ n_2\ G_2\ \Delta t + Q\ \bar{n}\ \Delta L\ \Delta t \tag{2.27}$$

or,

$$V(G_2\ n_2 - G_1\ n_1) = (Q_i\ \bar{n}_i - Q\ \bar{n})\ \Delta L \tag{2.28}.$$

As **ΔL** approaches zero, average values of "**n**" become point values, therefore,

$$V\frac{d(Gn)}{dL} = Q_i n_i - Qn \tag{2.29}$$

An MSMPR crystalliser at steady state would result that inlet flow rate, $\mathbf{Q_i}$ = outlet flow rate, **Q**. Thus $\mathbf{Q_i} = \mathbf{Q}$.

Therefore, **Eq. (2.29)** becomes

$$V\frac{d(Gn)}{dL} = Q_i(n_i - n) \tag{2.30}$$

or,

$$\frac{V}{Q}\frac{d(Gn)}{dL} = Q_i(n_i - n) \tag{2.31}$$

Meanwhile, the mean residence time of the system is **τ**, where:

$$\tau = \frac{V}{Q}$$

Therefore, **Eq.(2.31)** becomes,

$$\tau\frac{d(Gn)}{dL} = n_i - n \tag{2.32}$$

Integration of **Eq. (2.32)** yields,

$$n - n_i = (n^0)e^{-(\frac{L}{\tau G})} \tag{2.33}$$

where,

L = characteristic crystal size, (μm)

n = population density, (μm^{-1}. litre crystalliser suspension^{-1})

G = linear crystal growth rate, (μm. hour^{-1})

τ = mean crystalliser system residence time, (hour)

n^0 = nuclei population density, (μm^{-1}. litre crystalliser suspension^{-1})

n_i = inlet seed population density, (μm^{-1}. litre crystalliser suspension^{-1}).

2.9. Nucleation Rate

In an ideal MSMPR crystallisation system the plot of population density, **Ln n**, versus crystal size, **L**, results in a straight line as shown in **Figure 2.12**.

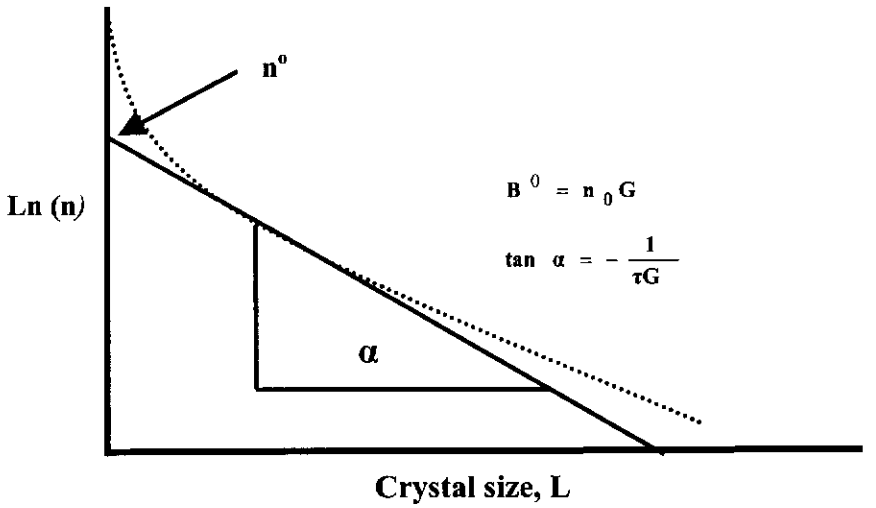

Figure 2.12 A typical semi-log plot of population density, Ln n, vs.crystal size

The slope and intercept of this straight line determine the growth rate, **G**, and the population density at zero size, $\mathbf{n^0}$. Then, the nucleation rate is calculated from the following equation.

$$B^0 = n^0 G \tag{2.34}$$

where,

B^0 = nucleation rate, (no.of nuclei)/(m^3 hour)

n^0 = population density at zero size

= number of nuclei at zero size, (no.of nuclei)/(micron m^3)

G = linear growth rate, micron/hour.

Some crystal systems, however, show deviations from the above expressions, especially at small crystal size regions. Instead of a linear relationship between **Ln n** and **L**, a distinct upward curvature occurs as shown by the dotted line in **Figure 2.12**, usually at sizes below about 20 micron (Jancic and Grootscholten 1984). In some other systems, the curved lines could begin to show at sizes below as large as 40 micron (Hartel *et al.* 1980; Sikdar and Randolph 1976), or even 100 micron (Liang and Hartel 1991). In such cases, therefore, the McCabe's ΔL law, where the growth rate, **G**, is not a function of crystal size, **L**, does not hold. If such deviations occur, a calculation procedure for crystallisation kinetics determination as proposed by Garside and Jancic (Garside and Jancic 1976; Garside and Jancic 1978) and Jancic

and Grootscholten (Jancic and Grootscholten 1984) is usually employed. The procedure was developed due to limitations imposed by particle sizing instruments, so that nucleation rate calculation has to resort to a particular technique, depending on the range of particle size data available (Jancic and Grootscholten 1984). As shown by Jancic and Grootscholten (previous citation) the population balance analysis is almost always subjected to a situation where data for a certain part of the particle size distribution, usually the small size region, is not available. As can be seen from **Figure 2.12**, it is possible to draw several different straight lines through the small size region of the plotted experimental data. Hence, nucleation and growth rate values may vary depending on the slope and intercept of the particular straight line chosen. This arbitrary choice is evidently one of several possible reasons why the resulting kinetics of one crystallising system can be different even when the same experimental conditions are carefully applied.

Obviously, for such a case where a curved line occurs, the slope of the line no longer has a single value and the intercept of it must accordingly be determined. Undoubtedly, the most appropriate intercept is one that sufficiently covers the smallest crystal size down to which the size analysis is performed. In this study, the technique for choosing a suitable intercept as proposed by Jancic and Grootscholten was adopted (Jancic and Grootscholten 1984). A linear regression through five smallest data points, which were obtained from CSD measurements, was carried out and the resulting equation yielded the slope and intercept of a straight line. The nucleation rate was then calculated using the obtained slope and intercept.

The experimental data obtained in the present study show a very sharp increase in the small size portion when plotted on a population density chart. Therefore, as suggested by Jancic and Grootscholten (previous citation), the smallest crystal size able to be detected by the particle analysis instrument was chosen. In fact, when dealing with crystals of microscopic sizes, an effective nucleation rate is generally used (Meadhra *et al.* 1996; Rusli *et al.* 1980). As the analytical instrument used in this study (= Malvern MasterSizer) is able to detect the smallest size as low as 1.18 micron, it was decided to select the five smallest crystal sizes: 1.18, 1.35, 1.55, 1.78, and 2.05 microns consecutively, for the nucleation rate determination.

2.10. Growth Rate

2.10.1. Mass growth rate

The mass growth rate is defined as the amount of mass of crystals deposited per unit surface area of seed crystals over a certain period of time (Witkamp *et al.* 1990). The mass growth rate is also termed the mass deposition rate. For MSMPR crystallisers it is usually measured over one residence time, because at steady state the crystals remain within the crystalliser over a period of one residence time. The following equation is used to determine the mass growth rate .

$$R_G = \frac{1}{A}\frac{dW}{dt} \tag{2.35}$$

where,

R_G = mass growth rate, (g)/(m^2)(hour)

A = sum of surface area of seeds + sum of surface area of product, m^2

dW/dt = differential rate of growth, (g)/(hour)

where,

dW = mass deposited or yield, gram

dt = residence time, hour.

Sum of surface area, A is calculated as,

$$A = n_i f_i L^2 \tag{2.36}$$

where,

n_i = population density, no./μm. litre

f_i = shape factor, dimensionless

L = characteristic crystal size, μm.

2.10.2. Linear growth rate

Another way to characterise the growth rate of crystals is to measure their linear dimension, and hence the term linear growth rate.

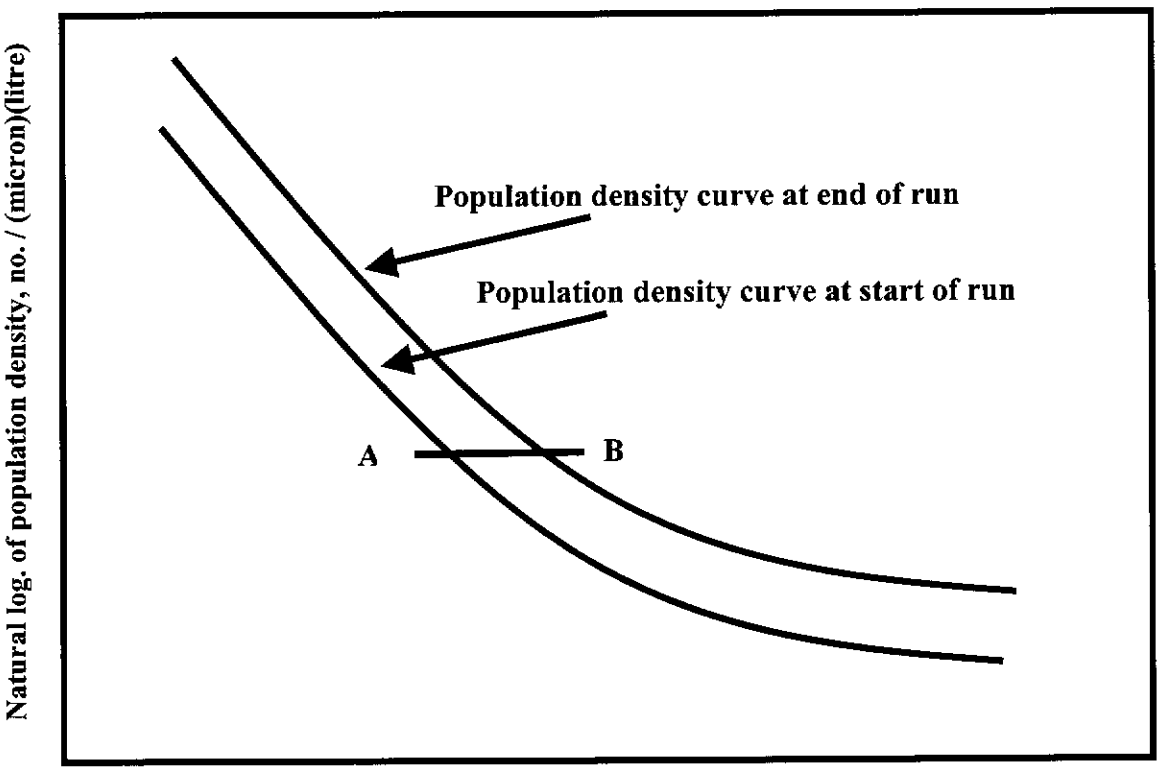

Figure 2.13 A typical linear growth rate calculation plot

The procedure is illustrated in **Figure 2.13** and is carried out by measuring the change of the characteristic dimension such as the crystal length with time. The distance between the two curves in **Figure 2.13**, as shown by the horizontal line **A-B**, is regarded as the linear growth rate of the crystals. It is important to note that for accurate results, the measurement should be made at points where the two curves are as closely parallel to each other as possible.

In a seeded MSMPR experiment by Chan (Chan 1997), the linear growth rate was evaluated by measuring the average distance between particle size distribution curve of seeds, which is at the beginning of the experimental run, and that at the end of the run when the steady state has been achieved. The procedure was adopted in this present study. Typical curves for the determination of the linear growth rate are

shown in **Figure 2.14**, which was taken from an experimental run with no admixtures and 15-minute residence time.

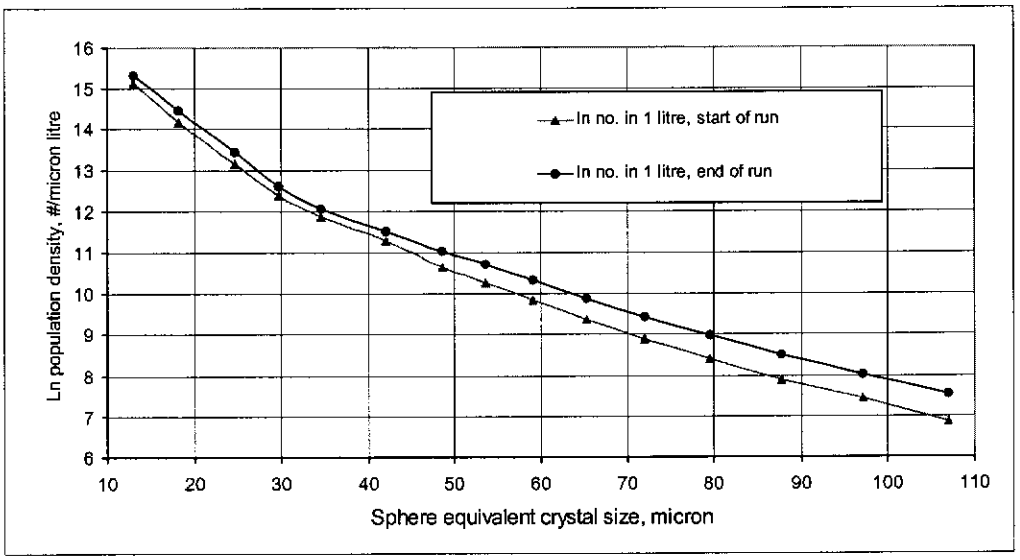

Figure 2.14 A typical population density plot for growth rate calculation

2.11. Yield

As crystallisation proceeds, concentration of the crystallising ions in the solution decreases to form crystals as solid phase. Yield, which is defined as the amount of crystal mass produced over a certain period of crystallisation run, can therefore be determined by calculating the difference between the initial and final concentrations of the crystallising ions. For gypsum crystallisation carried out in this study, this means to calculate the difference in Ca^{2+} concentrations at the beginning and the end of the crystallisation run. For MSMPR crystallisers the decrease in concentration can also be determined as the difference between the initial concentration and that at steady state, where the concentration has reached a constant value.

Summary

The literature review reveals the following features.

Crystallisation is a complex process. The properties of a crystallising solution are the decisive factors to influence the end product because the formation of a crystal

embryo or nucleation and its subsequent growth into a crystalline product are heavily dependent on such properties, particularly the level of supersaturation. The existing knowledge about nucleation is extensive and the origin of nucleation is two fold. Firstly, it originates from the dissolved solutes, which is described as true nucleation. Secondly, the origin can be the materials already undergoing the process of crystallisation but have not yet achieved their final form; hence the name is apparent nucleation. The growth of crystals is significantly influenced by the characteristics of the crystal surfaces.

It is almost impossible for a crystallisation process to proceed in a condition which is free from the presence of admixtures and that a minute amount of admixtures could have a very significant effect on crystallisation and its subsequent handling of the crystal products. The literature review also reveals that as yet there is no general conclusion or a systematic theory regarding the effect of admixtures on crystallisation. The effect is unique to crystallisation system under consideration.

Gypsum crystallisation is generally regarded as an unwanted phenomenon, due to its contribution to the scale formation, which is one of the persistent problems in many industries. Studies on the crystallisation of gypsum in the presence of admixtures are extensive, but general conclusions are yet widely varied.

MSMPR studies are regarded as a highly reliable and established technique to extract crystallisation kinetics such as nucleation and growth rates. However, in an MSMPR crystalliser, the crystallisation time is not an independent variable, so that it must first be selected. The selection can be carried out by examining the performance of a batch crystalliser.

Crystals are produced with varying sizes so that distribution of crystals with regard to their size, which is known as Crystal Size Distribution (CSD) is one of the main characterisation of crystals. The quality of a crystalline product is frequently related to its CSD.

CSD data of a crystallisation process is needed in order to extract the crystallisation kinetics, mainly, nucleation and growth rates, and this extraction is made possible through the utilisation of a Population Balance Equation (PBE). A Population Balance Equation is essentially a discreet accounting of crystal product, and

therefore it can also be applied to any particulate processes. While the PBE was originally developed for the unseeded MSMPR, it was later developed to cover the seeded MSMPR.

Calculation of nucleation and growth rates can be carried out in a number of ways depending on the characteristics of the CSD.

Crystallisation of gypsum is closely related to scale formation due to the following reasons. First, gypsum is crystalline matter formed through a crystallisation process. Second, one of the main components of the scale was frequently found to be gypsum. In the process of crystallisation, admixture effects cannot be overlooked since most crystallisation takes place in the presence of admixtures. A unified theory on the effects of admixtures on crystallisation of gypsum is as yet unavailable. Hence, it was felt that the crystallisation of gypsum in the presence of admixtures carried out in this study would add to the existing knowledge. The study was carried out in a continuous (MSMPR) crystalliser using three different admixtures: Fe^{3+} and Zn^{2+} (in their sulphate salts), and sodium isopropyl xanthate (SIPX) and their combinations. There were several reasons for the choice of the crystallising system. First, crystallisation process in an MSMPR can achieve steady state; hence extraction of experimental crystallisation kinetics under steady state condition is possible. Second, the Department of Chemical Engineering at Curtin University of Technology has been and is actively involved in assisting mineral processing industry to alleviate the burden of scaling problem with particular emphasis on gypsum scaling. Third, the flotation water in one of the mineral processing plants with which the Department of Chemical Engineering associates, was found to contain a significant amount of metallic ions: Fe^{3+} and Zn^{2+}.

Fourth, the use of sodium isopropyl xanthate (SIPX) as a flotation agent is widely recognised and it is one of the flotation agents used in the above-mentioned mineral processing plant.

The next chapter (Literature Review - Part 2: Gypsum Scaling: Effect of Admixtures on Gypsum Crystallisation Kinetics) discusses the scaling of gypsum, since gypsum is one of the main components of scale formed in many industries. Some researchers studied the crystallisation of gypsum with specific aim to reveal the phenomenon of

scaling and thereafter to develop methods to control its formation. Their studies were either carried out using a laboratory beaker test, crystallisers or piping system.

Bibliography

1. Jancic, S. J. and Grootscholten, P. A. M. (1984) *Industrial Crystallization,* Delft University Press and Reidel Publishing, Dordrecht, etc.
2. Mersmann, A. (1995) *Crystallization Technology Handbook*, Marcel Dekker, New York, etc.
3. Nyvlt et.al, (1985), The Kinetics of Industrial Crystallisation, Elsevier, Amsterdam, etc.
4. Myerson, A. S. (1993) Handbook of Industrial Crystallization, Butterworth-Heinemann, Boston, etc.
5. Ohara, M. and Reid, R. C. (1973) Modeling Crystal Growth Rates from Solution, Prentice-Hall, Englewood Cliffs, N.J.
6. Nyvlt, J., (1992) Design of Crystallizers, CRC Press, Boca Raton, USA.

References

1. Adams, J. F., and Papangelakis, V. G. (2000). "Gypsum Scale Formation in Continuous Neutralization Reactors." *Canadian Metallurgical Quarterly*, 39(4), 421-432.
2. Al-Sabbagh, A., Widua, J., and Offermann, H. (1996). "Influence of different admixtures on the crystallization of calcium sulfate crystals." *Chemical Engineering Communications*, 154, 133-145.
3. Amjad, Z. (1985). "Applications of Antiscalants to Control Calcium Sulfate Scaling in Reverse Osmosis Systems." *Desalination*, 54, 263-276.
4. Amjad, Z. (1988). "Kinetics of crystal growth of calcium sulfate dihydrate. The influence of polymer composition, molecular weight, and solution pH." *Canadian Journal of Chemistry*, 66, 1529-1536.
5. Amjad, Z., and Hooley, J. (1986). "Influence of Polyelectrolytes on the Crystal Growth of Calcium Sulfate Dihydrate." *Journal of Colloid and Interface Science*, 111(2), 496-503.

6. Amjad, Z., and Masler, W. F. (1985). "The inhibition of calcium sulfate dihydrate crystal growth by polyacrylates and the influence of molecular weight." *Corrosion 85*, Houston,TX.
7. Bansal, B., and Muller-Steinhagen, H. (1993). "Crystallization Fouling in Plate Heat Exchangers." *Journal of Heat Transfer*, 115(August), 584-591.
8. Bansal, B., Muller-Steinhagen, H., and Chen, X. D. (1997). "Effect of Suspended Particles on Crystallization Fouling in Plate Heat Exchangers." *Journal of Heat Transfer*, 119(August), 568-574.
9. Bansal, B., Muller-Steinhagen, H., and Chen, X. D. (2000). "Performance of plate heat exchangers during calcium sulphate fouling - investigation with an in-line filter." *Chemical Engineering and Processing*, 39, 507-519.
10. Bott, T. R. (1995). *Fouling of Heat Exchangers*, Elsevier, Amsterdam, New York.
11. Brandse, W. P., and van Rosmalen, G. M. (1977). "The influence of sodium chloride on the crystallization rate of gypsum." *Journal of Inorganic and Nuclear Chemistry*, 39, 2007-2010.
12. Budz, J., Jones, A. G., and Mullin, J. W. (1986). "Effect of Selected Impurities on the Continuous Precipitation of Calcium Sulphate (Gypsum)." *Journal of Chemical Technology and Biotechnology*, 36, 153-161.
13. Chamra, L. M., and Webb, R. L. (1994). "Modelling Liquid-side Particulate Fouling in Enhanced Tubes." *International Journal of Heat and Mass Transfer*, 37(4), 571-579.
14. Chan, V. A. (1997). "The Role of Impurities in the Continuous Precipitation of Aluminium Hydroxide," PhD thesis, Curtin University of Technology, Perth, Western Australia.
15. Christoffersen, M. R., Christoffersen, J., Weijnen, M. P. C., and van Rosmalen, G. M. (1982). "Crystal Growth of Calcium Sulphate Dihydrate at Low Supersaturation." *Journal of Crystal Growth*, 58, 585-595.
16. Davey, R. J. (1979). "The Control of Crystal Habit." INDUSTRIAL CRYSTALLIZATION 78, E. J. de Jong and S. J. Jancic, eds., North-Holland Publishing, 169-183.
17. de Jong, E. J. (1984). "Industrial Crystallization 84." *9th Symposium on Industrial Crystallization*, The Hague, the Netherlands, 177-184.

18. DeLong, J. D., and Briedis, D. (1985). "A technique for the study of growth rates of single crystals of sparingly soluble salts." *Journal of Crystal Growth*, 71, 689-698.
19. Desai, R. M., Rachow, J. W., and Timm, D. C. (1974). "Collision Breeding: A Function of Crystal Moments and Degree of Mixing." *AIChE Journal*, 20(1), 43-50.
20. Edinger, S. E. (1973). "The Growth of Gypsum.An investigation of the factors which affect the size and growth rates of the habit faces of gypsum." *Journal of Crystal Growth*, 18, 217-224.
21. Garside, J., and Jancic, S. J. (1976). "Growth and Dissolution of Potash Alum Crystals in the Subsieve Size Range." *AIChE Journal*, 22(5), 887-894.
22. Garside, J., and Jancic, S. J. (1978). "Prediction and Measurement of Crystal Size Distribution for Size-Dependent Growth." *Chemical Engineering Science*, 33, 1623-1630.
23. Hamdona, S. K., Nessim, R. B., and Hamza, S. M. (1993). "Spontaneous precipitation of calcium sulphate dihydrate in the presence of some metal ions." *Desalination*, 1(94), 69-80.
24. Hartel, R. W., Berglund, K. A., Gwynn, S. M., Schierholz, P. M., and Murphy, V. G. (1980). "Crystallization Kinetics for the Sucrose-Water System." *AIChE Symposium Series*, 76(193), 65-72.
25. Hasson, D., and Zahavi, J. (1970). "Mechanism of Calcium Sulfate Deposition on Heat-Transfer Surfaces." *Industrial and Engineering Chemistry Fundamentals*, 9(1), 1-10.
26. He, S., Oddo, J. E., and Tomson, M. B. (1994). "The Seeded Growth of Calcium Sulfate Dihydrate Crystals in NaCl Solutions up to 6 m and 90° C." *Journal of Colloid and Interface Science*, 163, 372-378.
27. Hodgson, T. D., and Jordan, T. W. J. (1976). "Scaling in Vertical Tube, Falling Film Evaporators." *5th International Symposium on Fresh Water from the Sea*, 295-303.
28. Jamialahmadi, M., and Muller-Steinhagen, H. (2000). "Crystallization of Calcium Sulphate Dihydrate from Phosphoric Acid." *Dev.Chem.Eng.Mineral Process.*, 8(5/6), 587-604.

29. Jancic, S. J., and Grootscholten, P. A. M. (1984). *Industrial Crystallization*, Delft University Press and Reidel Publishing, Dordrecht, Boston, Lancaster.
30. Klepetsanis, P. G., and Koutsoukos, P. G. (1998). "Kinetics of calcium sulfate formation in aqueous media: effect of organophosphorus compounds." *Journal of Crystal Growth*, 193, 156-163.
31. Klima, W. F., and Nancollas, G. H. (1987). "The Growth of Gypsum." *AIChE Symposium Series*, 83(253), 23-30.

32. Lahav, M., and Leiserowitz, L. (1990). "Tailor-made" auxiliaries for the control of nucleation, growth and dissolution of crystals." *11th Symposium on Industrial Crystallization*, Garmisch-Partenkirchen (Munich), 609-613.
33. Larson, M. A. (1984). "Advances in the Characterization of Crystal Nucleation." *AIChE Symposium series*, 80(240), 39-44.

34. Li, W., and Webb, R. L. (2000). "Fouling in enhanced tubes using cooling tower water. Part II: combined particulate and precipitation fouling." *International Journal of Heat and Mass Transfer*, 43, 3579-3588.
35. Liang, B., and Hartel, R. W. (1991). "Techniques for developing nucleation and growth kinetics from MSMPR data for sucrose crystallization in the presence of growth rate dispersion." *Journal of Crystal Growth*, 108, 129-142.
36. Lide, D. R. (1999). *CRC Handbook of Chemistry and Physics*, CRC Press, Boca Raton, USA.
37. Linnikov, O. D. (1999). "Investigation of the initial period of sulphate scale formation. Part 1. Kinetics and mechanism of calcium sulphate surface nucleation at its crystallization on a heat-exchange surface." *Desalination*, 122, 1-14.
38. Liu, S. T., and Nancollas, G. H. (1970). "The Kinetics of Crystal Growth of Calcium Sulphate Dihydrate." *Journal of Crystal Growth*, 6, 281-289.
39. Liu, S. T., and Nancollas, G. H. (1973). "The Crystal Growth of Calcium Sulfate Dihydrate in the Presence of Additives." *Journal of Colloid and Interface Science*, 44(3), 422-429.
40. Meadhra, R. O., Kramer, H. J. M., and van Rosmalen, G. M. (1996). "Model for Secondary Nucleation in a Suspension Crystalliser." *AIChE Journal*, 42(4), 973-982.

41. Middis, J., Paul, S. T., and Muller-Steinhagen, H. (1998). "Reduction of Heat Transfer Fouling by the Addition of Wood Pulp Fibers." *Heat Transfer Engineering*, 19(2), 36-44.
42. Mori, H., Nakamura, M., and Toyama, S. (1996). "Crystallization Fouling of Calcium Sulfate Dihydrate on Heat Transfer Surfaces." *Journal of Chemical Engineering of Japan*, 29(1), 166-173.
43. Moyers, C. G., Jr., and Rousseau, R. W. (1987). Handbook of Separation Technology, R. W. Rousseau, ed., John Wiley & Sons, New York.
44. Mullin, J. W. (1972). *Crystallisation*, Butterworths, London.
45. Mullin, J. W. (1979). "Crystal growth in pure and impure systems." INDUSTRIAL CRYSTALLIZATION 78, E. J. de Jong and S. J. Jancic, eds., North-Holland Publishing, Amsterdam, 93-103.
46. Myerson, A. S. (1993). *Handbook of Industrial Crystallization*, Butterworth-Heinemann, Boston, London, etc.
47. Nancollas, G. H. (1979). "The Growth of Crystals in Solution." *Advances in Colloid and Interface Science*, 10, 215-252.
48. Nancollas, G. H., White, W., Tsai, F., and Maslow, L. (1979a). "The Kinetics and Mechanism of Formation of Calcium Sulfate Scale Minerals - The Influence of Inhibitors." *Corrosion - NACE*, 35(7), 304-308.
49. Nancollas, G. H., White, W., Tsai, F., and Maslow, L. (1979b). "The Kinetics and Mechanism of Formation of Calcium Sulfate Scale Minerals. The Influence of Inhibitors." *Corrosion - NACE*, 35(7), 304-308.
50. Nyvlt, J. (1992). *Design of Crystallizers*, CRC Press, Boca Raton etc.
51. Nyvlt, J., Sohnel,O, Matuchova, M., Broul, M. (1985). *The Kinetics of Industrial Crystallization*, M. Stulikova, translator, Elsevier, Amsterdam, etc.
52. Ohara, M., and Reid, R. C. (1973). *Modeling Crystal Growth Rates from Solution*, Prentice-Hall, Englewood Cliffs, N.J.
53. Ohtaki, H. (1998). *Crystallization Processes*, John Wiley & Sons, Chichester etc.
54. Randolph, A. D., and, and Larson, M. A. (1988). *Theory of Particulate Processes.Analysis and Techniques of Continuous Crystallization*, Academic Press, San Diego,etc.
55. Rousseau, R. W., Li, K. K., and McCabe, W. L. (1976). "The Influence of Crystal Size on Nucleation Rate." *AIChE Symposium Series*, 72(153), 48-52.

56. Rusli, I. T., Larson, M. A., and Garside, J. (1980). "Initial Growth Rate of Secondary Nuclei Produced by Contact Nucleation." *AIChE Symposium Series*, 76(193), 52-58.

57. Sarig, S., Kahana, F., and Leshem, R. (1975). "Selection of threshold agents for calcium sulfate scalecontrol on the basis of chemical structure." *Desalination*, 17, 215-229.

58. Shinoda, K. (1978). *Principles of solution and solubility*, Marcel Dekker, New York & Basel.

59. Shor, S. M., and Larson, M. A. (1971). "Effect of Additives on Crystallisation Kinetics." *Chemical Engineering Progress Symposium Series*, 67(110), 32-42.

60. Sikdar, S. K., and Randolph, A. D. (1976). "Secondary nucleation of two fast growth systems in a mixed suspension crystalliser: magnesium sulfate and citric acid systems." *AIChE Journal*, 22(1), 110-117.

61. Smith, B. R., and Alexander, A. E. (1970). "The Effect of Additives on the Process of Crystallization. II. Further Studies on Calcium Sulphate (1)." *Journal of Colloid and Interface Science*, 43(1), 81-88.

62. Sohnel, O., and Garside, J. (1992). *Precipitation. Basic Principles and Industrial Applications*, Butterworth Heinemann, Oxford, etc.

63. Sudmalis, M., and Sheikholeslami, R. (2000). "Coprecipitation of $CaCO_3$ and $CaSO_4$." *The Canadian Journal of Chemical Engineering*, 78, 21-31.

64. Tadros, M. E., and Mayes, I. (1979). "Linear Growth Rates of Calcium Sulfate Dihydrate Crystals in the Presence of Additives." *Journal of Colloid and Interface Science*, 72(2), 245-254.

65. Tai, C. Y., and Wu, J.-F. (1992). "Interfacial supersaturation, secondary nucleation, and crystal growth." *Journal of Crystal Growth*, 116, 294-306.

66. van der Leeden, M. C., Kashchiev, D., and van Rosmalen, G. M. (1993). "Effect of additives on nucleation rate, crystal growth rate and induction time in precipitation." *Journal of Crystal Growth*, 130, 221-232.

67. van der Leeden, M. C., and van Rosmalen, G. M. (1987). "Aspects of additives in precipitation processes: Performance of polycarboxylates in gypsum growth prevention." *Desalination*, 66, 185-200.

68. van Rosmalen, G. M., Daudey, P. J., and Marchee, W. G. J. (1982). "Quantitative description of the influence of the inhibitor concentration on the growth rate of calcium sulfate dihydrate crystals in suspension." INDUSTRIAL

CRYSTALLIZATION 81, S. J. Jancic and E. J. de Jong, eds., North-Holland Publishing, Amsterdam, 147-154.

69. Weijnen, M. P. C., and van Rosmalen, G. M. (1984). "The Role of Additives and Impurities in the Crystallization of Gypsum." *Industrial Crystallization 84*, 61-66.
70. Weijnen, M. P. C., and van Rosmalen, G. M. (1985). "The influence of various polyelectrolytes on the precipitation of gypsum." *Desalination*, 54, 239-261.
71. Witkamp, G. J., van der Eerden, J. P., and van Rosmalen, G. M. (1990). "Growth of gypsum. I. Kinetics." *Journal of Crystal Growth*, 102, 281-289.
72. Witkamp, G. J., and van Rosmalen, G. M. (1987). "Incorporation of Cadmium and Aluminium Fluoride in Calcium Sulphate." *Industrial Crystallization 87*, 265-270.

CHAPTER 3 LITERATURE REVIEW – PART 2: GYPSUM SCALING: EFFECT OF ADMIXTURES ON GYPSUM CRYSTALLISATION KINETICS

3.1. Introduction

Scaling is the unwanted formation of a solid layer on equipment surfaces and piping systems and is one of the persistent problems encountered in many industrial operations such as distillation, cooling and heating of liquids, mixing, evaporation, crystallisation etc. The solid layer may become increasingly thicker during the process and the resulting deposit reduces the capacity of production through resistance to heat transfer, restriction of materials flow, corrosion and wearing out of construction materials etc. Research aimed at preventing or controlling the scaling problem has been extensive and significant advances have been made. However, currently available data have not yet been able to produce a general theory to elucidate all aspects of scaling phenomenon.

This chapter deals with the literature review pertinent to gypsum scale formation and inhibition, and is divided into the following sections:

1. Introduction
2. Background
3. Classification of Scaling
4. Mechanism of Scaling
5. Scale Formation of Gypsum.

3.2. Background

The term ***scaling*** is often used interchangeably with fouling (Krause 1993), although the two terms are not necessarily the same and hence, a clearer definition can be made about them. Scaling is the process of scale deposition on a surface such as the wall of a pipe or heat transfer surface (Epstein 1983). The term "**scale**" itself means a solid layer and in most cases it consists of crystalline materials (Forster and Bohnet 2000; Hasson 1981; Nulty *et al.* 1991). Fouling, on the other hand, refers to any

alteration on a surface of equipment due to accumulation of dirt, scale, corrosion products and other substances (Perry and Green 1997). Fouling is an unwanted phenomenon because it reduces the rate of heat transfer and/or the rate of flow, which ultimately translates into loss of production. Although a variety of measures have been taken to prevent its occurrence, it is still one of the serious problems encountered in industrial operations, particularly those involving heat transfer, piping system and liquid separation using membranes.

Briefly, scaling is one major category of fouling. Hasson (Hasson 1981) refers to scaling as precipitation fouling due to the fact that the scale deposited consists of hard crystalline layers formed through a crystallisation or precipitation process. Scaling is a persistent problem encountered in many industrial processes. Desalination installations (Amjad 1985; Linnikov 1999), cooling water systems (Nancollas and Klima 1982), chemical processes involving evaporation and/or crystallisation (Hasson 1981), potable water supply lines (Hasson 1981) and mineral processing plants (Northwood 1995) are some examples where the severe problem of scaling is usually encountered. In de-salting plants, for example, acid treatment or addition of scale inhibitors is usually required to suppress scale deposition. Distillation of sea and brackish water to produce potable water as practised in de-salting plants generates tenacious scale deposits containing calcium sulphate as one of the main constituents (Linnikov 1999). Apart from desalination operation, scaling problems in providing potable water results from the accumulation of $CaCO_3$ deposit on the inner wall of the pipe due to supersaturation with respect to $CaCO_3$ in the flowing water (Hasson 1981). Still another scaling problem can also be found in evaporation and crystallisation processes. The severity of scale deposition is enhanced in certain cases by the presence of contaminants, which either originate from the process solution, such as $CaCO_3$, $CaSO_4$ or Ca oxalate, or from the corrosion by-products (Hasson 1981). Scaling problems encountered in heat transfer equipment are intensified when the scale forming minerals show inverse solubility characteristics.

Scaling in pipes and on surfaces of vessels causes serious operational problems as well as increasing costs of pumping and replacement of parts. It decreases the performance of a heat exchanger due to higher resistance to heat transfer. The

resistance is the result of the build up of a thin film that grows into a solid layer and thus hinders the flow of heat. The solid layer also restricts the fluid flow causing a greater pressure drop and thus an increase in energy requirements for pumping operation. The scaling problem is technical as well as economical. Cleaning up the accumulation of scale on the heat exchanger surfaces or the wall of pipes can be a very difficult operation. In some cases, a process shut down is the only choice and consequently loss of production is inevitable.

Scaling is mainly caused by dissolved inorganic components crystallising out of the supersaturated solution with respect to the dissolved components. With supersaturation levels being the key factor, the scaling phenomenon is not necessarily confined to heat transfer surfaces, but also occurs under isothermal conditions or at ambient temperatures. One such condition is the scaling problem in the potable water supply system, where the pipes carrying the water do not undergo appreciable changes in temperatures and yet scale formation is prevalent. One of the major components of scale in some industries is calcium sulphate dihydrate or gypsum (Cowan and Weintritt 1976; Northwood 1995; Tadros and Mayes 1979). This chapter attempts to review the developments of scale prevention and control with regard to gypsum.

3.3. Classification of Scaling

Scaling is one of six major categories of fouling (Bott 1988b; Epstein 1983; Perry and Green 1997). These are:

1. *Particulate fouling*: due to the accumulation of suspended fine particles (in either a liquid or gaseous stream) onto a surface (Bossan *et al.* 1995; Chamra and Webb 1994; Epstein 1983; Grandgeorge *et al.* 1998; Gudmundsson 1981; Karabelas *et al.* 1997; Masri and Cliffe 1996).

2. *Chemical reaction fouling*: fouling due to the deposition of materials onto a surface caused by chemical reactions, such as auto-oxidation, polymerisation and thermal decomposition (Crittenden 1988; Watkinson and Wilson 1997).

3. *Corrosion fouling*: the deposition of corrosion products on the heat transfer surfaces (Crittenden 1988).

4. *Biological* or *bio fouling*: fouling of the surface due to growth and proliferation of micro- or macro-organisms, which are present in the fluid (Huttinger 1988; Sheikholeslami 1999; Sheikholeslami 2000b).

5. *Crystallisation fouling*: due to the deposition of crystals, which crystallise out of the solution, onto the surface (Bott 1988a; Epstein 1988; Helalizadeh *et al.* 2000).

6. *Freezing fouling*: fouling due to the freezing of process fluid, which then coats the heat transfer surface (Perry and Green 1997).

3.4. Mechanism of Scaling

A review on precipitation fouling or scaling given by Hasson (Hasson 1981) is probably one of the most comprehensive. The review describes the general mechanism of scaling once the supersaturated condition is established. The mechanism proceeds through five steps as explained below.

1. *Nucleation*: the formation of nuclei or active centres, which subsequently grow to become crystals.

2. *Diffusion*: the transport of the scale-forming components such as ionic species, solvated ions, molecules, particulate solids etc. to the solid surface.

3. *Deposition*: due to adsorption or attachment of the transported materials onto either the crystal surface or the solid surface.

4. *Removal*: detachment or removal of the deposit layer due to shear stress exerted by the flowing fluid.

5. *Ageing*: changes to the scale characteristics, caused by recrystallisation, phase transformation, Ostwald ripening, etc., which may either strengthen or weaken the scale deposit.

The five steps for scaling mechanism described above may occur concurrently or consecutively. In addition any two mechanisms may produce a synergistic effect (Hasson *et al.* 1996).

3.5. Scale Formation of Gypsum (Gypsum Scaling)

Many studies have been reported concerning gypsum scaling. Earlier studies (Amjad 1985; Amjad 1988a; Amjad 1988b; Amjad and Masler 1985; Edinger 1973; Gill 1980; Hasson and Zahavi 1970; Liu and Nancollas 1970; Liu and Nancollas 1973; McCartney and Alexander 1958; Nancollas 1983; Nancollas and Klima 1982; Nancollas and Reddy 1974; Nancollas *et al.* 1979a; Sarig *et al.* 1975; Sarig and Mullin 1982; Smith and Alexander 1970; Tadros and Mayes 1979; Vetter 1972) mainly focused on the kinetics of scale formation. They were either carried out in laboratory crystallisers of various configurations or on heated metal surfaces to simulate heat transfer equipment. The main concern was on the initial formation of the scale. Most of the later studies (Bansal and Muller-Steinhagen 1993; Bansal *et al.* 1997; Bansal *et al.* 2000; Bott 1995; Chamra and Webb 1994; Li and Webb 2000; Linnikov 1999; Middis *et al.* 1998; Mori *et al.* 1996; Sudmalis and Sheikholeslami 2000), on the other hand, have put emphasis on external factors influencing the deposition of the scale. These factors include hydrodynamics of the scale forming solutions, the characteristics of the solid surface, the behaviour of the particles suspended in the scaling solutions, the configuration of the heat transfer equipment etc.

3.5.1. Admixtures as scale inhibitors

Research on the effect of admixtures on gypsum crystallisation to develop strategies in preventing the occurrence of scaling is extensive as detailed in this section.

A rather comprehensive study was carried out way back in 1958 by McCartney and Alexander, which showed that nucleation and growth of gypsum were strongly suppressed by trace amounts (as low as 13 ppm) of colloidal particles (McCartney and Alexander 1958). They tested as many as 18 different organic as well as inorganic admixtures and concluded that the retardation effect of the admixtures on gypsum crystallisation was due to adsorption of the admixtures onto the crystal surface, thus preventing the advancement of the growth step. Moreover, their study showed that the strength of the adsorption has a positive correlation with the molecular weight of the admixtures. They later discovered that adsorption of scale inhibitors on crystal faces is selective or preferential.

Smith and Alexander (Smith and Alexander 1970) reported that polymers containing carboxyl (-COOH) groups are effective inhibitors for gypsum scale due to their ability to preferentially adsorb on the active growth sites of the gypsum crystal faces. The preferential adsorption was also confirmed by Edinger (Edinger 1973), and Liu and Nancollas (Liu and Nancollas 1973).

Due to the preferential adsorption and different density of growth sites, the habit of gypsum may change significantly, because different faces may have different growth rates. It is logical to assume that the most efficient growth retarder will be the inhibitor which is structurally well fitted to the crystal lattice of the precipitating crystals. Investigation on the effect of polyglutamic acid (= PGA) and polyvinyl sulphonate (= PVS) on gypsum growth by Sarig *et al.* (Sarig *et al.* 1975) lends support to this view. It was found that PGA was more effective than PVS as gypsum growth retarding agent because the carboxylic functional groups (-COOH) in PGA is structurally more compatible to $CaSO_4.2H_2O$ than the sulphonic groups in PVS.

Amjad and Masler (Amjad and Masler 1985) showed that trace amounts of polyacrylates affected the growth of gypsum significantly by incorporating into crystal lattices as the crystals grow.

The recent work of Oner *et al.* (Oner 1998) has compared the rate of crystallisation of calcium sulphate dihydrate in a pure solution with that in the presence of

admixtures. Various acrylics and methacrylics were used as admixtures. Rates of crystallisation in the pure solution were found to be between 1.4 to 2.2 times higher than those where admixtures were added.

In an earlier study (Tadros and Mayes 1979), the effect of admixtures on crystal habit was investigated by comparing the shape of the crystals formed with and without added admixtures. They found that carboxylic and phosphonic acid derivatives caused the gypsum crystals to grow more uniformly in size and shape than those formed in a pure solution.

The first step in scale formation is nucleation. Knowing the effect of admixtures on nucleation is therefore, undoubtedly important. It was reported that nucleation can either be promoted or suppressed by admixtures. Nucleation of gypsum in an ammoniacal solution was observed to be enhanced by the presence of calcium carbonate crystals (Kagawa *et al.* 1981). Sarig and Mullin (Sarig and Mullin 1982), on the other hand, reported that the nucleation rate of gypsum in the presence of Al^{+3} and F^- fluctuated with the admixture concentrations. In yet another case, the nucleation of gypsum was suppressed by the presence of either phosphonates or polycarboxylates as admixtures (He *et al.* 1994).

Considering the different responses of the nucleation rate of gyspum in the presence of different admixtures, a general explanation of the suppressing effect of admixtures on nucleation should not be attempted. In contrast, a case-by-case explanation would seem to be more convincing.

Research on growth kinetics of gypsum in impure solution by Amjad (Amjad 1988b) has suggested that the initial growth was dependent on the solution pH. Amjad explained that the pH level might have influenced the ionisation of the poly acrylic acid added into the crystallising solution as admixtures. The ionisation reaction should have provided more functional groups such as carboxyl, in the solution to retard the growth.

In another study, the dependence of gypsum growth on solution pH was substantiated (He *et al.* 1994). It is most likely that pH influences the degree of ionisation or

dissociation of certain organic admixtures, which results in more functional groups being available in the crystallizing solution. These ionised functional groups are then adsorbed onto active growth sites and decelerate or even stop the growth. Some other studies (Klepetsanis 1999; Klepetsanis and Koutsoukos 1989), however, suggested that pH did not affect the growth of gypsum crystals.

Al-Sabbagh *et.al* (Al-Sabbagh *et al.* 1996) studied the effect of different defoaming agents on the habit and filterability of gypsum crystals. The study showed that habit modification of gypsum was influenced by the functional groups adsorbed on specific surfaces of crystals. It was found that esterified citric acid was suitable as an admixture. This is due to the distance between carboxylate groups (COO-) of 3.5 Å, very similar to the distance between Ca ions in (111) face of gypsum. At pH values of $\geq$ 6, citric acid (one of the agents tested) was completely dissociated. Fully dissociated citric acid yields free COO-, which are then active as crystal modifiers by incorporation onto the crystal surface.

In order to better understand the scaling problem in industrial process waters, Chan and her group (Chan 1997) conducted a gypsum crystallization study using plant liquors from a particular mineral processing plant. It was observed that the plant liquors retarded the crystallisation reaction compared to pure synthetic liquors. It was believed that the retardation was due to the impurities, which were either dissolved or suspended in the liquors.

In an attempt to cover a wider temperature range of industrial processing applications, a gypsum scale control study was carried out by El Dahan and Hegazy (El Dahan and Hegazy 2000) who investigated phosphate esters as the admixtures at temperatures ranging from 40 to 90^{0}C. Their study showed that at the same supersaturation level and within the range of the temperatures selected, higher temperatures consistently required higher concentrations of admixtures to obtain the same percentage of scale reduction. This study suggests that the effect of admixtures on gypsum crystallisation can be temperature dependent.

A recent study on the crystallisation kinetics of gypsum in the presence of Fe^{3+}, Zn^{2+}, and sodium isopropyl xanthate (= a flotation agent) (Muryanto and Ang 2002) shows that nucleation rate was enhanced while growth was retarded.

3.5.2. Composite or mixed scaling of gypsum

In most cases, scaling occurs under impure conditions, in which the solutions may contain several different major components such as $CaSO_4$, $CaCO_3$ and $BaSO_4$, and various minor components in minute quantities. The effects of minor components and their combinations on scale formation have been investigated in various degrees and the results showed that some of these components were effective as scale inhibitors. Research on individual major components of scale has also been widely carried out, notably for sulphate and carbonate salts. Given the complexity of the scaling process, only a small number of studies have been done on composite scaling, where more than one major component was present. The salts may co-precipitate and their interactive behaviour can be an important aspect to the formation of scale. While studies on such co-precipitation are certainly worthwhile, they are still lacking, possibly due to the difficulty in determining the scale forming species, which should be chosen to represent a particular condition. Undoubtedly, investigation may start with the main species normally found in industrial waters, such as calcium sulphate, calcium carbonate, barium sulphate etc. and their combinations.

The work of Yuan *et al.* (Yuan *et al.* 1994), tried to address the problem of scaling normally encountered in offshore oil recovery using water flooding, where sulphate salts such as $BaSO_4$, $CaSO_4$ and $SrSO_4$ are usually present. Their work showed that competitive co-precipitation among sulphate salts occurred and that the severity of scaling was dependent on the ratio of injected seawater and formation water used. This result implies that both physical (temperature, pressure, etc.) and chemical properties (composition, concentration etc.) of the oil well solutions need to be taken into account when scaling problem is to be prevented.

Composite scaling of gypsum and biological matter may be non-existent. The presence of micro organisms could introduce CO_2 into the scaling solution due to the biological reactions (Sheikholeslami 1999). This may, in turn, affect the pH of the solution and/or promote the occurrence of calcium carbonate scale if Ca^{2+} is present in the solution. Thus, instead of gypsum, different forms of calcium carbonate scale such as calcite or aragonite may form. Investigation on composite scaling of $CaCO_3$ and micro organisms has never been done and may be worthwhile.

A study on co-precipitation of $CaCO_3$ and $CaSO_4$ was carried out by Sudmalis and Sheikholeslami (Sudmalis and Sheikholeslami 2000), whereby the experimental results in terms of induction time, species concentrations and deposit structure were compared with those of single species precipitation. It can be inferred from such comparison that co-precipitation of two or more species may not yield a synergistic or compounded effect.

Other studies on co-precipitation between two major constituents of scale: $CaSO_4$ and $CaCO_3$ (Chong and Sheikholeslami 2001; Sheikholeslami and Ng 2001) indicated that the concentration ratio of the two salts considerably dictates the kinetics of the scale formation. In addition, the scale characteristics (structure, adherence to the surface), was affected as well. Thus it appears that in composite scaling, the individual major components may behave as admixtures if they are present in minute amounts.

Research on composite or mixed scaling, such as inorganic and biological, can further be complicated if corroding solid surfaces were used (Sheikholeslami 2000b). In such a situation, another type of scaling, i.e. corrosion scaling may occur, thus three types of scaling will be present. The scaling characteristics will then be affected by various factors such as the availability Fe^{2+} as a corrosion product, for the growth and proliferation of the microorganisms (Characklis 1990).

A study on composite scaling of $CaSO_4$ and $CaCO_3$ by Helalizadeh *et al.* (Helalizadeh *et al.* 2000) revealed that the deposition rate of composite fouling could be either mass transfer or surface reaction-controlled depending on the rate of the fluid flow and the temperature of the solid surface. It could be argued that such

dependency should not be specific to composite fouling. As is known, the higher the flow rate the thinner the diffusion layer becomes and the transfer of scale growth units to the solid surface will be enhanced which results in more scale being deposited. The same tendency may be valid for temperature as higher temperatures may cause thinning of the diffusion layer. They also discovered that the mixed scale was weaker than that of pure $CaCO_3$ but stronger than that of pure $CaSO_4$. This finding about the change in deposit strength of composite scaling was later confirmed by similar research carried out by Chong and Sheikholeslami (Chong and Sheikholeslami 2001).

3.5.3. Prediction and modelling of scaling rate

Early researchers on calcium carbonate scale formation (Hasson 1981; Hasson *et al.* 1978) reported that the scaling process is primarily due to crystallisation fouling. It is interesting to note that gypsum, also a sparingly soluble salt, was reported to foul the surface mainly through a particulate deposition mechanism, rather than through the crystallisation mechanism (Sheikholeslami 2000a). A number of other researchers (Bansal and Muller-Steinhagen 1993; Bansal *et al.* 1997; Mori *et al.* 1996), however, maintained that the dominant factor is crystallisation mechanism. Yet another study (Middis *et al.* 1998) showed that the scaling process was a combination of crystallisation and particulate fouling. Hence, it is safe to conclude that in any gypsum scaling process a variety of factors, such as the supersaturation level of the fluid stream, flow velocity, temperature of the fluid, characteristics of the surface, type and concentration of dissolved admixtures, type and concentration of suspended particles, etc could be simultaneously operative. In brief, the scaling process of gypsum is system specific.

Nancollas *et al.* (Nancollas *et al.* 1979b) studied the influence of some scale inhibitors on the kinetics and formation of gypsum scale. They used a seeded method, which is believed to be highly accurate and reproducible. Their aim was to develop methods for scale prevention. Obviously, two approaches are important. The first is modification of the morphology of the scale crystals so as to lessen the tendency of sticking together to form agglomerates. The second is to stop or slow

down the rate of nucleation and growth so that less scale was deposited. An unseeded crystallisation method was clearly not suitable due to the demand of high supersaturations and thus the tendency of spontaneous nucleation. Moreover, in industrial applications such high supersaturations are rarely practised. The organic inhibitor (= DENPMP), which was selected for their study, was indeed able to inhibit both nucleation and growth.

The work of Linnikov (Linnikov 1999) showed that the nucleation rate of gypsum scale is linearly dependent on surface roughness. Hence it indicates that nucleation takes place directly on the surface of the heat exchanger (= HE) equipment. Further, if the nucleation rate also depends on the temperature of the surface of the HE, then the scaling phenomenon will be complicated, as it depends on the roughness and the temperature.

Undoubtedly, crystallisation fouling follows the rules that apply to crystallisation. Hence the relationship between crystallisation rate and supersaturation should apply. Researchers on the scaling of gypsum have adopted the following equation (Amjad 1988b; Klima and Nancollas 1987; Liu and Nancollas 1970; Nancollas and Reddy 1974):

$$m_d = k_r s \Delta C^n \tag{3.1}$$

where,

m_d = crystallisation or scale deposition rate, gram/sec

k_r = reaction rate constant, $ppm^{-1}\ min^{-1}$

s = a function of the number of nuclei sites, dimensionless

ΔC = concentration driving force, $gram/cm^3$

n = reaction rate order, 2.

An extensive investigation on the effect of admixtures on gypsum scaling was carried out by Amjad (Amjad 1988a). Various polymeric and non-polymeric admixtures were tested for their effect on gypsum scale formed on the surfaces of copper, brass and stainless steel under static conditions. It was reported that the

retarding effect of the selected admixtures on scale formation depended on molecular weight, functional groups and concentration. Different types of metals showed a different quantity of scale formed indicating that heat conductivity and surface roughness of the individual metals are likely important factors in gypsum scaling.

The seeded growth method for the investigation of the crystallisation kinetics of gypsum scale has been widely accepted as a highly reliable technique (Amjad 1988b; Liu and Nancollas 1973; Nancollas 1979; Smith and Alexander 1970). However, Nancollas (Nancollas 1983) suspected that the technique could be inaccurate for crystals showing appreciable dissolution behaviour because as the crystallisation proceeded, some of the crystals may undergo dissolution, thus the observation of the decrease in cation concentrations (in the case of gypsum: Ca^{2+} concentration) may be inaccurate. He proposes, therefore, the use of a constant composition method where the decrease in Ca^{2+} concentration in the crystallising solution is automatically compensated by addition of Ca^{2+} containing solution from an automatic burette (Weijnen and van Rosmalen 1984). For the seeded growth method to be reliable, therefore, the desupersaturation curve should show a smooth downward trend without any sign of fluctuation.

For crystallisation fouling, the rate of scale deposition can be presented as a function of surface area on which the scale grows and its crystallisation rate constant, $\mathbf{k_r}$ (Bott 1997). The surface area is readily obtained from measurement, but the rate constant, $\mathbf{k_r}$, has to be calculated according to the Arrhenius equation as follows:

$$k_r = Ae^{-\frac{E}{RT}} \tag{3.2}$$

where,

A = an Arrhenius constant, collisions/second

E = activation energy, kJ/mol

R = universal gas constant, (kJ)/(mol ^{0}K)

T = absolute temperature, ^{0}K.

As a crystallisation phenomenon, the scaling rate is also affected by the chemical properties of the solution such as ionic activity and pH. As the scale grows it is also

subjected to the shear stress exerted by the flowing fluid. These two factors, therefore, have to be taken into account. Hasson (Hasson 1981) proposes some kind of equation to accommodate this as follows:

$$\frac{dm}{dt} = KAP\Omega^{-\frac{E}{RT_s}} \tag{3.3}$$

where,

$\frac{dm}{dt}$ = rate of scale deposition, gram/sec

K = a dimensionless constant

A = area on which the scale grows, cm^2

P = sticking probability, dimensionless

Ω = chemical properties of the solution, e.g. concentration, $gram/cm^3$

T_s = absolute temperature of the surface, ^0K.

The sticking probability, **P**, is included to account for the removal mechanism, especially when the flow velocity is dominant. The precise magnitude of **P** is extremely difficult to calculate because it is dependent on various factors: characteristics (size, density, porosity etc.) of the scale, characteristics (roughness, topography etc.) of the surface, characteristics (flow rate, entrained particles etc.) of the flowing fluid. Its value is usually taken as less than unity (Bott 1995).

Some researchers (Muller-Steinhagen and Branch 1988) maintained that for scaling of calcium carbonate, the removal rate should not be ignored for flow velocities greater than 0.8 m/sec.

Measurement of scaling rate is usually carried out in two ways. Firstly, it can be done by measuring thermal resistance (= heat resistance of fouling layer), $\mathbf{R_f}$. Secondly, it can be achieved by measuring deposition rate, i.e. deposited mass per unit area. The first method is usually not preferred due to the complexity of the relationship between deposit structure and thermal resistance. It is clear that the

structure of the deposit varies in density, porosity etc. and this variation affects thermal resistance. Hence, the second method is preferred.

In nearly every industrial application where scaling is encountered, hydrodynamics of the fluid is involved. Thus, in predicting or modelling scaling rate, two factors must be taken into account; that is the chemical characteristics of the fluid and, its hydrodynamics. Furthermore, since during scaling processes it is very likely that two or more mechanisms are operative (Sheikholeslami 2000a), it is advantageous to formulate a composite model, whereby effects of two or more mechanisms are simultaneously investigated. Sheikholeslami (Sheikholeslami 2000a) proposed an equation to accommodate all possible aspects.

$$w_{net} = A.w_{part} + B.w_{precip} - w_{removal} \tag{3.4}$$

where,

w_{net} = net or overall deposition rate, gram/sec

A, B = dimensionless constants

w_{part} = deposition rate due to particulate fouling, gram/sec

w_{precip} = deposition rate due to precipitation fouling, gram/sec

$w_{removal}$ = removal rate, gram/sec.

Clearly, the surface of the materials as well as the flow configurations affect the scale deposition. Forster *et al.* (Forster *et al.* 1999) reported that scale reduction under pulsating flow is more effective. This could be due to the "jerking" action the pulsating flow exerts on the deposited scale, so that the removal force is increased. They also found that different metallic surfaces foul differently. Moreover, the surface topography of the different metal used was observed to affect the scale deposition rate. This could be due to the effect of the surface characteristics on the wetting angle of scale growth units attached to the surface.

Bansal and Muller-Steinhagen (Bansal and Muller-Steinhagen 1993) investigated the crystallisation fouling of gypsum in a plate and frame heat exchanger. They showed that the deposition rate of gypsum scale in such types of heat exchangers decreases

with an increase in flow velocity. It was obvious therefore that higher shear forces must have caused two things. Firstly, it caused the removal of the newly formed gypsum deposit and secondly, it resulted in the lowering of the deposition rate or transport of the scale building components onto the wall of the heat exchanger. Another work of Bansal and Muller-Steinhagen (Bansal *et al.* 1997) was an investigation on the effect of suspended particles on crystallisation fouling of gypsum in a plate heat exchanger (HE). It was found that non-crystallising particles may reduce the deposition rate of gypsum scale. These particles settled and loosely attached to the HE surface. Therefore, the gypsum scale attached to these particles will be swept away easily by the flowing fluid. Another of their findings was that the non-crystallising particles operated as retarding agents for the growth of the scale deposit.

The mechanism of gypsum scale deposition on heat transfer surfaces was investigated by Hasson and Zahavi (Hasson and Zahavi 1970). They used an annular HE and they managed to formulate a kinetic model for the rate of nucleation along the annular HE. It was found that nucleation on the surface of the HE occured in a non-uniform pattern influenced partly by the temperature of the surface. The nucleation rate was found fastest at the downstream edge compared to the inlet region. This phenomenon is actually caused by the induction time. At the start of the run, nucleation was not yet possible due to induction time. After a while, that is towards the end of the annular HE, sufficient time has elapsed to allow scale building components to reach a critical nuclei size. Hence, at the downstream side of the annulus more nucleation occurred and subsequently grew to become scale. Therefore, the downstream side showed the thickest scale deposit. Two important findings in the work of Hasson and Zahavi indicated that gypsum scale formation in pipes could be significantly promoted by surface nucleation. Firstly, when the flow of the scaling solution in pipes was reversed (= inlet became outlet region), while keeping all other conditions the same, a significant amount of scale was observed to form at the previously scale free inlet region. Secondly, (again keeping all other conditions constant), at a lower surface temperature of 80^0C, the outlet or downstream region was significantly fouled, whereas at a higher surface temperature (87^0C) the inlet region was free from scale.

Hodgson and Jordan (Hodgson and Jordan 1976) investigated the scaling of calcium sulphate in a vertical tube (falling film) evaporator (= **VTE**). They found that the tendency to form gypsum scale is dependent upon the heat flux and the fluid flow rate. The higher the heat flux the higher the tendency of scaling because of the inverse solubility of the gypsum scale. Similarly, the lower the flow rate the more time is available for the scale components to develop and attach onto the pipe wall.

Gas bubbles escaping from the heat exchanger surfaces can also significantly affect the initial formation of scale. This has been reported by Hasson and Zahavi (Hasson and Zahavi 1970) and Gill and Nancollas (Gill 1980) in their investigation on the mechanism and kinetics of gypsum scale at heated metal surfaces. It was assumed that the observed preferential nucleation on the surface of the bubbles was due to a temperature gradient, which could have existed across the bubble-liquid interface. Similar findings were later reported by Nancollas and Klima (Nancollas and Klima 1982), with respect to the effect of gas bubbles on the nucleation of calcium sulphate scale. Furthermore, addition of polyacrylic acid (PAA) into the crystallising system resulted in complete prevention of bubble formation so that less nucleation was observed. Presumably, the added PAA could have reduced the wettability of the bubble surface and subsequently increased the contact angle. Hence, nuclei attachment onto the bubble surface was prevented.

It has been postulated that calcium sulphate scale may undergo a phase transformation during the scaling process on a heat transfer surface (Cowan and Weintritt 1976; Gill 1980; Nancollas 1983). Thus, temperature is one of the important factors with regard to gypsum scaling. Consequently, researchers should be aware of the range of transition temperatures for the three hydrated salts of calcium sulphates: anhydrous calcium sulphate ($CaSO_4$), hemihydrate calcium sulphate ($CaSO_4.1/2H_2O$) and calcium sulphate dihydrate ($CaSO_4.2H_2O$). In this regard, Mori *et al.* (Mori *et al.* 1996) confirmed that the calcium sulphate scale deposited on the heat transfer surfaces at temperatures below 99^0C was found to be layers of gypsum .

Hasson *et al.* (Hasson *et al.* 1978) investigated the scale formation of $CaCO_3$ and formulated a model based on the diffusion of Ca^{2+} and CO_3^{2-} onto the interface. The

model is applicable under various flow rates and supersaturation levels. This is obvious because flow rate and supersaturation do not change the availability of Ca^{2+} and CO_3^{2-} in the solution. The applicability of the later model was later confirmed by Andritsos *et al.* (Andritsos *et al.* 1996) using the same $CaCO_3$ system.

Scaling in piping systems and surfaces of vessels is one of the dominant problems in mineral processing industries in Western Australia. The industries include copper and zinc, pigment, mineral sands etc. A number of studies (Chan 1997; Headley *et al.* 2001; Murray 1997; Northwood 1995) have been carried out to prevent the formation of scale in process water piping, of which gypsum is one of the main components. For one of these industries, a proposal was made (Northwood 1995) to suppress the accumulation of the gypsum scale, which comprises three different prevention measures. Firstly, a crystalliser unit could be installed within the water circuit to crystallise out calcium sulphate from the process water. Secondly, the process water circuit could be pumped into a large dam to allow crystallisation to occur over an extended period of time before recycling to the plant. Thirdly, the pH of the process water may be adjusted using a different alkali, NaOH instead of $Ca(OH)_2$. However, a serious difficulty remains, that is, that the chemical properties of the water process highly fluctuated (Northwood 1995). As reported by Northwood (Northwood 1995), the pH level of the flotation circuit water dropped considerably over a short period of a few hours. The dramatic change in pH level indicated that the solution might contain unstable substances, such as oxidisable components. Prediction of the mechanism of gypsum crystallisation in such a solution requires data, which span over a long period of time, until the pattern of the fluctuation is discovered.

A recent study on $CaSO_4.2H_2O$ scaling under isothermal conditions and negligible removal rate (Muryanto *et al.* 2002), has also tried to employ the previous model to predict the deposition rate. The modelling result shows that within the range of the experimental conditions used in the study, the predicted values of the deposition rate agree reasonably well with the measured values. Thus the ionic diffusion model developed previously for calcium carbonate scaling is also suitable for gypsum scaling phenomenon under isothermal conditions and no removal step.

Summary

Some conclusions may be drawn from this review.

Classification of fouling in industrial applications into six major categories is well defined from which methods of prevention and control of fouling may be developed.

The current understanding of the five steps of fouling is reasonably clear. Each step is affected by chemical and physical characteristics as well as the hydrodynamics of the system.

Admixtures of various types have been used to prevent and control scale formation, which leads to a clearer understanding of the scaling problems. The effect of admixtures on scale formation appears to be system-specific.

Scale deposit may likely consist of more than one main constituent, of which the process is labelled composite or mixed scaling. In such cases, the nature of the deposit is affected by the presence of co-precipitates and the resulting effect may not be additive. Most studies on composite scaling have been carried out for a mixture of $CaSO_4$ and $CaCO_3$.

Research on scale prevention has ultimately led to prediction and modelling of scaling rates. Attempts to model combined scaling mechanisms have been carried out but the results seem to be specific to the system under consideration. On the other hand, modelling based on one single operative mechanism has proved to be applicable in some systems such as calcium carbonate and gypsum scaling.

In mineral processing industries, unreliable data with respect to the chemical properties of the process water may be encountered, therefore a comprehensive and accurate documentation of such properties is required before any scale prevention measures are attempted.

The problem of scaling, including that of gypsum, is complex, depending not only on the nature of the scaling solutions and the presence of admixtures but also on external factors such as the hydrodynamics of the system. For these reasons, a unified theory, which will explain every aspect of scaling phenomenon satisfactorily, is very unlikely to be obtained. Instead, addressing the problem of scaling may have to greatly rely on specific empirical data. However, it should be sufficient to show that much gypsum scaling research has been found to be helpful in elucidating the scaling problem encountered by many industries.

References

1. Al-Sabbagh, A., Widua, J., and Offermann, H. (1996). "Influence of different admixtures on the crystallization of calcium sulfate crystals." *Chemical Engineering Communications*, 154, 133-145.
2. Amjad, Z. (1985). "Applications of Antiscalants to Control Calcium Sulfate Scaling in Reverse Osmosis Systems." *Desalination*, 54, 263-276.
3. Amjad, Z. (1988a). "Calcium Sulfate Dihydrate (Gypsum) Scale Formation on Heat Exchanger Surfaces: The Influence of Scale Inhibitors." *Journal of Colloid and Interface Science*, 123(2), 523-536.
4. Amjad, Z. (1988b). "Kinetics of crystal growth of calcium sulfate dihydrate. The influence of polymer composition, molecular weight, and solution pH." *Canadian Journal of Chemistry*, 66, 1529-1536.
5. Amjad, Z., and Masler, W. F. (1985). "The inhibition of calcium sulfate dihydrate crystal growth by polyacrylates and the influence of molecular weight." *Corrosion 85*, Houston,TX.
6. Andritsos, N., Kontopoulou, M., Karabelas, A. J., and Koutsoukos, P. G. (1996). "Calcium carbonate deposit formation under isothermal conditions." *Canadian Journal of Chemical Engineering*, 74(December), 911-919.
7. Bansal, B., and Muller-Steinhagen, H. (1993). "Crystallization Fouling in Plate Heat Exchangers." *Journal of Heat Transfer*, 115(August), 584-591.
8. Bansal, B., Muller-Steinhagen, H., and Chen, X. D. (1997). "Effect of Suspended Particles on Crystallization Fouling in Plate Heat Exchangers." *Journal of Heat Transfer*, 119(August), 568-574.
9. Bansal, B., Muller-Steinhagen, H., and Chen, X. D. (2000). "Performance of plate heat exchangers during calcium sulphate fouling - investigation with an in-line filter." *Chemical Engineering and Processing*, 39, 507-519.
10. Bossan, D., Grillot, J. M., Thonon, B., and Grandgeorge, S. (1995). "Experimental Study of Particulate Fouling in An Industrial Heat Exchanger." *Journal of Enhanced Heat Transfer*, 2(1-2), 167-175.
11. Bott, T. R. (1988a). "Crystallisation fouling - Basic science and models." Fouling Science and Technology, L. F. Melo, T. R. Bott, and C. A. Bernardo, eds., Kluwer Academic, Dordrecht, Boston, London, 251-260.

12. Bott, T. R. (1988b). "General Fouling Problems." Fouling Science and Technology, L. F. Melo, T. R. Bott, and C. A. Bernardo, eds., Kluwer Academics, Dordrecht, Boston, London, 3-14.
13. Bott, T. R. (1995). *Fouling of Heat Exchangers*, Elsevier, Amsterdam, New York.
14. Bott, T. R. (1997). "Aspects of Crystallization Fouling." *Experimental Thermal and Fluid Science*, 14, 356-360.
15. Chamra, L. M., and Webb, R. L. (1994). "Modelling Liquid-side Particulate Fouling in Enhanced Tubes." *International Journal of Heat and Mass Transfer*, 37(4), 571-579.
16. Chan, V. A., Ang, H.M., Kristall, Z. and Vautier, T. (1997). "Crystallization of Calcium Sulphate Dihydrate." *25th Australian and New Zealand Chemical Engineers' Conference and Exhibition,*, Rotorua, N Z.
17. Characklis, W. G. (1990). " Microbial Fouling." Biofilms, W. G. Characklis and K. C. Marshall, eds., Wiley, New York.
18. Chong, T. H., and Sheikholeslami, R. (2001). "Thermodynamics and kinetics for mixed calcium carbonate and calcium sulphate precipitation." *Chemical Engineering Science*, 56(18), 5391-5400.
19. Cowan, J. C., and Weintritt, D. J. (1976). *Water-Formed Scale Deposits*, Gulf Publishing, Houston, TX.
20. Crittenden, B. D. (1988). "Basic science and models of reaction fouling." Fouling Science and Technology, L. F. Melo, T. R. Bott, and C. A. Bernardo, eds., Kluwer Academics, Dordrecht, Boston, London, 293-313.
21. Edinger, S. E. (1973). "The Growth of Gypsum.An investigation of the factors which affect the size and growth rates of the habit faces of gypsum." *Journal of Crystal Growth*, 18, 217-224.
22. El Dahan, H. A., and Hegazy, H. S. (2000). "Gypsum scale control by phosphate ester." *Desalination*, 127, 111-118.
23. Epstein, N. (1983). "Thinking about Heat Transfer Fouling: A 5 x 5 Matrix." *Heat Transfer Engineering*, 4(1), 43-56.
24. Epstein, N. (1988). "General thermal fouling models." Fouling Science and Technology, L. F. Melo, T. R. Bott, and C. A. Bernardo, eds., Kluwer Academic, Dordrecht, Boston, London, 15-30.

25. Forster, M., Augustin, W., and Bohnet, M. (1999). "Influence of the adhesion force crystal/heat exchanger surface on fouling mitigation." *Chemical Engineering and Processing*, 38, 449-461.
26. Forster, M., and Bohnet, M. (2000). "Modification of molecular interactions at the interface crystal/heat transfer surface to minimize heat exchanger fouling." *International Journal of Thermal Sciences*, 39(7), 697-708.
27. Gill, J. S., Nancollas, G.H. (1980). "Kinetics of growth of calcium sulfate crystals at heated metal surfaces." *Journal of Crystal Growth*, 48, 34-40.
28. Grandgeorge, S., Jallut, C., and Thonon, B. (1998). "Particulate Fouling of Corrugated Plate Heat Exchangers - Global Kinetics and Equilibrium Studies." *Chemical Engineering Science*, 53(17), 3051-3071.
29. Gudmundsson, J. S. (1981). "Particulate Fouling." Fouling of Heat Transfer Equipment, E. F. C. Somerscales and J. G. Knudsen, eds., Hemisphere Publishing, Washington, D.C., 357-387.
30. Hasson, D. (1981). "Precipitation Fouling." Fouling of Heat Transfer Equipment, E. F. C. Somerscales and J. G. Knudsen, eds., Hemisphere, New York, 527-568.
31. Hasson, D., Bramson, D., Limoni-Relis, B., and Semiat, R. (1996). "Influence of the flow system on the inhibitory action of $CaCO_3$ scale prevention additives." *Desalination*, 108, 67-79.
32. Hasson, D., Sherman, H., and Biton, M. (1978). "Prediction of calcium carbonate scaling rates." *6th International Symposium on Fresh Water from the Sea*, 193-199.
33. Hasson, D., and Zahavi, J. (1970). "Mechanism of Calcium Sulfate Deposition on Heat-Transfer Surfaces." *Industrial and Engineering Chemistry Fundamentals*, 9(1), 1-10.
34. He, S., Oddo, J. E., and Tomson, M. B. (1994). "The inhibition of gypsum and barite nucleation in NaCl brines at temperatures from 25 to 90° C." *Applied Geochemistry*, 9, 561-567.
35. Headley, G., Muryanto, S., and Ang, H. M. (2001). "Effects of Additives on the Crystallisation Rate of Calcium Sulphate Dihydrate." *6th World Congress of Chemical Engineering,*, Melbourne, Australia, 2312.
36. Helalizadeh, A., Muller-Steinhagen, H., and Jamialahmadi, M. (2000). "Mixed salt crystallisation fouling." *Chemical Engineering and Processing*, 39, 29-43.

37. Hodgson, T. D., and Jordan, T. W. J. (1976). "Scaling in Vertical Tube, Falling Film Evaporators." *5th International Symposium on Fresh Water from the Sea*, 295-303.

38. Huttinger, K. J. (1988). "Surface Bound Biocides - A Novel Possibility to Prevent Biofouling." Fouling Science and Technology, L. F. Melo, T. R. Bott, and C. A. Bernardo, eds., Kluwer Academic, Dordrecht, Boston, London, 233-239.

39. Kagawa, M., Sheehan, M. E., and Nancollas, G. H. (1981). "The Crystal Growth of Gypsum in Ammoniacal Environment." *Journal of inorganic and nuclear chemistry*, 43, 917-920.

40. Karabelas, A. J., Yiantsios, S. G., Thonon, B., and Grillot, J. M. (1997). "Liquid-side Fouling of Heat Exchangers - An Integrated R-and-D Approach for Conventional and Novel Designs." *Applied Thermal Engineering*, 17(8-10), 727-737.

41. Klepetsanis, P. G., Dalas, E., Koutsoukos, P.G. (1999). "Role of Temperature in the Spontaneous Precipitation of Calcium Sulfate Dihydrate." *Langmuir*, 15, 1534-1540.

42. Klepetsanis, P. G., and Koutsoukos. (1989). "Precipitation of calcium sulfate dihydrate at constant calcium activity." *Journal of Crystal Growth*, 98, 480-486.

43. Klima, W. F., and Nancollas, G. H. (1987). "The Growth of Gypsum." *AIChE Symposium Series*, 83(253), 23-30.

44. Krause, S. (1993). "Fouling of heat transfer surfaces by crystallization and sedimentation." *International Chemical Engineering*, 33(3), 355-401.

45. Li, W., and Webb, R. L. (2000). "Fouling in enhanced tubes using cooling tower water. Part II: combined particulate and precipitation fouling." *International Journal of Heat and Mass Transfer*, 43, 3579-3588.

46. Linnikov, O. D. (1999). "Investigation of the initial period of sulphate scale formation. Part 1. Kinetics and mechanism of calcium sulphate surface nucleation at its crystallization on a heat-exchange surface." *Desalination*, 122, 1-14.

47. Liu, S. T., and Nancollas, G. H. (1970). "The Kinetics of Crystal Growth of Calcium Sulphate Dihydrate." *Journal of Crystal Growth*, 6, 281-289.

48. Liu, S. T., and Nancollas, G. H. (1973). "The Crystal Growth of Calcium Sulfate Dihydrate in the Presence of Additives." *Journal of Colloid and Interface Science*, 44(3), 422-429.
49. Masri, M. A., and Cliffe, K. R. (1996). "A Study of the Deposition of Fine Particles in Compact Plate Fin Heat Exchangers." *Journal of Enhanced Heat Transfer*, 3(4), 259-272.
50. McCartney, E. R., and Alexander, A. E. (1958). "The effect of additives upon the process of crystallisation. I.Crystallisation of calcium sulfate." *Journal of Colloid Science*, 13, 383-396.
51. Middis, J., Paul, S. T., and Muller-Steinhagen, H. (1998). "Reduction of Heat Transfer Fouling by the Addition of Wood Pulp Fibers." *Heat Transfer Engineering*, 19(2), 36-44.
52. Mori, H., Nakamura, M., and Toyama, S. (1996). "Crystallization Fouling of Calcium Sulfate Dihydrate on Heat Transfer Surfaces." *Journal of Chemical Engineering of Japan*, 29(1), 166-173.
53. Muller-Steinhagen, H., and Branch, C. A. (1988). "Calcium carbonate fouling of heat transfer surfaces." *CHEMECA*, Sydney, Australia, 101-106.
54. Murray, N. (1997). "Continuous Crystallisation of Calcium Sulphate Dihydrate," Final Year Undergraduate Project, Curtin University of Technology, Perth,Western Australia.
55. Muryanto, S., and Ang, H. M. "Crystallisation Kinetics of Calcium Sulphate Dihydrate in the Presence of Additives." (2002). *2nd World Engineering Congress*, Sarawak, Malaysia.
56. Muryanto, S., Ang, H. M., Santoso, E., and Parkinson, G. M. (2002). "Gypsum Scaling in Isothermal Flow Systems." *Regional Symposium on Chemical Engineering 2002*, Kuala Lumpur, Malaysia.
57. Nancollas, G. H. (1979). "The Growth of Crystals in Solution." *Advances in Colloid and Interface Science*, 10, 215-252.
58. Nancollas, G. H. (1983). "The Nucleation and Growth of Scale Crystals." Fouling of Heat Exchanger Surfaces, R. W. Bryers, ed., Engineering Foundation, New York.
59. Nancollas, G. H., and Klima, W. F. (1982). "Scale Formation at Heated Metal Surfaces - A Model Cooling Tower System." *Materials Performance*, 9-12.

60. Nancollas, G. H., and Reddy, M. M. (1974). "The Kinetics of Crystallization of Scale-Forming Minerals." *Society of Petroleum Engineers Journal*, 117-126.

61. Nancollas, G. H., White, W., Tsai, F., and Maslow, L. (1979a). "The Kinetics and Mechanism of Formation of Calcium Sulfate Scale Minerals - The Influence of Inhibitors." *Corrosion - NACE*, 35(7), 304-308.

62. Nancollas, G. H., White, W., Tsai, F., and Maslow, L. (1979b). "The Kinetics and Mechanism of Formation of Calcium Sulfate Scale Minerals. The Influence of Inhibitors." *Corrosion - NACE*, 35(7), 304-308.

63. Northwood, T. (1995). "Scale reduction in Process Water Pipes at Murchison Zinc," Final Year Undergraduate Project, Curtin University of Technology, Perth, Western Australia.

64. Nulty, J. H., Grace, B., and Cunningham, D. (1991). "Control of Calcium Based Scales in Australian Mineral Processing." *World Gold 91*, 185-188.

65. Oner, M., Dogan, O., Oner, G. (1998). "The influence of electrolytes architecture on calcium sulfate dihydrate growth retardation." *Journal of Crystal Growth*, 186, 427-437.

66. Perry, R. H., and Green, D. W. (1997). *Perry's Chemical Engineers' Handbook*, McGraw-Hill, New York, etc.

67. Sarig, S., Kahana, F., and Leshem, R. (1975). "Selection of threshold agents for calcium sulfate scalecontrol on the basis of chemical structure." *Desalination*, 17, 215-229.

68. Sarig, S., and Mullin, J. W. (1982). "Effect of Trace Impurities on Calcium Sulphate Precipitation." *Journal of Chemical Technology and Biotechnology*, 32, 525-531.

69. Sheikholeslami, R. (1999). "Composite fouling - inorganic and biological. A review." *Environmental Progress*, 18(2), 113-122.

70. Sheikholeslami, R. (2000a). "Calcium Sulfate Fouling - Precipitation or Particulate: A Proposed Composite Model." *Heat Transfer Engineering*, 21(3), 24-33.

71. Sheikholeslami, R. (2000b). "Composite Fouling of Heat Transfer Equipment in Aqueous Media - A Review." *Heat Transfer Engineering*, 21(3), 34-42.

72. Sheikholeslami, R., and Ng, M. (2001). "Calcium sulfate precipitation in the presence of nondominant calcium carbonate: Thermodynamics and kinetics." *Industrial and Engineering Chemistry Research*, 40(16), 3570-3578.

73. Smith, B. R., and Alexander, A. E. (1970). "The Effect of Additives on the Process of Crystallization. II. Further Studies on Calcium Sulphate (1)." *Journal of Colloid and Interface Science*, 43(1), 81-88.

74. Sudmalis, M., and Sheikholeslami, R. (2000). "Coprecipitation of $CaCO_3$ and $CaSO_4$." *The Canadian Journal of Chemical Engineering*, 78, 21-31.

75. Tadros, M. E., and Mayes, I. (1979). "Linear Growth Rates of Calcium Sulfate Dihydrate Crystals in the Presence of Additives." *Journal of Colloid and Interface Science*, 72(2), 245-254.

76. Vetter, O. J. (1972). "An evaluation of scale inhibitor." *Journal of Petroleum Technology*, 24, 997-1006.

77. Watkinson, A. P., and Wilson, D. I. (1997). "Chemical Reaction Fouling. A Review." *Experimental Thermal and Fluid Science*, 14(4), 361-374.

78. Weijnen, M. P. C., and van Rosmalen, G. M. (1984). "The Role of Additives and Impurities in the Crystallization of Gypsum." *Industrial Crystallization 84*, 61-66.

79. Yuan, M. D., Todd, A. C., and Sorbie, K. S. (1994). "Sulphate scale precipitation arising from seawater injection - A prediction study." *Marine and Petroleum Geology*, 11(1), 24-30.

CHAPTER 4 BATCH CRYSTALLISATION OF GYPSUM IN THE PRESENCE OF ADMIXTURES

4.1. Introduction

During a crystallisation process, admixtures play an important role. They can act as growth modifiers, growth inhibitors or nucleation controllers. Admixtures are sometimes added to the crystallising solution to produce end products with predetermined qualities. It is common practice to alter the shape of crystals using admixtures so that flowability and/or filterability of the crystals can be improved (Weijnen and van Rosmalen 1984). Since admixtures (= additives) can be selected and added in precise amount, they are also able to control the change of shape of the crystals. Admixtures can also be added with the purpose of restraining the growth of crystals. This is the case when fouling or scaling on pipes or other equipment is to be prevented. By adding admixtures it is hoped that the shape of the crystals will change so as to lessen the tendency of the crystals to agglomerate. Then, the crystals will not attach to the surface of equipment or pipes, but will float freely in solution and can be swept away by the flowing fluid easily. In addition, admixtures can also reduce scaling by decreasing crystal growth rates.

In an attempt to better understand the retarding effect of admixtures on gypsum scale formation found in mineral processing industries, for example in flotation water piping system, crystallisation of gypsum was investigated in the present study, in which two biodegradable admixtures normally used in copper/zinc concentrate production were investigated. A laboratory batch crystalliser was used in this study to obtain experimental data, which can later be used to determine the mean residence time and other parameters for a continuous crystallisation experiment.

The batch crystallisation experiments were run using seeded method and it was discovered that the added seed crystals start growing immediately upon addition into the supersaturated solution, i.e. there is no induction time in this particular system.

The typical curves for the desupersaturation of Ca^{2+} ions versus crystallisation run times show that the reduction of calcium ion concentrations takes place rapidly in the

first 5 to 10 minutes of the run. Hence this length of time will be a guide in establishing the mean residence time for subsequent crystallisation experiments on gypsum carried out in a continuous mode (see **Chapter 6**).

The results of this batch crystallisation study suggest that addition of admixtures individually or in combination, significantly affects the crystallisation kinetics and in particular, reduces the rate of crystallisation of gypsum from aqueous solution.

This chapter consists of the following subheadings.

1. Introduction
2. Experimental Design for Batch Crystallisation
3. Experimental
4. Determination of Reaction Rate Constant
5. Determination of Activation Energy
6. Morphology and Surface Topography of the Crystals
7. Adsorption of Admixtures on Crystal Surface
8. Conclusion
9. Summary.

4.2. Experimental Design for Batch Crystallisation

The experimental design used for this study of batch crystallisation of gypsum is the "**One-factor-at-a-time**" method (Davies 1978). This was necessary due to the lack of comparable studies on which to base crystalliser settings. Literature search revealed that batch crystallisation operating conditions for gypsum vary widely, as can be seen in **Table 4.1**. It was therefore decided that the variable under investigation was set at a value estimated to give meaningful results and was then adjusted based on the results of this initial estimate. The variable values selected by this method included admixture concentration, seed slurry density and crystallisation run times.

Table 4.1 Operating conditions of the seeded batch crystallisation of gypsum chosen by different researchers

Crystallising solution	Crystalliser volume	Slurry density	Admixture & concentration	Crystallisation time	References
$Ca(Cl)_2 + Na_2SO_4$	0.30 L	0.31 - 2.87 g/L	No admixtures	up to 180 minutes	Liu & Nancollas, 1970
$Ca(Cl)_2 + Na_2SO_4$	0.30 L	0.88 - 3.03 g/L	NTMP : $(0.2 - 10.9)x10^{-5}$ M ENTMP : $(0.01 - 1.1)x10^{-5}$ M EDTA : 2.70×10^{-5} M HEDP: 10.02×10^{-5} M $(NH_4)_6Mo_7O_{24}$: 0.94×10^{-5} M	up to 8 hours	Liu & Nancollas, 1973
$CaSO_4.½\ H_2O + H_2O$ + NaCl	0.10 L	20.00 g/L	0.5 - 1.0 M NaCl	up to 300 minutes	Brandse & van Rosmalen, 1977
$CaSO_4.½\ H_2O + H_2O$	0.30 L	Not stated	Polycarboxylates: 0.2 - 0.8 ppm HEDP: 0.2 - 0.8 ppm Cu^{2+} : $10^{-5} - 10^{-3}$ M Zn^{2+}: 10^{-4} M	up to 100 minutes	Weijnen & van Rosmalen, 1984
$Ca(Cl)_2 + Na_2SO_4$	0.15 L	1.30 - 2.10 g/L	Polymer: 0.1 - 1.0 ppm	up to 10 hours	Amjad, 1987
$Ca_3(PO_4)_2 + H_2SO_4$	1.00 L	2.00 g/L	0.5 % F^- 0.05 % Fe 0.02 % Al	1 to 10 minutes	White & Mukhopadhyay, 1989
$Ca(NO_3)_2 + Na_2SO_4$	1.00 L	100.00 g/L	$NaNO_3$: 0.1 - 1.0 M $NaClO_4$: 0.1 M	Not given	Witkamp *et al.*, 1990
$CaCl_2.2H_2O$ + NaCl + Na_2SO_4	0.50 L	0.20 - 4.00 g/L	0.1 - 6.0 M NaCl	up to 450 minutes	He *et al.*, 1994

Table 4.1 contains the operating conditions of several investigations on batch crystallisation of gypsum both in a pure system as well as in the presence of admixtures. As can be seen in the table, different values of slurry density have been used, as well as other parameters. The values could have been selected on the basis of the expected effect of the admixtures on crystallisation process, notably the crystallisation kinetics.

A slurry density of 15.00 g/L had been used in previous Chemical Engineering Projects on crystallisation of gypsum (Murray 1997; Northwood 1995). In the present study a value of 8.00 g/L was selected and it proved satisfactory for crystallisation kinetics determination, and had been used for all subsequent crystallisation runs.

A similar situation was experienced in the optimisation of crystallisation run times. Previous projects (Murray 1997) had used times of 120 minutes; however, upon investigation of initial results it was found that 90 minutes was sufficient to allow the crystallisation to come to equilibrium.

Initial admixture concentration levels tested were those currently used in mineral processing flotation circuits (Headley *et al.* 2001). If these concentration levels proved to significantly vary the crystallisation rate constant, a level of double and half the initial amount used could be tested. This gave three data sets with the remaining four runs allocated to each admixture being used to confirm trends (using intermediate admixture concentration levels) and for the investigation of temperature effects at plant concentration levels. The operating variables used for each crystallisation run are shown in **Tables 4.2** and **4.3**.

Table 4.2 Fixed variables used in the seeded batch crystallisation experiments

Variable	Set value
Slurry density, (g/L)	8.00
Impeller speed, (rpm)	125
Crystalliser volume, (L)	2.00
Crystallisation time, (minute)	90
Initial Ca^{2+} concentration, (ppm)	2,000

Two different admixtures were chosen for this study, namely sodium isopropyl xanthate (= SIPX) and isopropyl thionocarbamate. Both of them are common flotation agents used in mineral processing (Headley *et al.* 2001).

Table 4.3 Manipulated variables used in the seeded batch crystallisation experiments

Trial no.	SIPX concentration, (g/L)	Isopropyl thionocarbamate concentration, (g/L)	Crystalliser temperature, (^{0}C)
1	0.00	0.00	25
2	0.00	0.00	25
3	0.05	0.00	25
4	0.10	0.00	25
5	0.20	0.00	25
6	0.20	0.00	35
7	0.20	0.00	45
8	0.30	0.00	25
9	0.40	0.00	25
10	0.00	0.0175	25
11	0.00	0.035	25
12	0.00	0.07	25
13	0.00	0.07	35
14	0.00	0.07	45
15	0.00	0.14	25
16	0.00	0.21	25
17	0.20	0.07	25
18	0.05	0.035	25

4.3. Experimental

A crystalliser operating in a batch mode was utilised in this study. It has a working volume of two litres, made of stainless steel with four internal baffles to prevent vortex. The crystalliser was agitated using a variable speed 45^0 pitched blade impeller and was placed in a thermostatically controlled water bath. The experiment was carried out using seeded growth technique as it was found that the technique is highly reproducible (Gill and Nancollas 1980; Liu and Nancollas 1970). For the crystallising solution, a synthetic gypsum solution was used, made by dissolving calcium chloride dihydrate ($CaCl_2.2H_2O$) and anhydrous sodium sulphate (Na_2SO_4) in equimolar amounts in distilled water, respectively. Gypsum crystals sized 53 to 90 μm were used as seeds.

Stirring rate was fixed at a speed of 125 rpm as it was found that this speed was sufficient to make the seed crystals evenly suspended in the solution. Initial concentration of the synthetic gypsum solution in the crystalliser was 2,000 ppm of Ca^{2+}.

One litre each of 0.1 M calcium chloride solution and sodium sulphate solution were prepared according to the procedure set out in **section 4.2** (= **Experimental Design for Batch Crystallisation**). The two solutions were placed in the crystalliser, the impeller was started and the whole system was left to equilibrate to the designated temperatures: 25, 35 or 45^0C. Having reached the designated temperature, a 20 ml solution sample (which corresponds to **t = 0** or **zero time**) was taken and prepared for atomic absorption spectrometry (AAS) analysis. Sixteen grams of gypsum seed crystals were added into the crystalliser and the timer was started. During the experimental run, solution samples (each of 20 ml volume) were withdrawn from the crystalliser at 2, 5, 10, 15, 20, 30, 40, 60 and 90 minutes, respectively after the seed addition, filtered through 0.22-μm filter paper (Millipore™ Corp.), and stored in vials ready for AAS analysis. After the completion of one experiment, the crystalliser and its accessories were cleaned and prepared for the next run.

4.4. Determination of Reaction Rate Constant

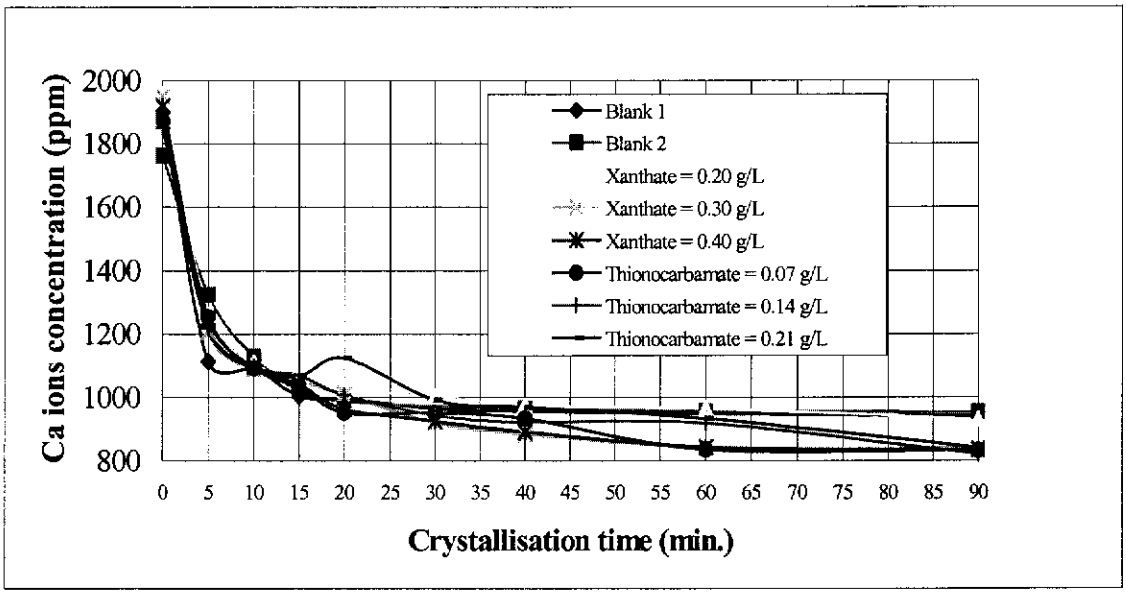

Figure 4.1 Typical desupersaturation curves for Ca^{2+} versus time in the batch crystallisation

The typical curves for desupersaturation of calcium ions against crystallisation time are shown in **Figure 4.1**. In each case the reduction of calcium ion concentrations takes place rapidly in the first 5 to 10 minutes of the run. It can be seen that the added seed crystals start growing immediately upon addition into the supersaturated solution; i.e. there is no induction time.

Determination of the reaction rate constant for subsequent crystal growth determination in solutions can be explained by using the diffusion model of Chernov (Myerson 1993). The model proposes that the diffusion of solute or growth units in the boundary layer and the thickness of the boundary layer are important aspects in controlling the growth.

The growth of crystals in a supersaturated solution according to the diffusion layer model of Chernov proceeds through the following steps. Firstly, transfer of growth units from the bulk of the solution to the diffusion layer. Secondly, diffusion of the transferred growth units in the diffusion layer. Finally, integration of the growth units onto the crystal surface and, further, into the crystal lattice.

As the growth units leave the diffusion layer toward the crystal surface, the integration of them onto the crystals causes an increase in the mass of the crystals, which can be expressed as the diffusion rate equation or Fick's first law (Nyvlt 1985) as follows.

$$\frac{\partial m}{\partial t} = DA\frac{\partial C}{\partial x} \tag{4.1}$$

where,

$\partial m/\partial t$ = rate of mass increase, g/sec

D = diffusion coefficient, cm^2/sec

A = surface area of crystal, cm^2

$\partial C/\partial x$ = concentration gradient of growth units in the diffusion layer, $g/cm^3.cm$

The concentration gradient of growth units in the diffusion layer is dependent on position. In other words, it represents the amount of growth units with respect to the position in the diffusion layer. It can be assumed that further away from the crystal-liquid interface and towards the bulk of the solution, the concentration will be higher and the difference acts as a driving force for the growth units to move towards the crystal-liquid interface or the diffusion layer. Thus the following equation can be proposed:

$$\frac{dC}{dx} = \frac{C - C_i}{\delta} \tag{4.2}$$

where,

C = concentration of growth units in the bulk of the solution, g/cm^3

C_i = concentration of growth units in the crystal/solution interface, g/cm^3

δ = thickness of diffusion layer or boundary layer, cm.

Substituting **Eq.(4.2)** into **Eq.(4.1)** results in **Eq. (4.3)** as follows:

$$\frac{dm}{dt} = k_d A(C - C_i) \tag{4.3}$$

where, $k_d = D/\delta$.

As can be seen in both **Eqs. (4.2)** and **(4.3)**, the rate of integration of growth units into the crystal lattice is dependent on the difference between their concentration in the diffusion layer and that in the bulk of the solution. Nyvlt (Nyvlt 1985) and Myerson (Myerson 1993) have used an approximation to **Eq. (4.3)**, which is written as **Eq. (4.4)** as follows:

$$\frac{dm}{dt} = k_i A(C_i - Ceq)^i \tag{4.4}$$

where,

k_i = proportionality or rate constant, dimensionless

C_{eq} = concentration of growth units in the bulk of the solution at equilibrium conditions, g/cm^3

i = an empirical exponent representing the reaction order, dimensionless.

The factor $\mathbf{k_i}$ in **Eq. (4.4)** is termed the proportionality or the rate constant for the integration of growth units into the crystal lattice. The empirical exponent, ***i***, depends on the crystallisation conditions and has values between **1** and **2**.

The interfacial concentration, $\mathbf{C_i}$, is difficult to measure and therefore elimination of it in the equation has been attempted by combining **Eqs. (4.3)** and **(4.4)**.

A simpler equation than that of **Eq. (4.4)** is generally used (Myerson 1993) which takes the following form:

$$\frac{dm}{dt} = K_G A\left(C - C_{eq}\right)^g \tag{4.5}$$

where the exponent, **g**, has values between **1** and **2**.

In many crystallisation studies, the constant, $\mathbf{K_G}$, and the surface area, **A**, are replaced by **k**, and is termed the crystallisation rate constant.

In crystallisation from solutions containing equimolar lattice ions, it is expected that the crystallisation rate follows **Eq. (4.5)** (Liu and Nancollas 1970). In many gypsum crystallisation system (Amjad and Hooley 1986; Amjad and Masler 1985; Christoffersen *et al.* 1982; He *et al.* 1994; Klima and Nancollas 1987; Liu and Nancollas 1970; Liu and Nancollas 1973; Nancollas *et al.* 1979), especially when no induction period was observed, the value of **g** in **Eq. (4.5)** was taken as equal to **2**, and that the value was used in this study. Furthermore, the surface area term, **A**, was assumed to be relatively constant.

With equimolar concentrations of lattice ions in the crystallisation solution, **Eq. (4.5)** can be rewritten as:

$$-\frac{dCa}{dt} = k\left(Ca_t - Ca_{eq}\right)^N \tag{4.6}$$

where,

- dCa/dt = rate of lattice ion concentration decrease due to crystallisation, (ppm. min^{-1})

Ca = lattice ion concentration of the crystallising solution, (in this study = concentration of Ca^{2+}, (ppm)

Ca_t = lattice ion concentration of the solution at time **t**, (ppm)

Ca_{eq} = lattice ion concentration of the solution at equilibrium,
= lattice ion concentration of the solution at **t** = 90 minutes, (ppm)

k = crystallisation rate constant, (ppm^{-1}. min^{-1})

N = reaction order = 2.

Upon integration, with **N = 2**, **Eq. (4.6)** yields the following:

$$\frac{1}{Ca_t - Ca_{eq}} - \frac{1}{Ca_0 - Ca_{eq}} = kt \qquad (4.7)$$

where,

Ca_0 = lattice ion concentration of the solution at **t = 0**, (ppm)

t = crystallisation time, (minutes).

Concentrations of the lattice ions were calculated as the concentrations of Ca^{2+} in the crystallising solution. Atomic absorption spectrometry (AAS) was used to calculate the concentrations as required. Using **Eq. (4.7)**, concentrations of Ca^{2+} obtained from AAS determination were then plotted versus time of crystallisation, which resulted in a straight line having slope equals to **k**, which is the reaction rate constant of the crystallisation process.

4.4.1. Sample calculation of the determination of reaction rate constant

A sample calculation of the reaction rate constant is presented below for the condition of crystallisation run with no admixtures.

Plotting **Eq. (4.7)** with the data as shown in **Table 4.4** will result in a graph as shown in **Figure 4.2**, where **F** or the **Y** axis represents the left hand side of **Eq. (4.7)**. The slope of the straight line is the reaction rate constant, **k**. As can be observed from

Figure 4.2, the slope of the straight line is 0.0014. The precise value of the slope was obtained from Data Analysis using Excell™, which is equal to 0.001405. Hence the value of the reaction rate constant **k**, is 0.0014 ppm^{-1} min^{-1}.

Table 4.4 Desupersaturation data for crystallisation run without admixtures

Sampling time, (minutes)	$[Ca^{2+}]$, (ppm)	$1/[Ca_t - Ca_{eq}]$ (ppm^{-1})	$1/[Ca_0 - Ca_{eq}]$ (ppm^{-1})
0	1901	0.00104	0.00104
2	1251	0.00321	0.00104
5	1112	0.00581	0.00104
10	1093	0.00653	0.00104
15	1004	0.01562	0.00104
20	995	0.01818	0.00104
30	965	0.04000	0.00104
40	957	0.05882	0.00104
60	949	0.11111	0.00104
90	940	∞	0.00104

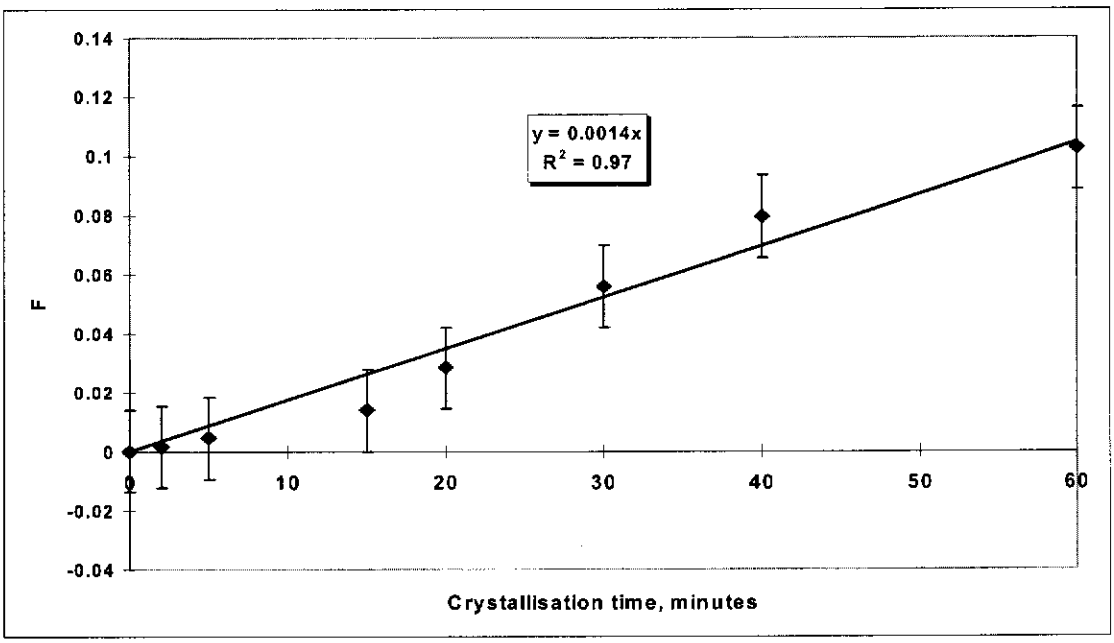

Figure 4.2 Typical plot of the determination of a second order reaction rate constant

The fully calculated results of the rate constant, **k**, for the entire batch crystallisation runs, are shown in **Tables 4.5 to 4.7**.

Table 4.5 Second order rate constant of gypsum crystallisation at 25^{0}C

Admixtures	Admixture concentration, (g/L)	2nd Order rate constant, (ppm^{-1} . min^{-1}) x 10^6
No admixture	0.000	1,405 ± 71
No admixture	0.000	1,561 ± 79
SIPX	0.050	871 ± 44
SIPX	0.100	568 ± 29
SIPX	0.200	475 ± 24
SIPX	0.300	440 ± 22
SIPX	0.400	365 ± 19
Isopropyl thionocarbamate	0.0175	830 ± 42
Isopropyl thionocarbamate	0.035	487 ± 25
Isopropyl thionocarbamate	0.070	254 ± 13
Isopropyl thionocarbamate	0.140	191 ± 10
Isopropyl thionocarbamate	0.210	171 ± 9

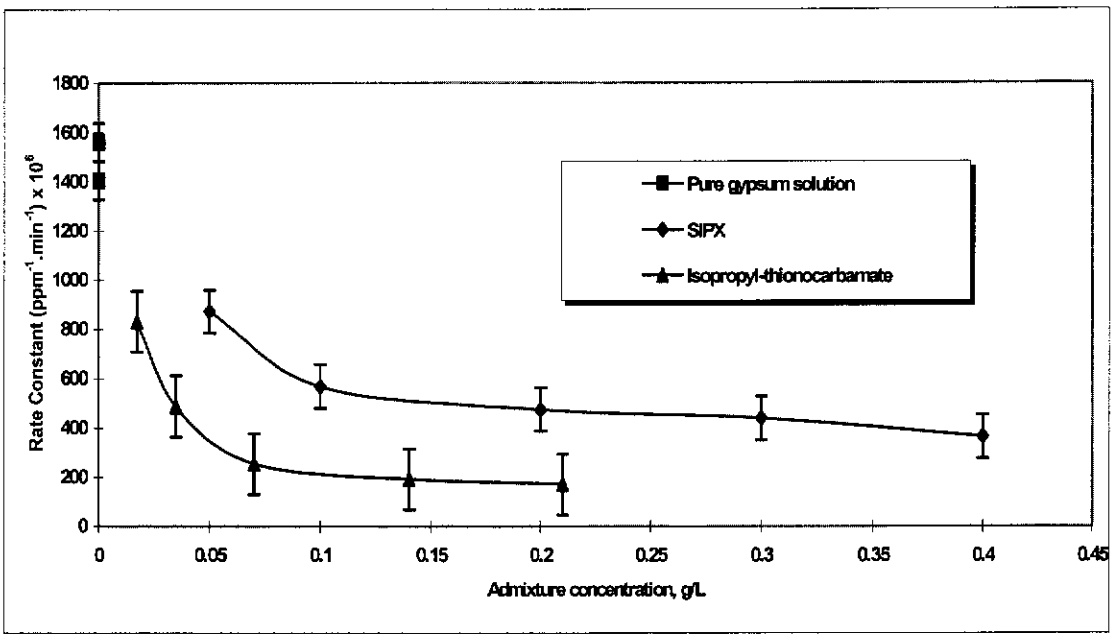

Figure 4.3 Second order rate constant of gypsum crystallisation at 25^{0}C (the data were taken from Table 4.5)

As can be seen from **Table 4.5** and **Figure 4.3**, admixtures drastically suppress the rate constant. For both admixtures, increasing the dosage will result in further suppression. At a plant dosing level of **0.20 g/L**, SIPX decreases the rate constant to about one-third of that without admixtures. It is obvious from the table that the isopropyl thionocarbamate has higher inhibition effect than SIPX. The plant dosing

level of isopropyl thionocarbamate is **0.070 g/L** and can control the rate constant to become around half that of SIPX (= SIPX at a plant dosing level, which is equal to **0.20 g/L**). Increasing the concentration of isopropyl thionocarbamate above plant dosing level, however, does not result in further significant reduction of rate constant. This could be caused by preferential adsorption of admixture molecules onto the crystal surfaces. At the beginning there are a lot of kink sites at the surface of the crystals where the molecules of admixtures tend to bond as kink sites have the highest binding energy. However, in a seeded growth technique, the large number of kinks, if any, will soon disappear due to the rapid 'self healing' of the surface (Nancollas 1979). Consequently, the rate constant will not change as the rest of the admixture molecules stay in the bulk solution and do not attach to the crystal surfaces.

Table 4.6 2^{nd} order rate constant of gypsum crystallisation at 25, 35, and 45 ^{0}C

Admixtures	Admixture conc., g/L	Temp., ^{0}C	k, $(ppm^{-1}\ min^{-1})x10^6$
SIPX	0.20	25	475 ± 24
SIPX	0.20	35	546 ± 28
SIPX	0.20	45	1,245 ± 63
Isopropyl thionocarbamate	0.07	25	254 ± 13
Isopropyl thionocarbamate	0.07	35	596 ± 30
Isopropyl thionocarbamate	0.07	45	1,088 ± 55

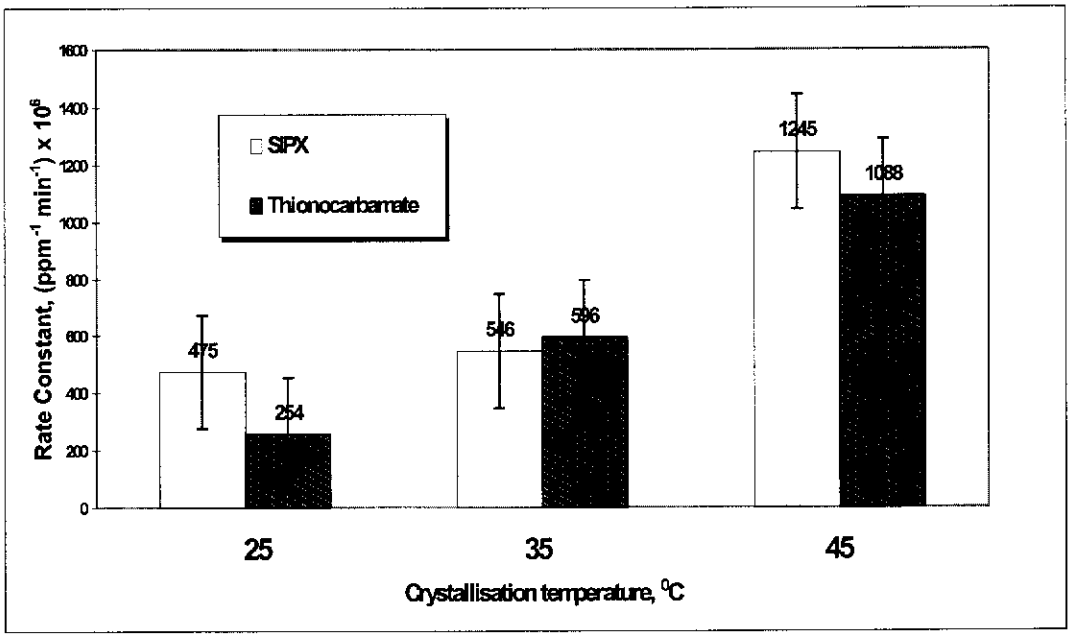

Figure 4.4 Comparison of the reaction rate constant for SIPX and isopropyl thionocarbamate at different crystallisation temperatures

Table 4.6 and **Figure 4.4** show that the rise in temperature enhances the rate constant, but at higher temperatures the effect of the two admixtures on the rate constant is almost the same. It appears that both admixtures have approximately the same effect on the rate constant at intermediate temperature of 35^0C. At lower and higher temperatures, however, the isopropyl thionocarbamate seems to be more effective in reducing the rate constant.

It can be seen from **Table 4.7** that there is a masking effect of isopropyl thionocarbamate on SIPX when these two admixtures are combined. Combination of SIPX and isopropyl thionocarbamate shows that only the effect of isopropyl thionocarbamate is obvious, that of SIPX seems to disappear. It is likely that the masking effect is due to the difference in molecular weight and the structure of the two admixtures. The molecular weight of SIPX ($C_4H_7OS_2Na$) is 158 whereas that of isopropyl thionocarbamate (as thiocarbamic acid, $C_{10}H_{16}Cl_3NOS$) is 304.68 (Howard 1972). The longer C chains of isopropyl thionocarbamate as the "backbone" of the molecular structure might have acted as a fence to block the growth sites and thus stopping the propagating steps (Amjad 1988; Oner 1998).

Table 4.7 Second order rate constant of gypsum crystallisation at 25^{0}C using SIPX, isopropyl thionocarbamate and combination of the two admixtures

Admixture	k, (ppm^{-1} min^{-1})x10^6
0.050 g/L SIPX	871 ± 44
0.035 g/L isopropyl thionocarbamate	487 ± 25
0.050 g/L SIPX + 0.035 g/L isopropyl thionocarbamate	482 ± 24
0.200 g/L SIPX	475 ± 24
0.070 g/L isopropyl thionocarbamate	254 ± 13
0.200 g/L SIPX + 0.070 g/L isopropyl thionocarbamate	244 ± 13

4.5. Determination of Activation Energy

In this seeded batch crystallisation of gypsum, the crystallisation process is essentially a chemical reaction between crystal lattice ions of gypsum: Ca^{2+} and SO_4^{2-}. A chemical reaction proceeds at a certain rate, which is influenced by a number of factors such as concentration, the exposed surface area and activity of seeds, the presence of admixtures, the temperature levels etc. In almost all cases, the rate of chemical reaction increases with increasing temperature. The relationship between the rate of chemical reaction and the temperature is generally explained through the use of Arrhenius law. Collision theory, which was originally developed for reactions in gaseous phase, is usually used to elaborate the rate of chemical reaction in conjunction with Arrhenius law.

Arrhenius law applies to such processes as diffusion, dissolution or crystallisation. In a crystallisation process, the amount of activation energy required for the crystal growth is dependent on the type of the driving force for the growth (Mullin 1972). For diffusion-controlled growth, lower values of activation energy (10 to 20 kJ mol^{-1}) are usually encountered. On the other hand, surface integration controlled growth requires higher activation energy: 40 to 60 kJ mol^{-1}.

The importance of Arrhenius law is that it can be utilised to investigate the effect of temperature on reaction rate with minimal data. The Arrhenius law is represented by **Eq.(4.8)** which shows the dependence of a reaction rate on temperature.

$$k = A\exp\left(\frac{-E_a}{RT}\right) \tag{4.8}$$

or in logarithmic form

$$\ln k = \ln A - \frac{E_a}{RT} \tag{4.8a}$$

where,

k = reaction rate constant, dimensionless

A = Arrhenius parameter
= total number of effective collisions of molecules per second

E_a = activation energy, kJ/mol

R = universal gas constant, 8.31 (kJ)/(mol)(^{0}K)

T = absolute temperature, ^{0}K.

For the experimental data obtained in this batch crystallisation by varying crystalliser temperature, with admixture dosing fixed at normal plant conditions, the Arrhenius parameter of the reaction has been determined. This was done by utilising both **Eq. (4.8)** and its logarithmic form as shown in **Eq. (4.8a)**.

Plotting the natural logarithm of the rate constants at varying temperatures against the inverse of the absolute temperature **(1/T)** results in a straight line. The slope of this line is **$-E_a/R$** and the intercept is the natural logarithm of the pre-exponential factor, **A**, where **E_a** is the activation energy and **R** is the universal gas constant. Typical plots of **1/T** versus **ln (k)** are shown in **Figures 4.5** and **4.6**.

The value of the activation energy, **E_a**, obtained for the isopropyl thionocarbamate admixture at plant dosing level of 0.07 g/L can be calculated from **Figure 4.5**. The slope of the line in **Figure 4.5** = **- E_a/R** = - 6903.4. Hence, **E_a** = 6903.4 x **R**, where **R** = universal gas constant = 8.314 x 10^{-3} kJ/mol. Thus, the activation energy, **E_a** = 6903.4 x 8.314 x 10^{-3} kJ/mol = 57.39 ± 2.87 kJ/mol. The activation energy values, **E_a**, for the three conditions: pure gypsum, in the presence of SIPX and in the presence of isopropyl-thionocarbamate, respectively, are calculated from a similar graph as shown in **Figure 4.6**.

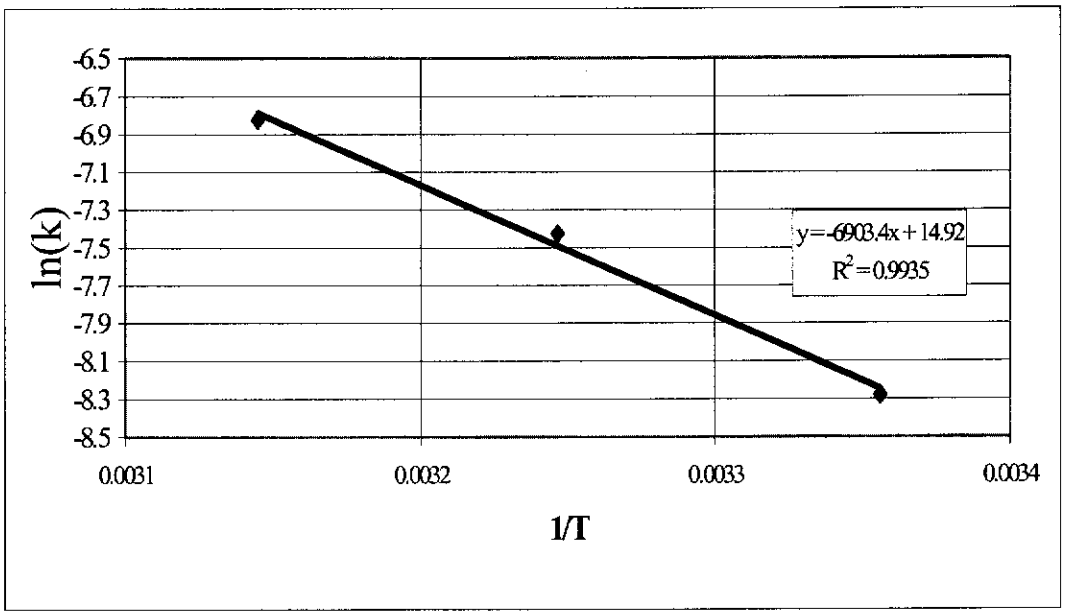

Figure 4.5 Plot of Arrhenius parameter for 0.07 g/L isopropyl thionocarbamate at 25, 35 and 45^{0}C

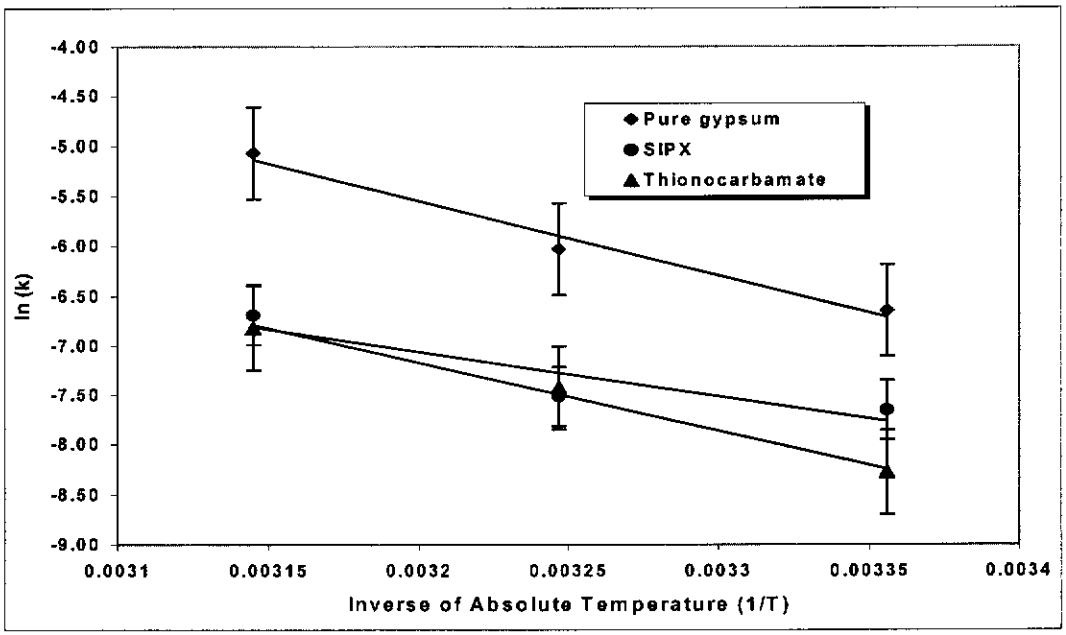

Figure 4.6 Plot of Arrhenius parameter for pure gypsum, SIPX and isopropyl thionocarbamate, respectively, at 25, 35 and 45^{0}C

The activation energy for the pure gypsum solution calculated from **Figure 4.6** is 60.00 kJ mol^{-1}. This value is in very good agreement with similar experiments carried out previously (Liu and Nancollas 1970; Nancollas and Reddy 1974).

Isopropyl thionocarbamate addition also yielded reasonable results compared with other published values for gypsum crystallisation system with admixtures (He *et al.* 1994; White and Hoa 1977). It would be expected that the activation energy calculated for SIPX would also be in the same range as that of isopropyl thionocarbamate since both of them are found as inhibitors for gypsum growth. It turned out, however, that the value of the activation energy for SIPX was lower, which should be contrary to the fact that SIPX hindered the growth. Overall, the activation energy values calculated from **Figure 4.6** are: 60.00 ± 3.00, 57.39 ± 2.87, and 37.65 ± 1.88 kJ/mol, for pure gypsum, isopropyl thionocarbamate, and SIPX, respectively. The corresponding Arrhenius factor, **A**, for the three activation energy values are: 3,017,684 ± 30,177; 89,791,422 ± 1,795,800 and, 1,686 ± 270, respectively. The value for SIPX may not be very accurate due to the poor correlation (coefficient of determination, $\mathbf{R^2 = 0.84}$) of the data obtained.

Table 4.8 Activation energies of several gypsum crystallisation studies

No	Crystallisation mode	Admixtures	Reaction order, N	Activation energy, (kJ/mol)	References
1	Unseeded batch	None	2	160	(Ching and McCartney 1973)
		2 ppm P A A [1)]		90 - 100	
2	Seeded batch	0.0 m NaCl [2)]	2	61	(He *et al.* 1994)
		0.1 m NaCl [2)]		59	
		1.0 m NaCl [2)]		58	
		3.0 m NaCl [2)]		53	
		6.0 m NaCl [2)]		55 (slight increase)	
3	Seeded batch	None	2	61 - 65	(Liu and Nancollas 1970)
4	Seeded batch	None	2	63	(Nancollas and Reddy 1974)
5	Seeded batch	Phosphonates [1)]	2	65	(Liu and Nancollas 1975b)
6	Seeded batch: $Ca_3(PO_4)_2 + H_2SO_4$	Fe^{3+} ,Al^{3+} ,F^- [2)]	2	49 - 59	(White and Hoa 1977)
7	Seeded batch	None	2	75.0	(Mile *et al.* 1982)
		> 0.1 M K_2SO_4 [2)]	1	29	
8	Seeded batch	Polyacrylates [1)]	2	65	(Amjad and Masler 1985)
9	Seeded continous $Ca_3(PO_4)_2 + H_2SO_4$	None	2	64	(White and Mukhopadhyay 1990)
10	Seeded batch	None	2	60	(Witkamp *et al.* 1990)
		1 M $NaNO_3$ [2)]	1.1 - 2.7	20 - 45	
11	Unseeded continous $Ca_3(PO_4)_2 + H_2SO_4$	None	2	65.2	(Jamialahmadi and Muller-Steinhagen 2000)
12	Seeded batch	None	2	64.0	(Kontrec *et al.* 2002)

Notes for **Table 4.8** column 3:

1. Decreasing crystal growth (measured as a function of supersaturation).
2. Increasing crystal growth (measured as a function of supersaturation).
3. Crystal growth increased with temperatures, but the effect of the admixtures used on the growth rate was not reported.

Literature search reveals one significant inconsistency in activation energy similar to that for SIPX obtained in this study, i.e. in the work of Ching and McCartney (Ching and McCartney 1973). These investigators found that adding trace amounts of polyacrylic acid (PAA) into a crystallising solution of gypsum, retarded the crystal growth but decreased the activation energy (see **Table 4.8** first row: the activation energy decreases from 160 to around 100 kJ/mol). They assumed that such a decrease was probably due to the defect or imperfection of the crystal surface, hence

caused easier incorporation of ions into the crystal lattice, which resulted in lower activation energy. The work of He *et al.* on seeded gypsum crystallisation (He *et al.* 1994) also shows such inconsistent calculated activation energies when impurities present in the crystallising solution at certain concentrations. As can be seen in **Table 4.8** (second row), increasing the NaCl concentration in the crystallising solution from 3.0 to 6.0 m, resulted in a slight increase of activation energy, $\mathbf{E_a}$, although the growth was reported to increase. It was thus postulated that the activation energy could be solution composition dependent.

In addition to the two previous reasoning, for the low activation energy for SIPX found in this study, several other possible reasons can be proposed. One possible reason is that the application of Arrhenius law to the system with SIPX might be inappropriate. This can also be seen from the low value of coefficient of determination, $\mathbf{R^2 = 0.84}$, obtained for the SIPX, whereas that for the isopropyl thionocarbamate, the $\mathbf{R^2}$ value is equal to **0.99**. Another possible reason is that a number of researchers have shown that it is very unlikely to find a chemical reaction, which is driven by only one single step process. In other words, two or more competing/opposing reactions might occur which results in inconsistency of the activation energy value (Masel 2001). Still another possible reason is the dependence of mechanism of crystal growth on supersaturation level. At low supersaturation levels, diffusion mechanism is the dominant mechanism while at higher levels the principal mechanism is surface reaction (Nancollas 1979). It could be assumed therefore, that a combination of mechanisms might be operative or competing in a system with intermediate supersaturation levels (as used in the present study), which may lead to the lowering of the activation energy. In a previous investigation on the rate of precipitation of gypsum under the influence of certain inorganic electrolytes, Mile *et al.* (Mile *et al.* 1982), found that the low activation energy value might result from competition between the surface integration and diffusion processes. The same phenomenon was also found in a batch crystallisation system of another sparingly soluble salt ($BaSO_4$) carried out by Taguchi *et al.* (Taguchi *et al.* 1996).

4.6. Morphology and Surface Topography of the Crystals

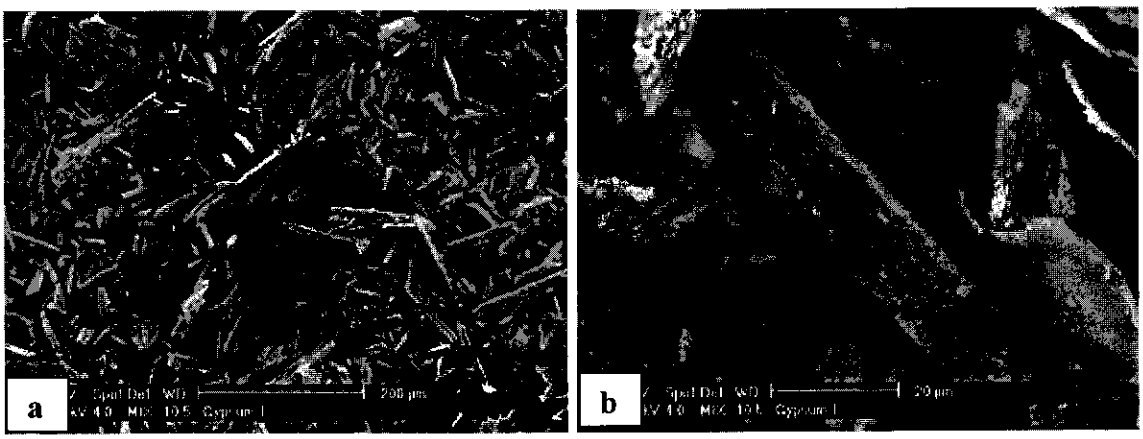

Figure 4.7 Gypsum seed crystals used for the batch experiment

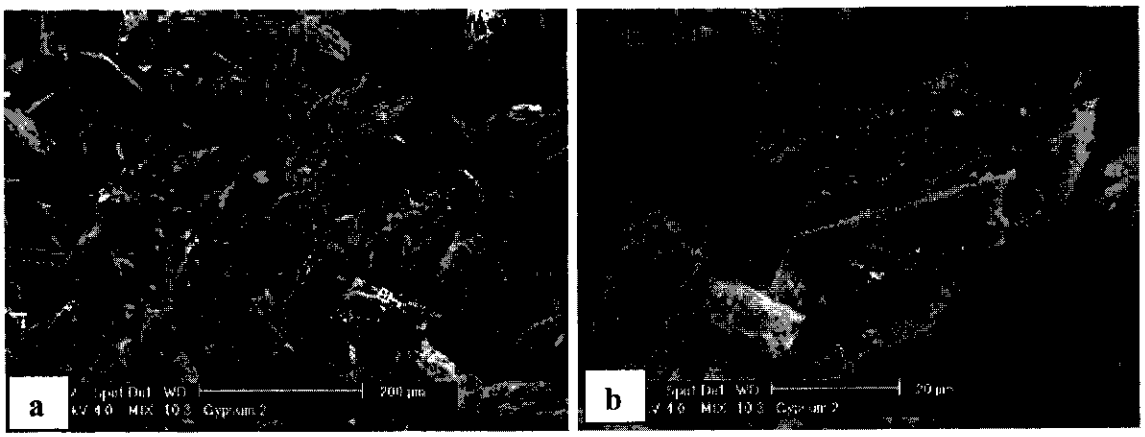

Figure 4.8 Crystal images of pure gypsum after 90 minute of batch crystallisation experiment

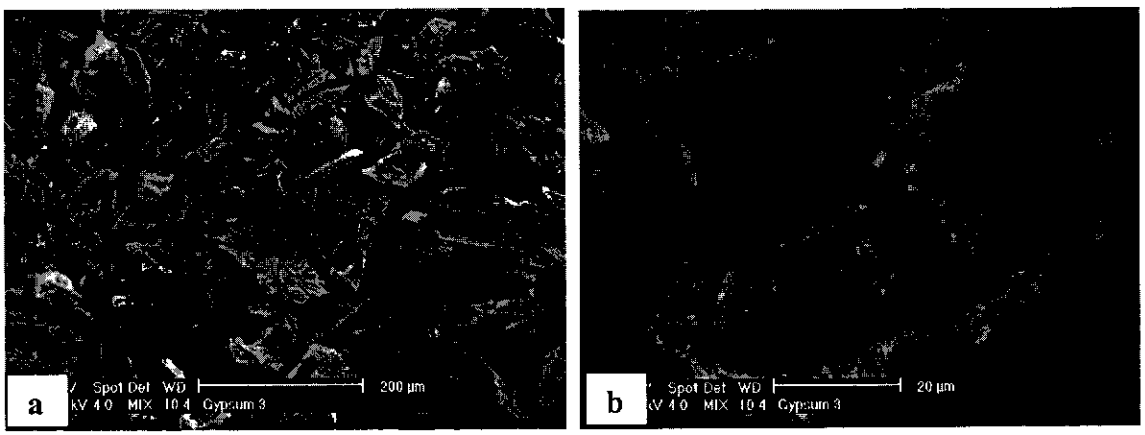

Figure 4.9 Crystal images of gypsum after 90 minute of batch crystallisation experiment in the presence of SIPX

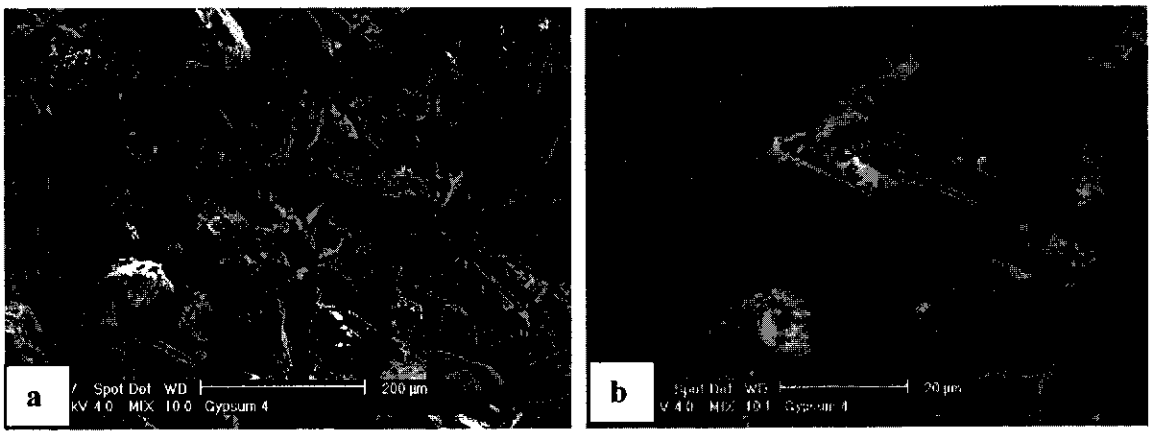

Figure 4.10 **SEM images of gypsum crystals after 90 minute of batch crystallisation experiment in the presence of isopropyl thionocarbamate**

The morphology and surface topography of crystals could be useful in determining the mechanism of crystallisation processes. In the present study, scanning electron micrographs were taken from the gypsum crystals, before as well as after the experiments. These micrographs are presented in **Figs. 4.7** to **4.10**, respectively. The rough surfaces of the seed crystals as shown in **Figure 4.7**, could be regarded as kink sites where the admixture molecules could have been attracted and attached, since such sites have the highest binding energy. In crystallisation experiments using seeded growth method, the large number of kinks, if any, will soon disappear due to the rapid 'self healing' of the surface (Nancollas 1979), coupled with the adsorption of the admixture molecules present in the solution. As a result, the crystal surfaces may become rather smooth, as can be seen in **Figures 4.8** to **4.10**, respectively. These figures also show that the crystals seem to be covered with small and fluffy masses, which could be crystallites or nuclei, indicating that the seeds were able to grow or that surface nucleation might have occurred. The SEM micrographs of the crystals as shown in these figures, however, would not likely be able to explain the effect of individual admixtures used, on the crystallisation kinetics.

In this study, both the pure system and the system with isopropyl thionocarbamate as admixtures produced high activation energies (**Ea > 40 kJ/mol**), which is indicative of a surface reaction process. The application of the second order kinetics model for

the two systems is, therefore, warranted. For the system with SIPX as admixtures, the use of the second order kinetics model yielded a low activation energy of about 38.00 kJ/mole, which indicates that the second order kinetics was probably not suitable. Another reaction order (= first order) was attempted, but was also found to be unsuitable, since the plot of $\mathbf{ln\ [Ca_t/Ca_0]}$ versus **t**, which should result in a straight line for the assumed first order reaction to be correct, resulted in a curved line. Therefore, the low value of activation energy found for the system with SIPX was probably caused by factors other than the reaction order assumed, as elaborated previously.

4.7. Adsorption of Admixtures on Crystal Surface

Adsorption of admixtures on the surface of crystals is one of the significant factors affecting the crystallisation kinetics, i.e. the nucleation and growth of the crystals. Research has shown that a direct relationship may exist between concentration of the adsorbed admixtures and the growth of crystals (Myerson 1993). Many admixtures are known to be able to retard the crystal growth process even if they are present in trace amounts (Amjad 1988; Amjad and Masler 1985; Ohara and Reid 1973; van Rosmalen *et al.* 1981; Weijnen and van Rosmalen 1985). It is therefore believed that this retardation occurs due to the preferential adsorption of the admixtures onto active growth sites available on the crystal surface. Otherwise, a substantial amount of the admixtures will be required in order to cover the entire surface of the crystals, and hence, stop the growth. Liu and Nancollas (Liu and Nancollas 1975a) observed the remarkable inhibiting effect of admixtures on the growth rate of barium sulphate crystals. It was found that at a concentration as low as 4.4×10^{-8} M, sodium tripolyphosphate was able to suppress the overall dissolution rate constant by as much as 90%. They also predicted, if all of the anions from the sodium tripolyphosphate were adsorbed onto the surface of the crystals, only about 30% of the total surfaces of the crystals were covered. Therefore, the surface of the crystals that can really be covered is even smaller, because some anions must have stayed in the bulk of the solution and not adsorbed onto the surface. Therefore, it was concluded that admixtures did not cover the entire surface of the crystals, but only

selectively adsorbed onto active growth sites of the crystals, most probably at kink sites, since such sites offer the highest binding energy.

Growth experiments of gypsum crystals also showed that a small crystal surface coverage of admixtures was sufficient to stop the growth. In one such case even a 5% crystal surface coverage of phosphonates was able to completely stop the growth (Weijnen 1986).

Measurement of admixture adsorption on the crystal surface can be carried out directly such as through the use of isotope labelling (Davey 1982), or an XPS analysis of the crystals after adsorption (Weijnen 1986), or indirectly such as electrophoresis or analysis of the crystallising solution (Davey 1982).

Nestler (Nestler 1968) was among the first researchers to investigate the adsorption of admixtures on gypsum. His experiment consisted of adding a certain amount of gypsum into a saturated gypsum solution in which a known concentration of poly acrylic acid (= PAA) had been added. The mixture was then "shaken" for 10 minutes. After being left to stand for a while, the supernatant was checked for its PAA concentration. The amount of the PAA adsorbed onto the crystals was calculated as the difference between the concentration of the PAA in the solution before and after the shaking. It was also found that the shaking time was not a critical factor. The results indicated that the amount of the PAA adsorbed onto the crystal was up to 3 mg per gram of gypsum, increases with the increase in pH level in the solution. The result is certainly dependent on the crystal surface area rather than on the mass.

The amount of admixtures adsorbed onto the crystals can also be directly calculated, as was carried out by Weijnen (Weijnen 1986). In her work, pre-weighed seeds were added into a certain volume of saturated solution of gypsum containing trace amounts of the admixtures to be investigated, and then the mixture was homogenised for a certain period of time, such as for 24 hours, until an equilibrium condition was reached. Next, the crystals were taken out of the suspension and analysed for their admixture content using XPS.

In the present study, the quantification of the admixture adsorbed on the crystal surface was carried out using the crystals obtained from the continuous crystallisation experiments (see **Chapter 6**). These crystals, which were stored in bottles, were ground, and subsequently dissolved in distilled water. The resulting solutions were then analysed using atomic absorption spectrometry (= AAS) analysis.

It was felt that for the continuous crystallisation experiments where admixture levels of 1 ppm had been used, the quantity of the adsorbed admixtures could be very low and, therefore the calculation might be prone to a significant error. Hence, it was decided that the measurement was only carried out for the level of concentrations: 10, 20, 25 and 50 ppm. The results of the AAS analysis were presented in ppm of admixtures (for either Fe^{3+} or Zn^{2+}), and then converted into mg. The result of the measurement is presented in **Figure 4.11**, where the ratio of the adsorbed admixtures per gram of gypsum crystals is plotted against the concentrations of the admixtures used.

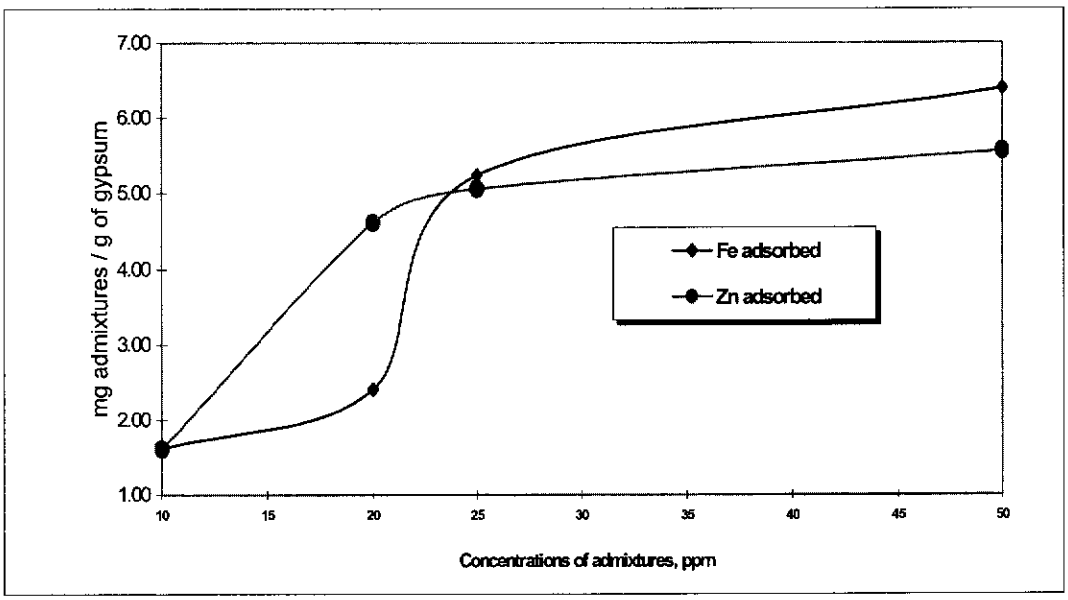

Figure 4.11 **Mass of admixtures adsorbed on the surface of gypsum crystals versus concentrations**

As can be seen in **Figure 4.11**, the adsorption measurements show that higher admixture concentrations result in more admixtures being adsorbed on the crystal

surface. These results may be discussed in conjunction with the continuous crystallisation experiments carried out in the present study (which is presented in **Chapter 6**). The continuous crystallisation experiments showed that the presence of admixtures, either individually or in combination of two or more admixtures resulted in an increase in nucleation rates, which increases with increasing admixture concentrations. One of the reasons for the increase may be the adsorption of the admixtures on the crystal surface, which causes the decrease in the critical free energy required for nucleation, as proposed by Nancollas and Reddy (Nancollas and Reddy 1974). Therefore, the results of the adsorption measurements as depicted in **Figure 4.11**, are in agreement with the reasoning for the nucleation rate increase put forward in the continuous crystallisation experiments (see **sections 6.6.1** to **6.6.2** in **Chapter 6**).

Measurement of the adsorption of admixtures on the crystal surfaces where the crystals are obtained from a suspension in a continuous crystalliser should be regarded as a preliminary study only. The reason is that, different crystal faces generally have different growth rates due to different structures and energy (Nyvlt and Ulrich 1995). It is therefore expected that the amount of the admixtures adsorbed, is also different for different crystal faces. From this analysis, it is logical to assume that an accurate quantification of adsorption of admixtures on crystal surface should be performed on a single crystal, or on a certain number of crystals with a very narrow size fraction.

4.8. Conclusion

The effects of admixtures, namely sodium isopropyl xanthate (= SIPX) and isopropyl thionocarbamate on the crystallisation rate of calcium sulphate dihydrate or gypsum have been investigated using a laboratory seeded batch crystalliser and by measuring the rate constant. It was found that adding the admixtures individually or in combination significantly affected the crystallisation kinetics and in particular reduced the rate of the crystallisation of gypsum from aqueous solution. The effect was measured using a second order kinetic model, that is using the difference between the initial and the equilibrium calcium ion concentrations. The mechanism of inhibition or reduction in the rate constant by both admixtures was assumed to be

one of adsorption of admixtures onto the gypsum crystal surface, thus blocking the active sites of the crystals. The effect of combinations of admixtures was seen to be equal to the effect of using only isopropyl thionocarbamate. Therefore, it was assumed that isopropyl thionocarbamate "overrode" the effect of SIPX by preferentially being adsorbed onto the gypsum crystal faces.

Activation energies were calculated using data from three different temperatures with admixtures levels fixed at typical plant values. The SIPX activation energy showed significant deviation from published values and thus indicated the apparent lack of fit to a second order reaction kinetics model. The value of activation energy calculated for isopropyl thionocarbamate results, however, showed satisfactory agreement with previous studies on gypsum in that comparable value of activation energy was obtained.

Due to the high activation energy values found, it was concluded that the use of the second order kinetics model for the batch crystallisation of gypsum carried out in this study is justified.

Measurement of the admixture adsorption on the crystal surface shows that higher admixture concentrations (within the range used in these batch crystallisation experiments) resulted in more admixtures being adsorbed onto the crystal surface. Moreover, the measurement results show good agreement with similar studies on gypsum conducted earlier by other researchers (Nestler 1968).

Summary

This chapter discusses the study of a seeded batch crystallisation of gypsum in the presence of admixtures. Two types of admixtures were selected: sodium isopropyl xanthate (= SIPX) and isopropyl thionocarbamate. The content of this chapter is summarised as follows:

1. *The experimental design used in this batch crystallisation study is exploratory using the so called "One-factor-at-a-time" method, since past research in this area had used various operating conditions. The variables investigated are the type and concentration of admixtures, seed slurry density and crystallisation run times. This was necessary due to the lack of comparable studies on which to base crystalliser settings.*

2. *The experimental set up and conditions for this seeded batch crystallisation are as follows:*

   - *Volume of crystalliser : 2 litres*
   - *Agitation speed : 125 rpm*
   - *Crystallisation temperature : 25, 35 and 45^{0}C*
   - *Crystallisation run times : up to 90 minutes*
   - *Method of analysis : atomic absorption spectrometry*
   - *Crystallising solutions : $CaCl_2$ and Na_2SO_4 solutions.*

3. *The crystallisation process was followed by measuring the desupersaturation of Ca^{2+} versus crystallisation time. Subsequently, the result of the crystallisation process was presented as the reaction rate constant, **k**, using a second order reaction rate constant.*

4. *In the presence of the admixtures used, the crystallisation rate decreases. For both admixtures increasing the concentrations will result in further decrease and the isopropyl thionocarbamate has higher inhibition effect than SIPX. The*

suppression or inhibition of the crystallisation may be a result of adsorption of the admixture molecules onto the crystal surfaces.

5. *The Arrhenius parameter, A, of the crystallisation reaction was calculated to determine the activation energy and subsequently the mechanism of the crystallisation process.*

6. *In this study, both the pure system and the system with isopropyl thionocarbamate as admixtures produced high activation energies (Ea > 40 kJ/mol), which is indicative of a surface reaction process. Hence, it was concluded that the use of the second order kinetics model for the batch crystallisation of pure gypsum and that in the presence of isopropyl thionocarbamate carried out in this study, is warranted.*

7. *In the presence of SIPX, the growth of the gypsum crystals was inhibited, but the activation energy decreased. Clearly, this finding is contrary to expectation. It was assumed that this discrepancy was probably caused by the nature of both the crystal surfaces and the crystallising solutions, and that different types of reaction mechanisms might occur at the same time resulting in lower activation energy.*

8. *Measurement of the admixture adsorption on the crystal surface shows that higher admixture concentrations (within the range used in this batch crystallisation experiments) resulted in more admixtures being adsorbed on the crystal surface. Moreover, the measurement results show good agreement with similar studies on gypsum conducted previously .*

The next chapter discusses the materials and methods for crystallisation of gypsum carried out in a continuous (= MSMPR) mode. Some parameters used in the continuous crystallisation experiments were taken from the results of the batch crystallisation discussed in the present chapter. These parameters include mean residence times, agitation speed and type of some admixtures used.

References

1. Amjad, Z. (1988). "Kinetics of crystal growth of calcium sulfate dihydrate. The influence of polymer composition, molecular weight, and solution pH." *Canadian Journal of Chemistry*, 66, 1529-1536.
2. Amjad, Z., and Hooley, J. (1986). "Influence of Polyelectrolytes on the Crystal Growth of Calcium Sulfate Dihydrate." *Journal of Colloid and Interface Science*, 111(2), 496-503.
3. Amjad, Z., and Masler, W. F. (1985). "The inhibition of calcium sulfate dihydrate crystal growth by polyacrylates and the influence of molecular weight." *Corrosion 85*, Houston,TX.
4. Ching, W., and McCartney, E. R. (1973). "The Use of a Membrane Electrode to Study the Crystallisation of Calcium Sulphate from Aqueous Solution. I. The Relation between Calcium Ion Activity and Crystallisation Rate." *Journal of Applied Chemistry and Biotechnology*, 23, 441-450.
5. Christoffersen, M. R., Christoffersen, J., Weijnen, M. P. C., and van Rosmalen, G. M. (1982). "Crystal Growth of Calcium Sulphate Dihydrate at Low Supersaturation." *Journal of Crystal Growth*, 58, 585-595.
6. Davey, R. J. (1982). "The Role of Additives in Precipitation Processes." Industrial Crystallization 81, S. J. Jancic and E. J. de Jong, eds., North-Holland Publishing, Amsterdam, 123-135.
7. Davies, O. L. (1978). *The Design and Analysis of Industrial Experiments*, Longman Group, London,New York.
8. Gill, J. S., and Nancollas, G. H. (1980). "Kinetics of growth of calcium sulfate crystals at heated metal surfaces." *Journal of Crystal Growth*, 48, 34-40.
9. He, S., Oddo, J. E., and Tomson, M. B. (1994). "The Seeded Growth of Calcium Sulfate Dihydrate Crystals in NaCl Solutions up to 6 m and 90° C." *Journal of Colloid and Interface Science*, 163, 372-378.
10. Headley, G., Muryanto, S., and Ang, H. M. (2001). "Effects of Additives on the Crystallisation Rate of Calcium Sulphate Dihydrate." *6th World Congress of Chemical Engineering,*, Melbourne, Australia, 2312.
11. Howard, P. H., Neal, M. (1972). *Dictionary of Chemical Names and Synonyms*, Lewis, Boca Raton, USA.

12. Jamialahmadi, M., and Muller-Steinhagen, H. (2000). "Crystallization of Calcium Sulphate Dihydrate from Phosphoric Acid." *Dev.Chem.Eng.Mineral Process.*, 8(5/6), 587-604.
13. Klima, W. F., and Nancollas, G. H. (1987). "The Growth of Gypsum." *AIChE Symposium Series*, 83(253), 23-30.
14. Kontrec, J., Kralj, D., and Brecevic, L. (2002). "Transformation of anhydrous calcium sulphate into calcium sulphate dihydrate in aqueous solutions." *Journal of Crystal Growth*, 240(1-2), 203-211.
15. Liu, S. T., and Nancollas, G. H. (1970). "The Kinetics of Crystal Growth of Calcium Sulphate Dihydrate." *Journal of Crystal Growth*, 6, 281-289.
16. Liu, S. T., and Nancollas, G. H. (1973). "The Crystal Growth of Calcium Sulfate Dihydrate in the Presence of Additives." *Journal of Colloid and Interface Science*, 44(3), 422-429.
17. Liu, S. T., and Nancollas, G. H. (1975a). "The Crystal Growth and Dissolution of Barium Sulfate in the Presence of Additives." *Journal of Colloid and Interface Science*, 52(3), 582-592.
18. Liu, S. T., and Nancollas, G. H. (1975b). "A Kinetic and Morphological Study of the Seeded Growth of Calcium Sulfate Dihydrate in the Presence of Additives." *Journal of Colloid and Interface Science*, 52(3).
19. Masel, R. I. (2001). *Chemical Kinetics and Catalysis*, John Wiley and Sons, New York etc.
20. Mile, B., Vincent, A. T., and Wilding, C. R. (1982). "Studies of the Effects of Electrolytes on the Rates of Precipitation of Calcium Sulphate Dihydrate using an Ion-selective Electrode." *Journal of Chemical Technology and Biotechnology*, 32, 975-987.
21. Mullin, J. W. (1972). *Crystallisation*, Butterworths, London.
22. Murray, N. (1997). "Continuous Crystallisation of Calcium Sulphate Dihydrate," Final Year Undergraduate Project, Curtin University of Technology, Perth,Western Australia.
23. Myerson, A. S. (1993). *Handbook of Industrial Crystallization*, Butterworth-Heinemann, Boston, London, etc.
24. Nancollas, G. H. (1979). "The Growth of Crystals in Solution." *Advances in Colloid and Interface Science*, 10, 215-252.

25. Nancollas, G. H., and Reddy, M. M. (1974). "The Kinetics of Crystallization of Scale-Forming Minerals." *Society of Petroleum Engineers Journal*, 117-126.
26. Nancollas, G. H., White, W., Tsai, F., and Maslow, L. (1979). "The Kinetics and Mechanism of Formation of Calcium Sulfate Scale Minerals - The Influence of Inhibitors." *Corrosion - NACE*, 35(7), 304-308.
27. Nestler, C. H. (1968). "Adsorption and Electrophoretic Studies of Poly (Acrylic Acid) on Calcium Sulfate." *Journal of Colloid and Interface Science*, 26, 10-18.
28. Northwood, T. (1995). "Scale reduction in Process Water Pipes at Murchison Zinc," Final Year Undergraduate Project, Curtin University of Technology, Perth, Western Australia.
29. Nyvlt, J., Sohnel,O, Matuchova, M., Broul, M. (1985). *The Kinetics of Industrial Crystallization*, M. Stulikova, translator, Elsevier, Amsterdam, etc.
30. Nyvlt, J., and Ulrich, J. (1995). *Admixtures in Crystallization*, VCH, Weinheim, New York, etc.
31. Ohara, M., and Reid, R. C. (1973). *Modeling Crystal Growth Rates from Solution*, Prentice-Hall, Englewood Cliffs, N.J.
32. Oner, M., Dogan, O., Oner, G. (1998). "The influence of electrolytes architecture on calcium sulfate dihydrate growth retardation." *Journal of Crystal Growth*, 186, 427-437.
33. Taguchi, K., Garside, J., and Tavare, N. S. (1996). "Nucleation and growth kinetics of barium sulphate in batch precipitation." *Journal of Crystal Growth*, 163, 318-328.
34. van Rosmalen, G. M., Daudey, P. J., and Marchee, W. G. J. (1981). "An analysis of growth experiments of gypsum crystals in suspension." *Journal of Crystal Growth*, 52, 801-811.
35. Weijnen, M. P. C. (1986). "The Influence of Additives on the Crystallisation of Gypsum," PhD Thesis, Delft University of Technology, Delft, the Netherlands.
36. Weijnen, M. P. C., and van Rosmalen, G. M. (1984) "The Role of Additives and Impurities in the Crystallization of Gypsum." *Industrial Crystallization 84*, 61-66.
37. Weijnen, M. P. C., and van Rosmalen, G. M. (1985). "The influence of various polyelectrolytes on the precipitation of gypsum." *Desalination*, 54, 239-261.
38. White, E. T., and Hoa, L. T. (1977) "Mass transfer studies in particulate systems using the population balance approach - The growth of gypsum crystals." *2nd*

Australasian Conference on Heat and Mass Transfer, University of Sydney, Australia, 401-408.

39. White, E. T., and Mukhopadhyay, S. (1990). "Crystallization of gypsum from phosphoric acid solutions." Crystallization as a Separation Process, A. S. Myerson and K. Toyokura, eds., ACS, Washington, DC, USA, 292-315.
40. Witkamp, G. J., van der Eerden, J. P., and van Rosmalen, G. M. (1990). "Growth of gypsum. I. Kinetics." *Journal of Crystal Growth*, 102, 281-289.

CHAPTER 5 MATERIALS AND METHODS FOR CONTINUOUS CRYSTALLISATION SYSTEM

5.1. Introduction

This chapter describes the experimental procedures and the experimental design for the continuous (MSMPR) crystallisation system carried out in this study.

As in other chemical processes, crystallisation requires the mass balance calculation to determine the quantities of raw materials needed and of crystal products produced. Moreover, such a balance will also determine the stream flow rates and their compositions. Hence, the mass balance is presented at the beginning of this chapter. Next, the crystallisation equipment and its operating conditions are discussed, including details of the schematic diagram, the geometry of the main components of the experimental rig, as well as the calibration and the performance test of the accessories. Then, the preparation of the experiments is presented, which includes the preparation of the crystallising solutions and the seed making. After discussion of the preparation stage, a typical experimental run and its subsequent sampling and measurements to extract the experimental data are elaborated. Finally, the "balanced incomplete randomised block design", selected as the experimental design for this continuous crystallisation study, is presented, which includes a table of "block" and "treatment" as a guideline for the experiments and for the data analysis.

This chapter contains the following subheadings:

5.2. Mass Balance for Continuous Crystallisation System

In an MSMPR crystalliser, the liquid and solid phases in the crystallisation process are related by three equations. For the liquid phase, there is an equation, which relates the variation of concentrations of species of the crystallising substances. For the solid phase or the crystals, the population balance equation (= PBE) is used. For both phases, the mass and energy balance is utilised (Lakatos and Sapundzhiev 1990). The present study investigates a crystallisation process in solution, hence the energy balance is not a critical factor (Mersmann 1995) and, therefore, not required. However, the mass balance was calculated to determine the quantities and compositions of the stream flows and their compositions, so that the raw materials needed and the products yielded can be quantified. Mass balance calculation for 8 residence times (1 residence time = 15 minutes) was carried out and the result is shown in **Table 5.1**. Detailed calculation of the mass balance is given in **Appendix B: Mass Balance for the Continuous Crystallisation System.**

Table 5.1 Mass balance for the continuous crystallisation for 8 residence times

Operating conditions	Seed Tank	Liquor Tank	Crystalliser
Concentration, ppm Ca^{2+}	611	1,348	1,200
Working volume, ml	3,000	10,000	1,500
Flow rate, ml/min	20	80	100
Slurry density, g/L	4.00	0.000	0.800

In a continuous crystallisation, the supersaturation level is not an independent variable. In fact, it is interrelated with residence times, and thus the capacity of the crystalliser. In this study, calculation has been made to evaluate the effect of residence time on the concentration level in the liquor tank, the results of which are presented in **Tables 5.2** to **5.4**.

Table 5.2 Crystallisation operating conditions for 10 minute residence time

Crystalliser		Seed Tank		Liquor Tank	
Flow rate (ml/min)	Concentration (ppm)	Flow rate (ml/min)	Concentration (ppm)	Flow rate (ml/min)	Concentration (ppm)
150	1,200	70	611	80	1,715
150	1,200	65	611	85	1,650
150	1,200	60	611	90	1,593
150	1,200	55	611	95	1,541
150	1,200	50	611	100	1,495

Table 5.3 Crystallisation operating conditions for 15 minute residence time

Crystalliser		Seed Tank		Liquor Tank	
Flow rate (ml/min)	Concentration (ppm)	Flow rate (ml/min)	Concentration (ppm)	Flow rate (ml/min)	Concentration (ppm)
100	1,200	20	611	80	1,347
100	1,200	15	611	85	1,304
100	1,200	10	611	90	1,265
100	1,200	5	611	95	1,231
100	1,200	0	611	100	1,200

Table 5.4 Crystallisation operating conditions for 20 minute residence time

Crystalliser		Seed Tank		Liquor Tank	
Flow rate (ml/min)	Concentration (ppm)	Flow rate (ml/min)	Concentration (ppm)	Flow rate (ml/min)	Concentration (ppm)
75	1,200	15	611	60	1,367
75	1,200	10	611	65	1,291
75	1,200	5	611	70	1,242
75	1,200	0	611	75	1,200

5.3. Description of Equipment and Operating Conditions

The schematic representation of the continuous crystallisation system is depicted in **Figure 5.1**. The major components of the system were a seed tank (= vessel I), a liquor tank (= vessel II) and a crystalliser vessel (vessel III). The crystalliser had a working volume of 1.5 litres, made of stainless steel with four internal baffles to prevent vortex formation. It was agitated using a variable speed 45^0 pitched blade impeller and was placed in a thermostatically controlled water bath. The crystalliser contained supersaturated solution of gypsum. An impeller speed of 125 rpm was found to be fast enough to prevent crystals from settling at the bottom of the crystalliser. A previous run carried out in an identical flexi-glass (transparent) crystalliser showed that the crystals were uniformly suspended. As the slurry density is low, that is 0.800 gram per litre of solution, it was considered unnecessary to increase the impeller speed as the crystallisation process proceeded. It was assumed that the increase in crystalliser slurry density due to nucleation and growth was minimal and did not significantly affect the required speed of the impeller for a completely mixed condition.

The seed tank contained seed crystals of gypsum suspended in a saturated solution of gypsum and it was also similarly agitated as that of the crystalliser. The liquor tank contained a supersaturated solution of gypsum and was immersed in a thermostatically controlled water bath. As the liquor tank did not contain any solids, it was only occasionally stirred to prevent hot spots and local supersaturation build up. Mass balance for the solution concentration level for varying residence times is given in **Tables 5.2** to **5.4**.

To ensure accurate flow rates, transfer of crystallisation solutions from one vessel to another throughout the system was facilitated by three Masterflex™ peristaltic pumps (supplied by Cole Palmer Instrument Company). The continuous crystallisation experiment consisted of three major steps: **Preparation of Crystallisation Solutions**, **Preparation of Seeds**, and **Crystallisation Run**. The full description of each of the three steps is given in **sections 5.4** to **5.5**.

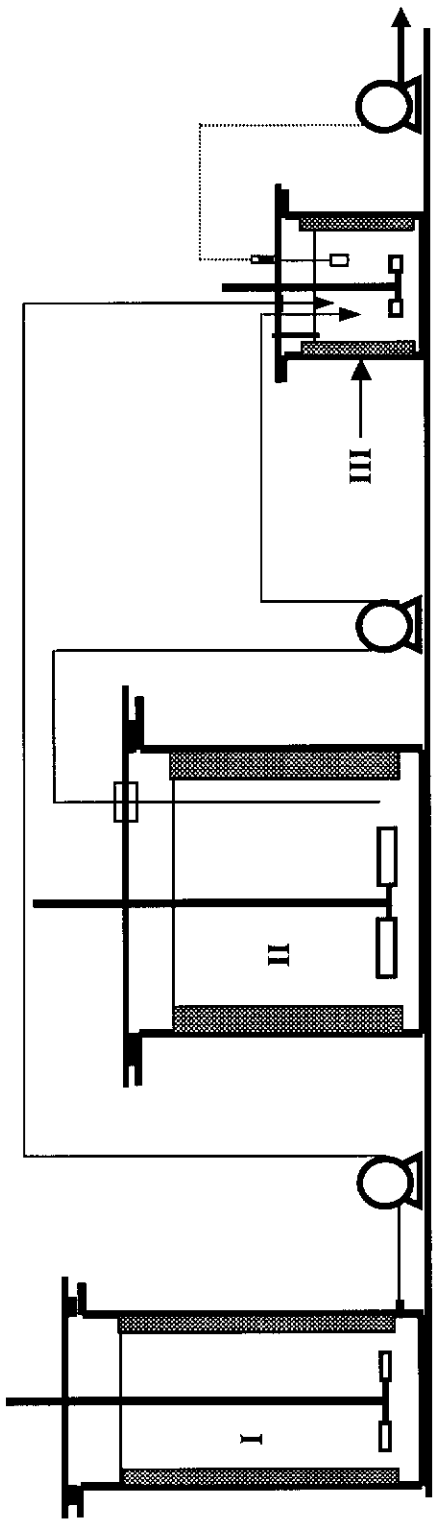

Figure 5.1 Schematic representation of the continuous (MSMPR) crystallisation system
I: Seed tank; II: Liquor tank; III: Crystalliser

5.3.1. Crystalliser vessel

A schematic picture of the crystalliser vessel is shown in **Figure 5.2**. It is a flat-bottomed cylindrical vessel (internal diameter (ID) = 15 cm) made of stainless steel (SS 316) with a working volume of 1,500 ml and was agitated using a four bladed variable pitched impeller with a diameter of 9 cm driven by a variable speed motor. The crystalliser vessel was fitted with four removable baffles connected to each other with two steel wires. To maintain the liquid level in the crystalliser at a constant level a polystyrene float level controller activated by an infra red sensor was used. The crystalliser was placed in a thermostatted water bath to obtain and maintain the desired temperature of crystallisation. Two separate SS 316 steel tubes (ID = 0.5 cm) were fitted to the lid of the crystalliser to facilitate the input flows from the seed tank and the liquor tank, respectively. To enhance the rapid mixing of the inlet streams with the crystalliser content, the two tubes were placed side by side and between two baffles. Moreover, the two tubes were extended from the lid down to mid height in the crystalliser. Product from the crystalliser was withdrawn using a peristaltic pump and was collected in a plastic bucket and was subsequently dumped into a waste tank in the laboratory. The product withdrawal was intermittent, delivering about 10% of the crystalliser content at a time. Owing to the low slurry density in the crystalliser (= 0.80 g/L) the intermittent withdrawal was considered sufficient to prevent classification of the suspended solids.

A batch mode operation was used to check the consistency of the slurry within the crystalliser. First, a saturated solution of 611 ppm of Ca^{2+} was prepared by mixing equimolar volume of calcium chloride and sodium sulphate solutions. The two solutions were mixed in the crystalliser and then agitated at 125 ppm. Next, 1.20 grams of gypsum was added into the crystalliser and the slurry was then taken from time to time to check the density. The sampling was done by taking 50 ml of slurry from the crystalliser using a syringe with an extended tubing attached to the tip of the syringe. The location of sampling was variously mid height of the crystalliser volume, at the centre of the crystalliser, and between two baffles. The samples were then filtered and the solids obtained were dried in an oven at 100^0C overnight. The

dried solids were weighed and the weight was calculated to give the slurry density in the crystalliser. The following table gives the result of the determination.

Table 5.5 Test for consistency of slurry density in the crystalliser

No.	Time of withdrawal after start, min	Density of slurry, gram per litre
1	2	0.792
2	5	0.796
3	15	0.801
4	20	0.800
5	45	0.799
6	60	0.800
7	90	0.798
8	120	0.801
9	150	0.801

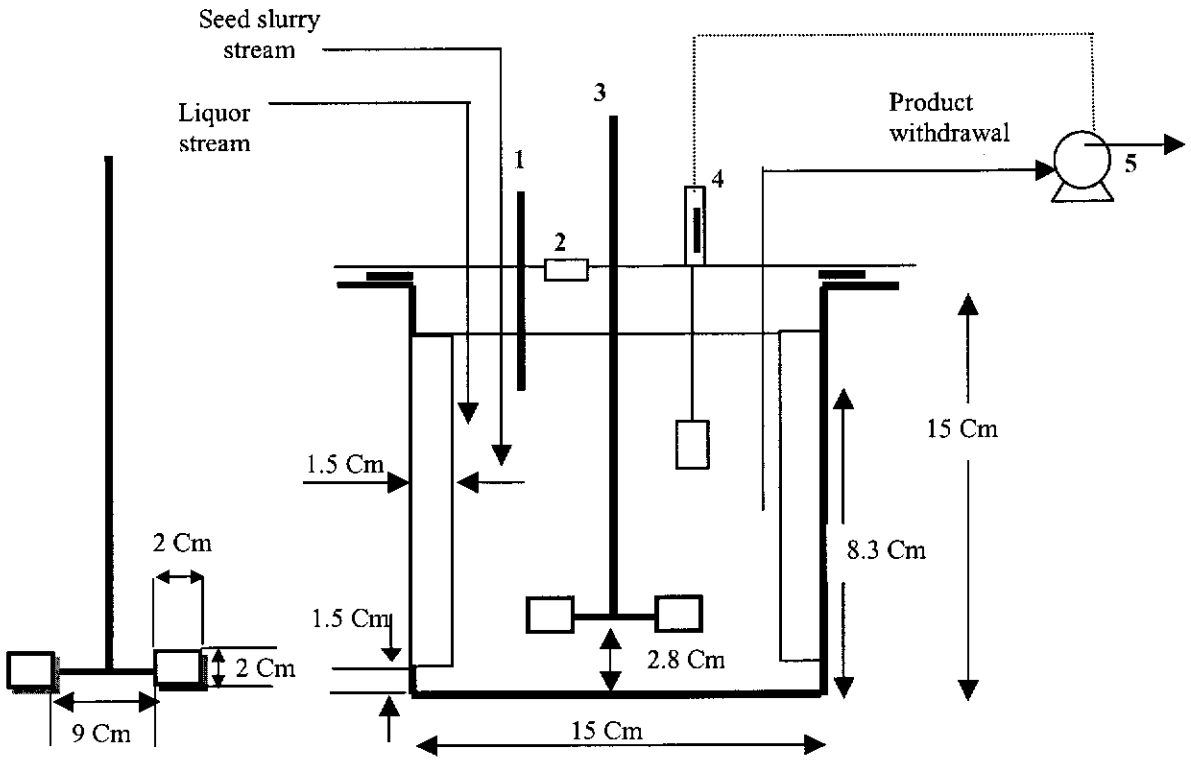

1 = Calcium ion selective probe 2 = sample port 3 = pitched blade turbine impeller
4 = polysterene float level controller 5 = peristaltic pump

Figure 5.2 Crystalliser and impeller geometry

5.3.2. Seed tank

The flow rate from the seed tank was checked to ensure the rate was sufficient to supply the crystalliser with adequate seeds. Seed slurry density in the seed tank was fixed at 4.00 g/L (see **Table 5.1**). To check the flow rate, the seed tank was filled with a saturated gypsum solution (= 611 ppm Ca^{2+}), the impeller was activated and a predetermined amount of gypsum was added to make the slurry density equal to 4.00 g/L. Then, a peristaltic pump was activated to withdraw the slurry from the seed tank at a flow rate of 20 ml/min. The volume of slurry withdrawn was 50.00 ml and it was collected into a measuring cylinder. Next, the slurry was filtered to obtain the solids. The solids obtained was dried in an oven at 100^0C overnight and then weighed. The weight corresponded to 50 ml of slurry. Then the weight was calculated to get the slurry density in g/L as shown in **Table 5.6**.

Table 5.6 Slurry density test for the stability of the seed tank flow rate

No.	Time of withdrawal after start, min.	Density of slurry, gram per litre
1	2	3.72
2	5	3.75
3	15	3.97
4	20	4.01
5	45	4.00
6	60	3.95
7	90	4.01
8	120	4.00
9	150	4.01

5.3.3. Liquor tank

The liquor tank is a cylindrical vessel made of stainless steel with an ID of 25.4 cm and the working volume of 10 litres. The liquor in the liquor tank was not continuously agitated because it did not contain any suspended solids. It was occasionally stirred gently, to prevent the occurrence of hot spots and local concentrations. A stainless steel tube with an ID of 3 mm was extended from the lid

of the liquor tank down to the bottom of the tank. The tube was then connected to a flexible Norprene™ tubing (supplied by Cole Palmer Instrument Company), to a peristaltic pump. The liquor tank was placed inside a thermostatic cylindrical water heater, the temperature of which can be adjusted to control the temperature of the liquor within the liquor tank. The temperature of the liquor was set at a higher level than that in the crystalliser so that when the two streams from the seed tank and the liquor tank were mixed in the crystalliser, the desired temperature was achieved.

The liquor was prepared with a slightly higher concentration level than that in the crystalliser in order to achieve the desired level of concentration in the crystalliser. Calculation of the level of concentration for the liquid within each tank (crystalliser, seed and liquor tanks) is elaborated in **Appendix B: Mass Balance for the Continuous Crystallisation System**. The concentrated liquor in the liquor tank was observed to be stable for the duration of the continuous crystallisation run.

5.3.4. Transport pumps

In this continuous crystallisation study three Masterflex™ peristaltic pumps (supplied by Cole Palmer Instrument Company) were used. One peristaltic pump was used to transport the slurry from the seed tank into the crystalliser. Another peristaltic pump was used for delivering the liquor from the liquor tank into the crystalliser. The third peristaltic pump was utilised for the withdrawal of the crystalliser product. The seed tank and the liquor tank peristaltic pumps were fitted with size 16 (3.1 mm inside diameter) MasterFlex™ tubing (supplied by Cole Palmer Instrument Company), while for the crystalliser withdrawal pump the same tubing but with a smaller inside diameter (= 1.6 mm) was used. Prior to the actual experimental runs, all of the pumps were calibrated to check their pumping capacity since they were only fitted with potentiometric set points with scales from 0 to 10, instead of direct measurement in unit volume per unit time. (The calibration procedure and results are presented in **section 5.3.4.2.**). Gypsum solution is neither toxic, nor corrosive, nor harmful, and therefore no specific requirement is necessary for the pumps and the tubing.

5.3.4.1. Transport pump settings

It is necessary to ensure that the flow rate of the slurry in the system is high enough to prevent the crystals from settling and/or classifying during transport. A calculation was carried out for the transport of the seed slurry from the seed tank to the crystalliser vessel to validate this condition. The calculation is as follows:

Cross section area of tube (A) $= \pi \times (0.31\ cm)^2/4.$

Volume of seed in 1 litre slurry $= 0.8\ g/2.32\ gr/cm^3$

$= 0.3448$ ml.

(density of gypsum = 2.32 g/cm^3) (Perry and Green 1997))

Volume of liquid in 1 litre slurry $= (1{,}000 - 0.3448)$ ml

$= 999.6552$ ml.

Seed slurry volumetric flow rate $= 20$ ml/min.

Volumetric flow rate of liquid in seed slurry $= (20 - 0.3448)$ ml/min

$= 19.6552$ ml/min.

Superficial velocity (v_o) of liquid in seed slurry = volumetric flow rate/A

$= (19.6552\ cm^3/min)/0.075\ cm^2$

$= 4.3678$ cm /sec

≈ 4.37 cm/sec.

Particle Reynolds number in the slurry inside the tube is defined as

$$N_{Re} = v_o \rho_{solution} L / \mu_{solution} \qquad (5.1)$$

where,

N_{Re} = particle Reynolds number, dimensionless

v_o = superficial velocity, cm/sec

$\rho_{solution}$ = density of gypsum-water solution (=1.0 g/cm^3)

L = crystal size, cm

$\mu_{solution}$ = viscosity of gypsum-water solution, g/cm sec.

Hence,

$\mathbf{N_{Re}}$ = (4.3678 cm/sec)(2.32 g/cm^3)(0.0125 cm)/(0.01 g/cm sec)

= 0.126666/0.01

= 12.7

= 13

The particle Reynolds number, $\mathbf{N_{Re}}$, equals 13, thus the terminal velocity of the particles in the slurry falls in the intermediate region between Newton's and Stoke's regimes. Therefore the terminal velocity of crystals in the slurry can be calculated by the following equation

$$u_t = 0.153 \frac{g^{0.71} L^{1.14} (\rho_{gypsum} - \rho_{water})^{0.71}}{\rho_{water}^{0.29} - \rho_{solution}^{0.43}} \qquad (5.2)$$

where,

u_t = terminal velocity of crystals in the slurry, cm/sec

g = gravitational constant, (g)(cm)/(dyne)(sec^2)

L = crystal size, cm

ρ_{gypsum} = density of gypsum, g/cm^3

ρ_{water} = density of water, g/cm^3

$\rho_{solution}$ = density of gypsum-water solution (=1.0 g/cm^3).

Solving the above equation with all the values available gives $\mathbf{u_t}$ = 1.21 cm/sec. As can be seen the terminal velocity of crystals in the slurry, $\mathbf{u_t}$ (=1.21 cm/sec), is much less than the superficial velocity of the liquid, $\mathbf{v_o}$ (= 4.37 cm/sec). Therefore it can be stated that the chances of crystals settling or undergoing classification during transport from the seed tank into the crystalliser is negligible.

5.3.4.2. Calibration of the peristaltic pump flow rates

The peristaltic pumps used for the transport of solutions were not equipped with flow meters by which the flow rate can be read directly. Instead, potentiometric set points

from 0 to 10, was used in each pump to regulate the flow rate. Hence, it is necessary to calibrate the exact flow rate for each representative set point. The calibration was carried out by measuring the volume of the solution delivered at each set point per minute. A stopwatch and a measuring cylinder were respectively used to measure the time and volume of the solution collected. Each measurement was done twice and the results were averaged. The results of the calibration are presented in the following charts: **Figures 5.3** to **5.5**.

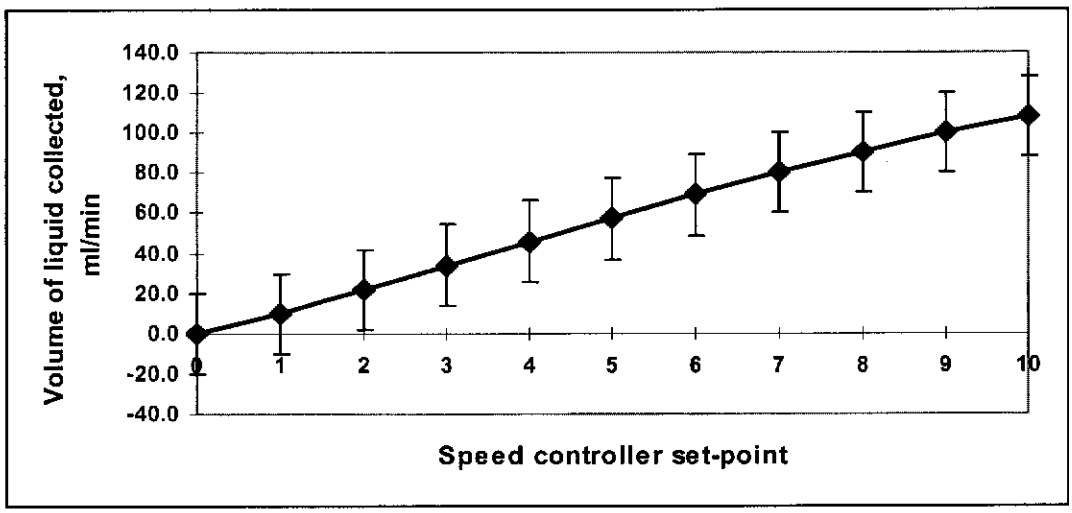

Figure 5.3 Calibration plot for the seed tank peristaltic pump

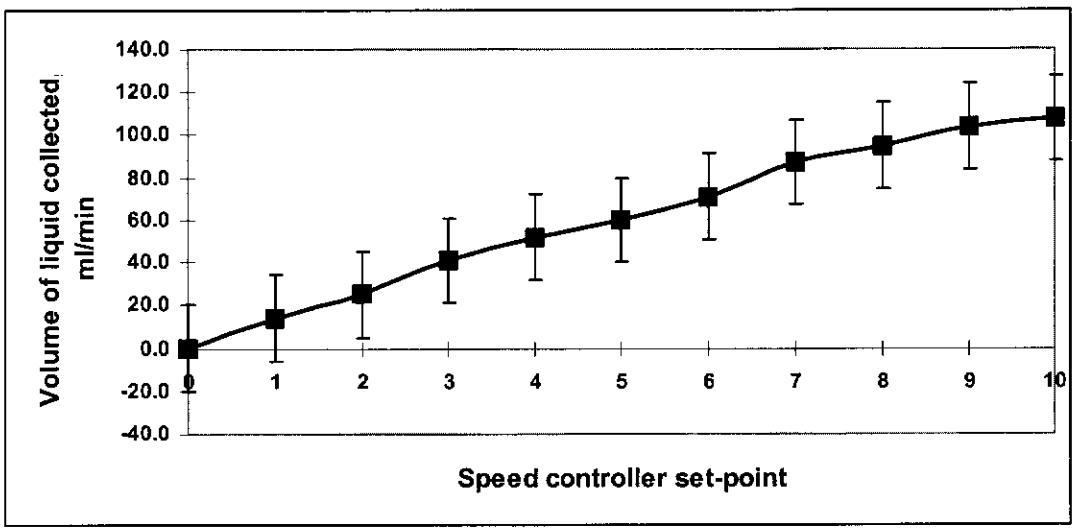

Figure 5.4 Calibration plot for the liquor tank peristaltic pump

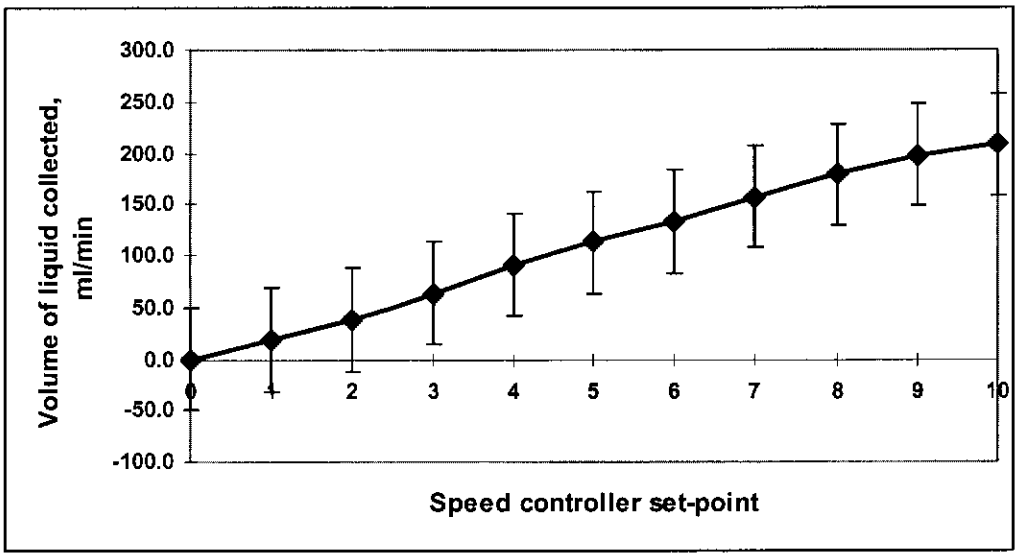

Figure 5.5 Calibration plot for the crystalliser peristaltic pump

5.3.5. Vessels and accessories

The three vessels, namely the seed tank, the liquor tank and the crystalliser were cleaned following the procedure adopted by Chan (Chan 1997). For the connection tubes, cleaning was carried out using a dilute hydrochloric acid solution followed by rinsing with distilled water. The use of the hydrochloric acid solution was especially adopted after each experimental run in order to dissolve trace amount of crystals that might have attached to the inner wall of the tubes.

5.4. Preparation of System

5.4.1. Preparation of crystallisation solutions

Gypsum solutions with different concentration levels with respect to Ca^{2+} were prepared by diluting and mixing stock solutions of $CaCl_2.2H_2O$ and Na_2SO_4, respectively. The stock solution of $CaCl_2.2H_2O$ as Ca^{2+} provider, was made by dissolving crystals of $CaCl_2.2H_2O$ in distilled water. The stock solution of Na_2SO_4, as $SO4^{2-}$ provider, was prepared in the same manner. The two solutions were kept separately and only mixed immediately prior to the experimental run. Extreme care

was taken to keep the solutions free from dust, insoluble matter etc. In addition, both solutions were filtered before being used for the experiments. Procedure for the preparation of crystallisation solutions is detailed in **Appendix B: Mass Balance for the Continuous Crystallisation System**. The preparation procedure was based on the selected operating conditions of the three main components of the crystallisation rig as tabulated in **Table 5.1** as follows:

1. Seed tank:

Concentration level	= saturated
	= 611 ppm of Ca^{2+}.
Flow rate	= 20.00 ml/min.
Slurry density	= 4.00 g/L.

2. Liquor tank:

Concentration level (calculated)	= 1,348 ppm of Ca^{2+}.
Flow rate	= 80.00 ml/min.
Slurry density	= 0.00 g/L.

3. Crystalliser: (= for 15 minute residence time)

Concentration level	= 1,200 ppm of Ca^{2+}.
Flow rate	= 100 ml/min.
Slurry density	= 0.800 g/L.

Briefly, the preparation of crystallisation solutions as detailed in **Appendix B** resulted in the following.

1. The crystallisation solutions were prepared by dilution with distilled water from the more concentrated stock solutions of 0.5 M of $CaCl_2$ and 0.5 M of Na_2SO_4, respectively.
2. The volume of 0.5 M of $CaCl_2$ stock solution required for the entire experimental runs was 20.25 litres. Likewise, the required volume of 0.5 M of Na_2SO_4 was 20.25 litres.
3. The amount of $CaCl_2.2H_2O$ crystals required for the stock solution was 10.125 mol or 1488.58 grams.

4. The amount of Na_2SO_4 crystals required for the stock solution was 10.125 mol or 260.36 grams.
5. The amount of seeds needed for one crystallisation run = 15.200 grams.
6. The total amount of seeds required for the entire experiments = 1094.4 grams
   ≈ 1095 grams.

5.4.2. Preparation of seeds

Gypsum crystals as seeds for this seeded continuous crystallisation were prepared by slow and accurate addition of 0.60 M calcium chloride solution to 0.60 M sodium sulphate solution in equal volumes at room temperature according to the following reaction:

$$\mathbf{CaCl_2.2H_2O + Na_2SO_4 \rightarrow CaSO_4.2H_2O + 2\ NaCl} \qquad (5.3)$$

The crystals obtained were filtered, washed, oven dried, sieved and stored. Before being used for the experiment the crystals were heated in an oven overnight at 60^0C. Then they were sieved within the sieve cuts +53 μm and –90 μm and characterised by optical microscopy and scanning electron microscopy (SEM) (Phillips XL30) (Amjad 1985). The sieved crystals were then ready for the experiment. Detailed description of gypsum seed preparation is well-documented (Amjad 1985; Amjad 1988; Liu and Nancollas 1970; Liu and Nancollas 1973).

5.4.2.1. Detailed description of the seed making

Two litres each of 0.6 M solutions of calcium chloride (= $CaCl_2$) and sodium sulphate (= Na_2SO_4) were prepared in two separate large glass beakers. The sodium sulphate solution was then transferred into an agitated vessel and the two solutions were agitated at 250 rpm, respectively. A peristaltic pump was used to withdraw the calcium chloride solution into the vessel containing the sodium sulphate solution. The pumping lasted about 10 minutes. After all the calcium chloride solution had been withdrawn, the pump was turned off, but the agitation in the vessel (in which the gypsum crystals were then growing) was continued at half the previous speed, i.e.

at 125 rpm for 30 minutes. Next, the stirring was stopped, the stirrer removed and the mixture was left to stand for five minutes to allow the seed crystals to settle. Subsequently, the supernatant was decanted.

The wet gypsum crystals in the vessel were then transferred into a large glass beaker and washed several times with plenty of distilled water to remove the Na^+, Cl^- and fines. Next, they were suction filtered. In order to prevent the crystals from forming aggregates or agglomerates, they were washed with iso-propanol (IPA) and suction filtered until dry enough so as not to form lumps when they were taken from the filter funnel. The crystals were then spread on a large filter paper and put in an oven at 90^0C for up to three days or until they became dry to the touch.

The seed making was repeated many times until enough crystals had been obtained for the entire experiment. It was observed that each seed making produced about 130 grams of seeds.

5.4.2.2. Uniformity of the seeds prepared

To ensure the uniformity of the gypsum seed crystals prepared, the following procedure was carried out. The crystals were initially stored in several small plastic bottles. From each bottle about 40 grams of seeds were taken and poured into a splitter (supplied by Metalcraft, Canningvale 6155 WA) which distributed the crystals into 22 chutes in the splitter and then into two collectors. After all the crystals from the small plastic bottles had been put into the splitter and collected in the two collectors, they were mixed in a large plastic bucket. From this plastic bucket, a small amount of the crystals (about 40 grams) was taken and put back into each of the small plastic bottles. This procedure was repeated five times and finally the mixed crystals were stored in the plastic bottles until they were used. The plastic bottles were shaken and inverted each day to ensure that the crystals remain in a homogeneous state and to prevent caking.

Before being used for the experiment, the crystals were put in an oven overnight at 60^0C. Then the crystals were sieved within the sieve cuts + 38 μm and – 90 μm. The sieved crystals were then ready for the experiment.

5.4.2.3. Characterisation of the seeds: morphology and purity

The seed crystals obtained from the seed making showed the characteristics of gypsum crystals formed from pure supersaturated solution, in that they were acicular or needle-like in shape as shown in **Figure 5.6** (Rolfe 1966; Weijnen and van Rosmalen 1984).

Figure 5.6 Scanning electron micrograph of gypsum as seeds

Chemically, the seeds were also confirmed as gypsum by the following method. A small amount of about five grams of purchased reagent grade gypsum and seed crystals were accurately weighed separately. The two crystal substances were then dried in an oven at 110^0C for several days. Each day the two substances were taken from the oven and weighted and put back into the oven if a constant weight had not been reached. As the constant weight of the purchased reagent grade gypsum was the same as that of the seed crystals, it was concluded that the seed crystals were indeed gypsum or calcium sulphate dihydrate. This method was similar to that used

by He *et al.* (He *et al.* 1994) for the preparation of calcium sulphate hemihydrate crystals from gypsum.

5.5. Description of a Typical Experimental Run

The crystallisation run was initially started in a batch mode for one residence time of 15 minutes. The crystalliser was placed in a thermostatically controlled water bath with accuracy to within 1^0C. It was heated until the desired temperature of the solution within the crystalliser was reached. After the attainment of the desired temperature, a sample for solution concentration was taken and then a predetermined weight of gypsum crystals was added into the crystalliser. Immediately after the seed addition, a stopwatch was started and the speed of the impeller was sharply increased for about 30 seconds so as to homogenise the contents of the crystalliser. After the vigorous stirring, the agitation speed was reduced to its predetermined value and the system was run in a batch mode. In a similar batch crystallisation experiment on gypsum (Murray 1999), an impeller speed of 225 rpm and a slurry density of 15.00 g/L were found to cause no attrition after an experimental run of 15 minutes. In this study both the impeller speed (= 125 rpm) and the slurry density (= 0.800 g/L) values were much less than those used by Murray (Murray 1999), and hence the vigorous stirring at the start of the experiments was believed not to cause attrition of the crystals. While the crystalliser was running in a batch mode, the seed tank was agitated to maintain homogeneous slurry of gypsum seeds. A sample for initial crystal size distribution (**CSD**) analysis was taken from the seed tank during this period. The liquor tank was agitated slowly just to maintain the liquor at uniform temperature and thus avoid the occurrence of hot spots. The flow rates of the three tanks were determined by adjusting the set point of the pumps connected to them through tubing (see **Figs. 5.3**, **5.4** and **5.5** in **section 5.3.4.2** for the calibration charts of the pump flow rates).

When the batch mode period was ended, the system was run in a continuous mode by activating the peristaltic pumps. The continuous mode was run uninterrupted for up to eight residence times to ensure that the system reached steady state. Throughout the run the agitation speed as well as the flow rates were periodically checked and

rectified if necessary. The running of a continuous crystallisation system could sometimes be hindered by a blockage in the tubing system. Blockages were usually easy to rectify, that is, by reversing the flow. For example, in this experiment the crystalliser product withdrawal was carried out by the peristaltic pump operated in reverse flow mode. If there is an obstruction in the crystalliser outlet tubing, the obstruction can be removed by reversing the pump operation from "REVERSE" to "FORWARD" mode for a few seconds and then back to "REVERSE" mode.

For the run with admixtures, the pre-weighed admixtures were added into the seed tank prior to the start of the continuous mode. Sampling during the continuous mode was carried out according to the experimental design. On completion of the continuous run, that is, after eight residence times, the system was stopped. This was done by switching the peristaltic pumps, the impeller motors and, the temperature controller off. The crystalliser content was discarded into a waste container and all the tanks and accessories were cleaned for subsequent runs according to the procedure adopted by Chan (Chan 1997).

5.6. Sampling and Measurements

5.6.1. Sampling for solution concentrations

As crystallisation proceeds, the Ca^{2+} concentration in the crystallising solution decreases due to the crystallisation of calcium sulphate dihydrate ($CaSO_4.2H_2O$) or gypsum. The decrease in Ca^{2+} concentration was continuously monitored using a Calcium Ion Selective Electrode (Orion™) (hereafter will be called the Ca^{2+} electrode). A sample hole was made on the crystalliser lid, through which the Ca^{2+} electrode was inserted into the crystalliser, such that the tip of the electrode was dipped into the solution. Once the crystallisation run was started, the Ca^{2+} electrode was switched on and the concentration of Ca^{2+} in the solution was continuously displayed on the screen. The Ca^{2+} electrode was calibrated before each crystallisation run to make sure that there was no potential drift. In addition, to stabilise the electrode-sensing module, that is, the part that measures the

concentrations, it was always soaked in the standard 100 ppm solution between experimental runs.

Calibration of the Ca^{2+} electrode

It is necessary to ensure that the Ca^{2+} electrode used in this study correctly measures the concentration of Ca^{2+} in the crystallising solution within the range of the concentration used. The lowest possible concentration of Ca^{2+} will be in the seed tank, which is equal to the saturated condition of 611 ppm of Ca^{2+} (at 25^0C). On the other hand, the liquor tank contains Ca^{2+} solution with the highest concentration, that is, about 1,350 ppm (see **Table 5.1. Mass balance for the continuous crystallisation for 8 residence times** in **section 5.2**). Therefore, the calibration of the Ca^{2+} electrode should cover at least the range: 611 ppm to 1,350 ppm of Ca^{2+}. The sensitivity of the Ca^{2+} electrode used is also shown as the change in electrode potential (measured in millivolts, mV) observed with every tenfold change in concentration (as explained in Ca^{2+} Electrode Instruction Manual, supplied by Orion Company). Therefore, for reasons of practicality as well as of the range of concentrations that needs to be covered, a calibration scheme shown in **Table 5.7** was carried out.

Table 5.7 Electrode potential for different solution concentrations

Solution concentration (ppm of Ca^{2+})	Electrode potential (mV)	
	1^{st}	2^{nd}
200	-29.7	-29.9
300	-26.7	-27.5
500	-14.7	-15.2
700	-14.8	-15.7
900	-8.6	-8.9
1000	-8.1	-8.9
1100	-7.9	-9.2
1300	-6.8	-7.3
1500	-3.6	-3.8
1600	-2.6	-2.6
2000	+0.3	+0.4

Temperature of standard solution: 27.5^0C

Concentration of standard solution: 100 ppm of Ca^{2+}

Electrode potential of standard solution: -34.4 mV

The standard solution for the calibration was prepared by dissolving $CaCl_2.2H_2O$ crystals in distilled water to make a 0.5 M $CaCl_2$ stock solution. From the stock solution, standard solutions with different concentrations can be made by appropriate dilution with distilled water.

It is also necessary to ensure that the Ca^{2+} electrode is stable for the duration of the crystallisation time. The continuous crystallisation will run for at least eight residence times and each residence time lasts 15 minutes. Therefore the Ca^{2+} electrode should be stable enough during that period. A scheme was carried out to check the stability of the Ca^{2+} electrode and the result is shown in **Table 5.8**.

Table 5.8 Electrode potential versus time for the 100 ppm standard solution

Time (hours)	Temp. of solution (^{0}C)	Electrode potential (mV)	PH
0	38.7	-8.2	7.136
1	38.9	-8.6	7.149
2	38.2	-8.3	7.147
3	38.2	-8.2	7.147
4	38.7	-8.2	7.147

Temperature of standard solution: 39^0C

Concentration of standard solution: 100 ppm of Ca^{2+}

Electrode potential of standard solution: -8.2.mV

Calibration of the Ca^{2+}electrode was also carried out to ensure its precision in measuring the Ca^{2+} concentration and the result is shown in **Table 5.9**.

Table 5.9 Accuracy of the Ca^{2+}electrode at different concentrations

Concentration, ppm Ca^{2+} (prepared)	Concentration, ppm Ca^{2+} (measured)		PH		Potential, mV	
	1st	2nd	1st	2nd	1st	2nd
10	10.00	10.05	7.151	7.151	-9.1	-9.2
100	100	100	6.696	6.696	17.8	17.6
1,000	1,000	998	6.287	6.286	42.1	42.2
1,350	1,350	1,348	6.226	6.227	45.5	45.5

5.6.2. Sampling for slurry density

Samples for the slurry density were taken at the beginning of the crystallisation run, that is, from the seed tank, and subsequently at the end of each residence time. A 50 ml sample was isokinetically withdrawn using a 50 ml plastic syringe and immediately filtered and washed using iso-propanol. The filtered solids were then dried in an oven until a constant weight was reached. The ratio between the weight of solids and the sample volume was taken as the slurry density.

5.6.3. Sampling for crystal size distribution (CSD)

One of the main characteristics of a crystal product is its crystal size distribution or CSD. The CSD is important for several reasons. First, it influences the process performance such as filtration of the mother liquor and the subsequent drying of the crystals. Second, it affects the storage and handling of the final product, such as flowability. Third, it affects the appearance and end use of the product such as the colour and dissolution properties. In this work, CSD sampling was carried out twice. The first sample was taken from the seed tank to represent initial CSD. The second sample was taken after steady state was achieved, that is at the end of the 8^{th} residence time, to correspond to the final CSD. A 50 ml sample was isokinetically withdrawn using a 50 ml plastic syringe and immediately filtered and washed with isopropanol solution. The solids obtained were transferred into a small beaker containing isopropanol and then ready for CSD analysis. Results of the analysis were used to calculate growth and nucleation rates respectively. An ideal MSMPR is

a well-mixed reaction vessel where the product CSD within the crystalliser is the same as that in the product withdrawal point.

The CSD was analysed indirectly because the particle size analyser used in this study, i.e. Malvern MasterSizer™, gives the results in terms of percentage volume distribution. However, since there is no evidence to the contrary, gypsum is believed to be a crystalline material that has a constant density, so that volume distribution is identical to weight distribution. The percentage volume distribution obtained from the Malvern MasterSizer™ was therefore, treated as such.

5.7. Experimental Design

5.7.1. Classification of research method

Research is an attempt to answer a question or to solve a problem utilising a systematic procedure supported by verifiable fact. The following classification of research methodology proposed by Leedy (Leedy 1989) is given to put the experiments carried out in this study into context.

- Historical method
- Descriptive survey method
- Analytical survey method
- Experimental method.

The experimental method is widely used in engineering and science, and therefore, it was used in this study and is elaborated in the following section.

5.7.2. Experimental method

The experimental method implies that the research work is basically carried out in research laboratories. The basic assumption of experimental method is that a given phenomenon follows a cause-and-effect pattern (page 218, Leedy 1989). Experimenter deals with two situations and assesses each of them for comparison. Then the experimenter goes on by introducing external factors into one of the

situations and observes the change, if any. The experiment assumes that whatever change is observed, is caused by the external factors introduced. In most cases, the experiment will conclude by stating that the external factors have either significant or insignificant effect(s) on the experimental subject.

Before any experimental research is carried out, it needs to be carefully planned or designed, so that the required information or data are accurate and reliable and can be gathered in an efficient way. The design of experiment, which is also called the experimental design, is intentionally employed as a powerful technique, that is one that yields reliable experimental data and accurate interpretation of it. In order to elaborate on the experimental design, several statistical terms are first introduced.

- **Experimental design**

Experimental design is a specific plan, which consists of a sequence of steps to be carried out for a research study to ensure that the experiment can be conducted efficiently and will yield an unambiguous and verifiable data. Furthermore, the design ensures that the analysis of the data will yield a valid statistical conclusion.

- **Treatment**

A treatment is a procedure or any controlled condition which is applied to the experimental material in order that its effect on it can be measured (Petersen 1985). Different processes, different operating conditions, are examples which are effectively called different treatments (page 199, Davies 1978). In this work three different admixtures (Fe^{3+}, Zn^{2+} and sodium isopropyl xanthate (=SIPX)) and their combinations (Fe^{3+}+ SIPX, Zn^{2+}+ SIPX, and Fe^{3+}+ Zn^{2} +SIPX) were investigated in order to assess their effects on the crystallisation kinetics. Thus, the treatment represents the different types of admixtures and their combinations.

- **Experimental unit**

Experimental unit is a unit or a group to which a treatment is applied, and which will be compared with a control group, that is the group which has not been given the treatment (page 42, Miller and Wilson 1983). Hence, in this study, an experimental

unit is represented by any cell, which denotes a combination of treatment and block as shown in **Tables 5.10** and **5.11** in **section 5.7.6.2 (The balanced incomplete block design used in this study).**

- **Block**

A block is a group of experimental units having certain inherent characteristics in common. In other words, it is a group of experimental units with homogeneous conditions (page 6, Petersen 1985). In this study, the effects of admixtures on the crystallisation kinetics were investigated at some operating conditions which involve varying the temperatures (**25^{0}C** and **40^{0}C**) and admixture concentrations (**1**, **10** and **50 ppm**). Thus, a block represents an operating condition, which involves temperature variation and different admixture concentration. **Tables 5.10** and **5.11** (in **section 5.7.6.2**) show different blocks designed for this study.

- **Replication**

A replication refers to the number of times any particular treatment appears throughout the experiment. Replication is carried out to provide an estimate of the magnitude of experimental error. Additionally, it helps calculate the level of the tests of significance (page 446, Bethea *et al.* 1985).

- **Observation**

Observation refers to a research activity in recording the information on certain characteristics of an object. The researcher records and analyses the characteristics without intentional intervention.

- **Randomisation**

Randomisation is done to eliminate any bias in the experimental unit (page 446, Bethea *et al.* 1985). As is already known, in every experiment there are always other variables which cannot fully be controlled, even if a good design has been made to control certain variables (page 3, Hicks 1973). Hence, bias might occur. It is assumed that through randomisation, the effects of extraneous factors are averaged

out so that bias is reduced to a minimum or eliminated altogether (page 9, Montgomery 1991).

- **Independent variable**

A certain characteristic that the researcher has control over and is able to manipulate it or change it at will.

- **Dependent variable**

A dependent variable is one over which the researcher has no direct control. It is the result of the effect of the independent variable.

- **Factor**

The term "factor" indicates any manipulable feature of the experimental conditions such as temperature, chemical concentrations, flow rate etc (page 248, Davies 1978).

5.7.3. Experimental design

There is no absolute classification about experimental design. Apparently, the classification is dictated by the academic discipline on which the research will be conducted. Literature survey on the experimental design for engineering and physical sciences (Bethea *et al.* 1985; Davies 1978; Hicks 1973; Montgomery 1991) shows that the following sequence of approach is widely known.

5.7.3.1. One-at-a-time approach

The researcher may be satisfied conducting the experiment conventionally using a one-at-a-time approach. This method is simple but may take a lot of time. Furthermore, it might lead to wrong conclusions if the factors interact (Davies 1978).

5.7.3.2. Randomised block design

It is obvious that if the number of experimental runs that has to be performed is large, the variability of the experimental materials and process expands. Therefore it becomes more difficult to obtain a high precision on the result data because identical conditions may not be available. This situation gives rise to the need of using block and randomisation. Hence, the randomised block design and its variation were adopted.

5.7.3.3. Factorial design

Many experiments involve examination of two or more factors. The factorial design allows such examination to be made. One of the advantages of factorial design is that the conclusions drawn are valid over a range of experimental conditions because the effects of one factor may be estimated at several levels of other factors (page 201, Montgomery 1991).

5.7.4. Requirements of a good experimental design

There are three requirements for a good experimental design, namely replication, randomisation and blocking (page 4, Petersen 1985). If repeated observations were applied to several experimental units receiving the same treatments, the experimental errors could be estimated more accurately. Therefore, replication can be used as a method to better estimate the experimental error. In addition, replication can also increase the precision because it minimises the standard error. As is known:

$$\text{Standard error} = \sqrt{\frac{s^2}{r}} \tag{5.4}$$

where,

$\mathbf{s^2}$ = sample variance

r = number of observations or replication.

It is clear from the above equation that as the number of observations, **r**, increases the standard error decreases. For reasons of practicality, however, replication is sometimes not justifiable. This is especially true for cases where preliminary

observations have shown that experimental data show a certain trend. The investigation on the effects of additives and impurities on the crystallisation of gypsum has shown that in most cases, the effect shows a particular trend with regard to the amount or concentration of impurities. Therefore, the need for replication in this work was seen as optional.

The second requirement is randomisation, that is a technique to ensure that treatments to the experimental units are equal and independent from each other. Hence, randomisation is utilised to minimise the effect of either known or unknown systematic disturbances (page 588, Davies 1978). Still another requirement for a good experimental design is to increase the precision by applying blocking. By blocking it is meant that the experimental materials are arranged into groups or blocks which consist of uniform experimental units. In the analysis of the results, differences among blocks are removed from the experimental error. The following section discusses the error analysis applied to this study.

- **Error Analysis**

It is obvious that each step of an experimental run is subject to both random and systematic errors. In this continuous crystallisation study, the random errors will very likely occur in the following steps.

1. Weighing and dissolving crystals of both $CaCl_2.2H_2O$ and Na_2SO_4 for the crystallisation solutions.
2. Subsequent measuring of the volumes of the crystallisation solutions.
3. Reaction time in starting and stopping the peristaltic pumps.
4. Reaction time in starting and stopping the stopwatch to time the experimental runs.
5. Weighing the mass of crystals obtained.

In addition, all the equipment used in the experiments (balances, volumetric flasks, peristaltic pumps, stopwatch etc.) is also subject to systematic errors. For example, if the pump was running consistently slow, then all the experimental flow rates will be underestimated and vice versa. In this study, the systematic uncertainties of all equipment used, in the absence of more specific information, were identified and established (Taylor 1997). As an example, a volumetric flask of two-litre capacity

has a systematic error or uncertainty of ± 0.6 ml at 20^0C. Similarly, it was decided that all balances have up to one percent uncertainty (Taylor 1997). Briefly, all of the equipment used in this crystallisation experiments was considered to have some known definite uncertainties, which contributes to the systematic error. Thus, in the error analysis both random and systematic errors were taken into account.

The general formula for error propagation as proposed by Taylor (Taylor 1997) was used for the error analysis as all errors are assumed to be independent and occur at random. The formula shows that uncertainties in a certain step propagate through the calculation so that the final result of the calculation will effectively include an accumulation of such error propagation.

5.7.5. Randomised complete block design

While factorial design can be very useful because a lot of factors and their interactions can be investigated, it is sometimes found that sufficient resources to carry out such a comprehensive experiment are not available. When this situation is encountered, most researchers in engineering and physical science usually choose the experimental design, known as **Randomised Complete Block Design**. With this design all sources of experimental variability can be systematically controlled through blocking arrangement.

5.7.6. Balanced incomplete block design

Although the randomised complete block design is an ideal technique, certain experimental conditions may not permit such design from being executed. Shortages of experimental equipment or facilities, physical size of the block or the volume of the experimental work sometimes prevent the use of such design. For such situations the randomisation of the experiment is still possible but the random treatment will not be represented in every block. Thus, examinations of all the treatments under comparable conditions are not possible. In such cases, an alternative design known as **Randomised Incomplete Block Design** may be chosen. It is usually further divided into balanced and unbalanced types. A balanced incomplete block design

would allow the condition where every pair of treatments occurs together in a block the same number of times (Davies 1978). With a balanced incomplete block design the analysis work is simplified and may then be systematised. The unbalanced design, on the other hand, would require a method so that the missing values or responses caused by the imbalance can be formulated.

5.7.6.1. Analysis of a balanced incomplete block design

Let us consider that,

b = number of blocks in the experiments

a = number of treatments in the experiments

k = number of treatments in one block

r = number of replications of a given treatment throughout the experiment

N = total number of observations.

It obviously follows that $\mathbf{N = a\ r = b\ k}$. In addition, there is a parameter, λ, which denotes the number of times each pair of treatments can occur in the same block throughout the experiment. Being "the number of times", hence λ must be an integer. The parameter λ can be explained as follows. In the same block any particular treatment, for example treatment **a**, appears **r** times together with other **r (k-1)** treatments. Since every one of the **(a-1)** other treatments appear λ times together with **a**, then,

$$\mathbf{r(k-1) = \lambda\ (a - 1)}, \text{ or } \lambda = \mathbf{r\ (k-1)/(a-1)} \qquad (5.5)$$

5.7.6.2. The balanced incomplete block design used in this study

The balanced incomplete block design was adopted in this study due to the following advantages (page 580, Davies 1978). First, maximum precision is ensured because variability among blocks is removed from the experimental error. Second, all treatments are compared with the same precision. Third, calculation can be simplified and systematised. Fourth, if by accident, a balanced incomplete block design cannot be fully implemented, an analysis of the available experimental data is still possible through the use of missing value estimation (Davies 1978).

A proper choice of experimental design is essential to obtain a better understanding of the effects of all the factors to be investigated. In this work, two factors were investigated, that is the temperatures in ^{0}C and the level of admixture concentrations in ppm. The temperature as a factor has two levels, that is **25^{0}C** and **40^{0}C**. For the admixture concentrations, three levels were chosen: **1 ppm, 10 ppm** and **50 ppm**. The levels of the two chosen factors were selected at random and it was assumed that they originate from an infinite population of possible levels.

A selection of balanced incomplete block designs formulated by Davies (see pp. 228-235, Davies 1978) was consulted and it was then decided that with two factors and three levels of each factor, an arrangement with blocks of five observations would be chosen. The arrangement consists of six treatments in six blocks of five. It comprises all possible combinations of the six treatments in groups of five as shown in **Tables 5.10** and **5.11**. The requirement of a balanced incomplete block design is satisfied in that every pair of treatments occurs together in the same block the same number of times (Davies 1978). In this case, each pair occurs four times, for example, treatments **A** and **B** in blocks **1** to **4**, treatments **B** and **C** in blocks **1, 2, 3** and **6**, treatments **C** and **D** in blocks **1, 2, 5** and **6**, and so on.

Table 5.10 Balanced incomplete randomised block design – general plan

Treatment	Block					
	1	2	3	4	5	6
A	✓	✓	✓	✓	✓	
B	✓	✓	✓	✓		✓
C	✓	✓	✓		✓	✓
D	✓	✓		✓	✓	✓
E	✓		✓	✓	✓	✓
F		✓	✓	✓	✓	✓

Table 5.11 Balanced incomplete randomised block design used in this study

Types of Admixtures	Admixture concentration (ppm) & Crystallisation temperature (^{0}C)					
	1 ppm & 25^{0}C	10 ppm & 40^{0}C	50 ppm & 25^{0}C	1 ppm & 40^{0}C	10 ppm & 25^{0}C	50 ppm & 40^{0}C
Fe^{3+}	✓	✓	✓	✓	✓	
Zn^{2+}	✓	✓	✓	✓		✓
SIPX	✓	✓	✓		✓	✓
Fe^{3+} + SIPX	✓	✓		✓	✓	✓
Zn^{2+} + SIPX	✓		✓	✓	✓	✓
Fe^{3+} + Zn^{2+} + SIPX		✓	✓	✓	✓	✓

In addition, two experimental runs at 25^{0}C and 40^{0}C each were conducted for the pure system, that is, without added admixtures. These two runs serve as a control on which comparison of effect is based.

By applying a balanced incomplete block design it is obvious that there will be some information loss in the experimental results compared with a factorial design (page 86, Dash 1993). This loss of information is defined as an efficiency factor, $\mathbf{E_f}$, that is a relative ratio of error variance of treatments using a factorial design and that using a balanced incomplete block design. The following equation is used to define the efficiency factor.

$$Ef = \frac{\left[\frac{2\sigma_a^2}{r}\right]}{\left[\frac{2\sigma_k^2 . k.(a-1)}{N_{actual}.(k-1)}\right]} \tag{5.6}$$

where,

E_f = efficiency factor

σ_a^2 = variance of the differences of two treatment values in a complete block design

σ_k^2 = variance of the differences of two treatment values in an incomplete block design

r = number of replications of a given treatment throughout experiment

a = number of treatments in the experiments

k = number of treatments per block

N_{actual} = total number of observations

$\frac{2\sigma_a^2}{r}$ = error variance of the difference of statistical means between any two blocks in a complete design.

$\frac{2\sigma_k^2.k.(a-1)}{N_{actual}(k-1)}$ = error variance of the difference of statistical means between any two blocks in an incomplete block design.

It is usually safe to assume (Dash 1993) that $\sigma_a^2 = \sigma_k^2$, so that the efficiency factor equation becomes:

$$Ef = \frac{a(k-1)}{k(a-1)} \tag{5.7}$$

In this work it was decided that **a** = **6** and **k** = **5**, where **a** is the number of blocks and **k** is number of treatment per block. Therefore $\mathbf{E_f}$ = (6)(5-1)/(5)(6-1) = 24/25 = 0.96 or 96 %. In other words, using the balanced incomplete block design for this work there is a loss of information of 100 – 96 = 4 %.

Summary

This chapter discusses the materials and methods used in the continuous (MSMPR) crystallisation experiments carried out in this study. The discussion covers six main topics as follows:

1. *Calculation of mass balance to determine the quantities of raw materials needed and crystal product produced, as well as the stream flow rates and their compositions.*

2. *Description of the laboratory continuous (MSMPR) crystalliser including an explanation of its major components: the seed tank, the liquor tank and the crystalliser, as well as considerations of the capability of the peristaltic pumps used.*

3. *Preparation of crystallising solutions: $CaCl_2$ and Na_2SO_4 solutions, respectively, and gypsum crystals as seeds. This section includes calculations of the quantities of solutions and seeds needed for the entire experiments. The preparation of gypsum crystals as seeds covers the seed making, the uniformity of the crystals produced and the characterisation with respect to morphology and chemical purity.*

4. *Description of how the continuous crystallisation run was performed, how to ensure achievement of steady state, and hence, a representative MSMPR crystallisation operation.*

5. *Sampling and measurements to extract the experimental data, which includes data for solution concentration with respect to Ca^{2+}, slurry density, and crystal size distribution (= CSD). This section covers an explanation of the accuracy of the Calcium Ion Selective Electrode used for the solution concentration measurement, the iso-kinetic sampling for the slurry density and the CSD.*

6. *Discussion on the selection of an appropriate experimental design to be adopted in this study by examining three factors: (1) type of admixtures, (2) concentration of admixtures, (3) crystallisation temperatures. Three different admixtures were used: Fe^{3+}, Zn^{2+}, and sodium isopropyl xanthate (SIPX). Concentrations of admixtures were varied as follows: (1) 1 ppm, (2) 10 ppm, (3) 50 ppm. Two levels of crystallisation temperatures were selected: (1) 25^0C, (2) 40^0C. A balanced incomplete randomised block design was considered appropriate for this continuous crystallisation study.*

References

1. Amjad, Z. (1985). "Applications of Antiscalants to Control Calcium Sulfate Scaling in Reverse Osmosis Systems." *Desalination*, 54, 263-276.
2. Amjad, Z. (1988). "Kinetics of crystal growth of calcium sulfate dihydrate. The influence of polymer composition, molecular weight, and solution pH." *Canadian Journal of Chemistry*, 66, 1529-1536.
3. Bethea, R. M., Duran, B. S., and Boullion, T. L. (1985). *Statistical Methods for Engineers and Scientists*, Marcel Dekker, New York & Basel.
4. Chan, V. A. (1997). "The Role of Impurities in the Continuous Precipitation of Aluminium Hydroxide," PhD, Curtin University of Technology, Perth, Western Australia.
5. Dash, S. R. (1993). "Crystallization Kinetics of KCl in Continuous and Batch Cooling Crystallizers: Effect of Magnesium and Sulfate Ions," PhD, University of Saskatchewan, Saskatoon,Saskatchewan, Canada, S7N 0W0.
6. Davies, O. L. (1978). *The Design and Analysis of Industrial Experiments*, Longman Group, London,New York.
7. He, S., Oddo, J. E., and Tomson, M. B. (1994). "The Seeded Growth of Calcium Sulfate Dihydrate Crystals in NaCl Solutions up to 6 M and 90^0 C." *Journal of Colloid and Interface Science*, 163, 372-378.
8. Hicks, C. R. (1973). *Fundamental Concepts in the Design of Experiments*, Holt, Rinehart and Winston, New York, etc.
9. Lakatos, B., and Sapundzhiev, T (1990). "Effect of Size-dependent Crystal Growth Rate on the Multiplicity and Stability of MSMPR Crystallisers." *11^{th} Symposium on Industrial Crystallization*, Garmisch-Partenkirchen (Munich), Germany, 41-46.
10. Leedy, P. D. (1989). *Practical Research. Planning and Design*, Macmillan Publishing, New York.
11. Liu, S. T., and Nancollas, G. H. (1970). "The Kinetics of Crystal Growth of Calcium Sulphate Dihydrate." *Journal of Crystal Growth*, 6, 281-289.
12. Liu, S. T., and Nancollas, G. H. (1973). "The Crystal Growth of Calcium Sulfate Dihydrate in the Presence of Additives." *Journal of Colloid and Interface Science*, 44(3), 422-429.

13. Mersmann, A. (1995). *Crystallization Technology Handbook*, Marcel Dekker, New York, Basel, Hong Kong.
14. Miller, P. M., and Wilson, M. J. (1983). *A Dictionary of Social Science Methods*, John Wiley & Sons, Chichester, etc.
15. Montgomery, D. C. (1991). *Design and Analysis of Experiments*, John Wiley & Sons, New York, etc.
16. Murray, M. (1999). "Batch Crystallisation of Gypsum," Final Year Undergraduate Project, Curtin University of Technology, Perth, Western Australia.
17. Perry, R. H., and Green, D. W. (1997). *Perry's Chemical Engineers' Handbook*, McGraw-Hill, New York, etc.
18. Petersen, R. G. (1985). *Design and Analysis of Experiments*, Marcel Dekker, New York ,Basel.
19. Rolfe, P. F. (1966). "Polymers that inhibit the deposition of calcium sulphate: Some interesting conductance observations." *Desalination*, 1, 359-366.
20. Taylor, J. R. (1997). *An Introduction to Error Analysis. The Study of Uncertainties in Physical Measurements*, University Science Books, Sausalito, California, USA.
21. Weijnen, M. P. C., and van Rosmalen, G. M (1984). "The Role of Additives and Impurities in the Crystallization of Gypsum." *Industrial Crystallization 84*, 61-66.

CHAPTER 6 CONTINUOUS CRYSTALLISATION OF GYPSUM IN THE PRESENCE OF ADMIXTURES

6.1. Introduction

In an industrial environment, gypsum usually crystallises in the presence of contaminants. Admixtures are almost always present in a crystallising system and influence the crystallisation process. It has been elaborated in the **Literature Review** in **Chapter 2**, that admixtures can have very significant effects on crystallisation processes, especially the crystallisation kinetics: nucleation and growth. Certain admixtures may also alter the shape of crystals and enhance the tendency of agglomeration (Al-Sabbagh *et al.* 1996).

Research on gypsum is very extensive and is mainly driven by the need to investigate the occurrence of gypsum scale formation, which is one of the main problems encountered by many industries. Water desalination by reverse osmosis, phosphoric acid production, secondary oil recovery by water flooding, water cooling towers and mineral processing such as copper and zinc extraction (Chan 1997b; Cowan and Weintritt 1976; He *et al.* 1994; Klepetsanis and Koutsoukos 1989), are a few examples of industrial processes where the occurrence of gypsum scales is prevalent.

In this study, an MSMPR laboratory crystalliser was used to investigate the crystallisation of gypsum. There are several reasons for this choice. Firstly, in an MSMPR crystalliser, steady state experimental data can generally be obtained. Secondly, the ultimate aim of this study is to investigate the accumulation of gypsum crystals as found in scaling. The scale formation develops over a relatively long period of time, usually in a flowing system, hence resembles a continuous process.

The methodology used for the continuous crystallisation experiments is presented in the previous chapter (= **Chapter 5**). Because of the high volume of physical work involved, a particular type of experimental design was adopted to reduce the number of experimental runs. A balanced incomplete block design was chosen and its rationale was detailed. With the reduction of the number of experimental runs, a loss

of information obviously takes place. However, the loss is considered acceptable and did not significantly affect the analysis.

The continuous crystallisation experiments were conducted at an initial concentration (supersaturated condition) level of 1,200 ppm of Ca^{2+} in the crystalliser to simulate the condition at a particular mineral processing industry in Western Australia (Northwood 1995). A total of **74** experiments were conducted as detailed in **Chapter 5** and **Appendix C**. Briefly, the matrix of experimental variables consisted of two crystalliser temperature levels of 25 and 40^0C, six different levels of admixture concentrations (1, 10, 20, 22, 25 and 50 ppm) and six different combinations of admixture types (Fe^{3+}, Zn^{2+}, SIPX (= sodium isopropyl xanthate), Fe^{3+}+SIPX, Zn^{2+}+SIPX and Fe^{3+}+Zn^{2+}+SIPX). It has already been elaborated in the experimental design (see **Chapter 5**, section **5.8.6.2**) that the number of experiments was reduced at the expense of only **4%** loss of information.

This chapter consists of three main parts: **Introduction**, **Attainment of Steady State**, and **Calculation of Crystallisation Kinetics**. In the section: **Attainment of Steady State**, the extraction of experimental data is explained. Kinetics of crystallisation, which comprises nucleation and growth of gypsum crystals as affected by the selected admixtures, is described in the section on **Calculation of Crystallisation Kinetics**. Discussion on the effects of admixtures (either used individually or in combination) on the linear growth rate is presented in section **6.4**. An attempt was made to correlate the linear growth rate, with both the crystal size and the concentration of admixtures, and this attempt is described in section **6.5**. In addition, the nucleation rate calculation is discussed in section **6.6**. This chapter closes with a summary, highlighting the main points of the discussion.

6.2. Attainment of Steady State

6.2.1. Attainment of steady state with respect to solution concentration and slurry density

As explained in **Chapter 5**, extraction of experimental data for a continuous crystallisation should be made after a steady state has been attained. An ideal MSMPR crystalliser should be able to reach such a steady state with respect to three parameters: solution concentration, slurry density, and crystal size distribution (CSD) (Chan 1997a).

Attainment of steady state with respect to solution concentration in the crystalliser is shown by the desupersaturation rate curve (= change of concentration with time) as depicted in **Figure 6.1**.

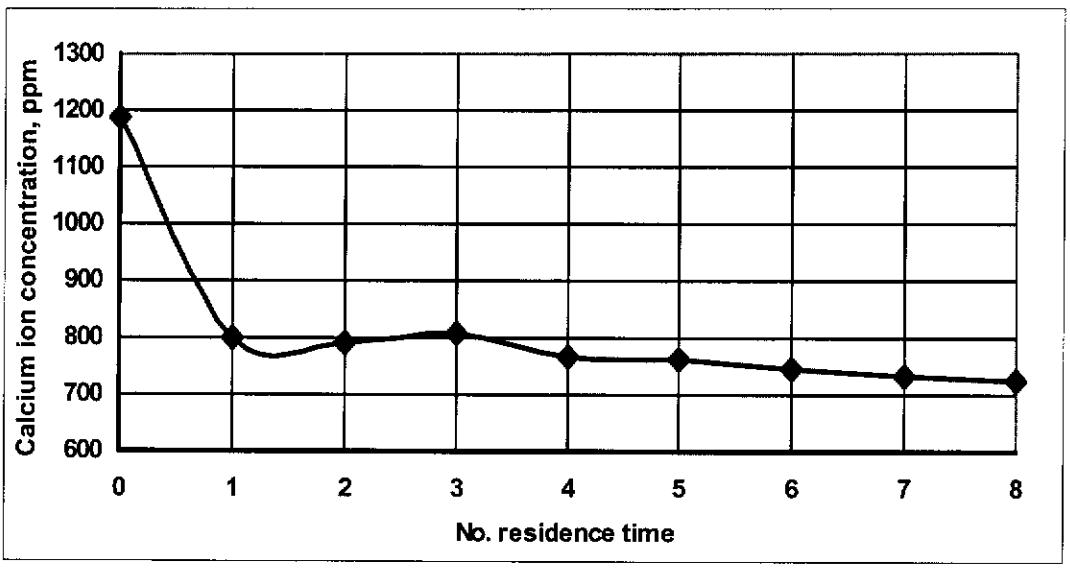

Figure 6.1 **A typical desupersaturation curve for pure gypsum crystallisation, showing the decrease of Ca^{2+}concentration as the crystallisation progresses (1 residence time = 15 minutes)**

As can be seen, the rate of desupersaturation is extremely fast for the first **15** minutes of the experimental run but the curve levels off from that time onwards. The levelling off in the decrease of Ca^{2+} is obviously due to nucleation and growth of gypsum crystals at the expense of Ca^{2+} ions. The desupersaturation curve in **Figure 6.1** confirms that steady state condition with respect to the solution concentration is

achieved after about the seventh residence time. He *et al.* (He *et al.* 1994) studied the growth rate of calcium sulphate dihydrate using seeded growth method and found that the crystallisation reaction was caused only by the added seeds. Their study revealed that no induction period was observed and that the gypsum crystals started growing immediately after seed addition. The same situation was observed in this study, namely that the induction period did not occur. **Appendix D** (= **Continuous Crystallisation Experimental Data**) tabulates the data on the decrease of Ca^{2+} concentrations for the entire experimental runs.

As crystallisation proceeds, new crystals will form and subsequently grow and the seeds added into the crystallising solution grow as well. Consequently, the number of crystals in the crystalliser increases which is reflected by an increase in slurry density (= mass of crystals per unit volume of crystalliser) as crystallisation progresses. A plot of slurry density versus time of crystallisation can then be made as shown in **Figure 6.2**.

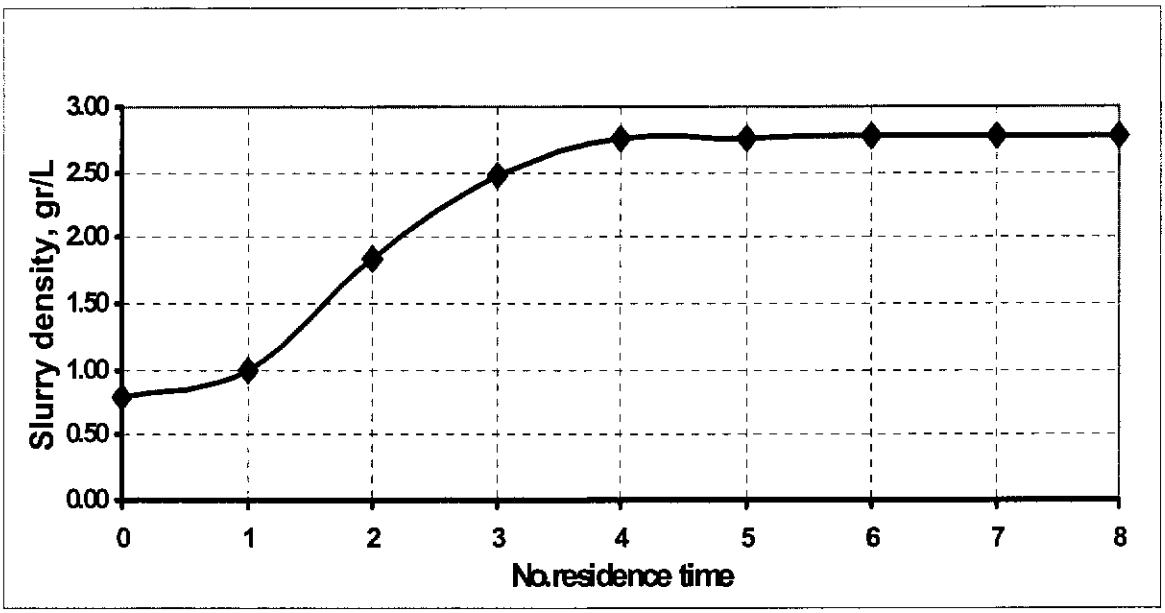

Figure 6.2 **A typical curve of slurry density versus residence time for pure gypsum crystallisation, showing an increase in slurry density as crystallisation progresses (1 residence time = 15 minutes)**

As can be seen, the slurry density gradually increases to ultimately reach a plateau at approximately the fourth residence time. It can thus be concluded that the experimental run started to reach steady state from the fourth residence time or after

60 minutes of crystallisation run time. **Appendix D (= Continuous Crystallisation Experimental Data)** includes data on the slurry density for this continuous crystallisation study.

Figures 6.1 and **6.2** are essentially mirror images of each other. The decrease in Ca^{2+} concentration, as depicted in **Fig.6.1**, is undoubtedly due to $CaSO_4.2H_2O$ or gypsum crystallising out of the solution. The sharp decrease of Ca^{2+}ions during the first residence time, however, should have been manifested in the sudden increase in slurry density in the same period of time. A lot of Ca^{2+} ions have gone out of the solution but this was not reflected in the small change in crystal mass. The reason for this is not exactly known, but it could be due to more nucleation occurring in the first residence time and fines not being collected or passed the filter paper. As a result, the density of slurry during the first 15 minutes of the crystallisation run was low.

Figure 6.2 also shows that the mass of gypsum crystals increases by as much as two to three times the weight of seed crystals added initially. It can be concluded, therefore, that the low initial seed concentration of 0.800 gram per litre of solution was adequate to facilitate the growth and thus the crystallisation experiment. Scanning electron microscopy (SEM) observation was made of the crystals on completion of the experimental run. The growing crystals show a surface roughening, which is characteristic of nucleation (Liu and Nancollas 1970).

Having established the steady state with respect to both solution concentration and slurry density, it was thought that the use of the admixtures should be tested to ascertain their ability to affect the crystallisation kinetics. The tests were carried out, and the graphs of the experimental data were compared as shown in **Figs 6.3** and **6.4**, which depict the desupersaturation profiles of the crystallisation runs at temperature levels of 25^0C and 40^0C, respectively. As can be seen in both figures, most of the desupersaturation curves for the system with admixtures show a lower decrease than that for the pure gypsum. This clearly indicates that the admixtures were capable of inhibiting the formation of gypsum, and hence confirms the expected aim of this continuous crystallisation study that the selected admixtures would be able to affect the crystallisation kinetics. In addition, the desupersaturation curves in both **Figs.**

6.3 and **6.4** show that a steady state condition for all admixture concentrations tested could be achieved in around the 8th residence time.

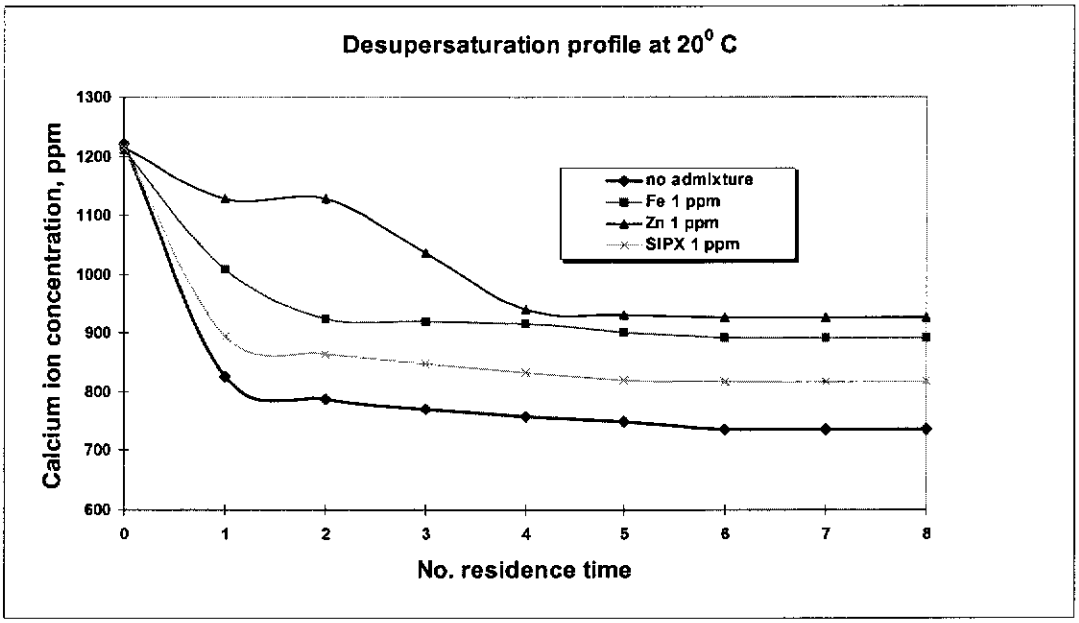

Figure 6.3 **Desupersaturation curves at 25^{0}C showing the decrease of Ca^{2+}concentration as crystallisation progresses (1 residence time = 15 minutes)**

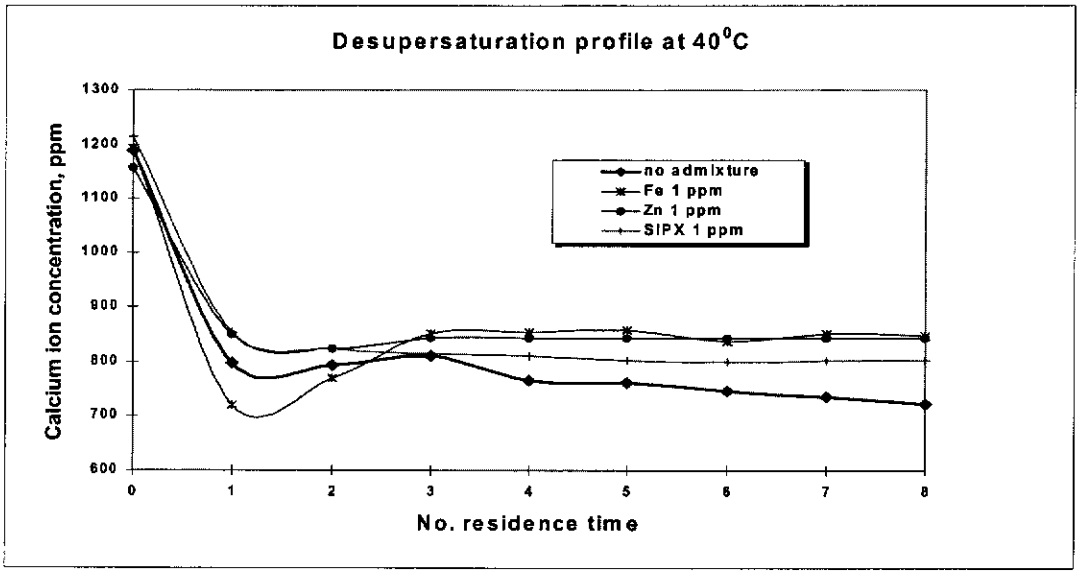

Figure 6.4 **Desupersaturation curves at 40^{0}C showing the decrease of Ca^{2+}concentration as crystallisation progresses (1 residence time = 15 minutes)**

6.2.2. Attainment of steady state with respect to CSD

The accuracy of results for particle size analysis depends very strongly on the dispersion of the particulate sample prior and during the analysis. As has been verified by Iacocca and German (Iacocca and German 1997), comparison of results of particle size measuring instruments shows that the dispersion is more important than the measurement technique used. In other words, regardless of the types of particle size measuring instruments used, the samples must be well dispersed to ensure homogeneity with respect to their particle distribution, to enable the results to be compared across the different measuring instruments. In order to verify that the dispersion of samples during analysis was adequate, and thus did not affect the CSD, a repetition of measurement was made, as shown in **Figures. 6.5** and **6.6**, respectively. Sonication of samples prior to analysis was not carried out for two reasons. Firstly, from visual inspection, the gypsum crystals used in this study did not show any agglomeration during storage, and the crystals flowed freely when taken out of the container. Secondly, gypsum crystals are brittle and rod-like in shape; hence sonication may break the crystals and hence affect the measured CSD.

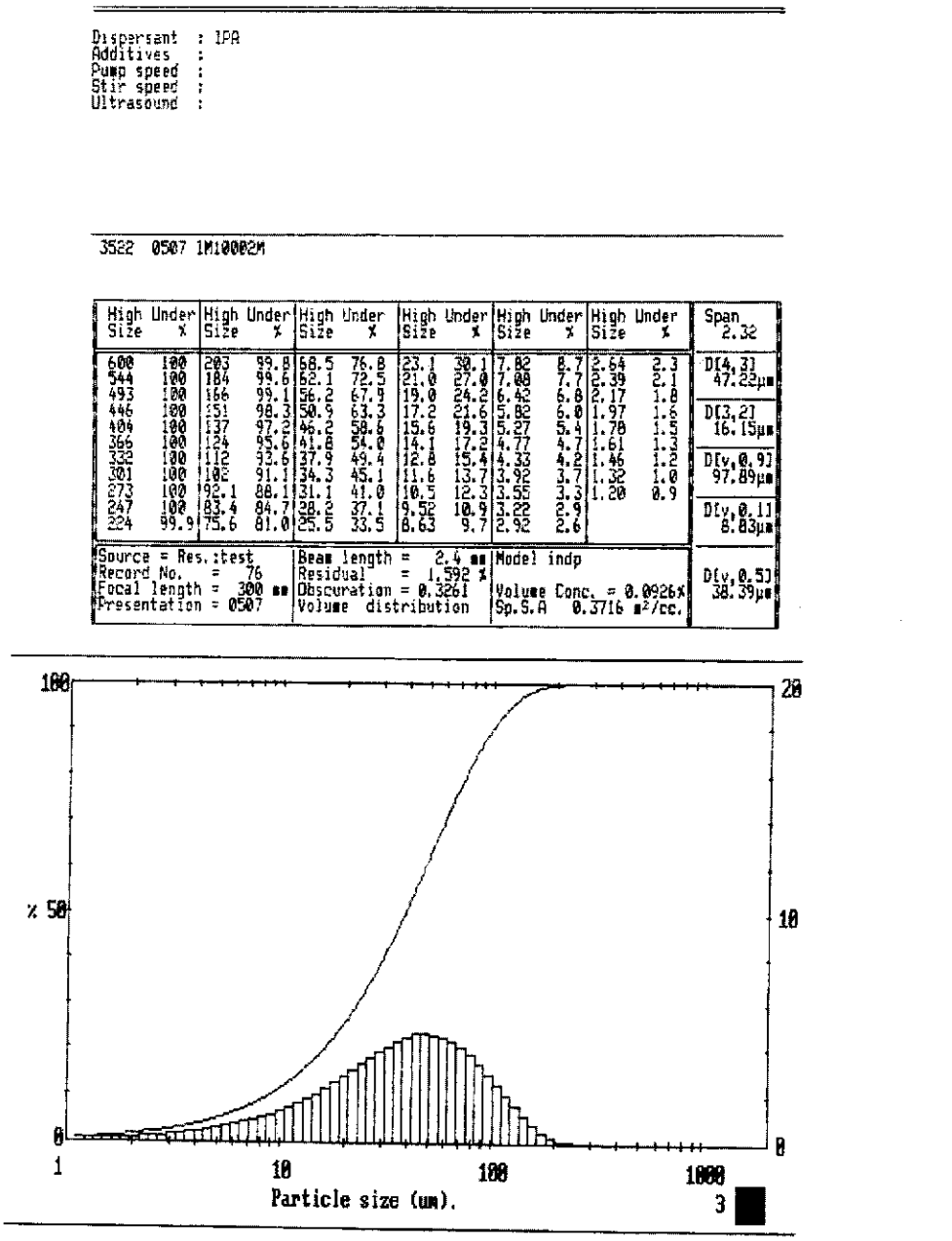

Figure 6.5 **A typical Malvern analysis of the gypsum crystals used in the experiments**

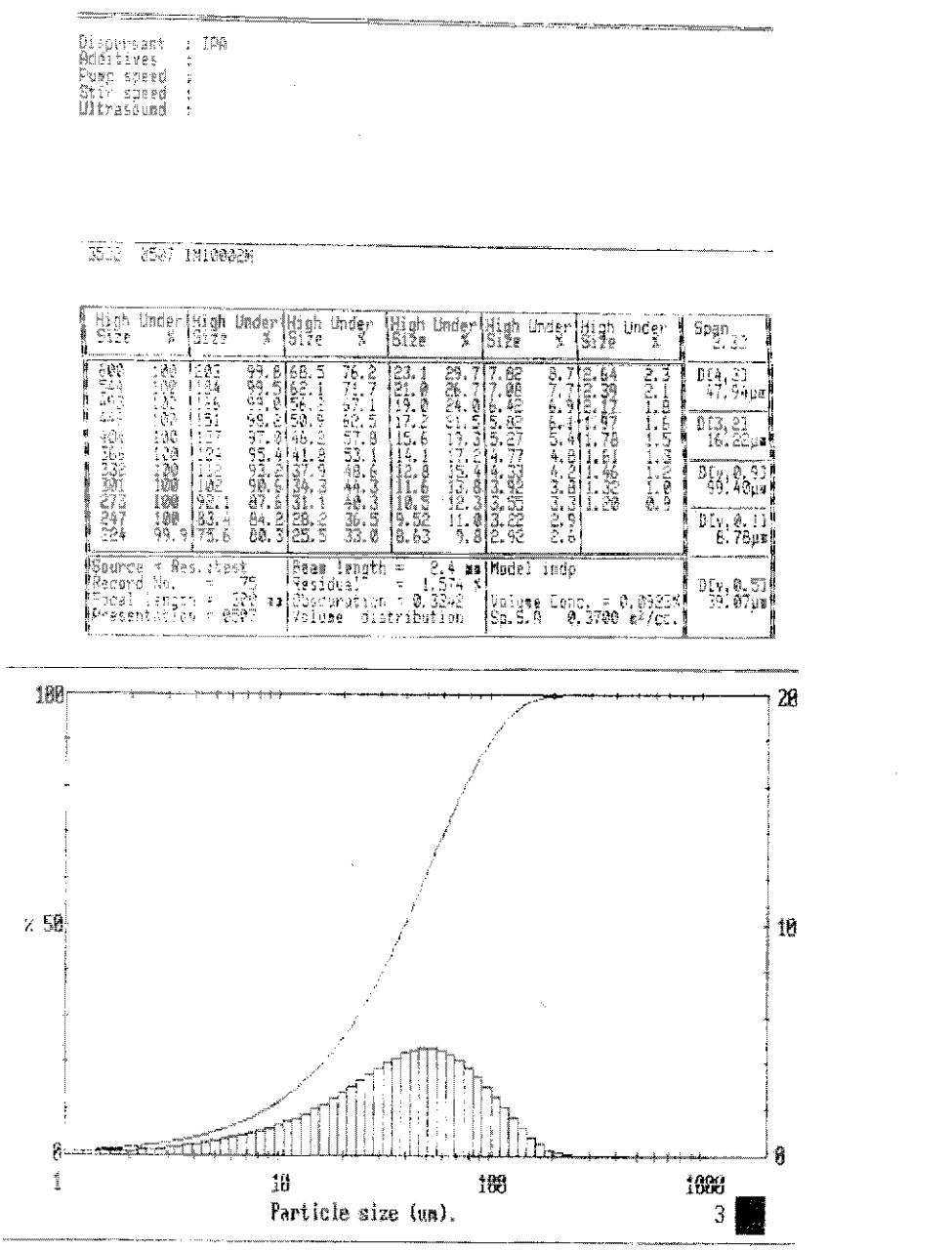

Figure 6.6 Repetition of Malvern analysis for the same sample analysed and presented previously in Figure 6.5

Data of Malvern analyses shown in both **Figures. 6.5** and **6.6** were obtained from one sample, namely, that of the seed crystals. **Figure 6.6** shows the result of a repetition of the Malvern analysis previously carried out and shown in **Figure. 6.5**. Malvern analysis requires dispersion of samples in a suitable liquid, which does not interact (either physically and/or chemically) with the particles suspended in it. Physical interaction with the crystals may manifest in phenomena such as agglomeration or dissolution, whereas the chemical interaction may result in the liquid reacting chemically with the crystals. Stirring is required to assist dispersion of particles in the liquid. Comparison of **Figures. 6.5** and **6.6** clearly shows that the CSD does not change appreciably. This means that the liquid used for the dispersion of the particles, namely, isopropyl alcohol (= IPA), neither interacted with nor dissolved the crystals so as to change the CSD. Therefore, the use of IPA as a dispersion medium was considered suitable. The observable consistency of the plots in **Figures. 6.5** and **6.6** also confirms that the intensity of stirring was appropriate so as not to cause any significant breakage or attrition of the crystals.

During each experimental run, two Malvern analyses for CSD were carried out, that is at the start (= CSD for seeds) and at the end (= CSD for product crystals) of a run. Typical data of Malvern analysis are presented in **Table 6.1** and further treatment of such raw data for the seeds and product crystals is tabulated in **Table 6.2** (see the next section). The next section on **Calculation of Crystallisation Kinetics** describes the determination of nucleation and growth rates based on the data obtained from Malvern analysis as presented in both **Tables 6.1** and **6.2**.

6.3. Calculation of Crystallisation Kinetics

Crystallisation kinetics arises from a combination of nucleation and growth of crystals. The population balance theory as developed by Randolph and Larson (Randolph and Larson 1988) is a well-established technique to derive crystallisation kinetics from steady state MSMPR crystalliser data. The theory is especially useful because it is capable of determining both nucleation and growth rates simultaneously. Under ideal conditions, such as when the growth of crystals is independent of size, the CSD of an MSMPR can be utilised to predict nucleation and

growth rates. Their method, however, was designed for the unseeded crystallisation systems, where no solids are present in the feed stream.

The technique developed by Chan (Chan 1997a) for the determination of nucleation and growth rates of crystals takes into account the distribution of seeds and was adopted in this study. Similar to the previous formula developed by Randolph and Larson, Chan's formula will first determine the growth rate. Then, based on the growth rate obtained, the nucleation rate can be calculated.

The technique developed by Randolph and Larson (Randolph and Larson 1988) assumes that nuclei are formed at one single size. As is shown in the technique, the nuclei density, $\mathbf{n_0}$, is calculated at zero size, that is **L = 0.00** micron. This assumption has proved to be unsatisfactory for some systems, that is those, which show the break down of the population density plot at small size fractions. In addition, the nucleation rate calculation may be erroneous due to conversion of the number of crystals into natural logarithmic number. In the present study, it was decided, therefore, to carry out the nucleation rate calculation using the technique developed by Jancic and Grootscholten (Jancic and Grootscholten 1984), where the five smallest size points obtained from the particle analysis were chosen as representative of the size of the nuclei.

6.3.1. Crystal size distribution (CSD) data

The CSD data were obtained by Laser diffraction particle sizing analysis using a Malvern Master Sizer™. Briefly, the Malvern instrument operates in the following way.

A parallel beam of monochromatic coherent light of fixed wavelength (λ = 670 nm) generated from He-Ne gas lasers was used to illuminate the crystals dispersed in a sample cell. Illumination of the crystals creates an array of Fraunhoffer diffraction pattern rings. A Fourier transform lens is placed in the light path after the crystals and a detector is placed at the focal plane of the lens. The detector consists of 16 to 32 concentric semicircular light sensitive diodes (= detector elements) radially

arranged from the centre. Crystals of different sizes generate different light intensity, which gives rise to different voltages in the detector element. Correlation between these voltages and crystal sizes is calculated using the Mie theory, and is subsequently displayed as digital data at every measurement time or sweep. The digital data were then used to calculate CSD (Brown and Felton 1985; Inaba and Matsumoto 1998; Rawle 2001).

Malvern analysis generates particle distribution data in either cumulative percentage volume distribution or cumulative percentage number distribution. The data obtained were then converted to obtain real or absolute number of the crystals or particles present in the system per unit volume.

Assuming that the density of gypsum crystals is constant, the Malvern data in percentage volume distribution is identical with that in percentage mass distribution. The assumption is considered valid since there is no evidence to the contrary. Therefore, knowing the total mass of the crystals per unit volume enables one to calculate the number of crystals for each particular size range.

Total mass of crystals:

$$M = \sum_{i=0}^{i=1} n_i k_v \rho_i L_i^3 \Delta L_i \tag{6.1}$$

where

M = total mass of crystals, mg

n_i = number of crystals in each size range, dimensionless

k_v = volumetric shape factor = 0.523, dimensionless (Jamialahmadi and Muller-Steinhagen 2000; Li *et al.* 1997)

ρ_i = density of crystal, mg/cm^3

L_i = characteristic crystal size for each size range, micron

ΔL = $L_i - L_{i-1}$

= difference in length between two adjacent sizes, micron.

The density of the crystals for the entire size range is constant, and therefore **Eq.(6.1)** can be written as:

$$M = 0.523\ \rho_i \sum_{i=0}^{i=1} n_i L_i^3 \Delta L_i \tag{6.2}$$

To calculate the number of crystals for each size range, $\mathbf{n_i}$, **Eq. (6.2)** was converted as follows:

$$n_i = \frac{M}{0.523\ \rho L_i^{\ 3} \Delta L_i} \tag{6.3}$$

Table 6.1 in the following page shows typical raw data of Malvern analysis to be used in conjunction with **Eq. (6.3)**.

Table 6.1 Typical raw data of Malvern analysis

High Size	Under, %	High Size	Under, %	High Size	Under, %	High Size	Under, %	High Size	Under, %
137	100	46.2	89.0	15.6	46.1	5.27	15.7	1.78	3.7
124	99.9	41.8	86.0	14.1	42.4	4.77	14.1	1.61	3.1
112	99.8	37.9	82.6	12.8	38.8	4.33	12.6	1.46	2.4
102	99.6	34.3	78.9	11.6	35.5	3.92	11.3	1.32	1.7
92.1	99.2	31.1	75.0	10.5	32.3	3.55	10.1	1.20	1.1
83.4	98.7	28.2	71.0	9.52	29.3	3.22	8.9		
75.6	98.0	25.5	66.8	8.63	26.6	2.92	7.8		
68.5	97.0	23.1	62.6	7.82	24.1	2.64	6.9		
62.1	95.6	21.0	58.3	7.08	21.7	2.39	6.0		
56.2	93.8	19.0	54.2	6.42	19.5	2.17	5.1		
50.9	91.6	17.2	50.1	5.82	17.5	1.97	4.4		

Note: High Size = crystal size (in microns),
Under % = cumulative undersize (in %).
The instrument used, can detect the crystal sizes up to 600 micron. Such high sizes are not shown in the above table since their percentage under size = 0 %. The largest size in the sample is 137 micron.

For crystals of 137 microns in size (1st row), the cumulative percentage undersize = 100 %, which means that all crystals in the population are smaller than 137 microns.

6.3.2. Sample calculation for Malvern analysis

As can be seen from **Table 6.1**, the largest crystals have sizes between **137.0** and **124.0** μm. In other words, all crystals (= **100 %**) have sizes below **137.0** μm. **Table 6.1** also shows that at the other extreme of the distribution, i.e. at the small fractions, **1.10 %** of the total number of crystals have sizes lower than 1.20 μm.

The CSD data shown in **Table 6.1** were then converted into percentage cumulative oversize and, together with the percentage cumulative under-size, are plotted against the crystal size, which results in cumulative distribution plots, as shown in **Figure 6.7**. The plot in **Figure 6.7** is similar to that in **Figure2.9** in **Chapter 2** section **2.6** (= **Literature Review – part 1**).

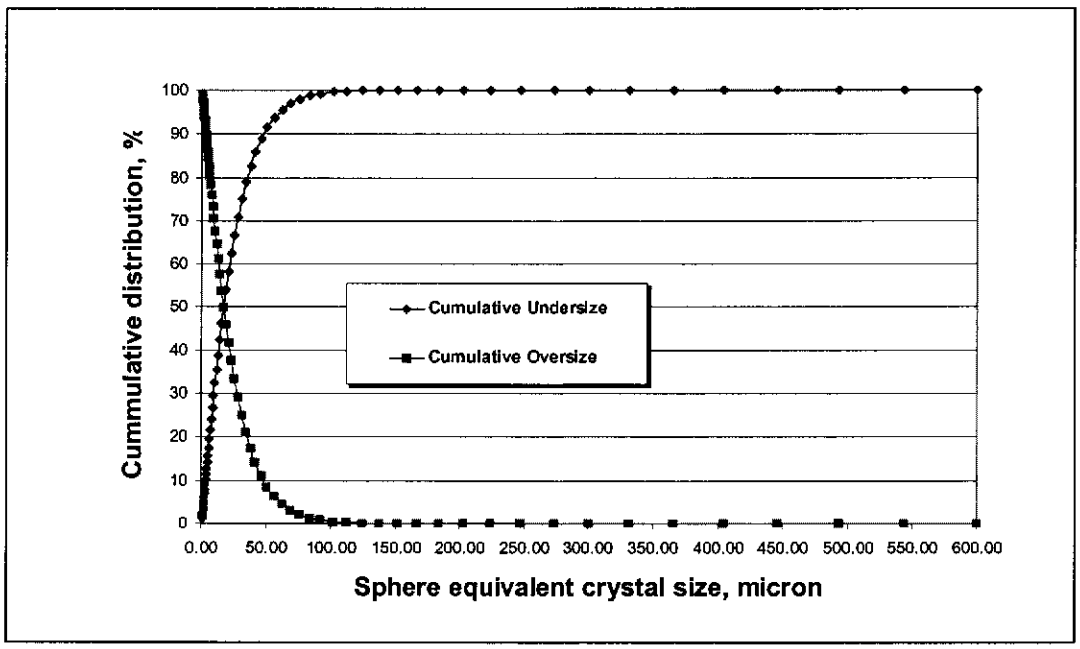

Figure 6.7 A typical cumulative plot of CSD

In order to determine the crystallisation kinetics, it is necessary to calculate the number of crystals for each size range, and this has been done and tabulated in **Table 6.2**. The contents of **Table 6.2** are explained as follows. **Column 1** contains data of the range of crystal sizes, which was measured by the Malvern particle analyser and was taken from the raw data in **Table 6.1**. **Column 2** shows the average size of each size range.

Table 6.2 Typical data of the number of crystals at the start and end of an experimental run

High size (micron)	Average size (micron)	Start of Run Undersize (%)	% of total (vol)	% of total (weight)	no. crystals/litre	End of Run Undersize (%)	% of total (vol)	% of total (weight)	no. crystals/litre
600.00	572.00	100.00	0.00	0.00	0	100.00	0.00	0.00	0
544.00	518.50	100.00	0.00	0.00	0	100.00	0.00	0.00	0
493.00	469.50	100.00	0.00	0.00	0	100.00	0.00	0.00	0
446.00	425.00	100.00	0.00	0.00	0	100.00	0.00	0.00	0
404.00	385.00	100.00	0.00	0.00	0	100.00	0.00	0.00	0
366.00	349.00	100.00	0.00	0.00	0	100.00	0.00	0.00	0
332.00	316.50	100.00	0.00	0.00	0	100.00	0.00	0.00	0
301.00	287.00	100.00	0.00	0.00	0	100.00	0.00	0.00	0
273.00	260.00	100.00	0.00	0.00	0	100.00	0.00	0.00	0
247.00	235.50	100.00	0.00	0.00	0	100.00	0.10	0.10	9
224.00	213.50	100.00	0.00	0.00	0	99.90	0.10	0.10	13
203.00	193.50	100.00	0.00	0.00	0	99.80	0.30	0.30	54
184.00	175.00	100.00	0.00	0.00	0	99.50	0.50	0.50	129
166.00	158.50	100.00	0.00	0.00	0	99.00	0.80	0.80	331
151.00	144.00	100.00	0.00	0.00	0	98.20	1.20	1.20	709
137.00	130.50	100.00	0.10	0.10	23	97.00	1.60	1.60	1368
124.00	118.00	99.90	0.10	0.10	33	95.40	2.20	2.20	2756
112.00	107.00	99.80	0.20	0.20	107	93.20	2.60	2.60	5242
102.00	97.05	99.60	0.40	0.40	288	90.60	3.00	3.00	8188
92.10	87.75	99.20	0.50	0.50	554	87.60	3.40	3.40	14285
83.40	79.50	98.70	0.70	0.70	1162	84.20	3.90	3.90	24576
75.60	72.05	98.00	1.00	1.00	2449	80.30	4.10	4.10	38130
68.50	65.30	97.00	1.40	1.40	5110	76.20	4.50	4.50	62364
62.10	59.15	95.60	1.80	1.80	9588	71.70	4.60	4.60	93042
56.20	53.65	93.80	2.20	2.20	17580	67.10	4.60	4.60	139585
50.90	48.55	91.60	2.60	2.60	31438	62.50	4.70	4.70	215808
46.20	44.00	89.00	3.00	3.00	52054	57.80	4.70	4.70	309687
41.80	39.85	86.00	3.40	3.40	89593	53.10	4.50	4.50	450296
37.90	36.10	82.60	3.70	3.70	142076	48.60	4.30	4.30	627017
34.30	32.70	78.90	3.90	3.90	226680	44.30	4.00	4.00	882880
31.10	29.65	75.00	4.00	4.00	344135	40.30	3.80	3.80	1241499
28.20	26.85	71.00	4.20	4.20	522629	36.50	3.50	3.50	1653888
25.50	24.30	66.80	4.20	4.20	793159	33.00	3.30	3.30	2366566
23.10	22.05	62.60	4.30	4.30	1242121	29.70	3.00	3.00	3290871
21.00	20.00	58.30	4.10	4.10	1666497	26.70	2.70	2.70	4167528
19.00	18.10	54.20	4.10	4.10	2498137	24.00	2.50	2.50	5784509
17.20	16.40	50.10	4.00	4.00	3685946	21.50	2.20	2.20	7698495
15.60	14.85	46.10	3.70	3.70	4898596	19.30	2.10	2.10	10558041
14.10	13.45	42.40	3.60	3.60	7401723	17.20	1.80	1.80	14053903
12.80	12.20	38.80	3.30	3.30	9849036	15.40	1.60	1.60	18134012
11.60	11.05	35.50	3.20	3.20	14022032	13.80	1.50	1.50	24960104
10.50	10.01	32.30	3.00	3.00	19848763	12.30	1.30	1.30	32662521
9.52	9.08	29.30	2.70	2.70	26398202	11.00	1.20	1.20	44553927
8.63	8.23	26.60	2.50	2.50	36073457	9.80	1.10	1.10	60274636
7.82	7.45	24.10	2.40	2.40	51009515	8.70	1.00	1.00	80711257
7.08	6.75	21.70	2.20	2.20	70486819	7.70	0.80	0.80	97335078
6.42	6.12	19.50	2.00	2.00	94572521	6.90	0.80	0.80	143654462
5.82	5.55	17.50	1.80	1.80	124837669	6.10	0.70	0.70	184359426
5.27	5.02	15.70	1.60	1.60	164505079	5.40	0.60	0.60	234263562
4.77	4.55	14.10	1.50	1.50	235366624	4.80	0.60	0.60	357518922
4.33	4.13	12.60	1.30	1.30	293783988	4.20	0.40	0.40	343272430
3.92	3.74	11.30	1.20	1.20	404807163	3.80	0.50	0.50	640517662
3.55	3.39	10.10	1.20	1.20	609721868	3.30	0.40	0.40	771799833
3.22	3.07	8.90	1.10	1.10	824132020	2.90	0.30	0.30	853531437
2.92	2.78	7.80	0.90	0.90	972950117	2.60	0.30	0.30	1231582427
2.64	2.52	6.90	0.90	0.90	1471732962	2.30	0.20	0.20	1241968745
2.39	2.28	6.00	0.90	0.90	2244686899	2.10	0.30	0.30	2841375821
2.17	2.07	5.10	0.70	0.70	2566241312	1.80	0.20	0.20	2784348621
1.97	1.88	4.40	0.70	0.70	3634804918	1.60	0.10	0.10	1971865236
1.78	1.70	3.70	0.60	0.60	4713393576	1.50	0.20	0.20	5966320982
1.61	1.54	3.10	0.70	0.70	8391162386	1.30	0.10	0.10	4552167660
1.46	1.39	2.40	0.70	0.70	12107823673	1.20	0.20	0.20	13136879211
1.32	1.26	1.70	0.60	0.60	16255444629	1.00	0.10	0.10	10288256094
1.20	1.20	1.10	1.10	1.10	3449913333	0.90	0.90	0.90	10718948215
			Total no. crystals		58811200213		Total no. crystals		58674954022

Thus, 572 μm (in **column 2 row 1**) is the average size between 600 and 544 μm shown in the first column. Similarly, 518.50 μm, is the average crystal size between

544 and 493 μm. The procedure was followed for the successive size ranges. The last row entry shows the high size and the average size = 1.20 μm, which is the limit of the capability of the Malvern particle sizer used in this study.

Column 3 shows the raw data of percentage cumulative under-size of the population as measured by the Malvern particle sizer.

The **fourth column** shows the percentage of each average size. Thus the number of crystals with average size of 572 μm equals zero. In other words, there are no particles with average size of 572 μm in the system. The average maximum size of the particle in the system is shown in row no.16 of the second column, which is 130.50 μm. It reveals that 0.10 % of the total number of crystals in the system have an average size of 130.50 μm. Next, the number of crystals of average size: 118.00 μm is also 0.10 % of the entire number of crystals in the system, as shown in row no.17.

Gypsum crystals were assumed to have constant density regardless of their size (Jamialahmadi and Muller-Steinhagen 2000; Li *et al.* 1997), and thus volume percentage is identical to weight percentage. This is shown by **column 5**.

Finally, using **Eq. 6.3**, the number of crystals for each size range was calculated and the results are presented in **column 6**.

Similar calculations were carried out for the product crystals, which are shown in **columns 7** to **10** in **Table 6.2**.

Having calculated the number of crystals both at the start and the end of the experimental run, it is now possible to plot the cumulative numbers in a population density plot. Data from **Table 6.2** were plotted as such and are shown in **Figure 6.8**. As can be seen from **Figure 6.8**, the population density plot for both the conditions at the start and end of the run does not yield a straight line. Instead, the plots show an upward curvature at the lower size regions.

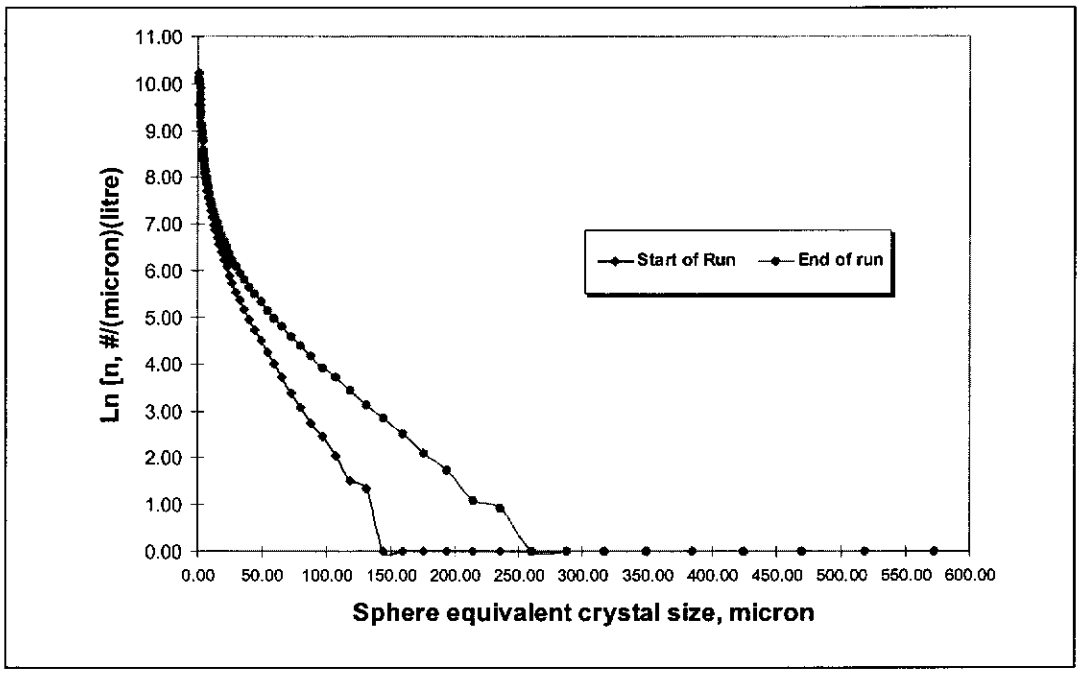

Figure 6.8 A typical population density plot, showing the condition at the start (lower curve) and end (upper curve) of an experimental run

In the present study, the growth rate calculation was carried out for crystals with average sizes between **13.05** and **107.00** microns. As can be seen from **Figure 6.8**, the population density plots show relatively smooth curves within the average size ranges: **10.00** to **110.00** microns. As was found later in all experimental runs in this study, plots of crystals with average sizes bigger than **110.00** microns always show irregular curves and thus measurement of linear growth rate in this region was not reliable.

It is well known that small crystals tend to agglomerate. In such cases it can be difficult to discern whether the crystals actually grow or that the change in size is due to agglomeration (Chan 1997a). To ensure that crystal growth was not due to agglomeration, only fractions of crystals above **10.00** microns in size were used to determine the growth rate.

The choice of size fractions between the size range: 13.05 and 107.00 micron was made and classified into 15 fractions as follows: **107.00, 97.05, 87.75, 79.50, 72.05, 65.30, 59.15, 53.55, 48.55, 42.05, 34.50, 29.65, 24.60, 18.30, 13.05** microns.

As it turned out later in the determination, the growth rate varies according to crystal size, increasing with the increase in size.

6.3.3. Calculation of the linear growth rate

Determination of linear growth rate is discussed in section **2.10.2** of the **Literature Review – part 1** (= literature review on crystallisation). A typical example of the experimental result is shown in **Figure 6.9**. It illustrates the population density plot at zero and eight residence times, which correspond to the start and end of an experimental run, respectively.

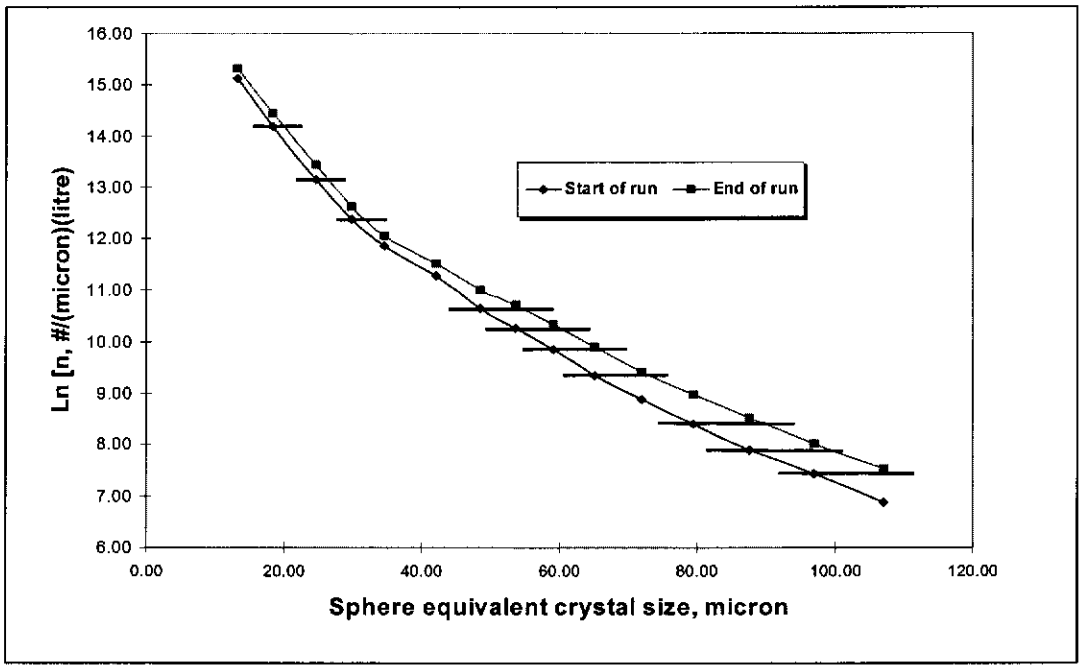

Figure 6.9 Determination of linear growth rate from the cumulative number oversize distribution

The distance between the two curves (measured by the straight lines connecting the two curves), was used to calculate the growth rate of the crystals. The distance represents one residence time chosen for this study (= 15 minutes), hence if the growth rate unit is in micron per hour, the measured distance needs to be adjusted accordingly, that is to be multiplied by 4. This procedure was proposed by Garside and Jancic (Garside and Jancic 1976; Garside and Jancic 1978) and Jancic and

Grootscholten (Jancic and Grootscholten 1984), and the results of such procedure are presented in **Table 6.3**. Several representative population density plots for the calculation of the linear growth rate are given in **Appendix D**.

Table 6.3 Typical growth rate of gypsum obtained in this study, showing the dependence of growth on crystal size (gypsum grown in a pure system without added admixtures)

Crystal size, L, (micron)	Growth rate, G, (micron)/(hour))
107.00	60.00
97.05	50.77
87.75	47.69
79.50	43.08
72.05	38.46
65.30	33.85
59.15	24.62
53.55	23.08
48.55	21.54
42.05	15.38
34.50	9.23
29.65	6.15
24.60	6.13
18.30	6.12
13.05	3.08

6.4. Effects of Admixtures on the Growth Rate

6.4.1. Effects of individual admixtures on the linear growth rate of gypsum

The presence of admixtures in a crystallising solution can have significant effect on crystallisation kinetics. Among crystallisation kinetics aspects, which are affected by the presence of admixtures, nucleation and growth of crystals are usually reported. Other aspects of crystallisation, which can be influenced by admixtures, include agglomeration, attrition, solubility of the crystals, width of metastable zones etc.

In some cases, nucleation is retarded by the presence of admixtures. In some other cases, it is enhanced. The same phenomenon occurs to growth, that is, growth can either be enhanced or retarded by admixtures. In this continuous crystallisation study, three types of admixtures were investigated for their effect on crystallisation

kinetics. In this section the effect of the three admixtures on crystal growth of gypsum is presented. It was found that the growth of gypsum is clearly retarded by the presence of the admixtures studied, whether they are present individually or in combination. **Tables 6.5** to **6.7** show the effect of individual admixtures on the growth rate. Subsequent tables showing the effect of combined admixtures on the growth rate are tabulated in **Tables 6.8** to **6.10** in section **6.4.2**. In all cases, the growth rates were calculated based on the experimental data for CSD at steady state, i.e. at equilibrium concentration of around 700 ppm of Ca^{2+}; while the initial concentration was 1,200 ppm of Ca^{2+}. The remaining data on the growth rate, especially those at an elevated temperature of 40^0C are given in **Appendix D**.

Table 6.4 Comparison of growth rate of gypsum (micron/hour) in a pure system at two different temperatures: 25^0C and 40^0C

Crystal size, (microns)	Growth rate in pure system, micron/hour	
	At 25^0C	At 40^0C
107.00	35.38	60.00
97.05	35.38	50.77
87.75	33.85	47.69
79.50	27.69	43.08
72.05	27.69	38.46
65.30	13.85	33.85
59.15	12.31	24.62
53.55	12.31	23.08
48.55	12.31	21.54
42.05	12.31	15.38
34.50	12.31	9.23
29.65	6.15	6.15
24.60	4.62	6.13
18.30	4.62	6.12
13.05	3.08	3.08

Table 6.5 Comparison of growth rate of gypsum (micron/hour) at different concentrations of Fe^{3+} at 25^0C

Crystal size, (microns)	Crystallisation temperature: 25^0C						
	0 ppm	1 ppm	10 ppm	20 ppm	22 ppm	25 ppm	50 ppm
107.00	35.38	28.15	20.80	13.79	0.00	0.00	0.00
97.05	35.38	25.19	17.60	13.79	0.00	0.00	0.00
87.75	33.85	20.74	16.00	13.79	0.00	0.00	0.00
79.50	27.69	14.81	14.40	13.79	0.00	0.00	0.00
72.05	27.69	5.93	13.79	13.79	0.00	0.00	0.00
65.30	13.85	5.93	12.80	13.79	0.00	0.00	0.00
59.15	12.31	5.93	5.17	5.17	0.00	0.00	0.00
53.55	12.31	5.93	5.17	0.00	0.00	0.00	0.00
48.55	12.31	5.93	3.45	0.00	0.00	0.00	0.00
42.05	12.31	5.93	0.00	0.00	0.00	0.00	0.00
34.50	12.31	0.00	0.00	0.00	0.00	0.00	0.00
29.65	6.15	0.00	0.00	0.00	0.00	0.00	0.00
24.60	4.62	0.00	0.00	0.00	0.00	0.00	0.00
18.30	4.62	0.00	0.00	0.00	0.00	0.00	0.00
13.05	3.08	0.00	0.00	0.00	0.00	0.00	0.00

Table 6.6 Comparison of growth rate of gypsum (micron/hour) at different concentrations of Zn^{2+} at 25^0C

Crystal size, (microns)	Crystallisation temperature: 25^0C						
	0 ppm	1 ppm	10 ppm	20 ppm	22 ppm	25 ppm	50 ppm
107.00	35.38	28.76	13.07	16.67	7.84	12.90	6.62
97.05	35.38	27.45	7.84	13.33	7.84	9.03	6.02
87.75	33.85	24.84	10.46	10.00	7.84	6.45	7.52
79.50	27.69	23.53	11.76	6.67	3.92	3.87	7.52
72.05	27.69	20.92	5.23	3.33	0.00	0.00	0.00
65.30	13.85	11.76	2.61	2.33	0.00	0.00	0.00
59.15	12.31	14.38	3.92	1.67	0.00	0.00	0.00
53.55	12.31	13.07	2.61	1.67	0.00	0.00	0.00
48.55	12.31	13.07	0.00	0.00	0.00	0.00	0.00
42.05	12.31	13.07	0.00	0.00	0.00	0.00	0.00
34.50	12.31	7.84	0.00	0.00	0.00	0.00	0.00
29.65	6.15	6.54	0.00	0.00	0.00	0.00	0.00
24.60	4.62	1.31	0.00	0.00	0.00	0.00	0.00
18.30	4.62	0.00	0.00	0.00	0.00	0.00	0.00
13.05	3.08	0.00	0.00	0.00	0.00	0.00	0.00

Table 6.7 Comparison of growth rate of gypsum (micron/hour) at different concentrations of sodium isopropyl xanthate (SIPX) at 25^{0}C

Crystal size, (microns)	Crystallisation temperature: 25^{0}C						
	0 ppm	1 ppm	10 ppm	20 ppm	22 ppm	25 ppm	50 ppm
107.00	35.38	25.71	12.31	10.53	5.03	0.00	0.00
97.05	35.38	24.29	10.77	7.89	5.03	0.00	0.00
87.75	33.85	20.00	9.23	7.89	5.03	0.00	0.00
79.50	27.69	18.57	7.69	6.58	2.52	0.00	0.00
72.05	27.69	12.86	6.15	5.26	2.52	0.00	0.00
65.30	13.85	14.29	6.15	3.95	2.52	0.00	0.00
59.15	12.31	11.43	3.08	3.95	2.52	0.00	0.00
53.55	12.31	7.14	3.08	2.63	1.26	0.00	0.00
48.55	12.31	5.71	3.08	2.63	0.00	0.00	0.00
42.05	12.31	0.00	0.00	0.00	0.00	0.00	0.00
34.50	12.31	0.00	0.00	0.00	0.00	0.00	0.00
29.65	6.15	0.00	0.00	0.00	0.00	0.00	0.00
24.60	4.62	0.00	0.00	0.00	0.00	0.00	0.00
18.30	4.62	0.00	0.00	0.00	0.00	0.00	0.00
13.05	3.08	0.00	0.00	0.00	0.00	0.00	0.00

6.4.2. Effects of combined admixtures on the linear growth rate of gypsum

Table 6.8 Comparison of growth rate of gypsum (micron/hour) at different concentrations of combined admixtures: Fe^{3+} and SIPX at 25^0C

Crystal size, (microns)	Crystallisation temperature: 25^0C						
	0 ppm	1 ppm	10 ppm	20 ppm	22 ppm	25 ppm	50 ppm
107.00	35.38	41.83	12.00	2.67	1.43	0.00	0.00
97.05	35.38	41.83	12.00	2.67	1.43	0.00	0.00
87.75	33.85	39.22	12.00	2.67	1.43	0.00	0.00
79.50	27.69	33.99	6.13	1.33	0.00	0.00	0.00
72.05	27.69	26.14	6.13	1.33	0.00	0.00	0.00
65.30	13.85	13.07	5.33	1.33	0.00	0.00	0.00
59.15	12.31	10.46	2.67	0.00	0.00	0.00	0.00
53.55	12.31	2.61	2.67	0.00	0.00	0.00	0.00
48.55	12.31	5.23	0.00	0.00	0.00	0.00	0.00
42.05	12.31	5.23	0.00	0.00	0.00	0.00	0.00
34.50	12.31	3.92	0.00	0.00	0.00	0.00	0.00
29.65	6.15	0.00	0.00	0.00	0.00	0.00	0.00
24.60	4.62	0.00	0.00	0.00	0.00	0.00	0.00
18.30	4.62	0.00	0.00	0.00	0.00	0.00	0.00
13.05	3.08	0.00	0.00	0.00	0.00	0.00	0.00

Table 6.9 Comparison of growth rate of gypsum (micron/hour) at different concentrations of combined admixtures: Zn^{2+} and SIPX at 25^0C

Crystal size, (microns)	Crystallisation temperature: 25^0C						
	0 ppm	1 ppm	10 ppm	20 ppm	22 ppm	25 ppm	50 ppm
107.00	35.38	31.30	21.48	18.67	13.33	13.01	10.37
97.05	35.38	27.83	21.48	17.33	12.00	11.38	5.93
87.75	33.85	24.35	21.48	14.67	10.67	11.38	4.44
79.50	27.69	20.87	14.77	10.67	9.33	11.38	2.96
72.05	27.69	17.39	9.40	8.00	9.33	8.13	2.96
65.30	13.85	17.39	5.37	4.00	8.00	6.50	4.15
59.15	12.31	15.65	2.68	3.20	5.33	3.25	0.00
53.55	12.31	13.91	0.00	0.00	4.80	1.63	0.00
48.55	12.31	10.43	0.00	0.00	4.00	1.63	0.00
42.05	12.31	6.96	0.00	0.00	2.67	0.00	0.00
34.50	12.31	3.48	0.00	0.00	1.33	0.00	0.00
29.65	6.15	3.48	0.00	0.00	0.00	0.00	0.00
24.60	4.62	3.48	0.00	0.00	0.00	0.00	0.00
18.30	4.62	0.00	0.00	0.00	0.00	0.00	0.00
13.05	3.08	0.00	0.00	0.00	0.00	0.00	0.00

Table 6.10 Comparison of growth rate of gypsum (micron/hour) at different concentrations of combined admixtures: Fe^{3+}, Zn^{2+} and SIPX at 25^0C

Crystal size, (microns)	Growth rate of gypsum, micron per hour						
	0 ppm	1 ppm	10 ppm	20 ppm	22 ppm	25 ppm	50 ppm
107.00	35.38	30.00	24.83	10.06	7.77	5.00	0.00
97.05	35.38	28.33	23.45	7.55	6.80	3.33	0.00
87.75	33.85	28.33	19.31	5.03	6.21	3.33	0.00
79.50	27.69	30.00	20.69	2.52	5.83	3.33	0.00
72.05	27.69	30.00	16.55	0.00	3.88	0.00	0.00
65.30	13.85	28.33	16.55	0.00	1.94	0.00	0.00
59.15	12.31	26.67	16.55	0.00	1.94	0.00	0.00
53.55	12.31	30.00	16.55	0.00	0.00	0.00	0.00
48.55	12.31	30.00	15.17	0.00	0.00	0.00	0.00
42.05	12.31	26.67	5.52	0.00	0.00	0.00	0.00
34.50	12.31	21.67	2.76	0.00	0.00	0.00	0.00
29.65	6.15	15.00	0.00	0.00	0.00	0.00	0.00
24.60	4.62	3.33	0.00	0.00	0.00	0.00	0.00
18.30	4.62	3.33	0.00	0.00	0.00	0.00	0.00
13.05	3.08	1.67	0.00	0.00	0.00	0.00	0.00

6.5. Calculation of the Growth Rate Correlation

As can be seen from all the tables on growth rate (**Table 6.3** to **Table 6.10**), the growth rate is clearly highly dependent on crystal size, increases with increasing crystal size. It indicates, therefore, that either size dependent growth or growth rate dispersion phenomena (or both) were operative. In addition, the tables also show that admixtures were observed to significantly inhibit the growth of gypsum. Therefore, it was decided to correlate the crystal growth, **G**, as a function of the characteristic crystal size, **L**, and the admixture concentration, **C**.

It has been known that there is a significant difference in effect between low and high concentration levels of admixtures on growth rate (Liu and Nancollas 1973; Mullin 1979; Nancollas 1983). Hence, the calculation of growth rate was carried out

with regard to two different levels of concentration of admixtures: lower level (**0.00** to **1.00** ppm) and, higher level (**10.00** to **50.00** ppm). To obtain a more general correlation, calculation of a correlation for the entire range of concentrations of admixtures, which covers both lower level and higher level was also carried out.

For a fixed level of supersaturation and crystal surface area, correlation between the growth rate, **G**, and the crystal size, **L**, as well as the admixture concentration, **C**, was proposed to take the following general equation:

$$G = k\, L^{\alpha}\, (1+C)^{\beta} \tag{6.4}$$

where,

G = linear growth rate, (micron)/(hour)

L = characteristic linear crystal size, micron

C = admixture concentration, ppm

k, α and **β** = dimensionless constants.

6.5.1. Sample calculation for the growth rate correlation

Correlating growth rate with admixture concentration was previously carried out by Dash (Dash 1993), for the crystallisation of KCl under the influence of Mg^{2+} and SO_4^{2-}, where the concentration was expressed as **(1+C)**. The expression **(1+C)** was used to facilitate a positive logarithmic number which was necessary when carrying out the calculation involving pure condition where **C** = 0.00 ppm.

In order to calculate the dimensionless constants: **k**, **α** and, **β** in **Eq. (6.4)**, the equation was linearised and takes the following form:

$$\ln G = \ln k + \alpha \ln L + \beta \ln (1+C) \tag{6.4a}$$

Regression analysis using Excell™ was then performed, to correlate **G** to **L** and **(1+C)**, which yielded the dimensionless constants: **k**, **α** and, **β**.

Because of the assumed linearity of the regression analysis in Excell™, it was considered necessary to repeat the regression analysis using other program, where a non-linear regression was performed. This non-linear regression was performed using SPSS™, and the values of **k**, **α** and, **β** obtained previously in Excell™ were used as initial values in the SPSS™. It was found that in most cases, the recalculation of regression analysis yielded higher values of $\mathbf{R^2}$ than was the case in the previous analysis. Therefore, all the regression calculations were carried out twice using both the Excell™ and the SPSS™ programs, and the higher values of $\mathbf{R^2}$ were chosen. Results of the non-linear regression calculations for the growth rate are presented in **Tables 6.11** to **6.16**.

6.5.2. Growth rate correlation at 25^{0}C

Table 6.11 Growth rate correlation for low admixture concentrations: 0.00 and 1.00 ppm, at 25^{0}C

Admixtures	Non linear growth rate correlation	R^2
Fe^{3+}	$G = 0.02\ L^{1.63}\ (1+C_{Fe})^{-46.10}$	**0.90**
Zn^{2+}	$G = 0.08\ L^{1.32}\ (1+C_{Zn})^{-13.11}$	**0.92**
SIPX	$G = 0.03\ L^{1.54}\ (1+C_{SIPX})^{-70.78}$	**0.92**
Fe^{3+} + SIPX	$G = 0.009\ L^{1.82}\ (1+C_{Fe})^{-201.84}\ (1+C_{SIPX})^{372.38}$	**0.90**
Zn^{2+} + SIPX	$G = 0.065\ L^{1.37}\ (1+C_{Zn})^{-61.67}\ (1+C_{SIPX})^{96.00}$	**0.92**
Fe^{3+} + Zn^{2+} + SIPX	$G = 0.09\ L^{1.30}\ (1+C_{Fe})^{187.97}(1+C_{Zn})^{-199.00}(1+C_{SIPX})^{-57.60}$	**0.83**

Table 6.12 Growth rate correlation for high admixture concentrations: 10.00 up to 50.00 ppm, at 25^{0}C

Admixtures	Non linear growth rate correlation	R^2
Fe^{3+}	$G = 0.001\ L^{2.12}\ (1+C_{Fe})^{0.94}$	**0.83**
Zn^{2+}	$G = 0.000013\ L^{3.09}\ (1+C_{Zn})^{-2.542}$	**0.83**
SIPX	$G = 0.0014\ L^{2.06}\ (1+C_{SIPX})^{-7.62}$	**0.90**
Fe^{3+} + SIPX	$G = 0.04\ L^{1.56}\ (1+C_{Fe})^{106}\ (1+C_{SIPX})^{-192}$	**0.93**
Zn^{2+} + SIPX	$G = 0.00033\ L^{2.48}\ (1+C_{Zn})^{0.09}\ (1+C_{SIPX})^{-5.40}$	**0.90**
Fe^{3+} + Zn^{2+} + SIPX	$G = 0.20\ L^{1.29}\ (1+C_{Fe})^{6127.22}(1+C_{Zn})^{-2982.70}\ (1+C_{SIPX})^{-3848.31}$	**0.77**

Table 6.13 Growth rate correlation for the entire admixture concentrations: 0.00 up to 50.00 ppm, at 25^{0}C

Admixtures	Non linear growth rate correlation	R^2
Fe^{3+}	$G = 0.007\ L^{1.81}\ (1+C_{Fe})^{-4.00}$	**0.80**
Zn^{2+}	$G = 0.04\ L^{1.46}\ (1+C_{Zn})^{-6.23}$	**0.90**
SIPX	$G = 0.018\ L^{1.63}\ (1+C_{SIPX})^{-16.69}$	**0.90**
Fe^{3+} + SIPX	$G = 0.008\ L^{1.85}\ (1+C_{Fe})^{801.60}\ (1+C_{SIPX})^{-1426.01}$	**0.94**
Zn^{2+} + SIPX	$G = 0.012\ L^{1.73}\ (1+C_{Zn})^{-9.46}\ (1+C_{SIPX})^{13.51}$	**0.91**
Fe^{3+} + Zn^{2+} + SIPX	$G = 0.0005\ L^{3.31}\ (1+C_{Fe})^{-5851.54}\ (1+C_{Zn})^{2665.79}\ (1+C_{SIPX})^{4033.59}$	**0.88**

6.5.3. Growth rate correlation at 40^{0}C

Table 6.14 Growth rate correlation for low admixture concentrations: 0.00 and 1.00 ppm, at 40^{0}C

Admixtures	Non linear growth rate correlation	R^2
Fe^{3+}	$G = 0.11\ L^{1.34}\ (1+C_{Fe})^{-0.17}$	**0.94**
Zn^{2+}	$G = 0.07\ L^{1.43}\ (1+C_{Zn})^{0.11}$	**0.96**
SIPX	$G = 0.03\ L^{1.69}\ (1+C_{SIPX})^{-0.73}$	**0.94**
Fe^{3+} + SIPX	$G = 0.04\ L^{1.56}\ (1+C_{Fe})^{106}\ (1+C_{SIPX})^{-192}$	**0.95**
Zn^{2+} + SIPX	$G = 0.03\ L^{1.70}\ (1+C_{Zn})^{-398.30}\ (1+C_{SIPX})^{-877.70}$	**0.94**
Fe^{3+} + Zn^{2+} + SIPX	$G = 0.09\ L^{1.40}\ (1+C_{Fe})^{68.70}\ (1+C_{Zn})^{-78.30}\ (1+C_{SIPX})^{-352.00}$	**0.95**

Table 6.15 Growth rate correlation for high admixture concentrations: 10.00 up to 50.00 ppm, at 40^{0}C

Admixtures	Non linear growth rate correlation	R^2
Fe^{3+}	$G = 0.005\ L^{2.00}\ (1+C_{Fe})^{-8.60}$	**0.87**
Zn^{2+}	$G = 0.0002\ L^{2.62}\ (1+C_{Zn})^{-2.31}$	**0.86**
SIPX	$G = 0.033\ L^{1.47}\ (1+C_{SIPX})^{-7.79}$	**0.84**
Fe^{3+} + SIPX	$G = 0.06\ L^{1.81}\ (1+C_{Fe})^{-349.30}\ (1+C_{SIPX})^{569}$	**0.90**
Zn^{2+} + SIPX	$G = 0.07\ L^{1.68}\ (1+C_{Zn})^{-13.00}\ (1+C_{SIPX})^{17.55}$	**0.89**
Fe^{3+} + Zn^{2+} + SIPX	$G = 0.07\ L^{1.98}\ (1+C_{Fe})^{-259.47}\ (1+C_{Zn})^{125.92}\ (1+C_{SIPX})^{164.86}$	**0.80**

Table 6.16 Growth rate correlation for the entire admixture concentrations: 0.00 up to 50.00 ppm, at 40^{0}C

Admixtures	Non linear growth rate correlation	R^2
Fe^{3+}	$G = 0.185\ L^{1.21}\ (1+C_{Fe})^{-10.24}$	**0.92**
Zn^{2+}	$G = 0.185\ L^{1.12}\ (1+C_{Zn})^{-7.84}$	**0.92**
SIPX	$G = 0.016\ L^{1.78}\ (1+C_{SIPX})^{-4.38}$	**0.93**
Fe^{3+} + SIPX	$G = 0.284\ L^{1.14}\ (1+C_{Fe})^{-78.40}\ (1+C_{SIPX})^{117.38}$	**0.93**
Zn^{2+} + SIPX	$G = 0.037\ L^{1.57}\ (1+C_{Zn})^{-2.20}\ (1+C_{SIPX})^{0.93}$	**0.82**
Fe^{3+} + Zn^{2+} + SIPX	$G = 0.264\ L^{1.17}\ (1+C_{Fe})^{-122.00}\ (1+C_{Zn})^{-65.20}\ (1+C_{SIPX})^{253}$	**0.88**

Interpretation of regression analysis is generally achieved, by firstly examining the values of the coefficient of determination, $\mathbf{R^2}$. The $\mathbf{R^2}$ values represent the percentage of variation in the values of the dependent variable by the change in the independent variable(s). In this study, the dependent variable is the crystal growth rate, **G**, whereas the independent variables are the crystal size, **L**, and the admixture concentration, **(1+C)**, respectively.

Examination of the $\mathbf{R^2}$ values contained in **Tables 6.11** to **6.16** indicates that all $\mathbf{R^2}$ values are $\geq$ **0.80** with the exception of one low value of **0.77** as shown in **Table 6.12** for the correlation at higher concentrations involving three different admixtures for the experiment conducted at 25^0C. The values of $\mathbf{R^2 \geq 0.80}$ implies that $\geq$ 80% of the variation in growth rate, **G**, is statistically directly caused by the change in both crystal size, **L**, and admixture concentration, **(1+C)**. Qualitatively, it means that within the conditions used in the experiments, the growth rate of gypsum is affected by the size of the crystals as well as the admixture concentration levels.

For both temperature levels of 25 and 40^0C, the dimensionless constant, **k**, is less than unity, which indicates that, **G**, is a weak function of **L** and **(1+C)**.

Most of the α values are greater than unity, which suggest that the growth of the crystals depends significantly on crystal size.

Admixture concentrations, however, show poor correlations. **Tables 6.11** to **6.16** show that individual and combined admixtures could have different effects. The combined admixtures have wider range of exponent values, β, compared to those of individual admixtures, increases with increasing combinations of admixtures. This might confirm the argument that the influence of admixtures on growth of crystals is highly dependent on particular solvent-solute systems and that the effect of admixtures on growth rate can already be significant even if they are present at a very low concentration. Furthermore, the fluctuation in exponent values, β, could have been caused by some interaction between the admixtures used. At the present time, however, the nature or existence of such interaction can only be speculated.

Two mechanisms of growth inhibition are proposed. Firstly, probably the more feasible mechanism, is that the admixtures were adsorbed and subsequently occupied active growth sites, such as kinks and steps, rendering the sites unavailable for attachment of solutes or growth units to the crystal surface (Klepetsanis and Koutsoukos 1998). This inhibition mechanism is invariably called "blocking" or "poisoning" of the active growth sites, which results in slowing down or stopping the crystal growth rate. Sarig and Mullin (Sarig and Mullin 1982) and more recently Hamdona *et al.* (Hamdona *et al.* 1993), Klepetsanis and Koutsoukos (Klepetsanis and Koutsoukos 1998) and El Dahan and Hegazy (El Dahan and Hegazy 2000), all investigating the effect of trace impurities on gypsum precipitation, reported the same inhibition behaviour as proposed in this study. Furthermore, the same inhibition mechanism was put forward by Benton *et al.* (Benton *et al.* 1993) in their study on the inhibitory effects of organic and inorganic additives on barium sulphate crystallisation.

The second mechanism is that, the admixtures were adsorbed onto the crystal surface, forming a physical barrier to ward off transfer of growth units from solution to the crystal surface, resulting in growth rate reduction. This type of mechanism is generally found in crystallisation research involving the use of tailor-made additives, such as the crystallisation of gypsum in the presence of α-amino acids (see page 409 Mersmann 1995).

The growth rates of gypsum found in this study are also comparable with those of White and Hoa (White and Hoa 1977), Murray (Murray 1997) and, White and Mukhopadhyay (White and Mukhopadhyay 1990) considering the difference in the seed slurry density and supersaturation values.

Investigation of calcium sulphate scale by Linnikov [Linnikov, 2000 #319] indicates that crystals of the same salts could have different growth rates even under the same experimental condition . The same phenomenon seems to occur in this work in that the growth rate of gypsum crystals was found to be size-dependent, whereas the results of a number of similar studies show the opposite, as discussed below.

The growth of potash alum and gypsum was found to be dependent on size at lower size regions (Garside and Jancic 1976; Klima and Nancollas 1987). Garside and Jancic used a 250 ml volume agitated vessel which behaved as an MSMPR for their investigation and measured the growth rate of potash alum over the size range 3.00 to 70.00 microns. Klima and Nancollas (Klima and Nancollas 1987) studying the growth of gypsum, found that growth rate was a linear function of size for crystal sizes below 100 microns. Large crystals greater than 100 microns (they used varying sizes of up to 700 microns) grew almost independently of size. Both Garside and Jancic (Garside and Jancic 1976) and Klima and Nancollas (Klima and Nancollas 1987) used seeded crystallisation technique and found that for small crystals ($\leq$ 100 microns), the overall kinetics of growth was determined solely by the surface integration mechanism. For such mechanism, the crystal growth rate becomes a function of the characteristics of the crystal surface. In a crystalliser vessel where a very large number of crystals with differing sizes are present (which was the case in this continuous crystallisation study), it was reasonable to expect that the growth rates of individual crystals would vary.

6.6. Nucleation Rate Calculation

The Population Balance Equation (**PBE**) developed by Randolph and Larson (Randolph and Larson 1988) is a well-defined method for the simultaneous determination of growth and nucleation rates of crystals grown in continuous MSMPR crystallisers. It is essentially an accounting for crystals with respect to size. As detailed in the **Literature Review** (**Chapter 2** section **2.9. Nucleation Rate**), the **PBE** first calculates the growth rate, **G**, and uses the value obtained to subsequently calculate the nucleation rate, $\mathbf{B^0}$. The population balance assumes that a plot of population density of crystals versus crystal size will yield a straight line and hence, the growth rate, **G**, is constant regardless of crystal size. However, it has been frequently observed that the plot breaks down at small size regions and the line is curved. The curved nature of the plot suggests that the extrapolation to initial or zero size required for the nucleation rate calculation is not warranted (Berglund and Larson 1982). Furthermore, the curved line would suggest that nuclei might be

created at several small sizes rather than at a single crystal size, **L = 0**, as determined by Randolph and Larson's PBE plot.

Due to limitations imposed by particle sizing instruments, nucleation rate calculation may sometimes have to resort to a particular technique, depending on the range of particle size data available (Jancic and Grootscholten 1984). As shown by Jancic and Grootscholten (previous citation) the population balance analysis is almost always subjected to a situation where data for a certain part of the particle size distribution, usually the small size region, is not available.

Clearly, if the population density plot curved in the small size region, the slope of such a plot no longer has a single value and the intercept of it must accordingly be determined. There can be several possible straight lines that can be drawn through the plotted experimental data. Hence, nucleation and growth rate values may vary depending on the slope and intercept of the particular straight line chosen. This arbitrary choice is evidently one of several possible reasons why the resulting calculations of the kinetics of one crystallising system can be different even when the same experimental conditions are carefully applied. Undoubtedly, the most appropriate intercept is one that sufficiently covers the smallest crystal size down to which the size analysis is performed.

In this study, the technique for selecting a suitable intercept that was proposed by Jancic and Grootscholten was adopted (Jancic and Grootscholten 1984). A linear regression through the five smallest data points, which were obtained from CSD analysis, was carried out as depicted in **Figure 6.10**, and the resulting equation yielded the slope and intercept of a straight line. The nucleation rate was then calculated using the obtained slope and intercept.

A sample calculation for nucleation rate using this method is presented for Fe^{3+} = 0.00 ppm at 40^0C. A regression line was drawn and the line obtained has the following equation,

$$Y = -2.1548\,X + 23.184 \qquad (6.6)$$

where,

Y = logarithmic number of nuclei density, (no.of nuclei)/(micron)(litre)

X = sphere equivalent nuclei size, micron

with coefficient of determination, $\mathbf{R^2 = 0.98}$.

Thus the growth rate, **G**, for the nuclei can be found from the slope of the straight line as represented **Eq. (6.6)**, as follows:

$\mathbf{-1/(\tau\, G)} = -2.1548$ or $\mathbf{G} = 1/(0.25)(2.1548) = 1.856$ μm/hour

where τ is the mean residence time and is equal to 15 minutes or 0.25 hour.

The intercept of **Eq. (6.6)** is 23.184, thus the number of crystals at effectively zero size, $\mathbf{n_0}$, is $e^{23.184}$ or 1.1713×10^{10} per micron litre. Further, the nucleation rate can be calculated using the following equation,

$$B^0 = n^0\, G \qquad (6.7)$$

where,

B^0 = nucleation rate, (no.of nuclei)/(micron)(hour)

n^0 = nuclei density, (no.of nuclei)/(micron)(litre)

G = growth rate of nuclei, (micron)/(hour).

Therefore, the nucleation rate,

$$\begin{aligned} \mathbf{B^0} &= (1.1713 \times 10^{10})(1.856) \\ &= 2.1739 \times 10^{10}\ \text{/(litre)(hour)} \\ &= 2.1739 \times 10^{13}\ \text{of nuclei/(m}^3\text{)(hour).} \end{aligned}$$

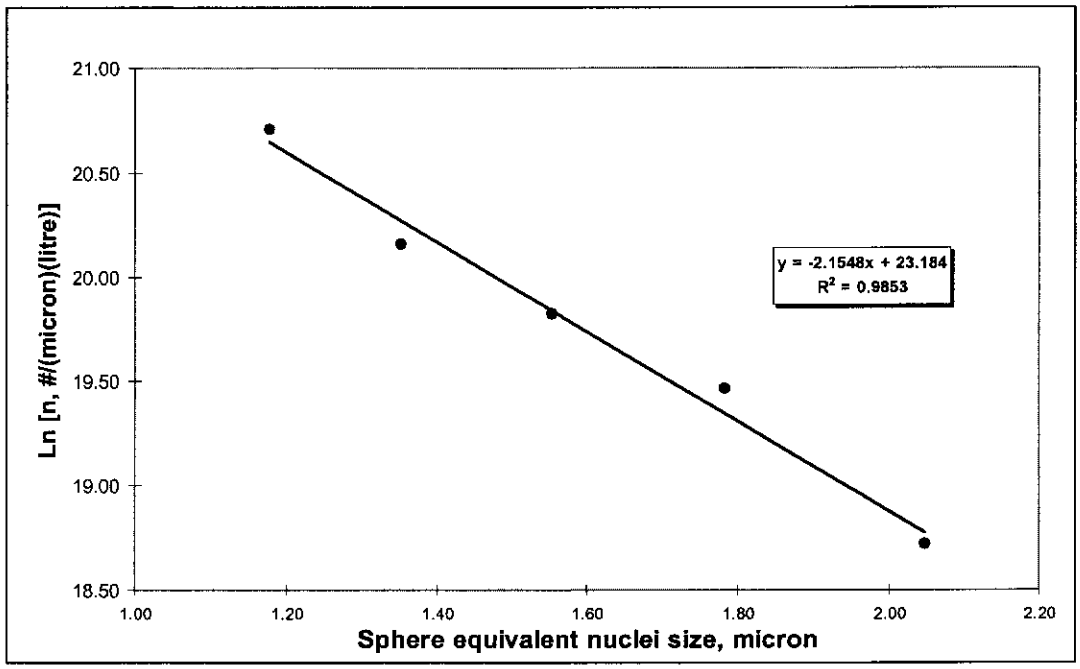

Figure 6.10 Cumulative density population at small size region for the determination of nucleation rate

6.6.1. Nucleation rate at 25^{0}C

Table 6.17 Nucleation rate of gypsum as affected by individual admixtures: Fe^{3+}, Zn^{2+}, and SIPX (no. nuclei x 10^{13})/(m^3)(hour) at crystallisation temperature of 25^{0}C

Concentration of admixtures, ppm	Nucleation rate and type of admixtures		
	Fe^{3+}	Zn^{2+}	SIPX
0.00	1.22	1.22	1.22
1.00	1.68	1.66	1.25
10.00	2.04	2.31	2.02
20.00	2.40	3.40	2.17
22.00	6.33	3.44	2.60
25.00	6.65	3.55	3.61
50.00	8.31	8.56	3.67

Table 6.18 Nucleation rate of gypsum as affected by combined admixtures of Fe^{3+}, Zn^{2+}, and SIPX (no. nuclei x 10^{13})/(m^3)(hour) at crystallisation temperature of 25^0C

Concentration of admixtures, ppm	Nucleation rate and type of admixtures		
	Fe^{3+} + SIPX	Zn^{2+} + SIPX	Fe^{3+} + Zn^{2+} + SIPX
0.00	1.22	1.22	1.22
1.00	2.04	1.48	1.25
10.00	2.15	1.54	1.68
20.00	2.44	1.80	1.94
22.00	3.89	1.97	4.68
25.00	5.25	2.48	6.57
50.00	7.08	4.16	7.14

6.6.2. Nucleation rate at 40^0C

Table 6.19 Nucleation rate of gypsum as affected by individual admixtures: Fe^{3+}, Zn^{2+}, and SIPX (no. nuclei x 10^{13})/(m^3)(hour) at crystallisation temperature of 40^0C

Concentration of admixtures, ppm	Nucleation rate and type of admixtures		
	Fe^{3+}	Zn^{2+}	SIPX
0.00	2.17	2.17	2.17
1.00	1.84	0.07	0.58
10.00	2.97	1.17	0.86
20.00	4.30	2.14	1.22
22.00	5.16	3.91	3.15
25.00	5.28	5.57	3.45
50.00	8.81	7.08	3.66

Table 6.20 Nucleation rate of gypsum as affected by combined admixtures of Fe^{3+}, Zn^{2+}, and SIPX (no. nuclei x 10^{13})/(m^3)(hour) at crystallisation temperature of 40^0C

Concentration of admixtures, ppm	Nucleation rate and type of admixtures		
	Fe^{3+} + SIPX	Zn^{2+} + SIPX	Fe^{3+} + Zn^{2+} + SIPX
0.00	2.17	2.17	2.17
1.00	0.39	1.36	1.34
10.00	1.62	3.60	1.45
20.00	2.57	3.78	1.68
22.00	6.57	6.45	2.84
25.00	7.86	8.48	3.45
50.00	8.56	8.72	7.18

Tables 6.17 to **6.20** summarise the nucleation rate values for all the admixtures used. As can be seen, in each case, the nucleation rate increases with increasing admixture concentrations. These results imply that the admixtures would have lowered the surface tensions in the crystallising solution, and consequently the contact angles of solute clusters with the crystal surfaces in the solution would have been decreased. As the contact angle decreases, the critical free energy of formation of solute clusters also decreases, causing an increase in nuclei formation.

The same phenomenon of increasing nucleation rate with the increase in temperature, was also reported by Shor and Larson (Shor and Larson 1971), in their study on the effect of surface active agents on the crystallisation kinetics of potassium nitrate crystals. Nucleation rate of calcium oxalate was also found to increase in the presence of low concentrations (up to 2.5 ppm) of glutamic acid (Azoury *et al.* 1983). A more recent study by Benton *et al.* (Benton *et al.* 1993) on the crystallisation of barium sulphate showed that phosphonate-based inhibitors also acted as nucleation promoters.

The apparent inconsistency of the nucleation rate values at 1 ppm and 40^0C, (which instead of gradually increases to be consistent with the general trend, decreases for all types of admixtures), can be attributed to a competition which exists between adsorption of the admixtures and of the nucleating substance onto the nucleus surface (Sohnel and Garside 1992). In the absence of admixture no competition exists and consequently a large quantity of nucleating substance is adsorbed onto the nucleus surface, resulting in subsequent growth of nuclei. In the presence of one ppm of admixture, however, both the nucleating units and the admixtures molecules must compete to arrive at the surface, hence the number of the nucleating units adsorbed onto the nucleus could be lower. In consequence, the nucleation rate decreases.

At higher concentrations of admixture (10 ppm and more) a large number of admixtures molecules can no longer be adsorbed onto the surface and thus stay in the solution acting as nucleus template. Thus, the nucleation rate increases again. Sarig and Mullin (Sarig and Mullin 1982) reported the same phenomenon of fluctuating nucleation behaviour in their study on the effect of Al^{3+} and F^- (both at concentrations of 0.00 to 81 ppm) on calcium sulphate precipitation. The

phenomenon of "non-steady state" rates of nucleation of $CaSO_4.2H_2O$ was also reported by Massey and Hileman (Massey and Hileman 1977). They found that such phenomenon occurred at low supersaturations, which is exactly the same case as in the present study.

The nucleation rate values over the range of the admixture concentrations used in the present work are comparable with other studies on the same crystallisation system. White and Hoa (White and Hoa 1977) investigated the growth of gypsum crystals under the influence of Fe^{2+}, Al^{3+}, and K^-, reported values for the nucleation rate within the limits from 7.2 x 10^{13} to 3.0 x 10^{14}/(m^3. hour), for concentration levels from 1,500 to 3,000 ppm Ca^{2+} and a crystallisation temperature of 40^0C. The slurry density, which should be a significant factor, however, was not reported. Similar laboratory continuous crystallisation of gypsum using seed slurry density of 15.00 g/L of solution, that is almost twenty times higher than that used in this study, was carried out by Murray (Murray 1997) and yielded nucleation rate values from 1.87 x 10^{14} to 2.94 x 10^{14} per (m^3.hour). The nucleation rate values reported in this study are, therefore, comparable with the results of the two previous studies.

Summary

In this chapter, experimental results and discussion of a seeded continuous crystallisation (MSMPR) of calcium sulphate dihydrate ($CaSO_4.2H_2O$) or gypsum in the presence of admixtures are presented. The aim of the experiment was to investigate the behaviour of gypsum crystallisation in the presence of admixtures, since the knowledge of such behaviour can be a useful tool for scale prevention measures especially when gypsum is one of the major components of the scale.

The following features were noted in this study:

1. *The seeded continuous crystallisation experimental runs reasonably satisfied the conditions of an ideal MSMPR, in terms of:*

    - *Solution concentration in the crystalliser*
    - *Slurry or magma density in the crystalliser*

- *Crystal size distribution (CSD) in the crystalliser.*

2. *The experimental data of crystal size distribution (CSD) were suitable to be used to calculate the linear crystal growth rate, G, and the nucleation rate, B^0.*

3. *The linear crystal growth rate, G, was found to be dependent on size, increases with increasing crystal size.*

4. *Both in the pure and in the presence of admixtures, the linear crystal growth rates were generally higher for the higher crystallisation temperature of 40^0C rather than for that at 25^0C.*

5. *In general, the admixtures tested were able to inhibit the crystal growth rates, but to enhance the nucleation rates.*

6. *In almost all cases, in the concentration range studied, higher admixture concentrations induce high retardation on the growth rates. On the contrary, the higher the admixture concentrations, the higher the nucleation rates.*

7. *Since the growth rate was found to be dependent on crystal size, a correlation between these two parameters and the admixture concentrations was attempted. For a fixed level of supersaturation and crystal surface area, it was proved that for each crystallisation temperature: 25^0C and 40^0C, the correlation function can be presented as the following general equation:*

$$G = k\,L^{\alpha}\,(1+C)^{\beta}$$

where:

G = *linear growth rate, micron/hour*

k, α *and* β = *dimensionless constants*

L = *crystal size, micron*

C *= concentration of the admixtures used, ppm*

8. *For both crystallisation temperatures of 25^0C and 40^0C, and within the range of the admixture concentrations used, the correlation is best presented in three separate categories: (a) low admixture concentrations, (b) high admixture concentrations, and (c) combined low and high admixture concentrations.*

9. *The correlation function is best applied to the low concentration category (= category (a)), followed by the combined low and high admixture concentration category (= category (c)). The high concentration category (= category (b)) shows the poorest correlation.*

10. *For both crystallisation temperatures of 25^0C and 40^0C, the correlation function reveals the following:*

    - *The growth rate, **G**, is significantly dependent on crystal size, **L**.*
    - *The growth rate, **G**, is a weak function of admixture concentrations, **C**.*

11. *The mechanism of crystal growth inhibition was assumed to be that of adsorption of admixtures onto the active growth sites, which resulted in decreasing or stopping the growth.*

12. *Since the growth rate was found to be size-dependent, the McCabe's ΔL law (see **section 2.9** in **Chapter 2**) for the calculation of crystal growth and nucleation is violated. Hence, the nucleation rates calculated and presented in this study are the "effective" nucleation rate, which means that the nuclei were not formed at one single size.*

13. *In either the absence or the presence of individual admixture of Fe^{3+}, Zn^{2+}, and SIPX, the nucleation rate calculation resulted in the following details:*

    - *For pure gypsum, higher crystallisation temperature results in higher nucleation rate.*

- *In the presence of Fe^{3+} as admixture, higher crystallisation temperature results in higher nucleation rate, increases with an increase in admixture concentrations.*

- *In the presence of either Zn^{2+} or SIPX as admixture, higher crystallisation temperature results in lower nucleation rate, decreases with an increase in admixture concentrations.*

14. *In the presence of combined admixtures, of either Fe^{3+} + SIPX, Zn^{2+} + SIPX, or Fe^{3+}+ Zn^{2+}+SIPX, higher crystallisation temperature results in lower nucleation rates for lower concentrations, but higher nucleation rates for higher concentrations.*

15. *Both the nucleation and growth rate values of gypsum found in this study, either in the absence or in the presence of admixtures, generally agree with those in the literature.*

*The next chapter (**Chapter** 7) deals with a once-through pipe flow experiment, where factors influencing gypsum scale formation on the inner surfaces of pipes under isothermal conditions are discussed. These factors include concentration levels, type of admixtures, fluid flow rate and type of piping materials. The intention is that the outcomes of this pipe flow experiment will be compared with those of the present chapter. Hence, a better understanding might be gained of the behaviour of gypsum crystallisation occurring in vessels and in flowing solutions.*

References

1. Al-Sabbagh, A., Widua, J., and Offermann, H. (1996). "Influence of different admixtures on the crystallization of calcium sulfate crystals." *Chemical Engineering Communications*, 154, 133-145.
2. Azoury, R., Randolph, A. D., Drach, G. W., and Perlberg, S. (1983). "Inhibition of Calcium Oxalate Crystallization by Glutamic Acid: Different Effects at Low and High Concentrations." *Journal of Crystal Growth*, 64, 389-392.

3. Benton, W. J., Collins, I. R., Grimsey, I. M., Parkinson, G. M., and Rodger, S. A. (1993). "Nucleation, Growth and Inhibition of Barium Sulfate-controlled Modification with Organic and Inorganic Additives." *Faraday Discussion*, 95, 281-297.
4. Berglund, K. A., and Larson, M. A. (1982). "Growth of contact nuclei of citric acid monohydrate." *AIChE Symposium Series*, 78(215), 9-13.
5. Brown, D. J., and Felton, P. G. (1985). "Direct measurement of concentration and size for particles of different shapes using laser light diffraction." *Chemical Engineering Research and Design*, 63, 125-132.
6. Chan, V. A. (1997a). "The Role of Impurities in the Continuous Precipitation of Aluminium Hydroxide," PhD thesis, Curtin University of Technology, Perth, Western Australia.
7. Chan, V. A., Ang, H.M., Kristall, Z. and Vautier, T. "Crystallization of Calcium Sulphate Dihydrate." *25th Australian and New Zealand Chemical Engineers' Conference and Exhibition,*, Rotorua, N Z.
8. Cowan, J. C., and Weintritt, D. J. (1976). *Water-Formed Scale Deposits*, Gulf Publishing, Houston, TX.
9. Dash, S. R. (1993). "Crystallization Kinetics of KCl in Continuous and Batch Cooling Crystallizers: Effect of Magnesium and Sulfate Ions," PhD, University of Saskatchewan, Saskatoon,Saskatchewan, Canada, S7N 0W0.
10. El Dahan, H. A., and Hegazy, H. S. (2000). "Gypsum scale control by phosphate ester." *Desalination*, 127, 111-118.
11. Garside, J., and Jancic, S. J. (1976). "Growth and Dissolution of Potash Alum Crystals in the Subsieve Size Range." *AIChE Journal*, 22(5), 887-894.
12. Garside, J., and Jancic, S. J. (1978). "Prediction and Measurement of Crystal Size Distribution for Size-Dependent Growth." *Chemical Engineering Science*, 33, 1623-1630.
13. Hamdona, S. K., Nessim, R. B., and Hamza, S. M. (1993). "Spontaneous precipitation of calcium sulphate dihydrate in the presence of some metal ions." *Desalination*, 1(94), 69-80.
14. He, S., Oddo, J. E., and Tomson, M. B. (1994). "The Seeded Growth of Calcium Sulfate Dihydrate Crystals in NaCl Solutions up to 6 m and 90° C." *Journal of Colloid and Interface Science*, 163, 372-378.

15. Iacocca, R. G., and German, R. M. (1997). "A comparison of powder particle size measuring instruments." *The International Journal of Powder Metallurgy*, 33(8), 35-47.
16. Inaba, K., and Matsumoto, K. (1998). "Continuous Measurement of Crystal Number Concentration in Crystallization of Fructose by Laser Diffraction Method." *Journal of Chemical Engineering of Japan*, 31(1), 122-125.
17. Jamialahmadi, M., and Muller-Steinhagen, H. (2000). "Crystallization of Calcium Sulphate Dihydrate from Phosphoric Acid." *Dev.Chem.Eng.Mineral Process.*, 8(5/6), 587-604.
18. Jancic, S. J., and Grootscholten, P. A. M. (1984). *Industrial Crystallization*, Delft University Press and Reidel Publishing, Dordrecht, Boston, Lancaster.
19. Klepetsanis, P. G., and Koutsoukos. (1989). "Precipitation of calcium sulfate dihydrate at constant calcium activity." *Journal of Crystal Growth*, 98, 480-486.
20. Klepetsanis, P. G., and Koutsoukos, P. G. (1998). "Kinetics of calcium sulfate formation in aqueous media: effect of organophosphorus compounds." *Journal of Crystal Growth*, 193, 156-163.
21. Klima, W. F., and Nancollas, G. H. (1987). "The Growth of Gypsum." *AIChE Symposium Series*, 83(253), 23-30.
22. Li, J., Wang, J. H., and Zhang, Y. X. (1997). "Effects of the Impurities on the Habit of Gypsum in Wet-Process Phosphoric Acid." *Industrial and Engineering Chemistry Research*, 36, 2657-2661.
23. Liu, S. T., and Nancollas, G. H. (1970). "The Kinetics of Crystal Growth of Calcium Sulphate Dihydrate." *Journal of Crystal Growth*, 6, 281-289.
24. Liu, S. T., and Nancollas, G. H. (1973). "The Crystal Growth of Calcium Sulfate Dihydrate in the Presence of Additives." *Journal of Colloid and Interface Science*, 44(3), 422-429.
25. Massey, R. E., and Hileman, O. E. (1977). "Toward an understanding of rates of crystal nucleation from solution with a variable driving force." *Canadian Journal of Chemistry*, 55, 1285-1293.
26. Mersmann, A. (1995). *Crystallization Technology Handbook*, Marcel Dekker, New York, Basel, Hong Kong.
27. Mullin, J. W. (1979). "Crystal growth in pure and impure systems." INDUSTRIAL CRYSTALLIZATION 78, E. J. de Jong and S. J. Jancic, eds., North-Holland Publishing, Amsterdam, 93-103.

28. Murray, N. (1997). "Continuous Crystallisation of Calcium Sulphate Dihydrate," Final Year Undergraduate Project, Curtin University of Technology, Perth,Western Australia.
29. Nancollas, G. H. (1983). "The Nucleation and Growth of Scale Crystals." Fouling of Heat Exchanger Surfaces, R. W. Bryers, ed., Engineering Foundation, New York.
30. Northwood, T. (1995). "Scale reduction in Process Water Pipes at Murchison Zinc," Final Year Undergraduate Project, Curtin University of Technology, Perth, Western Australia.
31. Randolph, A. D., and, and Larson, M. A. (1988). *Theory of Particulate Processes.Analysis and Techniques of Continuous Crystallization*, Academic Press, San Diego,etc.
32. Rawle, A. (2001). "Basic principles of particle size analysis.", Malvern Instruments Ltd., Malvern, Worcestershire, UK.
33. Sarig, S., and Mullin, J. W. (1982). "Effect of Trace Impurities on Calcium Sulphate Precipitation." *Journal of Chemical Technology and Biotechnology*, 32, 525-531.
34. Shor, S. M., and Larson, M. A. (1971). "Effect of Additives on Crystallisation Kinetics." *Chemical Engineering Progress Symposium Series*, 67(110), 32-42.
35. Sohnel, O., and Garside, J. (1992). *Prec ipitation. Basic Principles and Industrial Applications*, Butterworth Heinemann, Oxford, etc.
36. White, E. T., and Hoa, L. T. "Mass transfer studies in particulate systems using the population balance approach - The growth of gypsum crystals." *2nd Australasian Conference on Heat and Mass Transfer*, University of Sydney, Australia, 401-408.
37. White, E. T., and Mukhopadhyay, S. (1990). "Crystallization of gypsum from phosphoric acid solutions." Crystallization as a Separation Process, A. S. Myerson and K. Toyokura, eds., ACS, Washington, DC, USA, 292-315.

CHAPTER 7 GYPSUM SCALING IN ISOTHERMAL FLOW SYSTEM

7.1. Introduction

Scaling is the formation of a solid layer on equipment surfaces and piping systems and is one of the persistent problems encountered in many industrial operations such as distillation, cooling and heating of liquids, mixing, evaporation, crystallisation etc (Hasson 1981). The solid layer may become increasingly thicker during the process and the resulting deposit reduces the capacity of production through resistance to heat transfer, restriction of materials flow, corrosion and wearing out of construction materials etc (Bott 1988). Scale formation and its subsequent deposition increase the energy requirement, such as that for pumping, as well as the cost associated with maintenance and replacement of parts. Thus the operational and technical problems may eventually translate into substantial economic penalties (Bott 1995; Gill 1999; Pritchard 1988).

Scale formation is mainly due to dissolved inorganic components crystallising out of the solution, which is supersaturated with respect to the dissolved components. In many industrial processes and applications, gypsum or calcium sulphate dihydrate (= $CaSO_4.2H_2O$), was found to be one of the main constituents of the scale (He *et al.* 1994; Headley *et al.* 2001; Klepetsanis 1999; Liu and Nancollas 1973; Nancollas and Reddy 1974). The scale forms when crystals agglomerate and attach onto the wall of the pipes or processing equipment and gradually coat the surface as a scale layer.

Research aimed at preventing or controlling gypsum scaling has been very extensive, and significant advances have been made. Earlier studies by Hasson and Zahavi (Hasson and Zahavi 1970), Liu and Nancollas (Liu and Nancollas 1973) and many others, mainly focused on the kinetics of scale formation. Most of the later studies (Bansal and Muller-Steinhagen 1993; Bansal *et al.* 1997; Bansal *et al.* 2000; Bott 1995; Chamra and Webb 1994; Li and Webb 2000; Linnikov 1999; Middis *et al.* 1998; Mori *et al.* 1996; Sudmalis and Sheikholeslami 2000), on the other hand, have put emphasis on external factors influencing the deposition of the scale. These

factors include hydrodynamics of the scale forming solutions, the characteristics of the solid surface, the configuration of the heat transfer equipment etc.

Conflicting results on the effect of hydrodynamics on scale deposition have been reported by Andritsos and Karabelas (Andritsos and Karabelas 1992). They showed that the flow rate either increased or decreased the mass of scale deposited over a certain period of time. Clearly, this is due to the nature of the solid-fluid interface layer and the shear stress induced to the scale by the flow. These two incompatible forces are further complicated by other parameters such as the presence of admixtures, which may exert a significant effect on the nature of the interface layer as well as on the characteristics of the scale deposited (Myerson 1993).

This chapter presents an investigation on the formation of gypsum scale on the inner surfaces of pipes of different diameters and materials. Effects of supersaturation, type and dosage of inhibitor species type, fluid velocity, and type of piping materials on the scaling rate were examined. The experiments were performed in a once-through pipe flow system, where conditions were maintained so that effects caused by foreign particle deposition and removal of scale by shear forces were minimised. This chapter is divided into the following sections:

7.1. Introduction
7.2. Mechanism of Scale Formation
7.3. Experimental
7.4. Results and Discussion
7.5. Conclusions
7.6. Comparison between the Growth Rate of Gypsum in the Continuous Crystalliser and Gypsum Scale Formation in the Scaling Experiments.

Section 7.6 describes an attempt to correlate the growth of gypsum in a crystalliser vessel (as detailed previously in **Chapter 6**) with that in a flowing solution, which is discussed in this chapter.

7.2. Mechanism of Scale Formation

The main pre-requisite of scaling is the existence of adequate supersaturation. This is true for scale deposition in either a heated or an isothermal system. Once sufficient supersaturation is attained, the process of scaling begins and this may proceed through the following stages (Andritsos and Karabelas 1992; Hasson 1981).

1. **Nucleation**: creation of nuclei or growth centres, which can take place on the solid surface such as the wall of the pipe, as well as in the bulk of the solution.

2. **Diffusion**: transport of solvated ions, molecules or tiny crystalline matter to the solid surface. In a pipe the diffusion is assumed to proceed radially outward from the centre of the pipe.

3. **Deposition/Growth**: the transported scaling components are subsequently adsorbed either directly onto the solid surface or onto the surface of the crystals attached to the solid surface.

4. **Removal**: detachment of the deposit layer due to shear stress exerted by the flowing fluid.

5. **Ageing**: changes to the scale characteristics, caused by recrystallisation, phase transformation, Ostwald ripening, etc., which may either strengthen or weaken the scale deposits.

The five steps of scaling mechanism described above may occur concurrently or consecutively. In addition, any two or more mechanisms may produce a synergistic effect (Hasson *et al.* 1996).

Some scale formation in industries takes place without a temperature gradient that is, under isothermal conditions. This can be found, for example, in potable water supply lines (Hasson 1981) and in mineral processing plants (Northwood 1995). The scale formation study presented in this paper was carried out at ambient temperature of 25^0C to simulate the condition of the flotation piping system in a certain mineral processing plant (Headley *et al.* 2001; Northwood 1995).

7.3. Experimental

7.3.1. Choice of experimental variables

Since the formation of scale is essentially a crystallisation phenomenon, the level of supersaturation of the crystallising solution is a dominant factor. Therefore, the first factor to be investigated in this study was the supersaturation, which is presented as the concentration of the scaling solution in ppm of Ca^{2+}. All factors studied are listed as follows.

7.3.1.1. Concentration level

Preliminary trials showed that at concentrations below 2,000 ppm with respect to Ca^{2+}, the amount of scale formed on the surfaces of the coupons (explanation about the coupons is given in **section 7.3.2**) was very small, making accurate weighing of the scale extremely difficult. In addition, removal of the scale from the coupons for subsequent scanning electron microscopy (SEM) examination without damaging the scale structure proved to be difficult. On the other hand, using Ca^{2+} concentration above 6,000 ppm resulted in a very rapid scale deposition and in clogging of the test section. It was thus decided that the experiments be conducted at Ca^{2+} concentrations between 2,000 and 6,000 ppm. The preparation of the supersaturated solutions used in the experiment is detailed in **section 7.3.3**. The normal solubility of gypsum at 25^0C is at Ca^{2+} concentration of 611 ppm.

7.3.1.2. Type and concentration of admixtures

The effect of admixtures on gypsum and its related calcium sulphate salts has been an active area of research (as discussed in the **Introduction**). However, a unified theory is probably very unlikely. Instead, the effect appears to be system-specific, that is, dependent on the system under investigation.

Two different admixtures have been chosen for this study, namely Fe^{3+} and sodium isopropyl xanthate (SIPX). Fe^{3+} was selected as it is found in significant amounts in mineral processing water (Northwood 1995) and because it is one of the corrosion products of steel (Weijnen and van Rosmalen 1984). SIPX was chosen due to its popular usage as a flotation agent in mineral processing (Cousins and McPhail 1996; Headley *et al.* 2001; Verma *et al.* 1999).

7.3.1.3. Flow rate of solution

In most cases, scaling occurs in flowing systems, and thus fluid velocity can be an important factor. The effect of flow rate on scale formation is complex. As an example, the aging stage may weaken the deposit strength, but the actual detachment of the deposit is dependent on the intensity of shear stress exerted by the flow. It can be likened to the shedding of old leaves from trees (Epstein 1983). As the leaves grow older their bonds to the twigs weaken, but the final detachment is dependent on the strength of the wind, which is the flow of the air (= fluid). Further, as advanced by Bott (Bott 1995), the removal mechanism involves the "sticking probability" value of the scale to the solid substrate. The precise magnitude of sticking probability value is extremely difficult to obtain since it is dependent on various factors: characteristics (size, density, porosity etc.) of the scale, characteristics (roughness, topography etc.) of the substrate, characteristics (flow rate, entrained particles, temperature etc.) of the flowing solution.

To avoid such complexities, in this study, low flow rate values (0.4 to 1.3 cm per second), which correspond to the Reynolds number in the laminar region, were chosen in order that the effect of the removal phenomenon on the scale deposition could be considered negligible. Experimentally, it can be seen through the transparent plastic tubing (see **section 7.3.5. Description of a typical experimental run**), that there were no particles carried away by the upward flowing solution.

7.3.1.4. Type of piping materials

It is well known that process equipment uses different type of materials depending on the chemicals or substances to be processed. In this project, the effect of four types of piping materials, i.e. PVC, copper, brass and stainless steel was studied.

7.3.2. Description of the experimental set-up

The experimental set-up is illustrated in **Figure 7.1**. Briefly, it consists of two major parts: two vessels each with a working volume of up to eight litres where gypsum forming solutions are kept and a test section where gypsum scale is deposited. One of the vessels contains $CaCl_2$ solution as Ca^{2+} provider, the other vessel contains Na_2SO_4 solution as SO_4^{2-} provider. The two solutions were transported through the

test section using one peristaltic pump (Masterflex™ peristaltic pump supplied by Cole Palmer Instrument Co.) at predetermined flow rates. The peristaltic pump was fitted with two heads, to ensure the same and accurate flow rates of the two solutions.

To avoid the possibility of nucleation occurring in the solution before the test section, the two solutions were transported separately from their respective vessels and thus mixing of the solutions occurred just at the inlet of the test section where the two solutions met. The test section consists of two flanged tubular units which were made of stainless steel and eight pairs of semi annular coupons which can be inserted into the tubular units and serve as scale surfaces (Andritsos and Karabelas 1991). The flanged tubular units were made of stainless steel and have a length of 8 cm and an inner diameter of 1.8 cm. Each semi annular coupon has a length of two cm and its internal diameter is either 1.3 or 0.7 cm. In order to firmly fix the alignment of the two tubular units, tongues and grooves were machined onto their opposing flanges. The spent liquor coming out from the test section was collected into a vessel to allow more gypsum to crystallise out of the liquor. The spent liquor and the gypsum formed were then discarded. All accessories were thoroughly cleaned with flowing tap water followed by rinsing with distilled water to avoid contamination. Prior to cleaning, a dilute HCl solution was used to soak the tubular units and the coupons after each experimental run to dissolve and remove traces of adherent scales.

The admixtures used in the experiments were dissolved in distilled water and then added into the vessel containing the Na_2SO_4 solution. The solutions entered the test section from the bottom side in order to lessen the effect of gravity, which can induce removal of the scale. In addition, for a downward flow, the fluid must flow fast and fully occupy the pipe cross section for otherwise it will tend to flow down one side of the pipe. In such a case, parts of the pipe, which are not covered by the fluid, would stay dry, resulting in non uniform scaling.

7.3.3. Preparation of the supersaturated solutions

Gypsum-forming solutions for the experiment were prepared by making equimolar amounts of stock solutions of calcium chloride and sodium sulphate, respectively. Calcium chloride solution was made by dissolving $CaCl_2.2H_2O$ crystals in distilled water at room temperature followed by filtration through 0.22 μm Millipore™ filter paper (Amjad 1985). The solution of sodium sulphate was prepared in the same manner. The two solutions were kept separately and extreme care was taken to keep the solutions free from dust, insoluble matter etc. The chemicals, glasswares, filter paper etc used, were the same as those used in the batch and continuous crystallisation study carried out previously. It is obvious that each step of an experimental run is subject to both random and systematic errors. In this scale formation study, the random errors will likely occur in the following steps.

1. Weighing and dissolving crystals of both $CaCl_2.2H_2O$ and Na_2SO_4 for the stock solution.
2. Subsequent measuring of the volumes for the preparation of the scaling solutions.

Error estimation was calculated for the preparation of the supersaturated solutions and is tabulated below. A sample calculation for the error estimation with respect to this scaling experiment is presented in **Appendix E**.

Table 7.1 Supersaturated solutions of gypsum prepared for the scaling experiments

Ca^{2+} concentrations	
Expected, (ppm)	**Calculated, (ppm)**
2,000	2,000 ± 20
3,000	3,000 ± 42
4,000	4,000 ± 71
5,000	5,000 ± 109
6,000	6,000 ± 154

7.3.4. Preparation of the test section

Before each experimental run both the tubular units and the semi annular coupons were washed with detergent and flowing tap water followed by HCl soaking, and rinsing with acetone and distilled water. Subsequently, the coupons were dried in an

oven, allowed to cool and were then carefully weighed. Next they were inserted into the tubular units. Finally, the tubular units with the semi annular coupons inside were fitted onto the experimental rig.

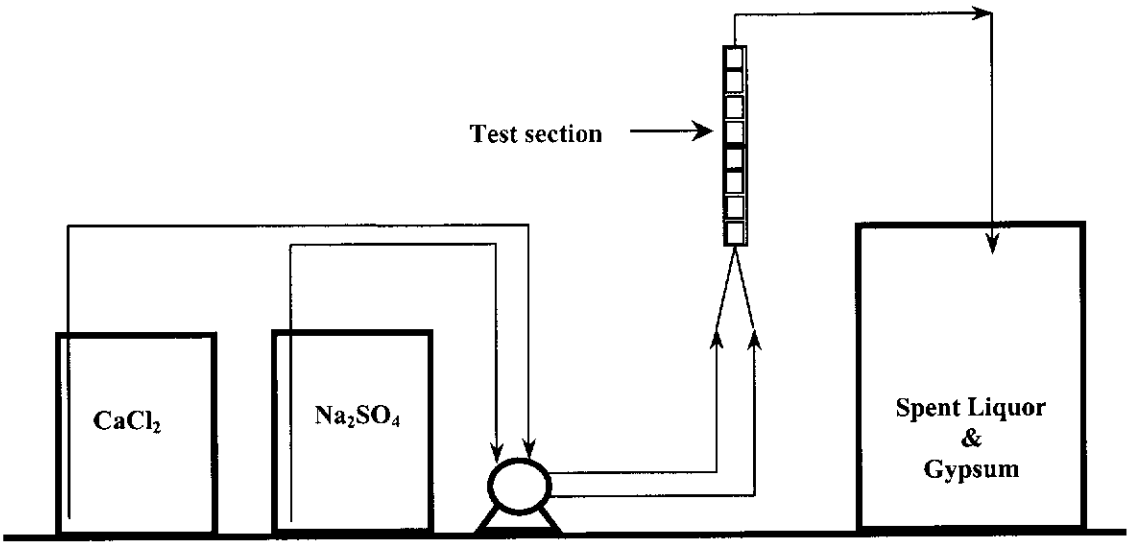

Figure 7.1 Schematic representation of the flow system experimental set up

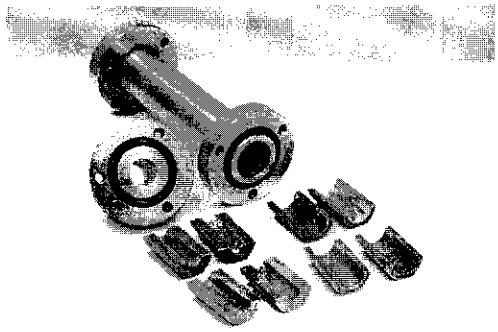

Figure 7.2 Photograph of the test section showing the coupons, the tubular unit and the flange

7.3.5. Description of typical experimental run

A predetermined amount of calcium chloride and sodium sulphate solutions were placed in separate vessels as described previously, to provide a certain supersaturated gypsum solution for the test section. For the experimental runs using admixtures, the admixture solution was added into the Na_2SO_4 solution. The pump was activated and the starting time was recorded. Occasionally, all the connecting tubes were checked for flow rate and leakage and to ensure that there were no air bubbles

formed inside the tubes, for otherwise the bubbles will interfere with either the flow rate uniformity and/or the deposition mechanism. At the end of the run, the pump was switched off. The tubular test section was disconnected and left in a vertical position until no more drippings of solution were seen. The semi-annular coupons were carefully withdrawn from the tubular units and were placed in an oven at a temperature of 60^0C overnight. The following day the coupons together with the adherent scale were weighed. The difference between the weight before and after the experiment is the weight of the mass of the scale deposit. The scale samples obtained were morphologically analysed using SEM (Phillips XL30).

7.3.6. SEM analysis of the scale samples

The scale deposited on the surface of the coupons was carefully removed using a paper tissue. It was then placed in vials ready for the SEM analysis. The analysis of the scale samples using SEM consisted of two steps: coating and imaging. Gold sputter coating was used and, it was done in a vacuum coating unit (DYNAVAC Sputter Coater Model SC150) as follows. First, some of the samples (= the scale crystals) were sprinkled onto double-sided sticky tape attached to an aluminium stub. Next, the stub with the attached samples was placed inside the vacuum coating unit and the unit was activated to remove the air inside its chamber, and replace it with argon gas. Replacing the air with the argon gas is necessary, since the latter is a better carrier for the gold atoms to transfer, sputter and cover the surface of the specimen. After a sufficient vacuum level had been achieved, the vacuum pump was switched off and the valve to sputter the gold coating was switched on. When the gold coating had achieved a certain thickness, it was stopped. The gold-coated specimen was left inside the vacuum chamber for a few minutes to cool. Finally, the specimen was removed from the chamber and placed inside the SEM unit (Phillips XL30), and the micrographs of the specimen were taken and printed. The micrographs were also saved into disk-files for future use.

7.4. Results and Discussion

7.4.1. Effect of supersaturation

Since supersaturation is the primary driving force for crystallisation, it is expected that an increase in supersaturation level will result in an increase in the amount of gypsum scale deposited on the pipe wall. **Figure 7.3** illustrates this situation. In all experiments using different type of piping materials, the mass of deposited gypsum increases with increasing concentration.

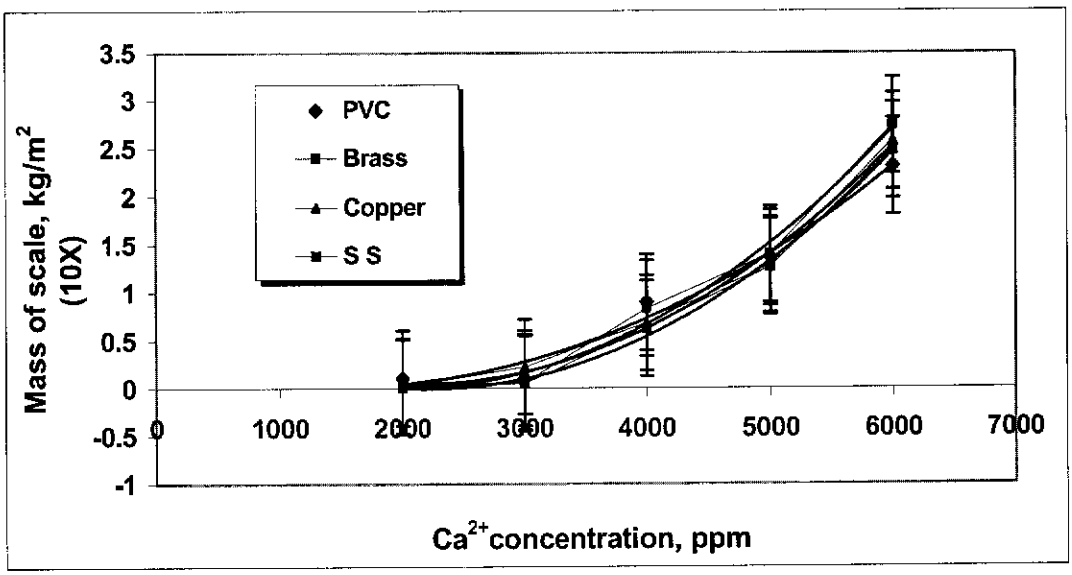

Figure 7.3 Effect of Ca^{2+} concentration level on scale deposition after four hours for various piping materials (at a low flow rate of 0.4 cm/sec)

Table 7.2 Regression correlation between type of pipe materials and mass of gypsum scale deposited

Type of pipe materials	Polynomial regression equation (Y = mass of scale, kg/m^2 ; X = calcium ion concentration, ppm)	R^2
P V C	$Y = 1.\ 10^{-7}\ X^2 - 0.0003\ X + 0.2550$	0.98
Brass	$Y = 2.\ 10^{-7}\ X^2 - 0.0007\ X + 0.6986$	0.99
Copper	$Y = 2.\ 10^{-7}\ X^2 - 0.0007\ X + 0.7748$	0.99
Stainless steel	$Y = 2.\ 10^{-7}\ X^2 - 0.0008\ X + 0.8350$	1.00

Polynomial regression lines (quadratic functions) were found to be suitable for the correlation between the concentration level and the mass deposited. As is shown in **Table 7.2**, the high $\mathbf{R^2}$ values ($\geq$ **0.98**) for all types of the piping materials indicate the suitability of the correlation.

7.4.2. Effect of flow rate and admixture concentrations

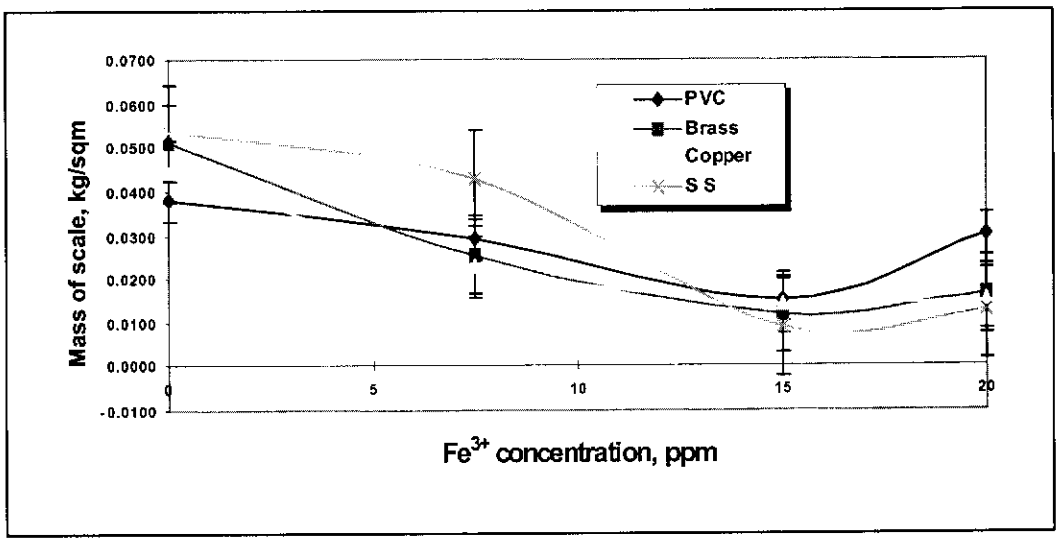

Figure 7.4 Effect of Fe^{3+} concentrations on gypsum scale deposited after four hours for various piping materials (at a low flow rate of 0.4 cm/sec and a concentration level of 2,500 ppm of Ca^{2+})

Figures 7.4 and **7.5** show the effects of Fe^{3+} concentrations at different fluid flow rates on the mass of gypsum scale deposited. As can be seen in the two figures, in general, higher concentrations of Fe^{3+} have higher retarding effect on the scale build up, up to about 15 ppm. Data for **Figure 7.4** were taken at a linear fluid flow rate of 0.4 cm per second while those for **Figure 7.5** were obtained at a linear fluid flow rate of 1.3 cm per second. **Figures 7.4** and **7.5** imply that the effect of flow rate depends on the pipe material, e.g. different strength of adhesion of the scale to different material (see **Table 7.3** for an easier comparison). Clearly, fluid moving at a higher flow rate exerts stronger shear stress on the scale deposit, which results in the removal of it.

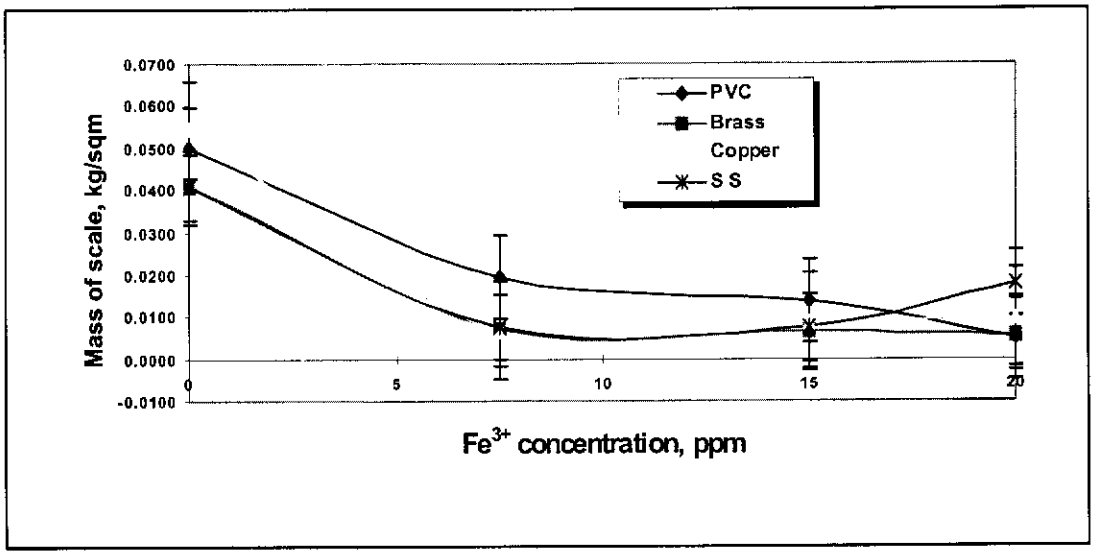

Figure 7.5 Effect of Fe^{3+} concentrations on gypsum scale deposited after four hours for various piping materials (at a higher flow rate of 1.3 cm/sec and a concentration level of 2,500 ppm of Ca^{2+})

Table 7.3 Mass of gypsum scale deposited after four hours in the presence of Fe^{3+} (at a concentration of 2,500 ppm of Ca^{2+}), in kg/m^2

Pipe materials	Admixture, ppm	Low flow rate, 0.4 cm/sec	High flow rate, 1.3 cm/sec
PVC	0	0.038 ± 0.001	0.050 ± 0.002
	7.5	0.029 ± 0.002	0.019 ± 0.001
	15	0.015 ± 0.001	0.014 ± 0.001
	20	0.030 ± 0.001	0.005 ± 0.000
Brass	0	0.051 ± 0.002	0.041 ± 0.002
	7.5	0.026 ± 0.002	0.007 ± 0.000
	15	0.012 ± 0.001	0.007 ± 0.000
	20	0.017 ± 0.001	0.006 ± 0.000
Copper	0	0.044 ± 0.002	0.054 ± 0.002
	7.5	0.023 ± 0.002	0.007 ± 0.000
	15	0.014 ± 0.001	0.009 ± 0.001
	20	0.015 ± 0.001	0.010 ± 0.001
Stainless steel	0	0.053 ± 0.002	0.041 ± 0.002
	7.5	0.043 ± 0.003	0.008 ± 0.001
	15	0.009 ± 0.000	0.007 ± 0.000
	20	0.022 ± 0.001	0.018 ± 0.001

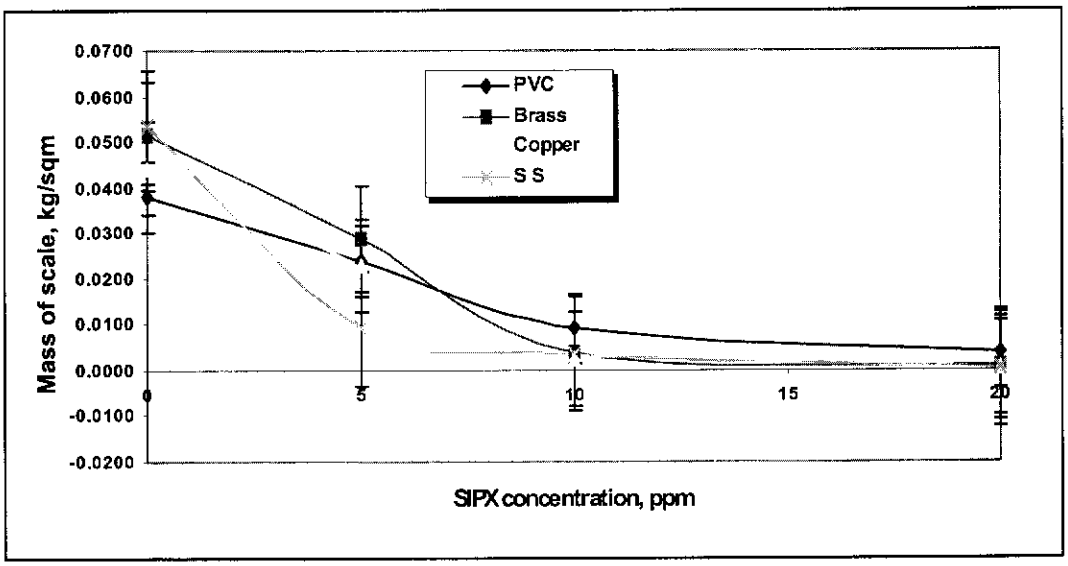

Figure 7.6 Effect of SIPX concentrations on gypsum scale deposited after four hours for various piping materials (at a low flow rate of 0.4 cm/sec and a Ca^{2+} concentration of 2,500 ppm)

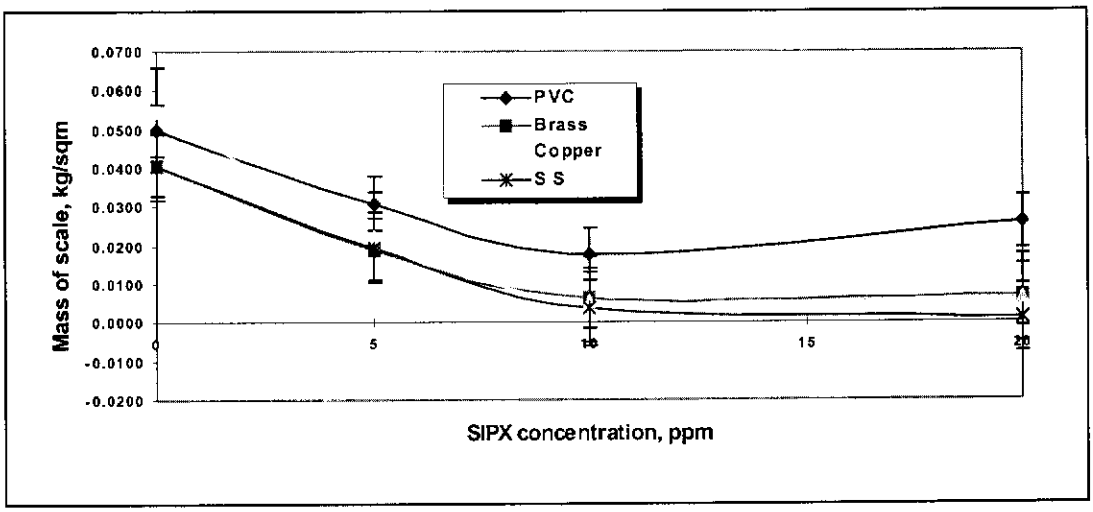

Figure 7.7 Effect of SIPX concentrations on gypsum scale deposited after four hours for various piping materials (at a higher flow rate of 1.3 cm/sec and a Ca^{2+} concentration level of 2,500 ppm)

The effect of SIPX on gypsum scale deposition is shown in both **Figures 7.6** and **7.7**. For an easier assessment, the effect of flow rate on the scale deposited for each type

of material is shown in **Figures 7.8** to **7.11**, respectively. In addition, the data for **Figures 7.6** and **7.7** are also presented in **Table 7.4**.

Table 7.4 Mass of gypsum scale deposited after four hours in the presence of SIPX (at a concentration of 2,500 ppm of Ca^{2+}), in kg/m^2

Pipe materials	Admixture, ppm	Low flow rate, 0.4 cm/sec	High flow rate, 1.3 cm/sec
PVC	0	0.038 ± 0.001	0.050 ± 0.002
	5	0.024 ± 0.003	0.031 ± 0.004
	10	0.009 ± 0.000	0.018 ± 0.002
	20	0.004 ± 0.000	0.026 ± 0.002
Brass	0	0.051 ± 0.002	0.041 ± 0.002
	5	0.029 ± 0.004	0.019 ± 0.003
	10	0.003 ± 0.000	0.006 ± 0.001
	20	0.001 ± 0.000	0.007 ± 0.000
Copper	0	0.044 ± 0.002	0.054 ± 0.002
	5	0.023 ± 0.003	0.022 ± 0.003
	10	0.002 ± 0.000	0.006 ± 0.000
	20	0.001 ± 0.000	0.006 ± 0.000
Stainless steel	0	0.053 ± 0.002	0.041 ± 0.002
	5	0.009 ± 0.000	0.019 ± 0.003
	10	0.003 ± 0.000	0.004 ± 0.000
	20	0.0003 ± 0.000	0.001 ± 0.000

As can be seen, in most cases, increasing the concentrations of SIPX resulted in less scale formation.

For the PVC, as shown in **Figure 7.8**, the mass of scale deposited was higher for a higher flow rate. A possible explanation for this behaviour is that the bonding between PVC and gypsum could be higher than that for the other materials tested.

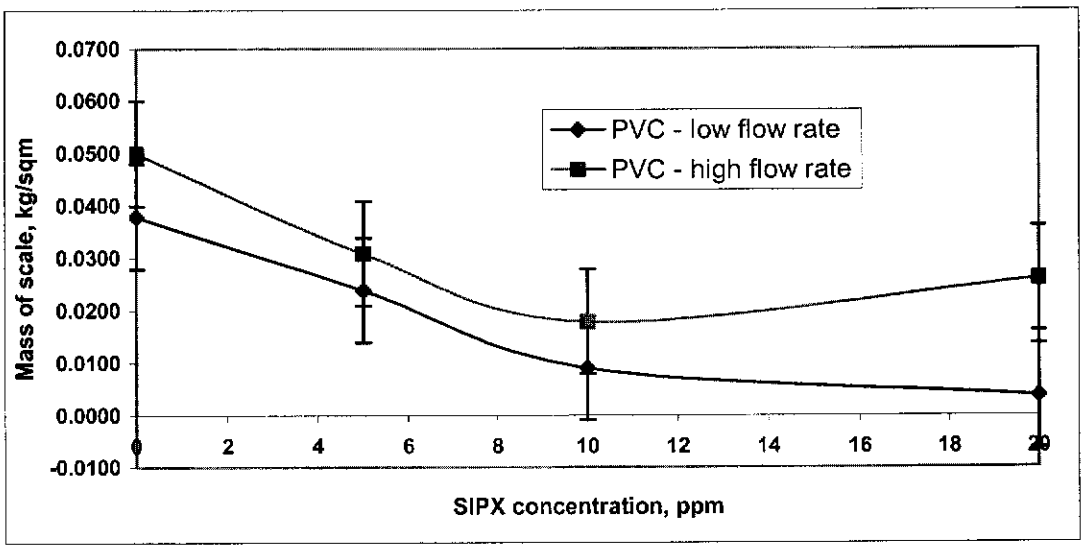

Figure 7.8 Effect of SIPX concentrations on gypsum scale deposited after four hours for PVC (at low and higher flow rates of 0.4 and 1.3 cm/sec, respectively and a Ca^{2+} concentration level of 2,500 ppm).

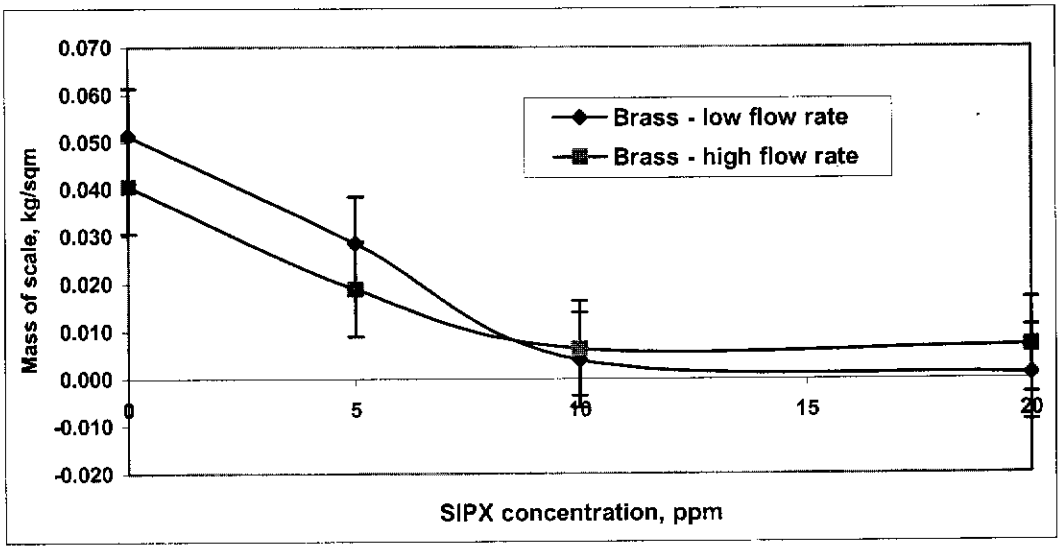

Figure 7.9 Effect of SIPX concentrations on gypsum scale deposited after four hours for brass (at low and higher flow rates of 0.4 and 1.3 cm/sec, respectively and a Ca^{2+} concentration level of 2,500 ppm).

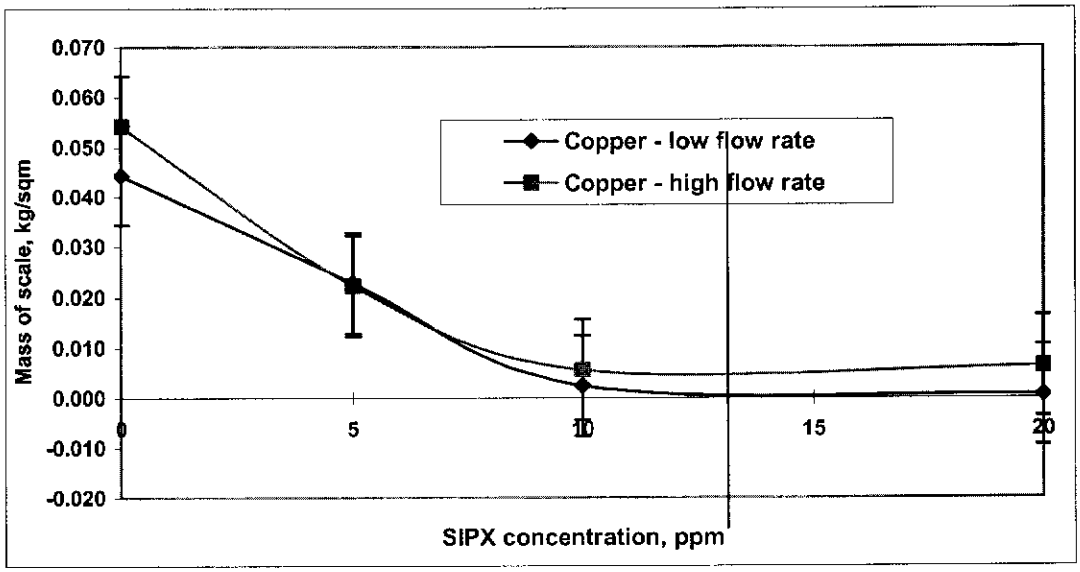

Figure 7.10 **Effect of SIPX concentrations on gypsum scale deposited after four hours for copper (at low and higher flow rates of 0.4 and 1.3 cm/sec, respectively and a Ca^{2+} concentration level of 2,500 ppm)**

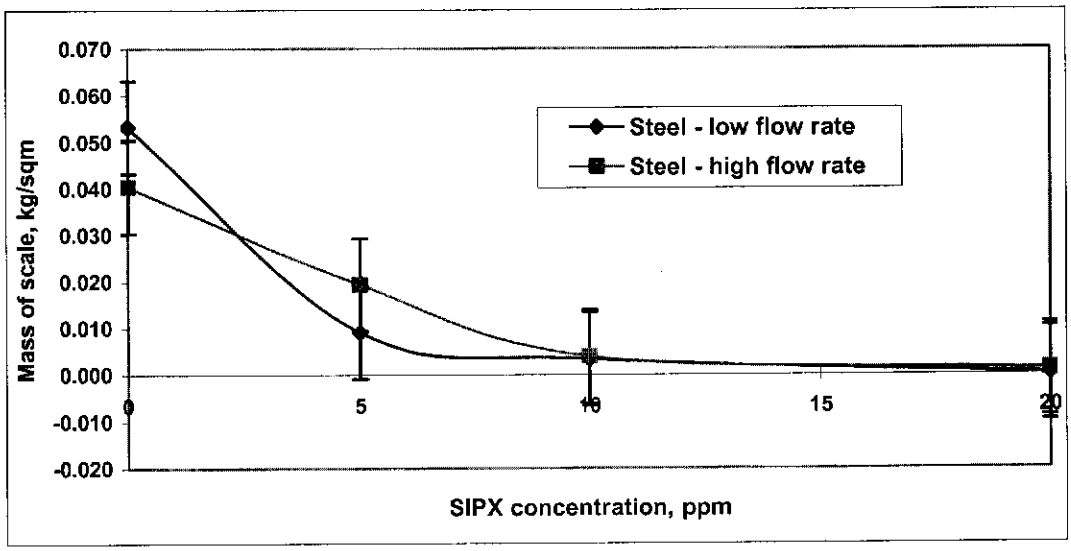

Figure 7.11 **Effect of SIPX concentrations on gypsum scale deposited after four hours for stainless steel (at low and higher flow rates of 0.4 and 1.3 cm/sec, respectively and a Ca^{2+} concentration level of 2,500 ppm)**

7.4.3. Effect of type of piping materials

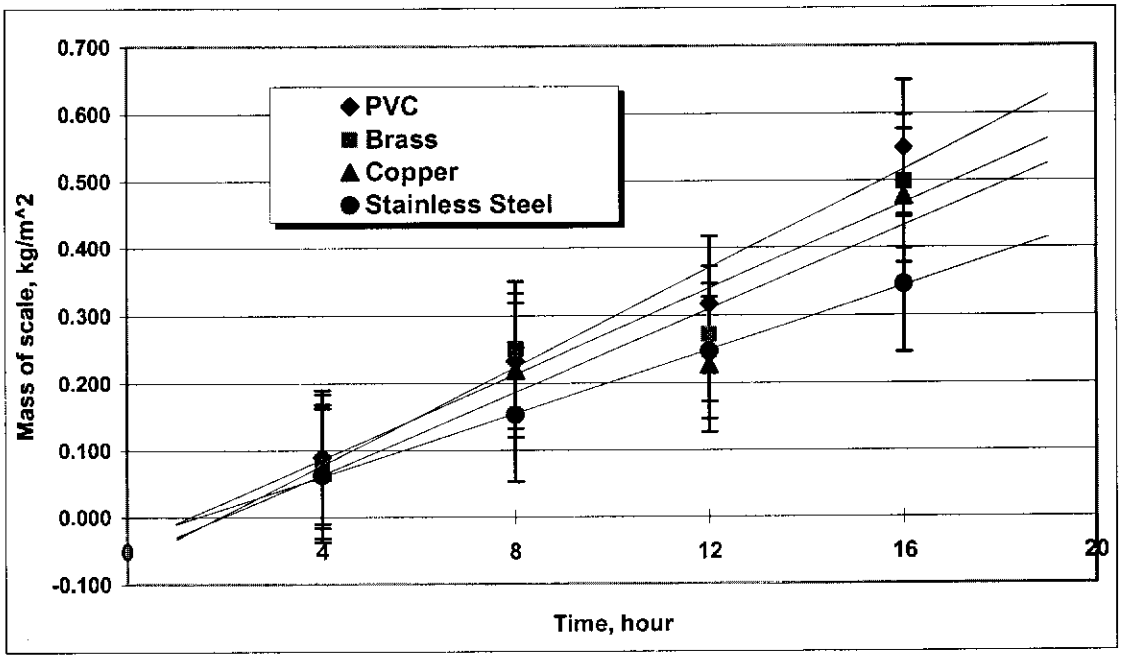

Figure 7.12 Effect of type of piping materials on gypsum scale deposited in the absence of admixtures (at a low flow rate of 0.4 cm/sec and a concentration level of 4,000 ppm Ca^{2+})

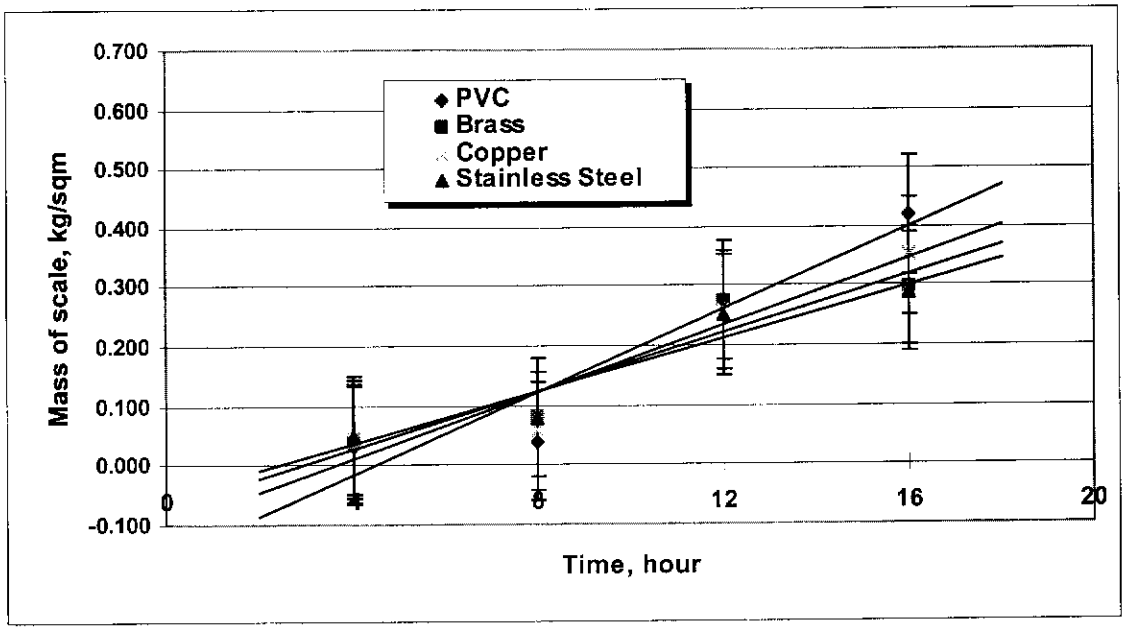

Figure 7.13 Effect of type of piping materials on gypsum scale deposited in the absence of admixtures (at a high flow rate of 1.3 cm/sec and a concentration level of 4,000 ppm Ca^{2+})

The effect of piping materials on scaling is not well understood. **Figures 7.12** and **7.13** show such effect, which is determined by the amount of scale deposited on the pipe made of particular materials, under otherwise the same operating conditions. Four linear regression lines were drawn to approximate the rate of formation for each type of the pipes used. As can be seen, the rate of formation seems to vary with different pipe materials: PVC the highest and stainless steel the lowest. Comparison of the two figures also shows that the higher flow rate seems to result in less scale deposit, which is consistent with the argument that the mass deposited decreases with increasing flow rate.

The effect of piping materials on scale deposition might be more related to the roughness of the surface, which could be inherently different in each type of material, as well as being a result of the methods of manufacture. It could be argued that once the pipe surfaces had been entirely covered by the scale layer, the roughness would have no appreciable effect on the scale growth. However, it may still influence the removal or the ageing processes. Microscopically, the entire surface of a pipe consists of crevices and cracks which provide sites for attachment of the scale building components when they are transferred towards the pipe wall. The characteristics of the crevices and cracks will affect the strength of the attachment. It can be assumed that the rougher the surfaces, the stronger the attachment, and hence the more difficult to detach. In another study (Linnikov 1999), it was observed that the nucleation rate of calcium sulphate crystals increases with surface roughness. In addition to the effect of the substrate microstructure/roughness, future studies may look into other possible effects as detailed in **section 8.2.3** in **Chapter 8**.

The linear regression lines that approximate to the rate of formation on each pipe material were extrapolated to obtain the projected values of induction time. It can be seen that the values are between 1 and 2 hours for a low flow rate (**Fig. 7.12**), and 2 to 4 hours for a high flow rate (**Fig. 7.13**). These predicted values are compared with the values of the induction time obtained in this scaling experiment, which is discussed in the following section.

In all cases, PVC was found to have the highest rate of gypsum scale deposition. In descending order from the highest to the lowest rate of deposition, the piping materials can be listed as follows: PVC, brass, copper and stainless steel.

7.4.4. Induction time

In a crystallisation process, there is usually a lapse of time between the attainment of supersaturation and the detectable changes in the crystallising solution property, signalling the onset of crystal formation. This period of time is widely known as the induction time or induction period, and consists of two successive parts, that is, (1) the period necessary for the formation of nuclei to reach a critical size, and (2) the time needed for these nuclei to grow to a detectable size. Since the term "detectable changes" is open to various interpretations; the concept of induction time could not be considered as fundamental in a crystallisation process (Sohnel and Mullin 1988). Different interpretations exist, because a variety of measurement techniques are available to determine the induction time. Four methods are generally used: visual, turbidimetry, by concentration, and by conductivity, respectively (Sohnel and Garside 1992). Therefore, for one crystallisation system, a discrepancy in results for the induction time may be obtained, depending on the method of measurement. For example, the visual method works by detecting the first visible crystals in the solution. It is perhaps the least recommended method, since it relies on the capability of the instrument, down to which smallest crystal size it can measure. Thus, even within one method, different values of induction time may exist. In other words, the exact duration of the induction period of a crystallisation process may not be found.

The induction time is affected by many factors. With respect to scale formation, it is related to the nature of the components in the scaling solutions and the characteristic of the surface (Bott 1997; Hasson *et al.* 1996). As an example, a rough surface is generally favourable for nucleation sites; hence the induction time could be short since such sites promote heterogeneous nucleation. Also, it was reported that the duration of induction period was greatly affected by the concentration of the admixtures present, the temperature, and the amount of seed crystals added into the

crystallisation system (Amjad 1985). In an attempt to better understand the behaviour of the crystallisation of gypsum in the presence of admixtures, including the scaling experiment, the induction time of each of the system was examined. As detailed in **Chapter 4**, during the batch crystallisation experiments carried out in this study, no induction time was observed. The same situation was found for the continuous crystallisation experiments, as presented in **Chapter 6**.

Several data on induction time with respect to gypsum crystallisation either in pure system or in the present of admixtures are presented in **Table 7.5**. As can be seen, the induction time may not be observed in crystallisation and/or scaling experiments, in either the absence or the presence of admixtures. In addition, the table indicates that investigation on gypsum scale formation using isothermal flow system has probably never been attempted. Experiments on scale formation using continuous crystallisation systems are also very few.

Table 7.5 Induction time in crystallisation/scaling experiments obtained by several authors

No.	Crystallisation or Scaling System	Admixtures	Induction time, (hours)	References
1	Unseeded batch (gypsum)	Citric acid, esterified citric acid, defoaming agent	0.0	(Al-Sabbagh *et al.* 1996)
2	Seeded batch (gypsum)	None	0.0	(Liu and Nancollas 1973)
		EDTA	0.0	
		NTMP	0 – 3.5	
		ENTMP	0 – 2.5	
		TENTMP	0 – 2.5	
		HEDP	0	
		$(NH_4)_6Mo_7O_{24}$	0	
3	Seeded batch (gypsum)	None	0	(Weijnen and van Rosmalen 1984)
		HEDP (10^{-6} – 10^{-5} M)	0	
4	Seeded batch (gypsum)	None	~ 0	(Chan 1997)
		Industrial process water	~ 0	
5	Seeded batch (gypsum)	None	0	(He *et al.* 1994)
		NaCl	0	
6	Isothermal flow ($CaCO_3$)	None	0.0	(Andritsos and Karabelas 1995)
7	Isothermal flow ($CaCO_3$)	None	0.0	(Andritsos and Karabelas 1992)
8	Isothermal flow (CdS)	None	0.0	(Andritsos and Karabelas 1992)
9	Isothermal flow (PbS)	None	0.0	(Andritsos and Karabelas 1992)
10	Isothermal flow (CdS & PbS)	None	0.0	(Andritsos and Karabelas 1992)
11	Isothermal flow ($CaCO_3$)	None	+)	(Hasson *et al.* 1996)
		Na-hexamethaphosphate	0	
		Acrylic polymer	0	
12	Seeded and unseeded continuous crystallisation (gypsum)	Fe^{3+}, Al^{3+}, Ni^{3+}	2 – 6 ++)	(Adams and Papangelakis 2000)
13	Seeded continuous crystallisation (gypsum)	None	0	(Jamialahmadi and Muller-Steinhagen 2000)

+) existed but not measured.

++) the measurement technique was not explained.

The induction time in the scaling experiments was determined by measuring the conductivity of the crystallising solution using a conductivity meter (Yokogawa, Model SC82).

It was discussed in **Chapter 4** that the second order kinetics shows a reasonable fit to the data obtained for the batch crystallisation of gypsum. In addition, the experiment shows that there was no induction period (as can be seen from **Figure 4.1** in **Chapter 4**), which is in agreement with some of the previous experiments listed in **Table 7.3**. In cases where induction period is not observed, the crystallisation of gypsum with equivalent concentration of ions could be considered to follow the second order kinetics (Amjad 1985).

In the scaling experiments carried out in the present study, a distinction should be made with respect to the induction period and the predicted time for the onset of the scale formation (as detailed in **section 7.4.3 Effect of type of piping materials**). Induction period, by definition, is the lapse of time from the achievement of supersaturation until the first visible nuclei are detected. Depending on the system under consideration, this period of time can be either long or short. On the other hand, the decrease in the concentration of Ca^{2+} of the solution as shown by the change in conductivity, was due to nuclei formation. It is logical, that the change/decrease in Ca^{2+} concentration could have been recorded, although the formation of scale had not yet started.

Once the nuclei formed and attached on the surface of the pipe wall, they accumulated, and after several hours, as predicted previously by **Figure 7.12** or **Figure 7.13**, these nuclei could have grown and accumulated as scale deposits. This phenomenon can be explained in connection with the topography of the pipe wall, which although visually smooth, may not be sufficiently smooth at the microscopic level. Therefore, nuclei formation was started immediately in the "cracks and pits" on the surface of the pipe wall. As scaling experiment progressed, the availability of relatively constant supersaturated flowing solution enhanced the formation of new nuclei, which might take place on top of the previously formed ones. In fact, Hasson and Zahavi (Hasson and Zahavi 1970) observed that the initial stage of scale deposition consisted of the nucleation of crystals, which adhered to the metal surface.

As explained previously, the induction time in the scaling experiments performed in the present work was investigated using a conductivity method. **Figures 7.14** and **7.15** show the results of this induction time measurement at a concentration level of 2,000 ppm of Ca^{2+}.

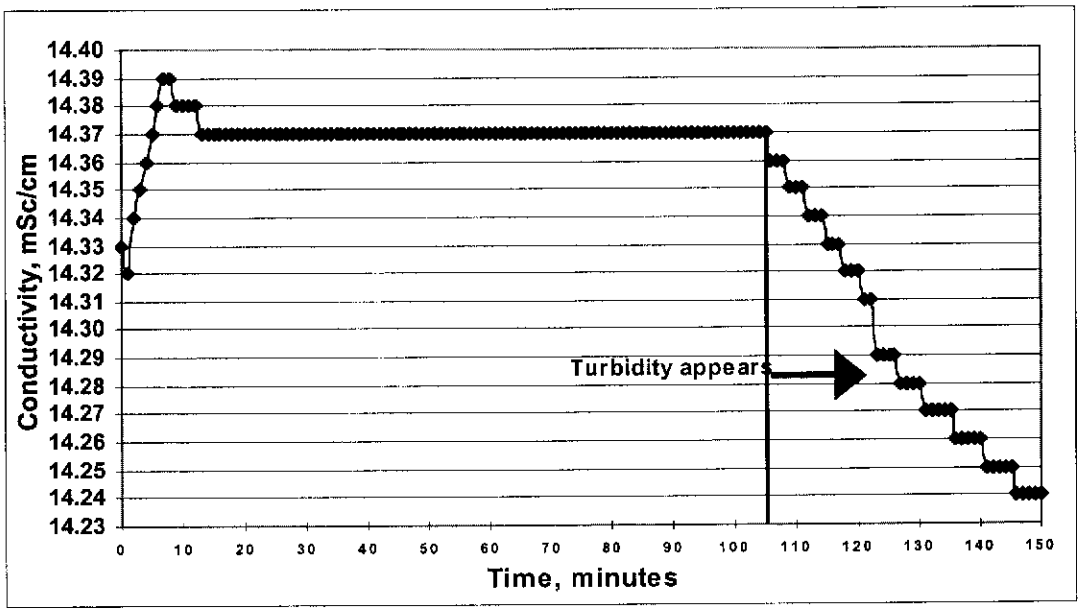

Figure 7.14 **The conductivity of the pure gypsum solution versus the scaling experiment time for an initial concentration of 2,000 ppm Ca^{2+} and solution temperature of 18.3^{0}C (first experiment)**

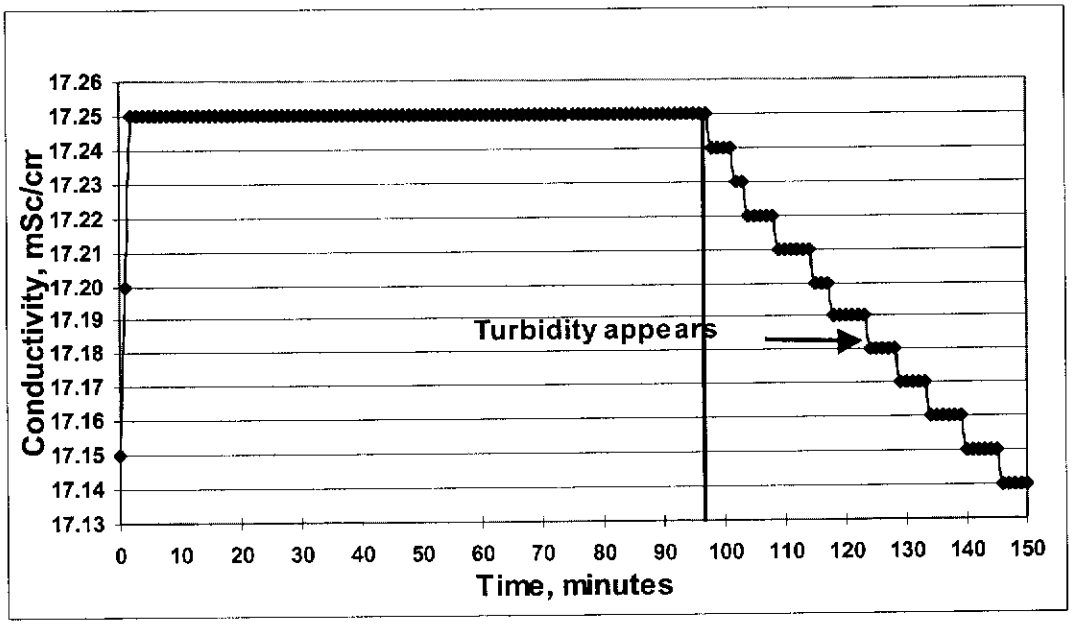

Figure 7.15 **The conductivity of the pure gypsum solution versus the scaling experiment time for an initial concentration of 2,000 ppm Ca^{2+} and solution temperature of 20.6^{0}C (second experiment)**

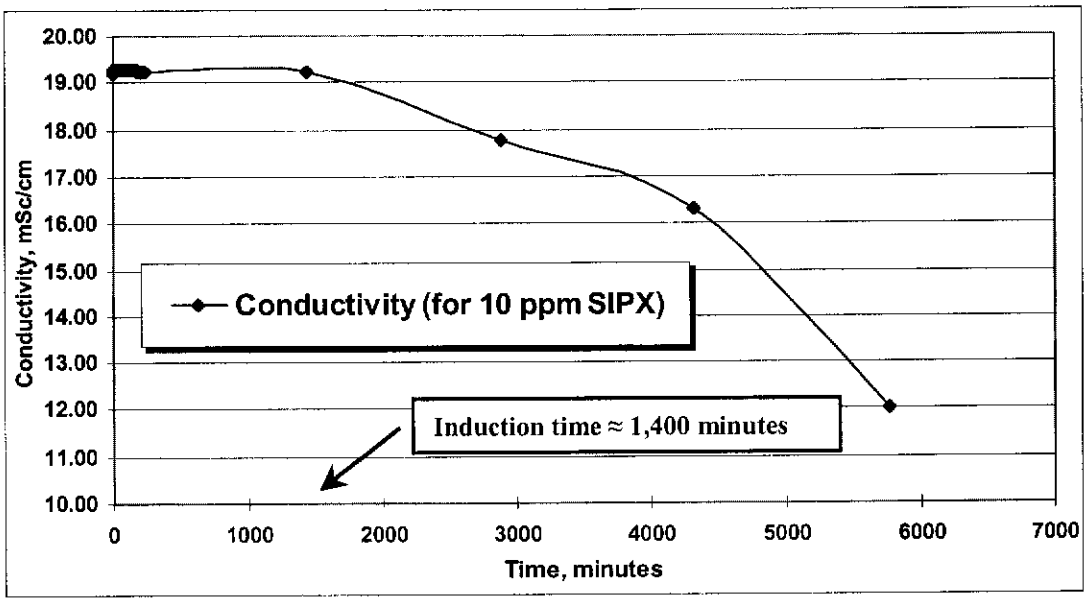

Figure 7.16 **The conductivity of the gypsum solution in the presence of 10 ppm of SIPX, versus the scaling experiment time for an initial concentration of 2,000 ppm Ca^{2+} and solution temperature of 19.2^{0}C**

Figures 7.14 and **7.15** clearly illustrate that at a concentration level of 2,000 ppm of Ca^{2+}, the gypsum solution shows significant or measurable induction time. It can be seen from the figures that the induction time is about 105 minutes at 10.3^{0}C and 97 minutes at 20.6^{0}C.

Induction time in the present of admixtures is usually longer than that in a pure system. This phenomenon is also prevalent in the present study, where the SIPX was added into the gypsum solution. As can be seen in **Figure 7.16**, the induction time as calculated from the intersection of tangents, in the present of SIPX is about 1,400 minutes.

Having observed the induction times as shown in **Figures 7.14** and **7.15**, it can be concluded that the predicted values of the induction time derived from **Figures 7.12** and **7.13** respectively, are reasonably materialized.

7.4.5. Morphology of the gypsum scale deposits

The morphology and surface topography of crystals may reveal information about the mechanism of crystal growth. A crystal morphological study may be of value in predicting the growth rate or to help prevent crystals from forming. With respect to scale formation processes such a study may indicate way to lessen scale formation, since some properties of scale deposit (especially physical properties) are related to morphology. As an example, a porous scale is obviously morphologically different from that of a dense or compact scale. The difference may, in turn, affect the thermal conductivity of the scale deposit. Further, the thermal conductivity as a temperature-related factor, may affect kinetics of scale formation. Thus, there could be a significant interrelationship between the scale formation process and the morphology of the scale.

Removal rate of a scale deposit formed in a flowing condition may also be affected by the morphology. It is logical to assume that a compact scale is more difficult to remove than a porous and loosely bound one.

In the gypsum scale formation in isothermal flow system experiments, carried out in the present study, the effect of admixtures on the morphology of the gypsum scale deposits was investigated. Scanning electron micrographs of the deposits were taken and subsequently used to reveal the morphology and surface topography of the deposits .

It is well known that calcium sulphate salts form different phases under different temperature levels. Hence, a once-through pipe flow experiment under isothermal condition was carried out and maintained to ensure that only one phase was formed, in this case, calcium sulphate dihydrate (= $CaSO_4.2H_2O$) or gypsum.

Scaling is a rate-driven phenomenon in which two simultaneous opposing steps, namely the deposition and removal stages determine its ultimate rate. The mass deposition rates of scale deposits are affected by several factors. It is therefore

important to observe how the scale morphology has been affected by such factors. In fact, it is common to include morphological studies in any investigation on scale formation. After each experimental run, therefore, the scale deposits formed inside the coupons were removed and collected for SEM analysis. Since SEM can produce pictures with high magnification and depth of fields, the micrographs obtained using SEM can easily be used to detect the structure of the deposits as well as any structural changes of the scale. **Figures 7.17** to **7.20** presented in the next section show such micrographs of the scale deposited on the surface of PVC coupons.

Figure 7.17 shows an SEM view of typical gypsum crystals obtained from the scale deposit after four hours, which formed in pure conditions, that is in the absence of admixtures. **Figure 7.17a** depicts the well-known needle and plate like shape of gypsum crystals precipitated from pure solutions. It can be seen that the deposits consist of crystals of different sizes. Such a feature is typical of pure gypsum scale deposit (Al-Sabbagh *et al.* 1996; El Dahan and Hegazy 2000; Klepetsanis and Koutsoukos 1998). Enlargement of the micrograph as depicted in **Figure 7.17b,** clearly shows the typical gypsum crystal morphology with dominant **(010)**, **(120)**, **(001)** and **(100)** faces, which are commonly observed (Bosbach *et al.* 1996; Rinaudo *et al.* 1988).

Figure 7.18 depicts the scanning electron micrographs of pure gypsum scale formation after 4 (**Fig. 7.18a**) and 8 hours (**Fig.7.18b**), respectively. As can be seen in **Figure 7.18b**, after 8 hours, the scale is seen to consist of clumps of leaf-like aggregates, which protrude in different directions and wedge into one another. **Figure 7.18b** may also indicate the tendency of the protruding crystals to orient to a certain direction, namely to the direction of flow (indicated by the direction of the white line).

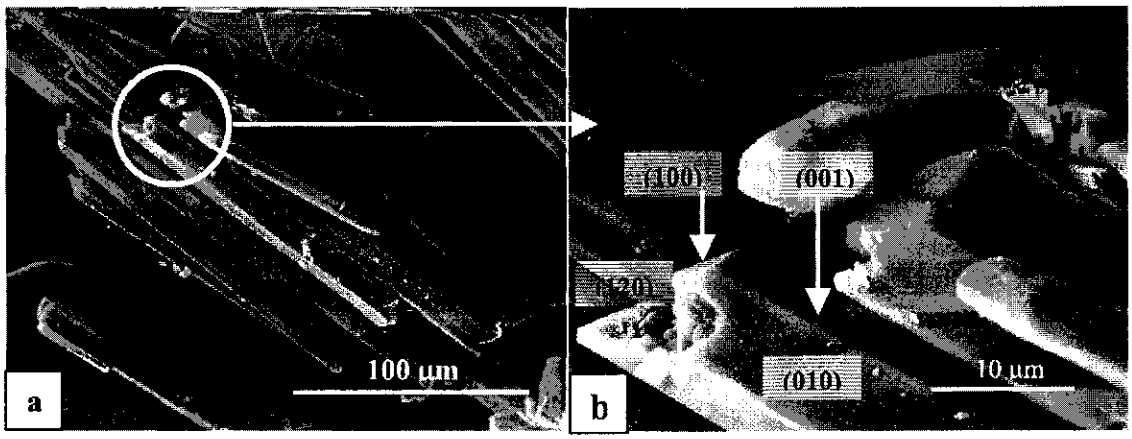

Figure 7.17 **Morphology of pure gypsum scale crystals after 4 hours of scaling, (b) enlargement of (a)**

This aggregation could be the result of a bridging mechanism in which nuclei formed between crystals grow and are simultaneously adsorbed onto more than one crystal face. Such mechanism was also observed during inhibition of the growth of gypsum by trace amount of polyacrylic acid (PAA) at room temperature (Oner 1998), and in the formation of gypsum scale layer on a heated metal pipe (Krause 1993).

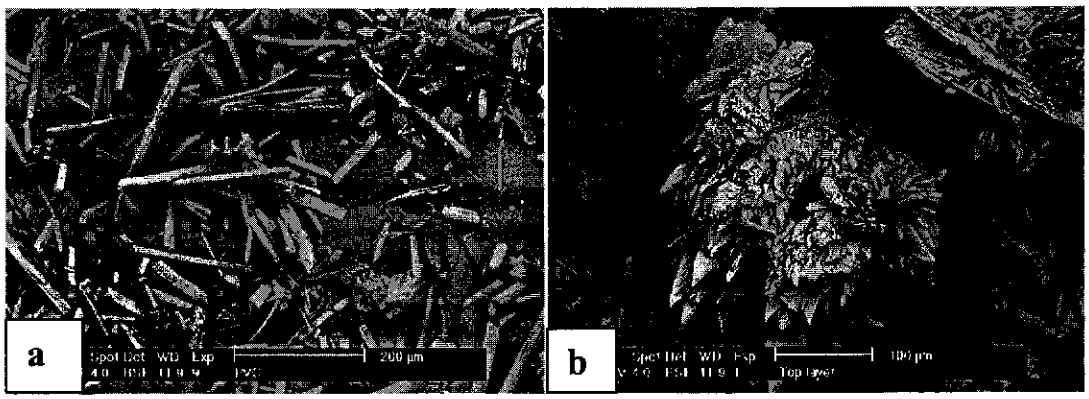

Figure 7.18 **Morphology of pure gypsum scale formed: (a) after 4 hours, (b) after 8 hours**

Figure 7.19 Morphology of gypsum scale after 4 hours: (a) pure gypsum, (b) in the presence of SIPX, (c) in the presence of Fe^{3+}

Figure 7.19 shows a typical series of micrographs of scale formed after 4 hours in pure gypsum solutions, in the presence of SIPX and in the presence of Fe^{3+}, respectively. All faces of pure gypsum crystals (**Fig. 7.19a**) are flat and smooth (even when viewed at higher magnification than those of **Figs. 7.19b** and **7.19c**), whereas those grown in the presence of admixtures are markedly rough and seem to be covered with cracks and masses of small crystallites. A similar roughening of crystal faces was reported in a number of investigations (Davey 1982; Rinaudo *et al.* 1988; Weijnen and van Rosmalen 1985). An investigation on the influence of various polycarboxylates on the precipitation of gypsum by Weijnen and van Rosmalen (Weijnen and van Rosmalen 1985), showed that the faces of the gypsum crystals obtained were highly roughened. They argued that the roughening effect is the result of the protonated carboxylic acid groups, which were adsorbed onto the crystal surface. Another explanation was given by Rinaudo *et al.* (Rinaudo *et al.* 1988) who maintained that the occurrence of fractures is due to the presence of metallic ions or their complexes making bonds with the uppermost oxygen atoms of the sulphate groups of the gypsum crystals. Such complexes may be weakly attached to the crystal surface and, being present at the surface, may be washed away by the flowing solution, and crack the surfaces open. Hence the surfaces are roughened. Still another explanation could be that adsorption of the admixtures onto the crystal surface results in the disruption of the otherwise "normal' growth rate of pure crystals (Ogden 2002). Since gypsum is a fast growing crystal, the disruption could be significant, so that the growth steps do not advance in a regular manner. Hence, the surface becomes rough.

Finally, there is another explanation for the roughening of the surface: the effect of the flow of the solution. Had the solution been kept stagnant, the effect of the admixtures could be the opposite, i.e. the smoothing of the surface (Dirksen and Ring 1991). The mechanism of this proposal is that the admixture molecules were adsorbed and filled in the step and kink faces making them gradually shallower and flatter, and thus a smooth surface is obtained. With the flowing solution, many admixture molecules were possibly not able to settle into the kinks and steps and, instead such molecules were carried away by the solution. Hence causing the surface of the scale to be uneven or rough.

It is difficult to distinguish the individual admixture effect, but it appears that both of the admixtures used caused the roughening of the scale surfaces. The micrographs indicate that agglomeration has extensively occurred and that some crystals no longer retain their straight needle-like shape but become slightly curved. Such curved crystals were also found in a number of investigations on gypsum either using a crystalliser vessel (McCartney and Alexander 1958; Rinaudo *et al.* 1988) or on heated metal surfaces (Amjad 1988). Rinaudo *et al.* (Rinaudo *et al.* 1988) argued that the occurrence of such curved gypsum crystals was caused by partial replacement of some water molecules by the admixtures either in their ionic forms or their complexes. Clearly, this could be a sound argument if the volume of the water molecules is different from that of the complexes, so that the complexes do not perfectly fit into the space left by the water molecules in the crystal structure. As a result the crystals might be curved. An earlier report on the effect of admixtures on gypsum by McCartney and Alexander (McCartney and Alexander 1958) showed that the curved gypsum crystals were obtained at an elevated temperature of 70^0C, in which the formation of the curved crystals was extremely rapid. Hence, it was argued that at the elevated temperature of 70^0C, the admixture could not effectively prevent nucleation. Once the nuclei formed, they might grow rapidly due to the high temperature. It is possible that the rapid growth causes imperfect surface structure and may result in curved crystals.

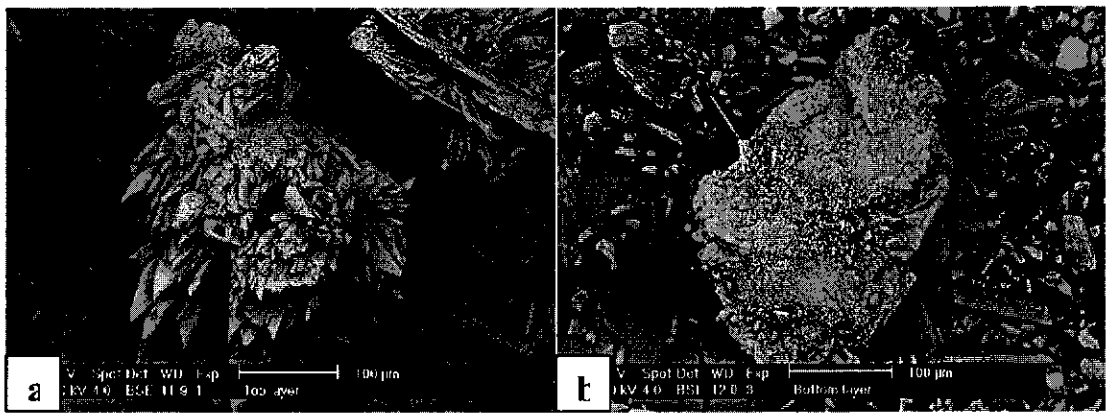

Figure 7.20 Morphology of scale in pure system after 8 hours: (a) top layer, (b) bottom layer

In practical situations, scale formation usually takes a long time and, thus cannot easily be simulated in a laboratory work. In this study a scale formation time of 8 hours has been chosen as the longest, for practical reasons. It was found that prolonging scaling experiments has the effect of making the scale deposits denser. In **Figure 7.20**, a micrograph is shown of the scale deposits after eight hours of experimental run. As can be seen, the compactness of the scale increases from the top of the scale to the bottom, and it was qualitatively noticed that the scale becomes more difficult to remove with time. In a once-through flow system, as was used in this study, the supersaturation is maintained at a constant level, and consequently the scale growth continues. In the beginning, when the first scale deposits attached to the pipe wall, the scale structure is relatively porous. This type of structure is favourable for nucleation sites and with the availability of supersaturated solution flowing past and between the cavities, which exist in the scale, more nuclei are generated. The nuclei created grow to become crystallites, filling the cavities. Hence, gradually the scale becomes denser. With the slow flow rate used in this study, it is believed that the nuclei are able to stick rather firmly onto the scale surface and grow, rather than being washed away as it might occur in a fast flowing solution. Obviously, as the scale formation proceeds, it accumulates, so that the bottom layer, having been longer in the process, becomes denser than the top layer.

7.5. Conclusions

7.5.1. Conclusions on the effects of the experimental parameters tested

Gypsum scaling experiments in an isothermal flow system were carried out to estimate the mass of gypsum scale deposited as affected by supersaturation level, admixtures, fluid flow rate and type of pipe materials. It was found that the mass of the gypsum scale deposited over a fixed period:

1. Increases with concentration (in the range 2,000 to 6,000 ppm of Ca^{2+}), and that the correlation can be represented by quadratic functions.

2. Decreases with increasing concentration of Fe^{3+} and SIPX.

3. Is little affected by the flow rate (in the range 0.4 - 1.3 cm sec^{-1}), over a narrow range of flow rates.

4. Is highest on PVC, followed by brass and copper, and lowest on stainless steel.

Measurement of the mass of the scale deposited could be improved by *in situ* monitoring using a quartz microbalance. Similar investigations to account for the effect of flow rate in the turbulent region, of other types of admixtures as well as of different piping materials would lead to a more comprehensive understanding about the scaling of gypsum and thereafter its prevention from occurring. Such investigations are currently being conducted independently in the research group.

7.5.2. Conclusions on the morphology of the gypsum scale deposits

Analyses of the morphology and surface topography of the scale samples result in the following:

1. The scale deposits obtained in this once-through isothermal flow system experiment were characteristic of gypsum crystals.

2. The scale deposits consisted of gypsum crystals, which grew and formed aggregates with one another. The aggregates oriented themselves with the direction of the fluid flow.

3. In the presence of admixtures the scaling solutions produced scale deposits with rough surfaces. This surface roughening may have been caused by a combined effect of the nature of the adsorbed admixtures and the fluid flow.

4. The observed roughening of crystal surfaces was found to be the same for both admixtures.

5. Prolonging the scaling time, while keeping all other factors constant, resulted in denser scale deposits. This might be caused by the formation and growth of crystals, which occur in the space between the crystals forming the scale deposits, and these then trapped and attached. The continuous formation and growth of the crystals was due to the relatively constant supersaturation conditions of the flowing fluid.

7.6. Comparison between the Growth Rate of Gypsum Crystals in the Continuous Crystalliser and Gypsum Scale Formation in the Scaling Experiments

The present study investigated the role of impurities and additives, collectively known as admixtures, in the crystallisation of gypsum. Three phases of experimental work were carried out: (1) batch crystallisation, (2) continuous crystallisation, and (3) scale formation in a once through pipe flow system. The results of the three phases of experiments show that in most cases the admixtures tested were able to reduce the growth rate of gypsum. It was described previously (see **Summary of Chapter 4**) that the residence time used in the continuous crystallisation experiment

was determined from the result of the batch crystallisation study. Thus, a link was established between phase 1 and phase 2 of the project. An attempt was also made to correlate the experimental results obtained from phase 2 and phase 3 of the project. This was carried out by quantitatively comparing the growth rate of the gypsum crystals obtained in the continuous crystallisation with the gypsum scale formation obtained in the scaling experiments.

7.6.1. Mass balance around the MSMPR crystalliser

A mass balance is calculated for the continuous crystallisation experiments carried out in this study. Such calculation is necessary since the mass growth rate of gypsum crystals in the crystalliser should correspond to the decrease in Ca^{2+} concentration (Ca^{2+} is one of the lattice ions) over the same period of time.

A sample calculation was carried out for the crystallisation of pure gypsum, that is, in the absence of any admixtures, at 25^0C.

One residence time	= 15 minutes.
Volumetric flow rate of gypsum solution	= 100 ml/min.
Therefore, volume of the solution for one residence time	= 15 x 100 = 1500 ml = 1.5 litre.

Slurry density in 1 litre solution at the beginning of the run = 0.7925 g (measured).

Slurry density at steady state	= 2.7689 g (measured).
Ca^{2+} concentration at the beginning of the run	= 1,221 ppm (measured).
Ca^{2+} concentration at steady state	= 735 ppm (measured).
The increase in slurry density	= (2.7689 – 0.7925) g = 1.9764 g.
The decrease in Ca^{2+} concentration	= (1221 – 735) ppm = 486 ppm.

The decrease in Ca^{2+} concentration should correspond to the gypsum crystals formed. Hence, gypsum crystals theoretically obtained at the expense of the decrease in Ca^{2+} concentration at the end of the experimental run (= steady state) can be calculated as follows:

The atomic weight of Ca^{2+} = 40 g/mol.

The molecular weight of gypsum ($CaSO_4.2H_2O$) = 172 g/mol.

Therefore, gypsum crystals theoretically obtained:

= 172/40 x 486 mg/L

= 2089.8 mg

= 2.0898 g.

Hence, the slurry density expected at steady state = slurry density at the beginning of the run + gypsum crystals formed

= (0.7925 + 2.0898) g/L

= 2.8823 g/L.

Slurry density measured at steady state = 2.7689 g/L.

The difference between the calculated and the experimental values of slurry density

= (2.8823 – 2.7689) g/L

= 0.1134 g/L.

The discrepancy between these two values could be argued as follows.

A 15 minute residence time may be too short for the calcium ions to become nuclei and subsequently grow to become gypsum crystals large enough to be retained by the filter paper used. Consequently, these small gypsum crystals passed the filter paper. Hence, the weight of the crystals obtained was lower than its calculated value. It is also likely that some of the gypsum crystals formed scaled up the wall of the crystalliser and the crystalliser internals. As a result, the expected increase in slurry density would be less.

Measurement of slurry density is described in **Chapter 5** (section **5.7.2. Sampling for slurry density**). A typical slurry density versus residence time plot is depicted in **Figure 6.2** in **Chapter 6** (section **6.2. Attainment of Steady State**).

Briefly, a 50 ml sample was isokinetically withdrawn from the crystalliser. It was immediately filtered and washed with isopropanol. The filtered solids were dried in an oven until a constant weight was reached. The difference in weight between the filter paper used and the filter paper plus the solids, equals the weight of the gypsum crystals obtained. This difference in weight was subsequently multiplied by 20 to give the weight of crystals in g/L of sample, which is equal to the slurry density in the crystalliser.

The sample calculation described previously, shows that the mass balance around the crystalliser could be considered as reasonable.

7.6.2. Calculation of the mass growth rate for the continuous crystalliser

The continuous crystallisation experiments were carried out using the seeded method: therefore, the growth was assumed to take place on the surface of the seeds. Since the small size crystals (below 13.05 microns) were found not to grow, only the surface area of the seeds with sizes from 13.05 microns to 107 microns was calculated. **Table 7.6** shows a sample calculation for the seed crystal surface for continuous crystallisation in the absence of admixtures, carried out in the present study.

The difference in slurry density at the beginning and at the end of the experimental run is the mass growth rate, and this was used to calculate the growth rate per surface area of the seeds.

The slurry density at the start of the run = 0.7925 g/L.
The slurry density reached a relatively stable value after 4 residence times (= 4 x 15 minutes = 1 hour), and at the end of the run the value = 2.7689 g/L.

The mass difference = 2.7689 – 0.7925 g = 1.9764 g.
Hence, the growth rate = the mass difference/the total surface area

$$= 1.9764 \text{ g}/0.050746514 \text{ m}^2$$
$$= 38.9465 \text{ g/m}^2$$
$$= 0.0389 \text{ kg/m}^2 \text{ hour.}$$

Table 7.6 Surface area of crystals in the continuous crystallisation of gypsum in the absence of admixtures

No. of crystals (#/litre)	Crystal size, micron	Surface area, micron^2	Surface area, m^2
1865	107	67080495.86	6.70805E-05
3031	97.05	89686461.28	8.96865E-05
4955	87.75	119863728.2	0.000119864
7966	79.5	158170115.6	0.00015817
12273	72.05	200155983.4	0.000200156
19685	65.3	263700925.7	0.000263701
30660	59.15	337001257.3	0.000337001
45112	53.55	406406742.6	0.000406407
60962	48.55	451427017.7	0.000451427
100224	42.05	556741512.2	0.000556742
172045	34.5	643324540.5	0.000643325
298503	29.65	824418954.7	0.000824419
685529	24.6	1303304571	0.001303305
19907476	18.3	20944415891	0.020944416
45569822	13.05	24380815517	0.024380816

Total surface area $= 0.050746514$ m^2

≈ 0.051 m^2.

7.6.3. Calculation of the scale formation scaling experiment

The scaling experiment was carried out at a volumetric flow rate of 30 ml/min. Hence, in one hour, the volume of solution that passed the test section = 30 x 60 = 1,800 ml. In addition, the scaling experiment was carried out for 4 hours. Since the induction time was approximately 2 hours (see **Figures 7.14** and **7.15**), the period taken for the calculation of the scale formation was 4 hours – 2 hours = 2 hours. The volume of the scaling solution used in 2 hours = 1,800 x 2 = 3,600 ml. The masses of scale shown in **Table 7.7** are those, which have been recalculated for the duration of 2 hours. **Table 7.7** presents the data of the scale formation in comparison with those of the continuous crystallisation experiments, in the presence of 0, 10 and 20

ppm of Fe^{3+}, respectively. In **Table 7.8**, similar data are presented for SIPX as admixtures.

Figures 7.21 to **7.24** display the rate of growth on scale formation on the inner walls of the pipe, as affected by the admixtures selected, as a function of the flow rate of the scaling solution. The mass growth rate of gypsum in the continuous crystalliser is included in all the graphs for comparison.

As can be seen, in the absence of any admixture (Fe = 0 ppm or SIPX = 0 ppm), the rate of growth of crystals in the crystalliser is consistently higher than the scale formation in the scaling system regardless of the flow velocity of the scaling solution.

Table 7.7 Data for the rate of growth/scale formation in the continuous crystallisation and scaling experiments, in the presence of 0, 10 and 20 ppm of Fe^{3+} at 25^0C

Admixtures	Growth rate in pipes, kg/m^2 hour				Growth rate in crystalliser [3], kg/m^2 hour
	Low flow rate, 0.4 cm/second [1]		High flow rate, 1.3 cm/second [2]		
Fe^{3+} = 0 ppm	PVC	0.0289	PVC	0.0249	0.0389
	Brass	0.0257	Brass	0.0203	
	Copper	0.0222	Copper	0.0271	
	Stainless steel	0.0267	Stainless steel	0.0202	
Fe^{3+}= 10 ppm	PVC	0.0121	PVC	0.0101	0.0196
	Brass	0.0100	Brass	0.0035	
	Copper	0.0095	Copper	0.0085	
	Stainless steel	0.0165	Stainless steel	0.0017	
Fe^{3+}= 20 ppm	PVC	0.0151	PVC	0.0021	0.0090
	Brass	0.0082	Brass	0.0059	
	Copper	0.0077	Copper	0.0072	
	Stainless steel	0.0063	Stainless steel	0.0071	

Notes:

1) The flow rate was in the laminar region.
2) The flow rate was in the laminar region.
3) The impeller speed was 125 rpm, just sufficient to keep the crystals thoroughly suspended in the solution and without noticeable attrition.

Table 7.8 Data for the rate of growth/scale formation in the continuous crystallisation and scaling experiments, in the presence of 0, 10 and 20 ppm of SIPX at 25^{0}C

Admixtures	Growth rate in pipes, kg/m^2 hour				Growth rate in crystalliser [3], kg/m^2 hour
	Low flow rate, 0.4 cm/second [1]		High flow rate, 1.3 cm/second [2]		
SIPX = 0 ppm	PVC	0.0289	PVC	0.0249	0.0389
	Brass	0.0257	Brass	0.0203	
	Copper	0.0222	Copper	0.0271	
	Stainless steel	0.0267	Stainless steel	0.0202	
SIPX = 10 ppm	PVC	0.0045	PVC	0.0089	0.0109
	Brass	0.0017	Brass	0.0032	
	Copper	0.0012	Copper	0.0028	
	Stainless steel	0.0017	Stainless steel	0.0019	
SIPX = 20 ppm	PVC	0.00185	PVC	0.0130	0.0062
	Brass	0.00055	Brass	0.0035	
	Copper	0.00030	Copper	0.0032	
	Stainless steel	0.0090	Stainless steel	0.0006	

Notes:

1) The flow rate was in the laminar region.
2) The flow rate was in the laminar region.
3) The impeller speed was 125 rpm, just sufficient to keep the crystals thoroughly suspended in the solution and without noticeable attrition.

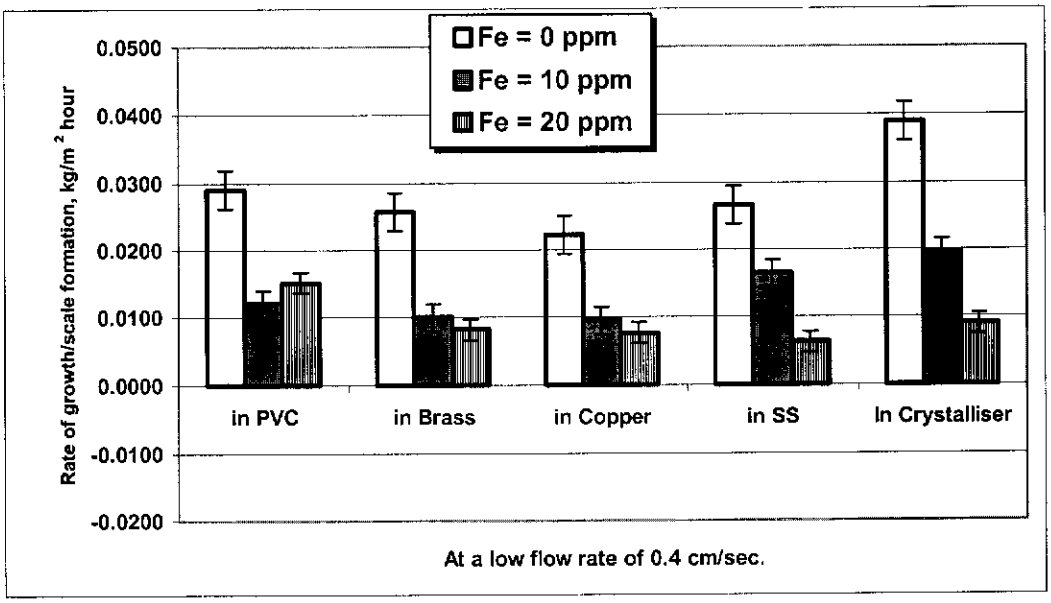

Figure 7.21 **Comparison between gypsum scale formation on the inner surfaces of different type of pipes and gypsum growth rate in crystalliser, showing the effect of Fe^{3+}**

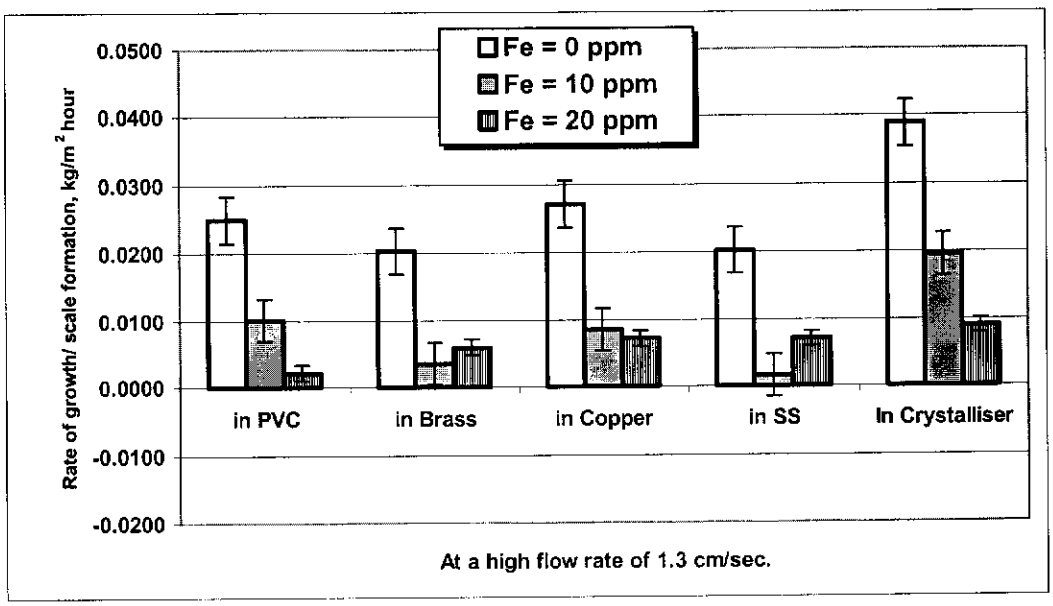

Figure 7.22 **Comparison between gypsum scale formation on the inner surfaces of different type of pipes and gypsum growth rate in crystalliser, showing the effect of Fe^{3+}**

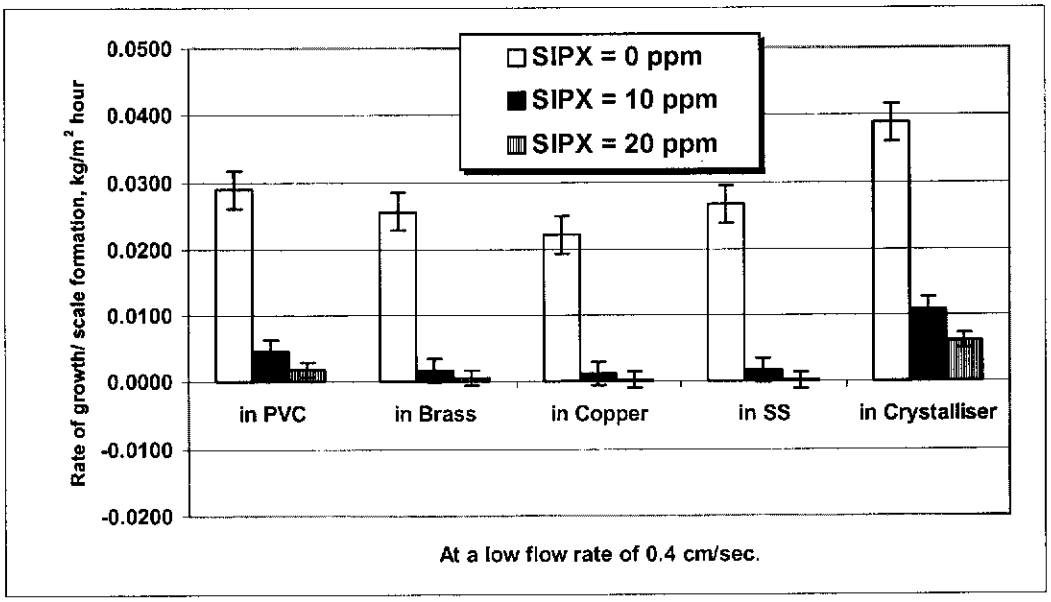

Figure 7.23 **Comparison between gypsum scale formation on the inner surfaces of different type of pipes and gypsum growth rate in crystalliser, showing the effect of SIPX**

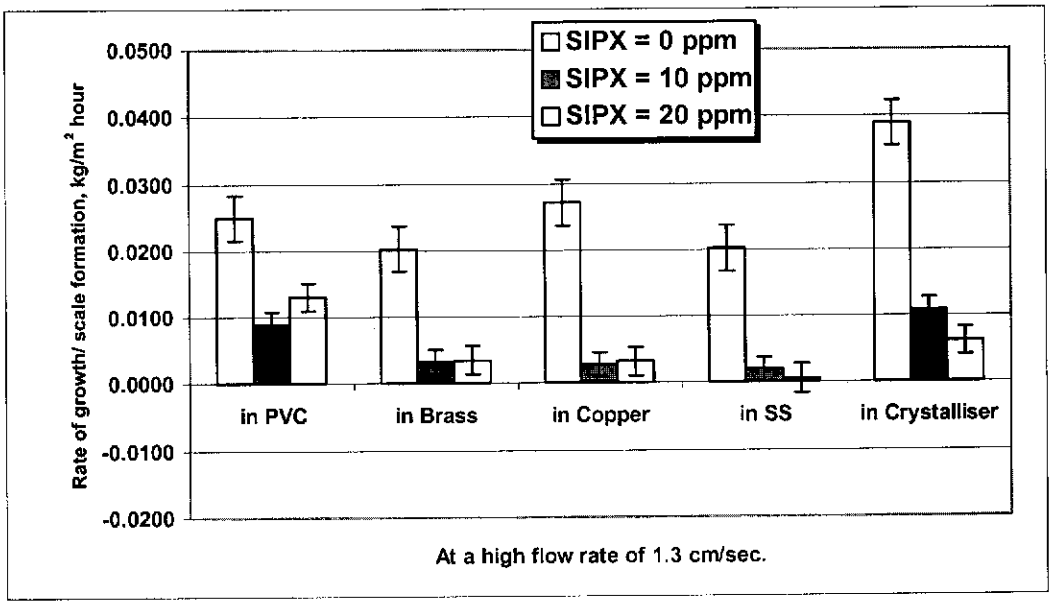

Figure 7.24 **Comparison between gypsum scale formation on the inner surfaces of different type of pipes and gypsum growth rate in crystalliser, showing the effect of SIPX**

Figures 7.21 to **7.24** display the rate of growth of scale formation on the inner walls of the pipe, as affected by the admixtures selected, as a function of the flow rate of the scaling solution. The mass growth rate of gypsum in the continuous crystalliser is included in all the graphs for comparison.

As can be seen, in the absence of any admixture (Fe = 0 ppm or SIPX = 0 ppm), the rate of growth of crystals in the crystalliser is consistently higher than the scale formation in the scaling system, regardless of the flow velocity of the scaling solution.

It could be postulated that the activation energy required for the formation of scale on the surface of the pipe walls is higher than that required for growth on the gypsum seeds in the crystalliser.

Figure 7.21 to **7.24** also indicate that SIPX is more effective in standing the scale formation than Fe^{3+}. This could be a result of the difference in molecular structure between SIPX and Fe^{3+}. The C chain structure in SIPX might have sealed as "blanket" on "fence" to cover the surface of the nuclei attached to the pipe surface. Hence, more nuclei are prevented from receiving the scale forming units which results in less growth.

This present study shows that the effect of flow rate on scale formation for the two admixtures tested appears to be conflicting. For Fe^{3+}, higher fluid flow rate resulted in less mass of scale. On the contrary, in the presence of SIPX, an increase in flow rate is reorganised by a corresponding increase in the mass of scale deposited.

Clearly, in the case of Fe^{3+}, the stronger shear stress exerted on the scale deposit by the fluid flowing at a higher flow rate, is sufficient to result in the partial removal of it.

The phenomenon observed for SIPX, especially for PVC, in which higher flow rate results in more scale deposit, could be due to the charge in the diffusional resistance (Andritsos and Karabelas 1992; Andritsos and Karabelas 1995; Andritsos *et al.* 1996).

Fluid moving at a high flow rate exerts stronger shear stress on the vicious diffusion layer covering the scale, which results in the thinning of the thickness of the layer. As the layer becomes thinner, the diffusion rate of the scale building components towards the wall of the pipes becomes faster. In other words, more ions or molecules or particulate matter are transported to the pipe walls. Hence, more scale may deposit. Clearly, the two effects of fluid flow rate are opposing, and different effects appear to be dominant in the two cases of Fe^{3+} and SIPX admixtures. This suggests that different scale morphologies and/or adhesion strengths participate in the observed phenomena.

Overall, as can be seen from **Figures 7.21** to **7.24**, the attempt to compare the rate of growth of gypsum crystals grown in a crystalliser with the rate of gypsum scale formation on the surface of pipe walls appears to be quantitatively reasonable.

Summary

This chapter presents experimental results and discussion of gypsum scale formation experiments in a once-through pipe flow system. The aim of the experiments was to investigate the behaviour of gypsum scale formation in flowing solutions and in the presence of admixtures, since the knowledge of such behaviour can be a useful tool for scale prevention measures especially when gypsum is one of the major components of the scale. The experimental parameters selected in this investigation are as follows:

1. *Concentrations: 2,000; 3,000; 4,000; 5,000 and 6,000 ppm of Ca^{2+}*
2. *Flow rates of scale forming solutions: 0.4 and 1.3 cm/second*
3. *Types of admixtures: Fe^{3+} and sodium isopropyl xanthate (= SIPX)*
4. *Concentrations of admixtures for each type: 0.00 to 20.00 ppm, tested at 5 ppm intervals.*

The scale forming solutions were prepared from calcium chloride dihydrate and sodium sulphate crystals, respectively, i.e. the same as the solutions used in the batch and continuous crystallisation studies discussed previously (in ***Chapters 4, 5 and 6).***

The experimental rig consists of two major parts: two 8-litre vessels, which separately contain the scale forming solutions, and the tubular test section which serves as the scale surface. The conditions of the experiment were maintained so that effects caused by foreign particle deposition and removal of scale by shear forces were minimised.

The effect of the chosen experimental parameters on the behaviour of gypsum scale formation was measured as the mass of the gypsum scale deposited on the inner wall of the pipes. The mass of gypsum scale was found:

1. *To increase with concentration (in the range 2,000 to 6,000 ppm of Ca^{2+}), and that the correlation between the mass of the deposited scale per unit tube area and the concentration can be presented by quadratic functions.*

2. *To decrease with increasing concentration of Fe^{3+} and SIPX.*

3. *To be little affected by the flow rate (in the range 0.4 - 1.3 cm per second).*

4. *To be highest on PVC, followed by brass and copper, and lowest on stainless steel.*

The scale samples obtained, were also analysed morphologically using SEM, and the analysis resulted in the following:

1. *The scale deposits were observed to be characteristic of gypsum crystals.*

2. *The scale deposits grow through crystal agglomeration mechanism, and it was observed that the direction of the fluid flow might effect the orientation of the growth.*

3. *In the presence of admixtures, the surface of the scale was rougher compared to that of pure gypsum scale. This surface roughness was assumed to be due to the effect of admixtures used and that of the flowing solutions. In addition, using SEM images alone, it was not possible to distinguish the effect of either the combined or the individual admixtures on the scale surface morphology.*

4. *Longer scale experiment time resulted in denser scale deposits. This was assumed to be the result of continuous formation and growth of the scale, since the flowing scaling solutions had relatively constant supersaturation.*

The findings of the gypsum scaling experiments discussed in this chapter are reviewed in comparison with that of the continuous crystallisation experiments, which has been presented previously in ***Chapter 6****. Overall, the attempt to compare the rate of growth of gypsum crystals grown in a crystalliser with that of gypsum scale formation on the surface of pipe walls appears to be quantitatively reasonable.*

References

1. Al-Sabbagh, A., Widua, J., and Offermann, H. (1996). "Influence of different admixtures on the crystallization of calcium sulfate crystals." *Chemical Engineering Communications*, 154, 133-145.
2. Amjad, Z. (1985). "Applications of Antiscalants to Control Calcium Sulfate Scaling in Reverse Osmosis Systems." *Desalination*, 54, 263-276.

3. Amjad, Z. (1988). "Calcium Sulfate Dihydrate (Gypsum) Scale Formation on Heat Exchanger Surfaces: The Influence of Scale Inhibitors." *Journal of Colloid and Interface Science*, 123(2), 523-536.
4. Andritsos, N., and Karabelas, A. J. (1991). "Crystallization and Deposit Formation of Lead Sulfide from Aqueous Solutions. I. Deposition Rates." *Journal of Colloid and Interface Science*, 145(1), 158-169.
5. Andritsos, N., and Karabelas, A. J. (1992). "Crystallization fouling: the effect of flow velocity on the deposition rate." *Eurotherm Seminar no.23*, Grenoble, France, 29-38.
6. Bansal, B., and Muller-Steinhagen, H. (1993). "Crystallization Fouling in Plate Heat Exchangers." *Journal of Heat Transfer*, 115(August), 584-591.
7. Bansal, B., Muller-Steinhagen, H., and Chen, X. D. (1997). "Effect of Suspended Particles on Crystallization Fouling in Plate Heat Exchangers." *Journal of Heat Transfer*, 119(August), 568-574.
8. Bansal, B., Muller-Steinhagen, H., and Chen, X. D. (2000). "Performance of plate heat exchangers during calcium sulphate fouling - investigation with an in-line filter." *Chemical Engineering and Processing*, 39, 507-519.
9. Bosbach, D., Junta-Rosso, J. L., Becker, U., and Hochella, M. F. (1996). "Gypsum growth in the presence of background electrolytes studied by Scanning Force Microscopy." *Geochimica et Cosmochimica Acta*, 60(17), 3295-3304.
10. Bott, T. R. (1988). "General Fouling Problems." Fouling Science and Technology, L. F. Melo, T. R. Bott, and C. A. Bernardo, eds., Kluwer Academics, Dordrecht, Boston, London, 3-14.
11. Bott, T. R. (1995). *Fouling of Heat Exchangers*, Elsevier, Amsterdam, New York.
12. Chamra, L. M., and Webb, R. L. (1994). "Modelling Liquid-side Particulate Fouling in Enhanced Tubes." *International Journal of Heat and Mass Transfer*, 37(4), 571-579.
13. Cousins, B. G., and McPhail, R. S. (1996). "Improvement of recoveries from copper bearing and copper-activated mineral ores using FLEX 31." *Minerals Engineering*, 9(5), 509-518.
14. Davey, R. J. (1982). "The Role of Additives in Precipitation Processes." Industrial Crystallization 81, S. J. Jancic and E. J. de Jong, eds., North-Holland Publishing, Amsterdam, 123-135.

15. Dirksen, J. A., and Ring, T. A. (1991). "Fundamentals of Crystallization: Kinetic effects on particle size distribution and morphology." *Chemical Engineering Science*, 46(10), 2389-2427.
16. El Dahan, H. A., and Hegazy, H. S. (2000). "Gypsum scale control by phosphate ester." *Desalination*, 127, 111-118.
17. Epstein, N. (1983). "Thinking about Heat Transfer Fouling: A 5 x 5 Matrix." *Heat Transfer Engineering*, 4(1), 43-56.
18. Gill, J. S. (1999). "A novel inhibitor for scale control in water desalination." *Desalination*, 124, 43-50.
19. Hasson, D. (1981). "Precipitation Fouling." Fouling of Heat Transfer Equipment, E. F. C. Somerscales and J. G. Knudsen, eds., Hemisphere, New York, 527-568.
20. Hasson, D., Bramson, D., Limoni-Relis, B., and Semiat, R. (1996). "Influence of the flow system on the inhibitory action of $CaCO_3$ scale prevention additives." *Desalination*, 108, 67-79.
21. Hasson, D., and Zahavi, J. (1970). "Mechanism of Calcium Sulfate Deposition on Heat-Transfer Surfaces." *Industrial and Engineering Chemistry Fundamentals*, 9(1), 1-10.
22. He, S., Oddo, J. E., and Tomson, M. B. (1994). "The Seeded Growth of Calcium Sulfate Dihydrate Crystals in NaCl Solutions up to 6 m and 90° C." *Journal of Colloid and Interface Science*, 163, 372-378.
23. Headley, G., Muryanto, S., and Ang, H. M. (2001). "Effects of Additives on the Crystallisation Rate of Calcium Sulphate Dihydrate." *6th World Congress of Chemical Engineering,*, Melbourne, Australia, 2312.
24. Klepetsanis, P. G., Dalas, E., Koutsoukos, P.G. (1999). "Role of Temperature in the Spontaneous Precipitation of Calcium Sulfate Dihydrate." *Langmuir*, 15, 1534-1540.
25. Klepetsanis, P. G., and Koutsoukos, P. G. (1998). "Kinetics of calcium sulfate formation in aqueous media: effect of organophosphorus compounds." *Journal of Crystal Growth*, 193, 156-163.
26. Krause, S. (1993). "Fouling of heat transfer surfaces by crystallization and sedimentation." *International Chemical Engineering*, 33(3), 355-401.

27. Li, W., and Webb, R. L. (2000). "Fouling in enhanced tubes using cooling tower water. Part II: combined particulate and precipitation fouling." *International Journal of Heat and Mass Transfer*, 43, 3579-3588.
28. Linnikov, O. D. (1999). "Investigation of the initial period of sulphate scale formation. Part 1. Kinetics and mechanism of calcium sulphate surface nucleation at its crystallization on a heat-exchange surface." *Desalination*, 122, 1-14.
29. Liu, S. T., and Nancollas, G. H. (1973). "The Crystal Growth of Calcium Sulfate Dihydrate in the Presence of Additives." *Journal of Colloid and Interface Science*, 44(3), 422-429.
30. McCartney, E. R., and Alexander, A. E. (1958). "The effect of additives upon the process of crystallisation. I.Crystallisation of calcium sulfate." *Journal of Colloid Science*, 13, 383-396.
31. Middis, J., Paul, S. T., and Muller-Steinhagen, H. (1998). "Reduction of Heat Transfer Fouling by the Addition of Wood Pulp Fibers." *Heat Transfer Engineering*, 19(2), 36-44.
32. Mori, H., Nakamura, M., and Toyama, S. (1996). "Crystallization Fouling of Calcium Sulfate Dihydrate on Heat Transfer Surfaces." *Journal of Chemical Engineering of Japan*, 29(1), 166-173.
33. Myerson, A. S. (1993). *Handbook of Industrial Crystallization*, Butterworth-Heinemann, Boston, London, etc.
34. Nancollas, G. H., and Reddy, M. M. (1974). "The Kinetics of Crystallization of Scale-Forming Minerals." *Society of Petroleum Engineers Journal*, 117-126.
35. Northwood, T. (1995). "Scale reduction in Process Water Pipes at Murchison Zinc," Final Year Undergraduate Project, Curtin University of Technology, Perth, Western Australia.
36. Ogden, M. (2002). "(Personal communication)." School of Applied Chemistry, Curtin University of Technology, Perth, Australia.
37. Oner, M., Dogan, O., Oner, G. (1998). "The influence of electrolytes architecture on calcium sulfate dihydrate growth retardation." *Journal of Crystal Growth*, 186, 427-437.
38. Pritchard, A. M. (1988). "The Economics of Fouling." Fouling Science and Technology, L. F. Melo, T. R. Bott, and C. A. Bernardo, eds., Kluwer Academic, Dordrecht, Boston, London, 31-45.

39. Rinaudo, C., Franchini-Angela, M., and Boistelle, R. (1988). "Gypsum crystallisation from cadmium-poisoned solutions." *Journal of Crystal Growth*, 89, 257-266.
40. Sudmalis, M., and Sheikholeslami, R. (2000). "Coprecipitation of $CaCO_3$ and $CaSO_4$." *The Canadian Journal of Chemical Engineering*, 78, 21-31.
41. Verma, B. C., Atwal, B. S., Singh, J., and Sharma, D. K. (1999). "A photometric titration method for the determination of xanthate-based flotation agents." *Indian Journal of Chemistry*, 38A, 91-92.
42. Weijnen, M. P. C., and van Rosmalen, G. M. (1984). "The Role of Additives and Impurities in the Crystallization of Gypsum." *Industrial Crystallization 84*, 61-66.
43. Weijnen, M. P. C., and van Rosmalen, G. M. (1985). "The influence of various polyelectrolytes on the precipitation of gypsum." *Desalination*, 54, 239-261.

CHAPTER 8 CONCLUSIONS AND RECOMMENDATIONS

8.1. Overall Conclusions

8.1.1. Batch crystallisation

1. In the presence of the admixtures used (= SIPX and isopropyl thionocarbamate), the crystallisation rate decreases. For both admixtures increasing the concentrations will result in further decrease and the isopropyl-thionocarbamate has higher inhibition effect than SIPX. Suppression or inhibition of the crystallisation rate may be caused by the adsorption of the admixture molecules onto the crystal surfaces.

2. Both the pure system and the system with isopropyl thionocarbamate as admixtures produced high activation energies (**Ea > 40kJ/mol**), which is indicative of surface reaction process. Hence, it was concluded that the use of the second order kinetics model for the batch crystallisation of pure gypsum and that in the presence of thionocarbamate carried out in this study, is warranted.

3. In the presence of SIPX, the growth of the gypsum crystals was inhibited, but the activation energy decreased. Initially, this finding is contrary to expectation. However, it can be rationalised that this discrepancy was probably caused by the nature of both the crystal surfaces and the crystallising solutions, and that different types of reaction mechanisms might simultaneously occur, resulting in lower activation energy.

4. The seeded batch crystallisation experiments carried out in the present study showed that the added seed crystals start growing immediately upon addition into the supersaturated solution, i.e. there is no induction time in this particular system. The reduction of calcium ion concentrations takes place rapidly in the first 5 to 10 minutes of the experimental run.

5. Addition of the selected admixtures either individually or in combination, significantly affects the crystallisation kinetics, that is, reduces the rate of crystallisation.

6. The value of the reaction order was taken as **2**, and was proved to be reasonably satisfactory.

7. An increase in temperature (25^0C to 45^0C) enhances the rate constant, but at higher temperatures the effect of the two admixtures on the rate constant is almost the same.

8. Isopropyl thionocarbamate seems to have a higher inhibition effect on gypsum growth than SIPX. This might be caused by the difference in molecular structure between the two admixtures. The longer C chains of isopropyl thionocarbamate compared to that of SIPX might have acted like a fence to more effectively block the growth sites and thus stopping the propagating steps.

9. Overall, the activation energy values calculated from this seeded batch crystallisation are: **60.00 ± 3.00**, **57.39 ± 2.87**, and **37.65 ± 1.88 kJ/mol**, for pure gypsum, and solutions containing isopropyl thionocarbamate, and SIPX, respectively. The value for SIPX may not be very accurate due to the poor correlation (coefficient of determination, $\mathbf{R^2 = 0.84}$) of the data obtained.

10. The low activation energy in the presence of SIPX might be the result of the following factors.

First, defects or imperfection of the crystal surfaces (which could be induced by the SIPX) might cause easier incorporation of the growth units resulting in lower activation energy. Second, the system with SIPX in this study does not satisfactorily obey the second order rate mechanism. Third, two or more competing reactions might occur resulting in inconsistency of the activation energy value. Finally, there may be competition between diffusion and surface integration processes, since the experiment was performed with an intermediate supersaturation level, which is a supersaturation ratio of **3.3**.

11. The SEM micrographs of the crystals obtained at the end of experimental run either with pure system or in the presence of either SIPX or isopropyl thionocarbamate show that the crystals are covered with small and fluffy masses. These small masses could be crystallites or nuclei, indicating that the seeds were possibly able to grow. Alternatively, they were unable to grow, therefore resulting in surface nucleation. However, these SEM micrographs would not likely be able to distinguish the effect of the individual admixtures used, on crystallisation kinetics.

12. Measurement of the admixture adsorption on the crystal surface shows that higher admixture concentrations (within the range used in the experiments) resulted in more admixtures being adsorbed on the crystal surface. These results show good agreement with similar studies on gypsum conducted earlier by other researchers (Nestler 1968).

8.1.2. Continuous (MSMPR) crystallisation

1. The seeded continuous crystallisation experimental runs reasonably demonstrated the conditions of an ideal MSMPR, in terms of:
   1) Solution concentration
   2) Slurry density
   3) Crystal size distribution (CSD).

2. The rate of de-supersaturation is extremely fast for the first 15 minutes of the experimental run, but changes to gradual decrease from that time onwards. The de-supersaturation curve indicates that steady state condition with respect to the solution concentration is achieved after the seventh residence time. Similar to the batch crystallisation (see section **8.1.1** no.**4**), in this continuous crystallisation the induction period did not occur.

3. The low initial seed concentration of 0.800 gram per litre of solution was adequate to facilitate the growth and thus the crystallisation experiment.

4. Most of the de-supersaturation curves for the system with admixtures show a lower decrease than was the case for the pure gypsum. This clearly indicates that the admixtures were capable of inhibiting the formation of gypsum, and hence confirms the expected aim of this continuous crystallisation study that the selected admixtures would be able to affect the crystallisation kinetics. In addition, the de-supersaturation curves show that a steady state condition for all admixture concentrations tested could be achieved in around the 8^{th} residence time.

5. It was found that the growth of gypsum is clearly retarded by the presence of the admixtures studied, whether they are present individually or in combination. In all cases, the growth rates were calculated based on the experimental data for CSD at steady state, i.e. at equilibrium supersaturation of around 700 ppm of Ca^{2+}; while the initial supersaturation was 1,200 ppm of Ca^{2+}.

6. The growth rate is highly dependent on crystal size, and increases with increasing crystal size. It indicates, therefore, that either size dependent growth or growth rate dispersion phenomena (or both) were operative. In this study, it was assumed that agglomeration phenomenon did not occur between crystals with sizes **>10 μm** (see **section 6.3.2** in **Chapter 6**). Future studies may verify this assumption, since the deviation of the population density versus size plot on semi-log scale could be partly the result of agglomeration effects.

7. Both in the absence and in the presence of admixtures, the linear crystal growth rates were generally higher for the higher crystallisation temperature of 40^0C compared to 25^0C.

8. For a fixed level of supersaturation, there is a correlation between the growth rate, **G**, and the crystal size, **L**, as well as the admixture concentration, **C**, and that the correlation was proposed to take the following general equation:

$$G = k\, L^{\alpha}\, (1+C)^{\beta}$$

where,

G	= linear growth rate, (micron)/(hour)
L	= characteristic linear crystal size, micron
C	= concentration of admixtures, ppm
k, α and β	= dimensionless constants.

9. For both crystallisation temperatures of 25^0C and 40^0C, and within the range of the admixture concentrations used, the correlation is best presented in three separate categories: (a) low admixture concentrations, (b) high admixture concentrations, and (c) combined low and high admixture concentrations.

10. The correlation function is best applied to the low concentration category (= category (a)), followed by the combined low and high admixture concentration category (= category (c)). The high concentration category (= category (b)) shows the poorest correlation.

11. For both temperature levels of 25 and 40^0C used in this continuous crystallisation study, the dimensionless constant, **k**, in the growth rate correlation, is less than unity, which indicates that the growth rate, **G**, is a weak function of crystal size, **L**, and the admixture concentration, **(1+C)**.

12. Most of the **α** values are greater than unity, which suggest that the growth of the crystals depends significantly on crystal size.

13. The exponent values, **β**, fluctuate significantly, which might indicate that the influence of admixtures on the growth of crystals is highly dependent on particular solvent-solute systems. In addition, fluctuation could have been caused by some interaction between the admixtures used. At the present time, however, the nature or existence of such interaction can only be speculated.

14. Two mechanisms of growth inhibition are proposed. Firstly, probably the more feasible mechanism, is that the admixtures were adsorbed and subsequently occupied active growth sites, such as kinks and steps, rendering the sites unavailable for attachment of solutes or growth units to the crystal surface (Klepetsanis and Koutsoukos 1998). This inhibition mechanism is invariably called "blocking" or "poisoning" of the active growth sites, which results in slowing down or stopping the crystal growth rate. The second mechanism is that the admixtures were adsorbed onto and covered the crystal surface, forming a physical barrier to ward off transfer of growth units from solution to the crystal surface, resulting in growth rate reduction.

15. The nucleation rate was calculated using the technique proposed by Jancic and Grootscholten (Jancic and Grootscholten 1984). The technique involves a linear regression through the five smallest data points from CSD analysis and the nucleation rate was calculated using the slope and intercept of the regression line. Hence, the nucleation rates calculated and presented in this study are the "effective" nucleation rate, which means that the nuclei were not formed at one single size.

16. In each case, the nucleation rate increases with increasing admixture concentrations. It was assumed that the admixtures could have lowered the surface tensions in the crystallising solution, and consequently the contact angles of solute clusters with the crystal surfaces in the solution could have been decreased. As the contact angle decreases, the critical free energy of formation of solute clusters also decreases, causing an increase in nuclei formation.

17. The variation of the nucleation rate values could be attributed to the following proposal. There could be a competition between adsorption of the admixtures and of the nucleating substance onto the nucleus surface (Sohnel and Garside 1992). In the absence of admixture no competition exists, and consequently a large quantity of nucleating substance is adsorbed onto the nucleus surface, resulting in subsequent growth of nuclei. Depending on the ratio of the quantity of the admixtures and the nucleating substance (or growth units) in the solution, the competition may result in decreasing or increasing the nucleation rates.

18. In either the absence or the presence of individual admixture of Fe^{3+}, Zn^{2+}, and SIPX, the nucleation rate calculation resulted in the following details:

    - For pure gypsum, higher crystallisation temperature results in higher nucleation rate.

    - In the presence of Fe^{3+} as admixture, higher crystallisation temperature results in higher nucleation rate, increasing with an increase in admixture concentrations.

    - In the presence of either Zn^{2+} or SIPX as admixture, higher crystallisation temperature results in lower nucleation rate, decreasing with an increase in admixture concentrations.

    - In the presence of combined admixtures, of either Fe^{3+} + SIPX, Zn^{2+} + SIPX, or Fe^{3+}+ Zn^{2+} + SIPX, higher crystallisation temperature results in lower nucleation rates for lower concentrations, but higher nucleation rates for higher concentrations.

8.1.3. Gypsum scale formation

1. The effect of the chosen experimental parameters on the behaviour of gypsum scale formation was investigated through measuring the mass of the gypsum scale deposited on the inner wall of the pipes. The mass of gypsum scale was found:

    - To increase with supersaturation (in the range 2,000 to 6,000 ppm of Ca^{2+}), and that the correlation between the mass of the deposited scale and the supersaturation can be represented by quadratic functions.

    - To decrease with increasing concentration of Fe^{3+} and SIPX. This indicates that both $Fe^{3+}$and SIPX are able to inhibit the growth rate of gypsum

- To be little affected by the flow rate (in the range 0.4 - 1.3 cm per second).

- To be highest on PVC, followed by brass and copper, and lowest on stainless steel.

- To be higher for higher flow rate for PVC, in the presence of concentrations of SIPX tested. The reason for this phenomenon (no.5) is not yet understood. One possible explanation could be that the higher flow rate might have caused the interface layer between the scale and the flowing solution to become thinner. Hence, more growth units were able to reach the pipe wall resulting in more scale being deposited. Undoubtedly, for this reasoning to be true, it should apply to all the pipe materials tested. Therefore, it would be likely that the scale structure and the adhesion strength between the scale and the substrate could have been participated in this phenomenon. Possibly, the adhesion between the scale and PVC is strong enough for the higher flow rate not to dislodge the scale on PVC, whereas it does dislodge it on other materials.

2. The effect of piping materials on scaling is not well understood. The rate of scale formation is roughly linear with time, but seems to vary with different materials: PVC is the highest and stainless steel the lowest. The effect might be more related to the roughness of the surface. In can be assumed that the rougher the surface the stronger the attachment, resulting in more scale deposited. In addition, substrate hydrophobicity/hydrophilicity and surface energy might affect the gypsum scale particle-substrate interactions and adhesion to the substrate.

3. The induction time for the pure solution of gypsum at 2,000 ppm of Ca^{2+} was about 2 hours. In the presence of admixtures (SIPX was selected) the induction time was significantly prolonged.

4. The scale samples obtained were also analysed morphologically using SEM, and the analysis resulted in the following:

   - The scale deposits were observed to be characteristic of gypsum crystals.

   - The scale deposits appear to grow through a crystal agglomeration mechanism.

   - In the presence of admixtures, the surface of the scale was rougher compared to that of pure gypsum scale. This surface roughness was assumed to be due to the combined effects of the admixtures used and the flowing solutions. Using SEM images alone, it was not possible to distinguish the effect of either the combined or the individual admixtures on the scale surface morphology.

   - Longer scale experiment times resulted in denser scale deposits. This was assumed to be the result of continuous formation and growth of the scale, since the flowing scaling solutions had a relatively constant supersaturation.

8.2. Recommendations

8.2.1. Batch crystallisation

1. It is suggested to investigate other types of flotation agents normally used in mineral processing industries. In addition, the crystallisation solution may be taken directly from plant site.

2. It is suggested to investigate the topography and morphology of the crystals before and after the experiment.

3. The amount of the admixtures adsorbed onto the crystal surface could be investigated further, to allow the calculation of the concentration of the admixtures adsorbed per area of crystal surface.

4. Based on SEM micrographs, the gypsum crystalline products were covered with small fluffy masses. This suggests that noticeable secondary nucleation occurred. Future studies should carry out a population balance analysis to confirm whether or not the total number of crystals increased (for secondary nucleation) or decreased (if significant agglomeration simultaneously occurred).

5. Due to the lower activation energies estimated, it is recommended to conduct batch crystallisation experiments involving the variation in agitation rate to verify if volume diffusion limitation played a significant role.

8.2.2. Continuous crystallisation

1. CSD measurements may be carried out using different techniques, which is not based on laser diffraction. In this way, the validity of the measurement of the CSD carried out in the present study could be compared.

2. It is suggested to conduct an experiment where crystallisers in series are used. This is to investigate the achievement of steady state.

3. It is suggested to apply this continuous crystallisation method to other systems, such as the continuous crystallisation of $CaCO_3$ or $BaSO_4$, both of which are among the main components of scale.

4. In this study, it was assumed that agglomeration phenomenon did not occur between crystals with sizes **>10 µm** (see **section 6.3.2** in **Chapter 6**). Future studies may verify this assumption, since the deviation of the population density versus size plot on semi-log scale could be partly the result of agglomeration effects.

5. It is suggested that to establish the crystallo-chemical identity of the seeds as pure gypsum (with no hemihydrate impurities), a powder XRD analysis could be more useful.

8.2.3. Gypsum scale formation

1. Since determination of the mass deposited on the pipe walls can be difficult if very small amount of scale is formed, it is suggested to conduct a similar study where in situ monitoring of the scale mass is applied. This could be accomplished using a Quartz Crystal Microbalance (QCM).

2. Future studies could utilise high resolution SEM back-scattered image analysis of the four different substrates before and after scale formation to further investigate the pivotal role played by the substrate surface structure or the surface chemistry. Accurate description of the sizes of asperities on the surfaces which might provide anchor sites for critical-size nuclei could be obtain by using atomic force microscopy (= AFM).

3. Looking at the greater fouling behaviour at PVC substrate surface, in comparison with brass, copper and stainless steel; it is suggested that future studies may look into that phenomenon by considering the following properties:

    - Substrate hydrophobicity/hydrophilicity
    - Substrate surface energy
    - Passivation effects due to possible metal oxide film formation.

4. A similar study with fluid rates in the turbulent region could be carried out. Such studies could be useful to determine the sticking probability values (as discussed in the **Literature Review – Part 2**). Such a study could also help explain the conflicting results obtained in the present work, i.e. the different effect of flow rate on the mass of the scale deposited under the influence of Fe^{3+} and SIPX, respectively.

5. A similar experiment but with a temperature gradient (= a non isothermal experiment) is suggested, the result of which could be compared to scaling problems in other areas, such as for the heat transfer equipment.

6. It is suggested to carry out similar studies where the first nuclei attached on the inner wall of the pipes can be observed. This would necessitate the use of flush

mounted small coupons inserted into the test section, which can be removed at any time without disrupting the experiment. To preserve the hydrodynamics of the system, similar coupons should replace the removed coupons immediately. This type of experiment will allow visual monitoring of the scale build up, which is the progress of the scale formation.

7. The possibility of particulate adsorption, viz. adsorption of fine crystals nucleated in the bulk liquor at the pipe walls needs to be looked at in future studies. Such studies could be useful since the process of scale formation may involve both precipitation and particulate fouling.

8. Different type of piping materials (other than those used in the present study) may be tested, so that a wider range of knowledge between piping materials and mass of scale deposited can be gained. Consequently, such studies could be applicable to different industrial settings.

References

1. Andritsos, N., and Karabelas, A. J. (1992). "Crystallization fouling: the effect of flow velocity on the deposition rate." *Eurotherm Seminar no.23*, Grenoble, France, 29-38.
2. Andritsos, N., and Karabelas, A. J. (1995). "Calcium carbonate scaling in isothermal flow systems." *IDA World Congress on Desalination and Water Science*, Abu Dhabi, UAE.
3. Andritsos, N., Kontopoulou, M., Karabelas, A. J., and Koutsoukos, P. G. (1996). "Calcium carbonate deposit formation under isothermal conditions." *Canadian Journal of Chemical Engineering*, 74(December), 911-919.
4. Chan, V. A. (1997). "The Role of Impurities in the Continuous Precipitation of Aluminium Hydroxide," PhD thesis, Curtin University of Technology, Perth, Western Australia.
5. Jancic, S. J., and Grootscholten, P. A. M. (1984). *Industrial Crystallization*, Delft University Press and Reidel Publishing, Dordrecht, Boston, Lancaster.

6. Klepetsanis, P. G., and Koutsoukos, P. G. (1998). "Kinetics of calcium sulfate formation in aqueous media: effect of organophosphorus compounds." *Journal of Crystal Growth*, 193, 156-163.
7. Nestler, C. H. (1968). "Adsorption and Electrophoretic Studies of Poly (Acrylic Acid) on Calcium Sulfate." *Journal of Colloid and Interface Science*, 26, 10-18.
8. Sohnel, O., and Garside, J. (1992). *Precipitation. Basic Principles and Industrial Applications*, Butterworth Heinemann, Oxford, etc.

CHAPTER 9 CHAPTER SUMMARIES

9.1. Summary of Chapter 2: the Literature Review – Part 1: Crystallisation of Gypsum in the Presence of Admixtures

The literature review reveals the following features.

Crystallisation is a complex process. The properties of a crystallising solution are the decisive factors to influence the end product because the formation of a crystal embryo or nucleation and its subsequent growth into a crystalline product are heavily dependent on such properties, particularly the level of supersaturation. The existing knowledge about nucleation is extensive and the origin of nucleation is two fold. Firstly, it originates from the dissolved solutes, which is described as true nucleation. Secondly, the origin can be the materials already undergoing the process of crystallisation but have not yet achieved their final form, hence the name is apparent nucleation. The growth of crystals is significantly influenced by the characteristics of the crystal surfaces.

It is almost impossible for a crystallisation process to proceed in a condition which is free from the presence of admixtures and that a minute amount of admixtures could have a very significant effect on crystallisation and its subsequent handling of the crystal products. The literature review also reveals that as yet there is no general conclusion or a systematic theory regarding the effect of admixtures on crystallisation. The effect is unique to crystallisation system under consideration.

Gypsum crystallisation is generally regarded as an unwanted phenomenon, due to its contribution to the scale formation, which is one of the persistent problems in many industries. Studies on the crystallisation of gypsum in the presence of admixtures are extensive, but general conclusions are yet widely varied.

MSMPR studies are regarded as a highly reliable and established technique to extract crystallisation kinetics such as nucleation and growth rates. However, in an MSMPR crystalliser, the crystallisation time is not an independent variable, so that it must first be selected. The selection was carried out by examining the performance of a batch crystalliser.

Crystals are produced with varying sizes so that distribution of crystals with regard to their size, which is known as Crystal Size Distribution (CSD) is one of the main characterisation of crystals. The quality of a crystalline product is frequently related to its CSD.

CSD data of a crystallisation process is needed in order to extract the crystallisation kinetics, mainly, nucleation and growth rates, and this extraction is made possible through the utilisation of a Population Balance Equation (PBE). A Population Balance Equation is essentially a discreet accounting of crystal product, and therefore it can also be applied to any particulate processes. While the PBE was originally developed for the unseeded MSMPR, it was later developed to cover the seeded MSMPR.

Calculation of nucleation and growth rates can be carried out in a number of ways depending on the characteristics of the CSD.

Crystallisation of gypsum is closely related to scale formation due to the following reasons. First, gypsum is crystalline matter formed through a crystallisation process. Second, one of the main components of the scale was found to be gypsum. In the process of crystallisation, admixture effects cannot be overlooked since most crystallisation takes place in the presence of admixtures. A unified theory on the effects of admixtures on crystallisation of gypsum is as yet unavailable. Hence, it was felt that the crystallisation of gypsum in the presence of admixtures carried out in this study would add to the existing knowledge. The study was carried out in a continuous (MSMPR) crystalliser using three different admixtures: Fe^{3+} and Zn^{2+} (in their sulphate salts), and sodium isopropyl xanthate (SIPX) and their combinations. There were several reasons for the choice of the crystallising system. First, crystallisation process in an MSMPR can achieve steady state, hence extraction of experimental crystallisation kinetics under state condition is possible. Second, the Department of Chemical Engineering at Curtin University of Technology has been and is actively involved in assisting mineral processing industry to alleviate the burden of scaling problem with particular emphasis on gypsum scaling. Third, the flotation water in one of the mineral processing plants with which the Department of Chemical Engineering associates, was found to contain a significant amount of

metallic ions: Fe^{3+} and Zn^{2+}. Fourth, sodium isopropyl xanthate (SIPX) is one of the flotation agents used in the above-mentioned mineral processing plant.

*The next chapter (**Literature Review – Part 2: Gypsum Scaling: Effect of Admixtures on Gypsum Crystallisation Kinetics**) discusses further the scaling of gypsum, as one of the main components of scale formation in industry. Some researchers studied the crystallisation of gypsum with specific aim to reveal the phenomenon of scaling and thereafter to control its formation. Their studies were either carried out using a laboratory beaker test, crystallisers or piping system.*

9.2. Summary of Chapter 3: the Literature Review – Part 2: Gypsum Scaling: Effects of Admixtures on Gypsum Crystallisation Kinetics

Some conclusions may be drawn from this review.

Classification of fouling in industrial applications into six major categories is well defined from which methods of prevention and control of fouling may be developed.

The current understanding of the five steps of fouling is reasonably clear. Each step is affected by chemical and physical characteristics as well as hydrodynamics of the system.

Admixtures of various types have been used to prevent and control scale formation, which leads to a clearer understanding of the scaling problems. The effect of admixtures on scale formation appears to be system-specific.

Scale deposit may likely consist of more than one main constituent, of which the process is labelled composite or mixed scaling. In such cases, the nature of the deposit is affected by the presence of co-precipitate and the resulting effect was not additive. Most studies on composite scaling have been carried out for a mixture of $CaSO_4$ and $CaCO_3$.

Research on scale prevention has ultimately led to prediction and modelling of scaling rates. Attempts to model combined scaling mechanism have been carried out but the results seem to be specific to the system under consideration. On the other

hand, modelling based on one single operative mechanism has proved to be applicable in some systems such as calcium carbonate and gypsum scaling.

In mineral processing industries, unreliable data with respect to the chemical properties of the process water may be encountered, therefore a comprehensive and accurate documentation of such properties is required before any scale prevention measures are attempted.

The problem of scaling, including that of gypsum, is complex, depending not only on the nature of the scaling solutions and the presence of admixtures but also on external factors such as the hydrodynamics of the system. For these reasons, a unified theory, which will explain every aspect of scaling phenomenon satisfactorily, is very unlikely to be obtained. Instead, addressing the problem of scaling may have to greatly rely on specific empirical data. However, it should be sufficient to show that much gypsum scaling research has been found to be helpful in elucidating the scaling problem encountered by many industries.

9.3. Summary of Chapter 4: Batch Crystallisation of Gypsum in the Presence of Admixtures

This chapter discusses the study of a seeded batch crystallisation of gypsum in the presence of admixtures. Two types of admixtures were selected: sodium isopropyl xanthate (= SIPX) and isopropyl thionocarbamate. The content of this chapter is summarised as follows:

1. *The experimental design used in this batch crystallisation study is exploratory using the so called "One-factor-at-a-time" method, since past research in this area had used various operating conditions. The variables investigated are the type and concentration of admixtures, seed slurry density and crystallisation run times. This was necessary due to the lack of comparable studies on which to base crystalliser settings.*

2. *The experimental set up and conditions for this seeded batch crystallisation are as follows:*

- *Volume of crystalliser* : *2 litres*
- *Agitation speed* : *125 rpm*
- *Crystallisation temperature* : *25, 35 and 45^{0}C*
- *Crystallisation run times* : *up to 90 minutes.*
- *Method of analysis* : *atomic absorption spectrometry.*
- *Crystallising solutions* : *$CaCl_2$ and Na_2SO_4 solutions.*

3. *The crystallisation process was followed by measuring the desupersaturation of Ca^{2+} versus crystallisation time. Subsequently, the result of the crystallisation process was presented as the reaction rate constant, **k**, using a second order reaction rate constant.*

4. *In the presence of the admixtures used, the crystallisation rate decreases. For both admixtures increasing the concentrations will result in further decrease and the isopropyl thionocarbamate has higher inhibition effect than SIPX. The suppression or inhibition of the crystallisation may be caused by adsorption of the admixture molecules onto the crystal surfaces.*

5. *The Arrhenius parameter, **A**, of the crystallisation reaction was calculated to determine the activation energy and subsequently the mechanism of the crystallisation process.*

6. *In this study, both the pure system and the system with isopropyl thionocarbamate as admixtures, produced high activation energies (Ea > 40 kJ/mol), which is indicative of a surface reaction process. Hence, it was concluded that the use of the second order kinetics model for the batch crystallisation of pure gypsum and that in the presence of isopropyl thionocarbamate carried out in this study, is warranted.*

7. *In the presence of SIPX, the growth of the gypsum crystals was inhibited, but the activation energy decreased. Clearly, this finding is contrary to the theory. It was assumed that this discrepancy was probably caused by the nature of both the crystal surfaces and the crystallising solutions, and that different types of reaction mechanisms might occur at the same time resulting in lower activation energy.*

8. *Measurement of the admixture adsorption on the crystal surface shows that higher admixture concentrations (within the range used in this batch crystallisation experiments) resulted in more admixtures being adsorbed on the crystal surface. Moreover, the measurement results show good agreement with similar studies on gypsum conducted previously .*

The next chapter discusses the materials and methods for crystallisation of gypsum carried out in a continuous (= MSMPR) mode. Some parameters used in the continuous crystallisation experiments were taken from the results of the batch crystallisation discussed in the present chapter. These parameters include mean residence times, agitation speed and type of some admixtures used.

9.4. Summary of Chapter 5: Materials and Methods for Continuous Crystallisation

This chapter discusses the materials and methods used in the continuous (MSMPR) crystallisation experiments carried out in this study. The discussion covers six main topics as follows:

1. *Calculation of mass balance to determine the quantities of raw materials needed and crystal product produced, as well as the stream flow rates and their compositions.*

2. *Description of the laboratory continuous (MSMPR) crystalliser including an explanation of its major components: the seed tank, the liquor tank and the crystalliser, as well as considerations of the capability of the peristaltic pumps used.*

3. *Preparation of crystallising solutions: $CaCl_2$ and Na_2SO_4 solutions, respectively, and gypsum crystals as seeds. This section includes calculations of the quantities of solutions and seeds needed for the entire experiments. The preparation of gypsum crystals as seeds covers the seed making, the uniformity of the crystals produced and the characterisation with respect to morphology and chemical purity.*

4. *Description of how the continuous crystallisation run was performed, how to ensure achievement of steady state and hence representative MSMPR crystallisation operation.*

5. *Sampling and measurements to extract the experimental data, which includes data for solution concentration with respect to Ca^{2+}, slurry density, and crystal size distribution (= CSD). This section covers an explanation of the accuracy of the Calcium Selective Electrode used for the solution concentration measurement, the iso-kinetic sampling for the slurry density and the CSD.*

6. *Discussion on the selection of an appropriate experimental design to be adopted in this study by examining three factors: (1) type of admixtures, (2) concentration of admixtures, (3) crystallisation temperatures. Three different admixtures were used: Fe^{3+}, Zn^{2+}, and sodium isopropyl xanthate (SIPX). Concentrations of admixtures were varied as follows: (1) 1 ppm, (2) 10 ppm, (3) 50 ppm. Two levels of crystallisation temperatures were selected: (1) 25^0C, (2) 40^0C. A balanced incomplete randomised block design was considered appropriate for this continuous crystallisation study.*

9.5. Summary of Chapter 6: Continuous Crystallisation of Gypsum in the Presence of Admixtures

In this chapter, experimental results and discussion of a seeded continuous crystallisation (MSMPR) of calcium sulphate dihydrate ($CaSO_4.2H_2O$) or gypsum in the presence of admixtures are presented. The aim of the experiment was to investigate the behaviour of gypsum crystallisation in the presence of admixtures,

since the knowledge of such behaviour can be a useful tool for scale prevention measures especially when gypsum is one of the major components of the scale.

The following features were noted in this study:

1. *The seeded continuous crystallisation experimental runs reasonably satisfied the conditions of an ideal MSMPR, in terms of:*

- *Solution concentration in the crystalliser*
- *Slurry or magma density in the crystalliser*
- *Crystal size distribution (CSD) in the crystalliser.*

2. *The experimental data of crystal size distribution (CSD) were suitable to be used to calculate the linear crystal growth rate, G, and the nucleation rate, B^0.*

3. *The linear crystal growth rate, G, was found to be dependent on size, increases with increasing crystal size.*

4. *Both in the pure and in the presence of admixtures, the linear crystal growth rates were generally higher for the higher crystallisation temperature of 40^0C rather than for that at 25^0C.*

5. *In general, the admixtures tested were found to be able to inhibit the crystal growth rates, but to enhance the nucleation rates.*

6. *In almost all cases, in the concentration range studied, higher admixture concentrations induce high retardation on the growth rates. On the contrary, the higher the admixture concentrations, the higher the nucleation rates.*

7. *Since the growth rate was found to be dependent on crystal size, a correlation between these two parameters and the admixture concentrations was attempted. It was proved that for each crystallisation temperature: 25^0C and 40^0C, the correlation function can be presented as the following general equation:*

$$G = k\,L^{\alpha}\,(1+C)^{\beta}$$

where:

G = *linear growth rate, micron/hour*

k, α *and* β = *dimensionless constants*

L = *crystal size, microns*

C = *concentration of the admixtures used, ppm*

8. *For both crystallisation temperatures of 25^0C and 40^0C, and within the range of the admixture concentrations used, the correlation is best presented in three separate categories: (a) low admixture concentrations, (b) high admixture concentrations, and (c) combined low and high admixture concentrations.*

9. *The correlation function is best applied to the low concentration category (= category (a)), followed by the combined low and high admixture concentration category (= category (c)). The high concentration category (= category (b)) shows the poorest correlation.*

10. *For both crystallisation temperatures of 25^0C and 40^0C, the correlation function reveals the following:*

- *The growth rate, **G**, is significantly dependent on crystal size, **L**.*
- *The growth rate, **G**, is a weak function of admixture concentrations, **C**.*

11. *The mechanism of crystal growth inhibition was assumed to be that of adsorption of admixtures onto the active growth sites, which resulted in decreasing or stopping the growth.*

12. *Since the growth rate was found to be size-dependent, the McCabe's ΔL law (see **section 2.8** in **Chapter 2**) for the calculation of crystal growth and nucleation is violated. Hence, the nucleation rates calculated and presented in this study are the "effective" nucleation rate, which means that the nuclei were not formed at one single size.*

13. *In either the absence or the presence of individual admixture of Fe^{3+}, Zn^{2+}, and SIPX, the nucleation rate calculation resulted in the following details:*

- *For pure gypsum, higher crystallisation temperature results in higher nucleation rate.*
- *In the presence of Fe^{3+} as admixture, higher crystallisation temperature results in higher nucleation rate, increasing with an increase in admixture concentrations.*
- *In the presence of either Zn^{2+} or SIPX as admixture, higher crystallisation temperature results in lower nucleation rate, decreasing with an increase in admixture concentrations.*

14. *In the presence of combined admixtures, of either Fe^{3+} + SIPX, Zn^{2+} + SIPX, or Fe^{3+}+ Zn^{2+} + SIPX, higher crystallisation temperature results in lower nucleation rates for lower concentrations, but higher nucleation rates for higher concentrations.*

15. *Both the nucleation and growth rate values of gypsum found in this study, either in the absence or in the presence of admixtures, generally agree with those in the literature.*

*The next chapter (**Chapter 7**) deals with a once-through pipe flow experiment, where factors influencing gypsum scale formation on the inner surfaces of pipes under isothermal conditions are discussed. These factors include concentration levels, type of admixtures, fluid flow rate and type of piping materials. The intention is that the outcomes of this pipe flow experiment will be compared with those of the present chapter. Hence, a better understanding might be gained of the behaviour of gypsum crystallisation occurring in vessels and in flowing solutions.*

9.6. Summary of Chapter 7: Gypsum Scaling in Isothermal Flow System

This chapter presents experimental results and discussion of gypsum scale formation experiments in a once-through pipe flow system. The aim of the experiments was to investigate the behaviour of gypsum scale formation in flowing solutions and in the presence of admixtures, since the knowledge of such behaviour can be a useful tool for scale prevention measures especially when gypsum is one of the major components of the scale. The experimental parameters selected in this investigation are as follows:

1. *Concentration levels: 2,000; 3,000; 4,000; 5,000 and 6,000 ppm of* Ca^{2+}
2. *Flow rates of scale forming solutions: 0.4 and 1.3 cm/second*
3. *Types of admixtures:* Fe^{3+} *and sodium isopropyl xanthate (= SIPX).*
4. *Concentrations of admixtures for each type: 0.00 to 20.00 ppm, tested at 5 ppm intervals.*

The scale forming solutions were prepared from calcium chloride dihydrate and sodium sulphate crystals, respectively, i.e. the same as the solutions used in the batch and continuous crystallisation studies discussed previously (in Chapters 4, 5 and 6).

The experimental rig consists of two major parts: two 8-litre vessels, which separately contain the scale forming solutions, and the tubular test section which serves as the scale surface. The conditions of the experiment were maintained so that effects caused by foreign particle deposition and removal of scale by shear forces were minimised.

The effect of the chosen experimental parameters on the behaviour of gypsum scale formation was measured as the mass of the gypsum scale deposited on the inner wall of the pipes. The mass of gypsum scale was found:

1. *To increase with concentration (in the range 2,000 to 6,000 ppm of* Ca^{2+}*), and that the correlation between the mass of the deposited scale and the concentration can be presented by quadratic functions.*

2. *To decrease with increasing concentration of Fe^{3+} and SIPX.*

3. *To be little affected by the flow rate (in the range 0.4 - 1.3 cm per second)..*

4. *To be highest on PVC, followed by brass and copper, and lowest on stainless steel.*

The scale samples obtained, were also analysed morphologically using SEM, and the analysis resulted in the following:

1. *The scale deposits were observed to be characteristics of gypsum crystals.*

2. *The scale deposits grow through crystal agglomeration mechanism, and the growth was seen to orient to the direction of the fluid flow.*

3. *In the presence of admixtures, the surface of the scale was rougher compared to that of pure gypsum scale. This surface roughness was assumed to be due to the effect of admixtures used and that of the flowing solutions. In addition, using SEM images alone, it was not possible to distinguish the effect of either the combined or the individual admixtures on the scale surface morphology.*

4. *Longer scale experiment time resulted in denser scale deposits. This was assumed to be the result of continuous formation and growth of the scale, since the flowing scaling solutions had relatively constant supersaturation.*

The findings of the gypsum scaling experiments discussed in this chapter are reviewed in comparison with that of the continuous crystallisation experiments, which has been presented previously in ***Chapter 6****. Overall, the attempt to compare the rate of growth of gypsum crystals grown in a crystalliser with that of gypsum scale formation on the surface of pipe walls appears to be quantitatively reasonable.*

Nomenclature

S.I. (Système International d'Unités) units are used in this work.

Greek notation

α, β : dimensionless constants, (Eq. 6. 4)

γ : interfacial free energy, (Eqs. 2.2; 2.15)

λ : a parameter, denoting the number of times any particular treatment appears in the experiment (sec. 5.8.6.1)

Δ : incremental quantity

δ : thickness of the diffusion (unstirred) layer, μm, (Eq. 2.15)

δ : thickness of the diffusion or boundary layer, cm, (Eq. 4.2)

ΔC : concentration driving force, (Eq 3.1)

ΔG : Gibbs free energy, (sec. 2.2.2.2.a)

$\Delta G_{homogeneous}$: Gibbs free energy for homogeneous nucleation, (Eq 2.6)

$\Delta G_{heterogeneous}$: Gibbs free energy for heterogeneous nucleation, (Eq 2.6)

ΔG_{volume} : free energy change for the phase transformation per unit volume, (Eq. 2.1)

$\Delta G_{surface}$: free energy change for the formation of nucleus surface, (Eq. 2.2)

$\Delta\mu$: chemical potential difference per solute molecule, (Eq. 2.1)

σ : supersaturation

: = S-1, where S = c/c*, dimensionless, (Eq. 2.14)

σ_i : specific energy of the **i**-th plane, erg/particle (Eq. 2.7)

σ_a^2 : variance of the differences of two treatment values in a complete block design, (Eq. 5.6)

σ_k^2 : variance of the differences of two treatment values in an incomplete block design, (Eq. 5.6)

$\rho_{solution}$: density of gypsum-water solution = 1.0 g/cm^3, (Eq.5.1)

ρ_{gypsum} : density of gypsum, g/cm^3, (Eq. 5.2)

ρ_{water} : density of water, g/cm^3,(Eq. 5.2)

ρ_i : density of crystal, mg/ml, (Eq. 6.1)

Σ : Summation.

$\mu_{solution}$: viscosity of gypsum-water solution, g/cm.sec, (Eq. 5.1)

θ : wetting angle, (Eq. 2.6)

τ : mean residence time, (Eq 2.18)

Ω : volume of the growth particle in the crystal, ml, (Eq. 2.15)

: chemical properties of the solution, (Eq. 3.3).

General notation

A : a temperature dependent constant, (Eq. 2.14)

: Arrhenius parameter (Eq. 4.8a)

: area for scale growth

: a dimensionless constant, (Eq.3.4)

: surface area of crystal, (Eqs. 2.17; 2.18 and 4.5)

: cross section area of tube, cm^2 , (section 5.4.4.1)

: notation for treatment in experimental design, (Table 5.10)

a : surface area of a solute entity in the cluster surface, (sec. 2.2.2.1.a)

: mean distance between growth units in crystal, μm, (Eq. 2.15)

: number of treatments in an experiments, (section 5.8.6.1)

B : a temperature dependent constant, (Eq. 2.14)

: a factor, dimensionless, (Eq. 2.15)

: a dimensionless constant, (Eq. 3.4)

: notation for treatment in experimental design, (Table 5.10)

B^0 : nucleation rate, (Eq. 6.7)

b : number of blocks in an experiment, (sec. 5.8.6.1)

C : solution concentration, (Eq. 2.21)

: concentration of growth units in the bulk of the solution, g/cm^3, (Eq. 4.2)

: concentration of admixtures used, ppm

: notation for treatment in experimental design, (Table 5.10)

Ca : lattice ion concentration in the crystallising solution, (in this present work = concentration of Ca^{2+})

Ca_0 : lattice ion concentration of the solution at time **t = 0**, ppm, (Eq. 4.7)

Ca_t : lattice ion concentration of the solution at time **t**, ppm, (Eq. 4.6)

Ca_{eq} : lattice ion concentration of the solution at equilibrium, ppm, (Eq. 4.6)

C_b : concentration in the bulk of the solution, (sec. 2.2.3.2.f)

C_{eq} : concentration of growth units in the bulk of the solution at equilibrium conditions, g/cm^3, (Eq. 4.4)

C_i : concentration of growth units in the crystal/solution interface, g/cm^3, (Eq. 4.2)

C_{Fe} : concentration of Fe^{3+}, ppm, (Table 6.19)

C_s : saturation concentration at particular ionic strength, (Eq. 2.21)

CSD : crystal size distribution

C_{SIPX} : concentration of SIPX, ppm, (Table 6.19)

C_{Zn} : concentration of Zn^{2+}, ppm, (Table 6.19)

c : a factor, (Eq. 2.15)

c_{eq} : equilibrium concentration of a saturated solution, (particles)/(ml), (Eq. 2.15)

dC/dx : concentration gradient of growth units in the diffusion layer, $g/(cm^3)(cm)$, (Eq. 2.8)

- dC/dt : growth rate, (Eq. 2.21)

- dCa/dt : rate of lattice ion concentration decrease due to crystallisation, ppm/min

dm/dt : rate of scale deposition, (Eq. 3.3)

dm/dt : rate of mass increase, g/sec, (Eq. 4.1)

dW/dt : differential rate of growth, g/hour, (Eq. 2.35)

D : coefficient of surface self-diffusion, cm^2/sec, (Eqs. 2.13; 2.15; 2.17)

: diffusion coefficient, cm^2/sec, (Eq. 4.1)

: notation for treatment in experimental design, (Table 5.10)

d : average distance between adsorbed species in the boundary layer, μm, (Eq. 2.13)

E : activation energy, (Eq. 3.2)

: notation for treatment, (Table 5.10)

e : elementary charge, (Eqs. 2.8 to 2.11)

E_a : activation energy, kJ/mol, (Eqs. 3.2 & 4.8)

E_f : efficiency factor, (Eq. 5.6)

E : amount of energy liberated, erg/particle, (Eqs. 2.8 to 2.11)

f_i : shape factor, (Eq.2.36)

F : notation for treatment in experimental design, (Table 5.10)

g : gravitational constant, (g)(cm)/(dyne)(sec^2) (Eq. 5.2)

G : rate of crystal growth, (Eq. 2.18)

: linear growth rate, micron/hour, (Eq. 6.4)

: growth rate of nuclei, micron/hour, (Eq. 6.7)

HE : heat exchanger, (sec. 3.5.3)

h : step height, micron, (Eq. 2.18)

h_i : distance of the i-th plane from the centre of the crystal, micron (Eq. 2.7)

I : rate of formation of a critical nucleus per unit surface area per unit time, (Eq. 2.18)

ID : internal diameter, (sec. 5.4.1)

J : a constant factor, (Eq. 2.19)

k : Boltzmann constant, (erg)/(particle)(^{0}K), (Eq. 2.15)

: crystallisation rate constant, (Eq. 2.26)

: growth rate constant, (Eq. 2.21)

: crystallisation rate constant, $ppm^{-1}\ min^{-1}$, (Eq. 4.6)

: reaction rate constant, (Eq. 4.8a)

: number of treatments in one block, (sec. 5.8.6.1)

: a dimensionless constant, (Eq. 6.4)

k_a : surface shape factor, (Eq. 2.2)

k_d : D/δ, (Eq. 4.3)

k_i : proportionality or rate constant, dimensionless, (Eq. 4.4)

k_r : reaction rate constant, (Eq. 3.1)

k_v : volumetric shape factor, dimensionless, (Eq. 2.1) & (in Chapter 6)

K : a dimensionless constant, (Eq. 3.3)

: a dimensionless constant, (Eq. 3.3)

K_G : a dimensionless constant, (Eq. 2.26)

L : size of cluster, (Eq. 2.1)

: crystal size, cm or micron, (in Chapter 5 and Chapter 6)

L_i : characteristic linear crystal size for the ***i*-th** size range, micron, (Eq. 6.1)

l : linear rate of face growth perpendicular to crystal surface, (μm)/(sec), (Eq. 2.15)

ΔL : difference in length between two adjacent crystal size ranges, micron, (Eq. 6.1)

m_d : crystallisation rate or scale deposition rate, (Eq. 3.1)

mV : electrode potential, (Table 5.7)

M : total mass of crystals, mg, (Eq. 6.1)

MSMPR : mixed suspension mixed product removal, (in Chapter 5)

n : step density,

= number of steps per unit length in a given area, (Eq. 2.16)

: growth order or reaction rate order, (Eq. 2.21) or (Eq. 3.1)

: population density of crystals, (Eq. 2.30)

n_i : total number of crystals in the *i*-th size range, (Eq. 6.1)

n^0 : nuclei density, (no. of nuclei/(micron)(litre)), (Eq. 6.7)

n(L) : population density of crystals of size L, (Eq. 2.22)

N : reaction order, dimensionless, (Eq. 2.27)

: total number of particles in the phase layer, (Eq. 2.12)

: total number of observations, (in Chapter 5)

N_{actual} : total number of observations, (in Chapter 5)

N_C : number of crystals, dimensionless

N_{nf} : total number of liquid species in the phase layer, (Eq. 2.12)

N_{ns} : total number of solid species in the phase layer, (Eq. 2.12)

N_{Re} : particle Reynolds number, dimensionless, (Eq. 5.1)

P : sticking probability, dimensionless, (Eq. 3.3)

PBE : Population Balance Equation, (sec. 5.3)

PGA : polyglutamic acid, (sec. 2.4)

PSD : Particle size distribution, (sec. 2.6)

PVS : polyvinyl sulfonate, (sec. 2.4)

Q_i : volumetric flow rate, (Eq. 2.32)

q : step flux,

= number of steps passing a given point per unit time, (Eq. 2.16)

r : radius of cluster, (Eq. 2.3)

: number of observations or replication, (in Chapter 5)

: ion distance, (Eqs. 2.8 to 2.11)

R : crystal growth rate, g/sec, (Eq. 2.14)

: universal gas constant, 8.31 (kJ)/(mol)(^{0}K), (Eq. 4.8)

R^2 : correlation coefficient, (Eq. 4.2)

R_f : heat resistance of fouling layer, (sec. 3.5.3)

R_G : mass growth rate, g/m^2 hour, (Eq.2.35)

s : number of cooperating spirals on crystal surface, (Eq. 2.15)

: a function of the number of nuclei sites, (Eq. 3.1)

s^2 : sample variance, (Eq. 5.4)

S : supersaturation level, (Eq. 2.5)

: number of growing sites, (Eq. 2.21)

SEM : scanning electron microscopy

SIPX : sodium isopropyl xanthate, (in Chapter 4)

T : absolute temperature, ^0K, (Eq. 4.8a)

T_s : absolute temperature of the surface where scale develops, ^0K, (Eq. 4.7)

t : mean time period, (Eq. 2.13)

: crystallisation time, minutes, (Eq. 2. 28)

u : step velocity, (Eq. 2.16)

u_t : terminal velocity of crystal in the slurry inside the tubing, cm/sec, (Eq. 5.2)

v_0 : superficial velocity, cm/sec, (Eq.5.1)

v* : rate of spread of nucleus, (Eq. 2.20)

Vm : molecular volume, (Eq. 2.1)

V : crystalliser volume, (Eq. 2.30)

VTE : vertical tube evaporator, (sec. 3.5.3)

w_{net} : net or overall deposition rate, (Eq. 3.4)

w_{part} : deposition rate due to particulate fouling, (Eq. 3.4)

w_{precip} : deposition rate due to precipitation fouling, (Eq. 3.4)

$w_{removal}$: removal rate, (Eq. 3.4)

X : sphere equivalent nuclei size, micron, (Eq. 6.6)

: Ca^{2+} concentration, ppm, (Table 7.2)

Y : log. number of nuclei density, (no. of nuclei/(micron)(litre)), (Eq.6.6)

: mass of scale, kg/m^2, (Table 7.2)

Subscripts

1,2	: input and output conditions, respectively, (Eq 2.30)
b	: quantity related to the bulk of the solution, (sec. 2.2.3.2.f)
c	: value at critical state, (Eq. 2.19)
d	: deposition
H	: "half-central" position of growth unit relative to crystal plane, (Eq. 2.8)
i	: quantity related to the interface, (sec. 2.2.3.2.f)
K	: position of growth unit at the edge of a completed plane, (Eq. 2.10)
P	: position of growth unit in the centre of a completed plane, (Eq. 2.11)
R	: position of growth unit in a corner of a completed plane, (Eq. 2.9)
r	: reaction
s	: value at the surface
net	: net or overall value
part	: particulate
precip	: precipitation
i	: value in crystal/solution interface
eq	: value at equilibriun
G	: growth
t	: value at time t
0	: value at time = 0
a	: value at activation
re	: Reynold number
solution	: value for gypsum-water solution
t	: terminal value
gypsum	: value for gypsum
water	: value for water
f	: value for factor
i	: value for the *i*th component
v	: volumetric
Fe	: value for Fe^{3+}
Zn	: value for Zn^{2+}
SIPX	: value for SIPX

Superscripts

*	: quantity related to critical state, (Eqs. 2.4 to 2.5)
	: quantity related to saturated condition, (sec. 2.2.3.2.f)
	: quantity related to nucleus, (Eq. 2.20)
g	: reaction order, (Eq. 4.5)
i	: an empirical exponent representing reaction order, dimensionless
‾	: indicating average amount, (Eq. 2.32)

Appendix A: Batch Crystallisation Experimental Data

Appendix A Batch Crystallisation Experimental Data

Table A – 1 Desupersaturation of Calcium ions versus crystallisation time in the batch crystallisation (see Figure 4.1 in Chapter 4)

Admixtures (g/L)	Crystallisation time, (minutes)	Ca^{2+} concentrations, (ppm)
No admixtures (blank #1)	0	1901
	5	1112
	10	1093
	15	1004
	20	995
	30	965
	40	957
	60	949
	90	940
No admixtures (blank #2)	0	1762
	5	1325
	10	1130
	15	1020
	20	988
	30	971
	40	965
	60	956
	90	954
0.20 SIPX	0	1956
	5	1260
	10	1109
	15	1040
	20	1026
	30	1003
	40	973
	60	965
	90	929

0.30 SIPX	0	1951
	5	1208
	10	1088
	15	1050
	20	1010
	30	919
	40	883
	60	844
	90	839
0.40 SIPX	0	1919
	5	1248
	10	1097
	15	1041
	20	963
	30	925
	40	892
	60	842
	90	833
0.07 isopropyl thionocarbamate	0	1875
	5	1253
	10	1093
	15	1033
	20	952
	30	952
	40	932
	60	836
	90	832
0.14 isopropyl thionocarbamate	0	1851
	5	1218
	10	1097
	15	1069
	20	1006
	30	943
	40	921
	60	918
	90	821

0.21 isopropyl thionocarbamate	0	1868
	5	1213
	10	1092
	15	1068
	20	1125
	30	992
	40	968
	60	933
	90	840

Table A-2 Typical data for the calculation of reaction rate constant (data for Figure 4.2 in Chapter 4)

Admixture	Crystallisation time, (minutes)	Ca^{2+} concentrations, (ppm)	F
None = blank #2	0	1762	0
	2	1325	0.001455
	5	1130	0.004429
	15	1020	0.013801
	20	988	0.028175
	30	971	0.055906
	40	965	0.079672
	60	956	0.102454
	90	954	-

Notes:

$$\frac{1}{Ca_t - Ca_{eq}} - \frac{1}{Ca_0 - Ca_{eq}} = kt$$

where,
kt = F
Ca_t = Ca^{2+} concentrations at time t,

Ca_{eq} = Ca^{2+} concentrations at t = 90 minutes,

Ca_0 = Ca^{2+} concentrations at t = 0 minutes.

Table A-3 **Typical data for the determination of activation energy, E_a (to be read in conjunction with Figure 4.5 in Chapter 4: 0.07 g/L isopropyl thinocarbamate at 25, 35 and 45°C respectively)**

Absolute temp. (T) (°K)	1/T	Time, (minutes)	Ca^{2+} (ppm)	F	ln k
298	0.0033	0	1875	0	- 8.2782
		5	1253	0.0014	
		10	1093	0.0029	
		15	1033	0.0040	
		20	952	0.0074	
		30	952	0.0074	
		40	932	0.0090	
		60	836	0.2847	
		90	832	-	
308	0.0032	0	1834	0	- 7.4253
		5	1053	0.0029	
		10	956	0.0052	
		15	886	0.0098	
		20	874	0.0115	
		30	836	0.0228	
		40	831	0.0260	
		60	824	0.0318	
		90	794	-	
318	0.0031	0	1880	0	- 6.8234
		5	1038	0.0031	
		10	915	0.0069	
		15	873	0.0106	
		20	854	0.0139	
		30	816	0.0329	
		40	804	0.0562	
		60	802	0.0615	
		90	787	-	

Appendix B: Mass Balance for the Continuous Crystallisation

Appendix B Mass Balance for the Continuous Crystallisation System

Stream Flow Rates and Feed Consumption

One residence time	= 15 minutes
	= 0.25 hour.
Crystalliser working volume	= 1.5 litres.
Slurry density in the crystalliser	= 0.800 g/L.
Seed tank working volume	= 4.0 litres.
Slurry density in the seed tank	= 4.00 g/L.
Liquor tank working volume	= 9.6 litres.
Slurry density in the liquor tank	= 0.00 g/L.

Crystalliser product flow rate	= 1.5 L/15 min
	= 1,500 mL/15 min
	= 100 mL/min.
Amount of seed crystals in crystalliser	= (0.800 g/L)(1.5 L)
	= 1.200 grams.
Flow rate for 0.800 g of seeds	= 1.200 g/15 min
	= 0.08 g/min.
Slurry density in seed tank	= 4.00 g/L
	= 4.00 g/1000 ml
	= 0.0040 g/ml.

Therefore, volumetric seed flow rate entering the crystalliser is:

= (0.08 g/min)(ml/0.0040 g)

= 20 ml/min.

Material balance equation:

Flow rate in = Flow rate out

Flow rate in	= seed tank flow rate + liquor tank flow rate.
Flow rate out	= crystalliser product rate
	= 100 ml/min.
Therefore, the flow rate in	= 100 ml/min.
Seed tank flow rate (calculated)	= 20 ml/min.
Therefore, liquor tank flow rate	= (100 - 20) ml/min
	= 80 ml/min.

The total consumption of the solution was calculated by assuming the number of residence times to achieve a steady state condition.

1. Assuming six residence times

Six residence time	= 6 x 15 minutes
	= 90 minutes.
Seed slurry consumption	= (90 min)(20 ml/min)
	= 1,800 ml
	= 1.8 litres.
Liquor consumption	= (90 min)(80 ml/min)
	= 7,200 ml
	= 7.2 litres.

2. Assuming eight residence times

Eight residence time	= 8 x 15 minutes
	= 120 minutes.
Seed slurry consumption	= 120 min x 20 ml/min
	= 2,400 ml
	= 2.4 litres.
Liquor consumption	= (120 min)(80 ml/min)
	= 9,600 ml
	= 9.6 litres.

Concentration level

In Crystalliser	= 1,200 ppm.
In Seed Tank	= 611 ppm.
In Liquor Tank	= to be determined from the calculation of mass balance on Ca^{2+} in the following section.

Mass balance on Ca^{2+}

Amount of Ca^{2+}:

1.In Crystalliser	= 100 mL (1,200 mg/1,000 ml)
	= 120.00 mg.
2.In Seed Tank	= 20 mL (611 mg/1,000 ml)
	= 12.22 mg.
3.In Liquor Tank	= (120.00-12.22) mg
	= 107.78 mg.

Assuming the level of concentration in the Liquor Tank = X.

Then, X	= 107.78 (1000/80)
	= 1347.25 mg /1,000 ml
	= 1,347.25 ppm
	≈ 1,350 ppm.

Preparation of the Crystallisation Solutions

Gypsum solutions with different concentration levels with respect to Ca^{2+} were prepared by mixing solutions of $CaCl_2.2H_2O$ and Na_2SO_4, respectively. The solution of $CaCl_2.2H_2O$ as Ca^{2+} provider was made by dissolving crystals of $CaCl_2.2H_2O$ in distilled water. Similarly, the solution of Na_2SO_4 as SO_4^{-2} provider was prepared in the same manner. The two solutions were separately kept and only mixed immediately prior to the experimental run. Extreme care was taken to keep the solutions free from dust, insoluble matter etc.

The following material balance shows a sample calculation for the preparation of the gypsum solutions.

Sample Calculation: basis 1 minute

Crystalliser seed density	= 0.800 g/L.
Residence time	= 15 minutes.
Crystalliser working volume	= 1,500 ml.
Product withdrawal	= crystalliser volume/residence time
	= 1,500 ml /15 minutes
	= 100 ml/min.

Amount of seeds in the crystalliser for the batch mode, that is at the start of the crystallisation run = seed density in crystalliser x crystalliser volume
= (0.800 g/litre)(1.5 litres)
= 1.200 g.

Flow rate of seeds in the crystalliser = amount of seeds in crystalliser/residence time
= 1.200 g/15 minutes
= 0.0800 g/min.

Seed slurry density in the seed tank = 4.00 g/L
= 0.004 g/ml.

Flow rate of slurry from the seed tank:
= seed flow rate in crystalliser/seed slurry density in seed tank
= (0.0800 g/min)/(0.0040 gr/ml)
= 20 ml/min.

Flow rate from liquor rate = product withdrawal – seed slurry flow rate
= (100 ml/min) – (20 ml/min)
= 80 ml/min.

Concentration level

In crystalliser = 1,200 ppm of Ca^{2+}.

In seed tank = 611 ppm of Ca^{2+} (=saturation level at $25^{O}C$).

In liquor tank = to be determined.

Calculation of the amount of Ca^{2+}

In Crystalliser = product flow rate x (1,200 mg/1,000 ml)
= (100 ml/min) x (1,200 mg/1,000 ml)
= 120.00 mg.

In Seed Tank = seed tank flow rate x (611 mg/1,000 ml)
= (20 ml/min) x (611 mg/1,000 ml)
= 12.220 mg.

In Liquor Tank = in Crystalliser – in Seed Tank
= (120 – 12.22) mg
= 107.780 mg.

Thus the concentration level in the liquor tank :
= amount of Ca^{2+} in liquor tank x (1,000/liquor tank flow rate)
= 107.78 mg x (1,000/80 ml)
= 1,347.25 ppm
≈ 1,348 ppm.

Calculation of the amount of $CaSO_4.2H_2O$ and Na_2SO_4 required for the crystallisation solutions

1. In Crystalliser

Working volume = 1,500 ml.

Concentration level = 1,200 ppm,
= 1,200 mg of Ca^{2+} per 1,000 ml solution.

For 1,500 ml, the amount Ca^{2+} of required = (1,500 ml/1,000 ml) x 1,200 mg

= 1,800 mg.

The solution for the crystalliser was prepared by dilution of the stock solutions of 0.5 M of $CaCl_2$ and 0.5 M of Na_2SO_4, respectively. Stock solution of 0.5 M $CaCl_2$ contains 0.5 mol of $CaCl_2$ per litre. Meanwhile, 0.5 mol of $CaCl_2$ equals 0.5 mol of Ca^{2+}.

0.5 mol of Ca^{2+} = 0.5 x 40 g = 20 g of Ca^{2+} per litre.

20 g of Ca^{2+} per litre = 20,000 mg of Ca^{2+} per 1,000 ml.

Therefore, for 1,800 mg of Ca^{2+} the stock solution which should be taken

= (1,800 mg/20,000 mg)(1,000 ml)

= 90 ml.

90 ml of 0.5 M $CaCl_2$ solution = (90 ml/1,000 ml) x 0.5 mol

= 0.045 mol.

Thus, the stock solution of 0.5 M of Na_2SO_4 which should be taken

= (0.045 mol/0.5 mol) x 1,000 ml

= 90 ml.

Procedure for the preparation of the crystalliser solution

Take 90 ml of 0.5 M $CaCl_2$ solution and dilute it with distilled water to make 500 ml. Take 90 ml of 0.5 M Na_2SO_4 solution and dilute it with distilled water to make 500 ml. Pour both solutions into the crystalliser while stirring, and then, add 500 ml of distilled water to make 1,500 ml of solution.

For the entire experiments, the stock solutions required were:

For 0.5 M $CaCl_2$ solution = 90 ml x 30

= 2,700 ml.

For 0.5 M Na_2SO_4 solution = 90 ml x 30

= 2,700 ml.

$CaCl_2.2H_2O$ required = (0.5 mol/1,000 ml) x 2,700 ml

= 1.35 mol

= (1.35 mol) x (MW of $CaCl_2.2H_2O$)

= (1.35 mol) x (147.02 g/mol)

= 198.477 g.

Na_2SO_4 required = (0.5 mol/1,000 ml) x 2,700 ml

= 1.35 mol

= (1.35 mol) x (MW of Na_2SO_4)

= (1.35 mol) x (142.04 g/mol)

= 191.754 g.

2. In Seed Tank

Working volume = 3.5 litres.

Volume of the solution prepared = 4.0 litres.

Concentration of Ca^{2+} = saturated solution

= 611 ppm

= 611 mg Ca^{2+} per 1,000 ml solution.

Therefore, the amount of Ca^{2+}required = (4,000 ml/1,000 ml) (611 mg)

= 2,444 mg.

The saturated solution was prepared from the stock solutions of 0.5 M $CaCl_2$ and 0.5 M Na_2SO_4 respectively. The stock solution of 0.5 M $CaCl_2$ contains 20,000 mg Ca^{2+} per litre of solution (see previous calculation for Crystalliser). Hence, the stock solution required for 2,444 mg Ca^{2+} = (2,444/20,000) (1,000 ml)

= 122.2 ml.

= (122.2/1,000)(0.5 mol)

= 0.0611 mol.

Since the saturated solution consists of equimolar amounts of $CaCl_2$ and Na_2SO_4 solutions, the stock solution of Na_2SO_4 required is also 0.0611 mol.

Procedure for the preparation of the seed tank solution

Place three litres of distilled water in the Seed Tank. Add 122.2 ml of 0.5 M $CaCl_2$ stock solution slowly with stirring. Next, add 122.2 ml of 0.5 M Na_2SO_4 stock

solution also slowly with stirring. Finally, add an additional of 755.6 ml of distilled water to obtain 4,000 ml of saturated solution of gypsum.

For the entire experiments, the stock solutions required were:

For 0.5 M $CaCl_2$ solution = 122.2 mlx30
= 3,666 ml.

For 0.5 M Na_2SO_4 solution = 122.2 mlx30
= 3,666 ml.

$CaCl_2.2H_2O$ required = (0.5 mol/1,000 ml) x 3,666 ml
= 1.833 mol
= (1.833 mol) x (MW of $CaCl_2. 2H_2O$)
= (1.833 mol) x (147.02 g/mol)
= 269.4877 g.

Na_2SO_4 required = (0.5 mol/1,000 ml) x 3,666 ml
= 1.833 mol
= (1.833mol) x (MW of Na_2SO_4)
= (1.833mol) x (142.04 gr/mol)
= 260.3593 g.

3. In Liquor Tank

Working volume = 9.6 litres
= 10,000 ml.

Concentration level = 1,350 ppm of Ca^{2+}.
= 1,350 mg Ca^{2+}per 1,000 ml of solution.

For 10,000 ml, the amount of Ca^{2+} required:
= (10,000/1,000)(1,350 mg
= 13,500 mg.

The supersaturated solution for the Liquor Tank was prepared by diluting the stock solutions. The stock solution of 0.5 M $CaCl_2$ contains 20,000 mgr of Ca^{2+} per 1,000 ml solution (see previous calculation for Crystalliser). Therefore, the stock solution required for 13,500 mg Ca^{2+} = (13,500/20,000) (1,000) ml
= 675 ml
= 0.3375 mol.

Likewise, the stock solution of 0.5 M Na_2SO_4 required

= 0.3375 mol

= (0.3375/0.5)(1,000)

= 675 ml.

Procedure for the preparation of the liquor tank solution

Place four litres of distilled water in the liquor tank. Add 675 ml of 0.5 M $CaCl_2$ stock solution slowly with stirring. Next, add four litres of distilled water followed by 675 ml of 0.5 M Na_2SO_4 stock solution, also slowly with stirring. Finally, add an additional of 650 ml distilled water to obtain 10,000 ml solution.

For the entire experiments, the stock solutions required were:

For 0.5 M $CaCl_2$ solution = 675 ml x 30

= 20,250 ml.

For 0.5 M Na_2SO_4 solution = 675 ml x 30

= 20,250 ml.

$CaCl_2.2H_2O$ required = (0.5 mol/1,000 ml) x 20,250 ml

= 10.125 mol

= (10.125 mol) x (MW of $CaCl_2.2H_2O$)

= (10.125 mol) x (147.02 gr/mol)

= 1488.5775 g.

Na_2SO_4 required = (0.5 mol/1,000 ml) x 20,250 ml

= 10.125 mol

= (10.125) x (MW of Na_2SO_4)

= (10.125) x (142.04 g/mol)

= 260.3593 g.

Calculation of the amount of seeds for one crystallisation run

1. In Crystalliser

Seed density = 0.800 g/L.

Amount of seeds for the batch mode = seed density x crystalliser volume

= (0.8 g/L) x (1.5 L)

= 1.200 g.

2. In Seed Tank

Seed density in seed tank = 4.00 g/L.

Seed tank flow rate = 20 ml/min.

One residence time in the crystalliser = 15 minutes.

Crystallisation time = 8 residence times

= 8 x 15 minutes

= 120 minutes.

Volume of the solution required = flow rate x crystallisation time

= (20 ml/min) x 120 minutes

= 2,400 ml

= 2.4 litres.

Volume at the bottom of seed tank which was unable to be pumped = 1 litre.

Therefore, volume to be prepared = (2.4 + 1) litres

= 3.4 litres ≈ 3.5 litres.

Amount of seeds required = volume x seed density

= (3.5 L) x (4g/L)

= 14.00 g.

Therefore, the total amount of seeds required for one crystallisation run

= (1.2 + 14) g

= 15.200 g.

The amount of crystal as seeds required for the entire experiments

= (15.2000) (30) g = 456.00 g.

Appendix C: Assessment of the Experimental Design Used in the Continuous Crystallisation Experiments

Appendix C Assessment of the Experimental Design Used in the Continuous Crystallisation Experiment

In any experimental work, especially when a large number of repetitive measurements have to be made, it is useful at some stage, to assess whether the selected experimental design will be able to yield data from which conclusive inferences may be drawn.

From the implementation of the balanced incomplete block design used in the continuous crystallisation experiments (the experimental design scheme is presented in **Table 5.11** in **Chapter 5**), the results for the 50 ppm admixture concentration level are shown in **Table C-1** as follows.

Table C-1 Growth rates of gypsum crystals at 50 ppm admixture concentrations

Types of Admixtures	Growth rates of crystals	References
Fe^{3+}	No growth at 25^{0}C for all crystal sizes	Table 6.5 Ch.6
SIPX	No growth at 25^{0}C for all crystal sizes	Table 6.7 Ch.6
	No growth at 40^{0}C for all crystal sizes	Table D-5 Appendix D
Fe^{3+} + SIPX (50 ppm each)	No growth at 40^{0}C for all crystal sizes	Table D-6 Appendix D
Fe^{3+} + Zn^{2+} + SIPX (50 ppm each)	No growth at 25^{0}C for all crystal sizes	Table 6.10 Ch.6

Table C-1 shows that, for both individual and combined admixtures, a concentration of 50 ppm resulted in complete growth retardation, and thus might be too high for the reduction of gypsum crystal growth investigated in this study. Hence, it is useful to

see, whether a lower concentration level would be sufficient for a complete growth retardation.

In the original experimental design (in **Table 5.11** in **Chapter 5**), the medium concentration level of admixtures was set at 10 ppm (the overall range used as shown in **Table 5.11**, is: 0, 1, 10, 50 ppm). Therefore, it was believed that a concentration level of 10 ppm could give a clue as at what concentration level the complete retardation of growth might occur.

Table C-2 Growth rates of gypsum crystals at 10 ppm admixture concentrations

Types of Admixtures	Growth rates of crystals	References
Fe^{3+}	At 25^{0}C: no growth for crystals with sizes ≤ 42.05 μm	Table 6.5 Ch.6
Zn^{2+}	At 40^{0}C: no growth for small crystals (≤ 24.60 μm)	Table D-4 Appendix D
SIPX	At 25^{0}C: no growth for crystals with sizes ≤ 42.05 μm	Table 6.7 Ch.6
	At 40^{0}C: no growth for very small crystals (≤ 18.30μm)	Table D-5 Appendix D
Fe^{3-} + SIPX (10 ppm each)	At 25^{0}C: no growth for crystals with sizes ≤ 48.55 μm	Table 6.8 Ch.6
	At 40^{0}C: no growth for very small crystals (≤ 18.30μm)	Table D-6 Appendix D
Zn^{2+} + SIPX (10 ppm each)	At 25^{0}C: no growth for crystals with sizes ≤ 59.15 μm	Table 6.9 Ch.6
Fe^{3+}+ Zn^{2+} + SIPX (10 ppm each)	At 25^{0}C: no growth for small crystals (≤ 29.65 μm)	Table 6.10 Ch.6
	At 40^{0}C: no growth for very small crystals (≤ 24.60 μm)	Table D-8 Appendix D

Table C-2 shows that in general, small crystals were not able to grow in the presence of 10 ppm of the admixtures studied. It was then concluded that a complete crystal growth inhibition might take place somewhere between 10 and 50 ppm, and therefore, an arbitrary value of 25 ppm concentration was chosen, and some of the results for this selected concentration level are tabulated in **Table C-3**.

Table C-3 Growth rates of gypsum crystals at 25 ppm admixture concentrations

Types of Admixtures	Growth rates of crystals	References
Fe^{3+}	At 25^{0}C: no growth for all crystal sizes	Table 6.5 Ch.6
SIPX	At 25^{0}C: no growth for all crystal sizes	Table 6.7 Ch.6
Fe^{3+} + SIPX (10 ppm each)	At 40^{0}C: no growth for all crystal sizes	Table D-6 Appendix D

Experiments at 25 ppm show that, in some cases, a complete reduction of growth is noted. This situation is shown in **Table C-3** and indicates that even the 25 ppm concentration level might still be too high for a complete growth retardation. Therefore, a lower concentration level between 10 and 25 ppm was chosen, i.e. 20 ppm. Results from the experiments at 20 ppm is tabulated in **Table C-4** and show that in general, for both individual and combined admixtures, small crystals experienced no growth. Yet no complete growth reduction for all crystal sizes was found. Hence, it would be reasonable to expect that the complete growth retardation might take place between 20 and 25 ppm.

Table C-4 Growth rates of gypsum crystals at 20 ppm admixture concentrations

Types of Admixtures	Growth rates of crystals	References
Fe^{3+}	At 25^{0}C: no growth for crystals with sizes ≤ 53.55 μm	Table 6.5 Ch.6
Zn^{2+}	At 40^{0}C: no growth for crystals with sizes ≤ 42.05 μm	Table D-4 Appendix D
SIPX	At 25^{0}C: no growth for crystals with sizes ≤ 42.05 μm	Table 6.7 Ch.6
	At 40^{0}C: no growth for very small crystals (≤ 24.60μm)	Table D-5 Appendix D
Fe^{3+} + SIPX (20 ppm each)	At 25^{0}C: no growth for crystals with sizes ≤ 59.15 μm	Table 6.8 Ch.6
	At 40^{0}C: no growth for crystals with sizes ≤ 79.50μm	Table D-6 Appendix D
Zn^{2+} + SIPX (20 ppm each)	At 25^{0}C: no growth for crystals with sizes ≤ 53.55 μm	Table 6.9 Ch.6
	At 40^{0}C: no growth for very small crystals (≤ 24.60μm)	Table D-7 Appendix D
Fe^{3+} + Zn^{2+} + SIPX (20 ppm each)	At 25^{0}C: no growth for crystals with sizes ≤ 72.05 μm	Table 6.10 Ch.6
	At 40^{0}C: no growth for very small crystals (≤ 24.60μm)	Table D-8 Appendix D

It was found that a complete growth retardation occurred for Fe^{3+} at 22 ppm and 25^{0}C. It would be likely that a concentration level of as either 20 or 21.5 or 22.5 ppm resulted in the same complete growth inhibiton. Based on the result at 22 ppm of Fe^{3+}, the original experimental design was adjusted to include admixture concentrations of: 20, 22 and 25 ppm. Thus, the implementation of the continuous crystallisation studies was that of "exploratory" experiment. The same type of experiment was then adopted for the third phase of project, that is the scaling of gypsum.

The assessment on the selected experimental design, its implementation and its adjustments is summed up as follows.

1. In general, the upper level of admixture concentration in the original experimental design, which is equal to 50 ppm, was found to be too high for complete growth retardation.

2. The experimental design selected (as discussed and tabulated in **section 5.8.6.2** in **Chapter 5**), was implemented, but additional admixture concentration levels were needed and so they were tested. These are: 20, 22 and 25 ppm, respectively.

3. Within the range of the experimental conditions selected for this continuous crystallisation experiments, it was assumed that 22 ppm was probably the lowest concentration level, at which a complete growth retardation could be expected.

4. It was indicated that the crystallisation of gypsum in the presence of admixtures, might better be investigated by the method of exploratory experiment rather than by a well defined experimental design.

5. Having found a discrepancy between the selected experimental design and its implementation, it was decided that the subsequent experiments on gypsum scaling be performed in an exploratory manner.

Appendix D: Continuous Crystallisation Experimental Data

Appendix D Continuous Crystallisation Experimental Data

Table D-1 Comparison of growth rate of gypsum (micron/hour) in pure system and in 1.00 ppm of Fe^{3+} at 25^0C

Crystal size, (microns)	Crystallisation temperature: 25^0C	
	Growth rate in pure system	Growth rate in 1.00 ppm Fe^{3+}
107.00	35.38	28.15
97.05	35.38	25.19
87.75	33.85	20.74
79.50	27.69	14.81
72.05	27.69	5.93
65.30	13.85	5.93
59.15	12.31	5.93
53.55	12.31	5.93
48.55	12.31	5.93
42.05	12.31	5.93
34.50	12.31	0.00
29.65	6.15	0.00
24.60	4.62	0.00
18.30	4.62	0.00
13.05	3.08	0.00

Table D-2 Comparison of growth rate of gypsum (micron/hour) in pure system and in 1.00 ppm of Fe^{3+} at 40^0C

Crystal size, (microns)	Crystallisation temperature: 40^0C	
	Growth rate in pure system	Growth rate in 1.00 ppm Fe^{3+}
107.00	60.00	36.67
97.05	50.77	31.67
87.75	47.69	30.33
79.50	43.08	28.33
72.05	38.46	25.00
65.30	33.85	23.33
59.15	24.62	23.33
53.55	23.08	23.33
48.55	21.54	23.33
42.05	15.38	16.67
34.50	9.23	10.00
29.65	6.15	8.33
24.60	6.13	6.67
18.30	6.12	5.00
13.05	3.08	3.03

Table D-3 Comparison of growth rate of gypsum (micron/hour) at different concentrations of Fe^{3+} at 40^0C

Crystal size, (microns)	Crystallisation temperature: 40^0C						
	0 ppm	1 ppm	10 ppm	20 ppm	22 ppm	25 ppm	50 ppm
107.00	60.00	36.67	17.78	18.5	6.2	0.00	0.00
97.05	50.77	31.67	16.30	16.9	6.2	0.00	0.00
87.75	47.69	30.33	14.81	13.8	3.1	0.00	0.00
79.50	43.08	28.33	11.85	12.3	0.00	0.00	0.00
72.05	38.46	20.00	10.37	9.2	0.00	0.00	0.00
65.30	33.85	23.33	8.89	3.1	0.00	0.00	0.00
59.15	24.62	23.33	8.30	1.5	0.00	0.00	0.00
53.55	23.08	23.33	7.41	1.5	0.00	0.00	0.00
48.55	21.54	23.33	5.93	0.00	0.00	0.00	0.00
42.05	15.38	16.67	4.44	0.00	0.00	0.00	0.00
34.50	9.23	10.00	2.96	0.00	0.00	0.00	0.00
29.65	6.15	8.33	0.00	0.00	0.00	0.00	0.00
24.60	6.13	6.67	0.00	0.00	0.00	0.00	0.00
18.30	6.12	5.00	0.00	0.00	0.00	0.00	0.00
13.05	3.08	3.33	0.00	0.00	0.00	0.00	0.00

Table D-4 Comparison of growth rate of gypsum (micron/hour) at different concentrations of Zn^{2+} at 40^0C

Crystal size, (microns)	Crystallisation temperature: 40^0C						
	0 ppm	1 ppm	10 ppm	20 ppm	22 ppm	25 ppm	50 ppm
107.00	60.00	45.16	30.00	19.35	14.19	22.67	20.00
97.05	50.77	43.87	26.67	14.19	10.32	17.33	13.85
87.75	47.69	41.29	20.00	10.32	10.32	18.67	13.85
79.50	43.08	37.42	10.00	6.45	10.32	12.00	10.77
72.05	38.46	36.13	5.00	6.45	10.32	5.33	10.77
65.30	33.85	33.55	5.00	5.16	9.03	5.33	12.31
59.15	24.62	32.26	5.00	3.87	3.87	2.67	10.77
53.55	23.08	28.90	5.00	2.58	2.58	2.67	6.15
48.55	21.54	27.10	3.33	1.29	1.94	0.00	3.08
42.05	15.38	20.65	3.33	0.00	0.00	0.00	0.00
34.50	9.23	15.48	1.67	0.00	0.00	0.00	0.00
29.65	6.15	14.19	1.67	0.00	0.00	0.00	0.00
24.60	6.13	7.74	0.00	0.00	0.00	0.00	0.00
18.30	6.12	3.87	0.00	0.00	0.00	0.00	0.00
13.05	3.08	2.58	0.00	0.00	0.00	0.00	0.00

Table D-5 Comparison of growth rate of gypsum (micron/hour) at different concentrations of sodium isopropyl xanthate (SIPX) at 40^0C

Crystal size, (microns)	Crystallisation temperature: 40^0C						
	0 ppm	1 ppm	10 ppm	20 ppm	22 ppm	25 ppm	50 ppm
107.00	60.00	57.14	18.46	12.41	10.32	5.26	0.00
97.05	50.77	55.71	18.46	12.41	10.32	5.26	0.00
87.75	47.69	54.29	16.92	12.41	10.32	5.26	0.00
79.50	43.08	51.43	15.38	12.41	11.61	0.00	0.00
72.05	38.46	14.29	10.77	12.41	5.16	0.00	0.00
65.30	33.85	14.29	6.15	12.41	3.87	0.00	0.00
59.15	24.62	14.29	6.15	12.41	2.58	0.00	0.00
53.55	23.08	11.43	6.15	12.41	1.29	0.00	0.00
48.55	21.54	7.14	6.15	5.52	0.00	0.00	0.00
42.05	15.38	7.14	3.08	2.76	0.00	0.00	0.00
34.50	9.23	7.14	3.08	1.38	0.00	0.00	0.00
29.65	6.15	5.71	3.08	1.38	0.00	0.00	0.00
24.60	6.13	0.00	3.08	0.00	0.00	0.00	0.00
18.30	6.12	0.00	0.00	0.00	0.00	0.00	0.00
13.05	3.08	0.00	0.00	0.00	0.00	0.00	0.00

Table D-6 Comparison of growth rate of gypsum (micron/hour) at different concentrations of combined admixtures: Fe^{3+} and SIPX at 40^0C

Crystal size, (microns)	Crystallisation temperature: 40^0C						
	0 ppm	1 ppm	10 ppm	20 ppm	22 ppm	25 ppm	50 ppm
107.00	60.00	45.26	14.40	7.14	12.00	0.00	0.00
97.05	50.77	40.88	14.40	7.14	8.00	0.00	0.00
87.75	47.69	36.50	12.80	4.29	5.33	0.00	0.00
79.50	43.08	36.50	12.80	0.00	2.67	0.00	0.00
72.05	38.46	33.87	11.20	0.00	2.67	0.00	0.00
65.30	33.85	33.58	9.60	0.00	2.67	0.00	0.00
59.15	24.62	32.12	8.00	0.00	2.67	0.00	0.00
53.55	23.08	30.66	6.40	0.00	1.33	0.00	0.00
48.55	21.54	29.20	4.80	0.00	0.00	0.00	0.00
42.05	15.38	29.20	4.80	0.00	0.00	0.00	0.00
34.50	9.23	20.44	3.20	0.00	0.00	0.00	0.00
29.65	6.15	11.68	1.60	0.00	0.00	0.00	0.00
24.60	6.13	2.92	1.60	0.00	0.00	0.00	0.00
18.30	6.12	2.84	0.00	0.00	0.00	0.00	0.00
13.05	3.08	0.88	0.00	0.00	0.00	0.00	0.00

Table D-7 Comparison of growth rate of gypsum (micron/hour) at different concentrations of combined admixtures: Zn^{2+} and SIPX at 40^0C

Crystal size, (microns)	Crystallisation temperature: 40^0C						
	0 ppm	1 ppm	10 ppm	20 ppm	22 ppm	25 ppm	50 ppm
107.00	60.00	63.33	34.67	26.67	25.81	22.45	14.81
97.05	50.77	60.00	33.33	26.67	25.81	22.45	5.93
87.75	47.69	33.33	32.00	26.67	25.81	22.45	5.93
79.50	43.08	26.67	28.00	26.67	25.81	22.45	5.93
72.05	38.46	26.67	20.00	26.67	20.97	22.45	5.93
65.30	33.85	23.33	10.67	26.67	20.65	22.45	5.93
59.15	24.62	15.00	9.33	26.67	15.48	14.29	5.93
53.55	23.08	15.00	6.67	26.67	2.58	10.20	5.93
48.55	21.54	10.00	6.67	13.33	6.45	0.00	0.00
42.05	15.38	6.67	4.00	6.67	5.16	0.00	0.00
34.50	9.23	5.00	2.67	5.33	5.16	0.00	0.00
29.65	6.15	3.33	1.33	1.33	0.00	0.00	0.00
24.60	6.13	3.33	2.67	0.00	1.29	0.00	0.00
18.30	6.12	0.00	2.67	0.00	2.58	0.00	0.00
13.05	3.08	0.00	0.80	0.00	0.00	0.00	0.00

Table D-8 **Comparison of growth rate of gypsum (micron/hour) at different concentrations of combined admixtures: Fe^{3+}, Zn^{2+} and SIPX at 40^0C**

Crystal size, (microns)	Growth rate of gypsum, micron per hour						
	0 ppm	1 ppm	10 ppm	20 ppm	22 ppm	25 ppm	50 ppm
107.00	60.00	52.80	25.00	24.00	16.77	12.66	6.67
97.05	50.77	52.80	20.00	24.00	16.77	12.66	6.67
87.75	47.69	44.80	16.67	24.00	16.77	12.66	6.67
79.50	43.08	40.00	16.67	24.00	16.77	10.13	6.67
72.05	38.46	38.40	15.00	17.33	16.77	7.59	1.67
65.30	33.85	36.80	13.33	17.33	16.77	7.59	0.00
59.15	24.62	36.80	11.67	17.33	16.77	5.06	0.00
53.55	23.08	35.20	8.33	17.33	2.58	1.27	0.00
48.55	21.54	32.00	8.33	17.33	2.58	1.27	0.00
42.05	15.38	32.00	6.67	13.33	2.58	0.00	0.00
34.50	9.23	16.00	3.33	2.67	2.58	0.00	0.00
29.65	6.15	16.00	1.67	1.33	2.58	0.00	0.00
24.60	6.13	12.80	0.00	0.00	1.29	0.00	0.00
18.30	6.12	4.80	0.00	0.00	1.29	0.00	0.00
13.05	3.08	3.20	0.00	0.00	0.00	0.00	0.00

Table D-9 Desupersaturation data for Fe^{3+} as admixtures at 25°C

No. of residence time	Ca^{2+} concentrations, ppm						
	Fe = 0 ppm	Fe = 1 ppm	Fe = 10 ppm	Fe = 20 ppm	Fe = 22 ppm	Fe = 25 ppm	Fe = 50 ppm
0	1221	1209	1205	1232	1227	1218	1229
1	825	1007	1129	1151	1171	1158	1209
2	786	925	1123	1149	1145	1147	1204
3	770	920	1121	1148	1138	1145	1203
4	757	916	1121	1147	1135	1145	1201
5	748	901	1113	1139	1130	1144	1199
6	735	892	1109	1131	1130	1144	1198
7	735	892	1109	1131	1129	1144	1198
8	735	892	1109	1131	1129	1144	1198

Table D-10 Desupersaturation data for Zn^{2+} as admixtures at 25°C

No. of residence time	Ca^{2+} concentrations, ppm						
	Zn = 0 ppm	Zn = 1 ppm	Zn = 10 ppm	Zn = 20 ppm	Zn = 22 ppm	Zn = 25 ppm	Zn = 50 ppm
0	1221	1214	1235	1197	1219	1224	1198
1	825	1129	1083	1084	1128	1172	1167
2	786	1128	1041	1049	1107	1156	1146
3	770	1036	1012	1028	1087	1131	1140
4	757	940	992	1026	1079	1122	1138
5	748	930	965	1025	1068	1098	1135
6	735	927	963	1025	1051	1094	1135
7	735	927	963	1025	1051	1094	1135
8	735	927	963	1025	1051	1094	1135

Table D-11 Desupersaturation data for SIPX as admixtures at 25°C

No. of residence time	Ca^{2+} concentrations, ppm						
	SIPX = 0 ppm	SIPX = 1 ppm	SIPX = 10 ppm	SIPX = 20 ppm	SIPX = 22 ppm	SIPX = 25 ppm	SIPX = 50 ppm
0	1221	1215	1219	1220	1224	1207	1223
1	825	894	1170	1181	1201	1186	1213
2	786	864	1152	1165	1195	1179	1210
3	770	847	1148	1159	1187	1171	1208
4	757	831	1146	1151	1171	1169	1207
5	748	820	1134	1148	1158	1167	1207
6	735	817	1131	1145	1149	1167	1207
7	735	817	1130	1145	1149	1167	1207
8	735	817	1130	1145	1149	1167	1207

Table D-12 Desupersaturation data for Fe^{3+} + SIPX as admixtures at 25°C

No. of residence time	Ca^{2+} concentrations, ppm						
	Fe + SIPX = 0 ppm	Fe + SIPX = 1 ppm	Fe + SIPX = 10 ppm	Fe + SIPX = 20 ppm	Fe + SIPX = 22 ppm	Fe + SIPX = 25 ppm	Fe + SIPX = 50 ppm
0	1221	1210	1224	1211	1214	1218	1218
1	825	1097	1195	1185	1198	1207	1213
2	786	1061	1176	1173	1186	1197	1208
3	770	1039	1171	1158	1181	1194	1205
4	757	1028	1168	1151	1179	1193	1203
5	748	1017	1162	1149	1178	1192	1201
6	735	1009	1158	1146	1178	1190	1201
7	735	1002	1157	1143	1178	1189	1201
8	735	1002	1157	1143	1178	1189	1201

Table D-13 Desupersaturation data for Zn^{2+} + SIPX as admixtures at 25°C

No. of residence time	Ca^{2+} concentrations, ppm						
	Zn + SIPX = 0 ppm	Zn + SIPX = 1 ppm	Zn + SIPX= 10 ppm	Zn + SIPX= 20 ppm	Zn + SIPX= 22 ppm	Zn + SIPX= 25 ppm	Zn + SIPX= 50 ppm
0	1221	1213	1224	1215	1198	1214	1224
1	825	1073	1088	1114	1115	1188	1221
2	786	1041	1069	1096	1092	1180	1214
3	770	1015	1060	1091	1087	1174	1211
4	757	1011	1056	1089	1084	1176	1198
5	748	1005	1049	1082	1076	1178	1194
6	735	1002	1042	1079	1072	1172	1193
7	735	1000	1039	1079	1072	1170	1193
8	735	1000	1039	1079	1072	1170	1193

Table D-14 Desupersaturation data for Fe^{3+} + Zn^{2+} + SIPX as admixtures at 25°C

No. of residence time	Ca^{2+} concentrations, ppm						
	Fe + Zn + SIPX = 0 ppm	Fe + Zn + SIPX = 1 ppm	Fe + Zn + SIPX= 10 ppm	Fe + Zn + SIPX= 20 ppm	Fe + Zn + SIPX= 22 ppm	Fe + Zn + SIPX= 25 ppm	Fe + Zn + SIPX= 50 ppm
0	1221	1214	1218	1223	1201	1217	1203
1	825	1093	1161	1174	1166	1186	1188
2	786	1025	1138	1145	1147	1177	1181
3	770	1016	1130	1133	1139	1178	1182
4	757	1002	1124	1127	1132	1170	1181
5	748	989	1121	1121	1127	1165	1181
6	735	984	1115	1119	1122	1163	1181
7	735	982	1113	1119	1120	1163	1181
8	735	982	1113	1119	1120	1162	1181

Table D-15 Desupersaturation data for Fe^{3+} as admixtures at 40°C

No. of residence time	Ca^{2+} concentrations, ppm						
	Fe = 0 ppm	Fe = 1 ppm	Fe = 10 ppm	Fe = 20 ppm	Fe = 22 ppm	Fe = 25 ppm	Fe = 50 ppm
0	1189	1194	1197	1216	1212	1209	1205
1	798	720	1120	1132	1140	1152	1190
2	792	769	1104	1151	1167	1180	1184
3	810	851	1090	1144	1159	1162	1182
4	765	853	1098	1119	1142	1151	1182
5	761	857	1098	1085	1131	1146	1182
6	746	836	1080	1062	1102	1137	1182
7	735	851	1086	1084	1102	1135	1182
8	723	847	1074	1084	1102	1133	1182

Table D-16 Desupersaturation data for Zn^{2+} as admixtures at 40°C

No. of residence time	Ca^{2+} concentrations, ppm						
	Zn = 0 ppm	Zn = 1 ppm	Zn = 10 ppm	Zn = 20 ppm	Zn = 22 ppm	Zn = 25 ppm	Zn = 50 ppm
0	1189	1156	1225	1212	1219	1196	1219
1	798	848	1066	1100	1122	1136	1168
2	792	823	1020	1068	1095	1116	1140
3	810	842	981	1042	1075	1112	1131
4	765	842	953	1045	1063	1100	1126
5	761	842	937	1032	1064	1089	1126
6	746	842	937	1021	1044	1088	1126
7	735	842	937	1019	1043	1083	1126
8	723	842	937	1019	1043	1083	1126

Table D-17 Desupersaturation data for SIPX as admixtures at 40°C

No. of residence time	Ca^{2+} concentrations, ppm						
	SIPX = 0 ppm	SIPX = 1 ppm	SIPX = 10 ppm	SIPX = 20 ppm	SIPX = 22 ppm	SIPX = 25 ppm	SIPX = 50 ppm
0	1189	1214	1215	1220	1216	1216	1207
1	798	852	1167	1178	1185	1190	1195
2	792	822	1144	1159	1180	1184	1192
3	810	815	1133	1140	1172	1176	1192
4	765	809	1126	1139	1151	1170	1192
5	761	801	1126	1132	1142	1162	1192
6	746	800	1126	1130	1142	1158	1192
7	735	801	1126	1130	1142	1158	1192
8	723	801	1126	1130	1142	1158	1192

Table D-18 Desupersaturation data for Fe^{3+} + SIPX as admixtures at 40°C

No. of residence time	Ca^{2+} concentrations, ppm						
	Fe + SIPX = 0 ppm	Fe + SIPX = 1 ppm	Fe + SIPX= 10 ppm	Fe + SIPX= 20 ppm	Fe + SIPX= 22 ppm	Fe + SIPX= 25 ppm	Fe + SIPX = 50 ppm
0	1189	1204	1202	1218	1211	1226	1217
1	798	1091	1169	1190	1195	1216	1210
2	792	1047	1146	1175	1183	1197	1198
3	810	1020	1135	1161	1178	1192	1196
4	765	997	1132	1156	1169	1190	1196
5	761	986	1132	1149	1167	1186	1196
6	746	986	1132	1149	1167	1186	1196
7	735	986	1132	1149	1167	1186	1196
8	723	986	1132	1149	1167	1186	1196

Table D-19 Desupersaturation data for Zn^{2+} + SIPX as admixtures at 40°C

No. of residence time	Ca^{2+} concentrations, ppm						
	Zn + SIPX = 0 ppm	Zn + SIPX = 1 ppm	Zn + SIPX= 10 ppm	Zn + SIPX= 20 ppm	Zn + SIPX= 22 ppm	Zn + SIPX= 25 ppm	Zn + SIPX= 50 ppm
0	1189	1223	1215	1202	1211	1209	1227
1	798	1067	1076	1094	1125	1178	1201
2	792	1032	1053	1087	1093	1172	1192
3	810	986	1044	1072	1080	1169	1188
4	765	978	1041	1074	1075	1169	1181
5	761	978	1039	1067	1062	1169	1181
6	746	978	1039	1057	1059	1162	1181
7	735	978	1032	1057	1059	1162	1181
8	723	978	1033	1055	1059	1162	1181

Table D-20 Desupersaturation data for Fe^{3+} + Zn^{2+} + SIPX as admixtures at 40°C

No. of residence time	Ca^{2+} concentrations, ppm						
	Fe + Zn + SIPX = 0 ppm	Fe + Zn + SIPX = 1 ppm	Fe + Zn + SIPX= 10 ppm	Fe + Zn + SIPX= 20 ppm	Fe + Zn + SIPX= 22 ppm	Fe + Zn + SIPX= 25 ppm	Fe + Zn + SIPX= 50 ppm
0	1189	1204	1207	1216	1212	1220	1219
1	798	1074	1144	1170	1174	1198	1215
2	792	1003	1121	1141	1152	1182	1187
3	810	972	1108	1132	1150	1173	1175
4	765	969	1096	1125	1142	1170	1175
5	761	969	1096	1106	1129	1164	1175
6	746	969	1096	1106	1127	1153	1175
7	735	969	1096	1107	1127	1154	1175
8	723	969	1096	1106	1127	1154	1175

Table D-21 Slurry density at 25°C for Fe^{3+}

No. of residence time	Slurry density, gram/L						
	Fe = 0 ppm	Fe = 1 ppm	Fe = 10 ppm	Fe = 20 ppm	Fe = 22 ppm	Fe = 25 ppm	Fe = 50 ppm
0	0.7925	0.8097	0.8017	0.7894	0.8026	0.8094	0.7898
1	0.9891	0.9794	0.9892	0.8412	0.8942	0.8372	0.8176
2	1.8447	1.5242	1.1246	0.9001	0.9974	0.8627	0.8316
3	2.4843	-	-	-	-	-	-
4	2.7618	1.8477	1.1927	0.9294	1.0926	0.9245	0.9102
5	2.7601	-	-	-	-	-	-
6	2.7705	1.9405	1.1769	1.0128	1.1972	0.9832	0.9645
7	2.7704	-	1.1988	1.0110	1.2011	0.9882	0.9662
8	2.7689	2.0723	1.1946	1.0149	1.2017	0.9884	0.9675

Table D-22 Slurry density at 25°C for Zn^{2+}

No of residence time	Slurry density, gram/L						
	Zn = 0 ppm	Zn = 1 ppm	Zn = 10 ppm	Zn = 20 ppm	Zn = 22 ppm	Zn = 25 ppm	Zn = 50 ppm
0	0.7925	0.7246	0.7991	0.8124	0.8119	0.8072	0.8114
1	0.9891	0.9121	0.9002	0.9442	0.9745	0.9702	0.9076
2	1.8447	-	0.9026	-	-	-	0.9103
3	2.4843	1.4202	1.4902	1.2610	1.3260	0.9906	-
4	2.7618	-	-	-	-	-	0.9142
5	2.7601	1.8976	1.8560	1.4051	1.4179	1.0794	-
6	2.7705	1.9115	1.8572	1.4074	1.5104	1.2356	0.9202
7	2.7704	1.9104	1.8565	1.4092	1.5174	1.2497	0.9225
8	2.7689	1.9123	1.8560	1.4082	1.5160	1.2489	0.9216

Table D-23 Slurry density at 25°C for SIPX

No of residence time	Slurry density, gram/L						
	SIPX = 0 ppm	SIPX = 1 ppm	SIPX = 10 ppm	SIPX = 20 ppm	SIPX = 22 ppm	SIPX = 25 ppm	SIPX = 50 ppm
0	0.7925	0.7952	0.8012	0.7942	0.8071	0.8143	0.8978
1	0.9891	0.9727	0.9241	0.8724	0.8489	0.8271	0.9026
2	1.8447	1.1849	0.9874	0.9451	0.9271	0.8386	0.9002
3	2.4843	-	-	-	-	-	-
4	2.7618	2.2856	1.1275	0.9725	0.9574	0.8371	0.9023
5	2.7601	-	-	-	-	-	-
6	2.7705	2.4715	1.1801	1.0059	1.0041	0.8454	0.9111
7	2.7704	2.4662	1.1521	1.0040	1.0026	0.8427	0.9112
8	2.7689	2.4791	1.1792	1.0076	1.0419	0.8496	0.9105

Table D-24 Slurry density at 25°C for Fe^{3+} + SIPX

No. of residence time	Slurry density, gram/L						
	Fe + SIPX = 0 ppm	Fe + SIPX = 1 ppm	Fe + SIPX = 10 ppm	Fe + SIPX = 20 ppm	Fe + SIPX = 22 ppm	Fe + SIPX = 25 ppm	Fe + SIPX = 50 ppm
0	0.7925	0.8012	0.7982	0.7694	0.8124	0.8075	0.7927
1	0.9891	0.8941	0.8004	0.8071	0.8479	0.8447	0.8004
2	1.8447	0.9273	0.8095	0.8194	0.8527	0.8579	0.7928
3	2.4843	-	-	-	-	-	-
4	2.7618	1.0075	0.9278	0.9042	0.9117	0.8881	0.8092
5	2.7601	-	-	-	-	-	-
6	2.7705	1.1478	0.9804	0.9235	0.9201	0.8974	0.8101
7	2.7704	1.1502	0.9862	0.9272	0.9214	0.9004	0.8124
8	2.7689	1.1729	0.9874	0.9251	0.9285	0.8978	0.8104

Table D-25 Slurry density at 25°C for Zn^{2+} + SIPX

No of residence time	Slurry density, gram/L						
	Zn + SIPX= 0 ppm	Zn + SIPX= 1 ppm	Zn + SIPX= 10 ppm	Zn + SIPX= 20 ppm	Zn + SIPX= 22 ppm	Zn + SIPX= 25 ppm	Zn + SIPX= 50 ppm
0	0.7925	0.7867	0.7746	0.7995	0.8213	0.8164	0.8009
1	0.9891	1.2481	0.8174	0.8570	0.9107	0.8274	0.8251
2	1.8447	1.5194	0.9091	0.9152	0.9570	0.8596	0.8414
3	2.4843	-	-	-	-	-	-
4	2.7618	1.7079	1.1269	0.9718	0.9904	0.8802	0.8375
5	2.7601	-	-	-	-	-	-
6	2.7705	1.8083	1.2610	1.0992	1.1673	0.8842	0.8869
7	2.7704	1.8179	1.2642	1.1211	1.1592	0.8821	0.8805
8	2.7689	1.8212	1.2673	1.1264	1.1726	0.8796	0.8872

Table D-26 Slurry density at 25°C for Fe^{3+} + Zn^{2+} + SIPX

No of residence time	Slurry density, gram/L						
	Fe + Zn + SIPX = 0 ppm	Fe + Zn + SIPX = 1 ppm	Fe + Zn + SIPX= 10 ppm	Fe + Zn + SIPX = 20 ppm	Fe + Zn + SIPX = 22 ppm	Fe + Zn + SIPX= 25 ppm	Fe + Zn + SIPX = 50 ppm
0	0.7925	0.8356	0.8077	0.8201	0.8095	0.7992	0.7029
1	0.9891	1.0793	0.8526	0.9017	0.8246	0.8014	0.7109
2	1.8447	1.2095	0.9947	0.9703	0.9093	0.8108	0.7202
3	2.4843	-	-	-	-	-	-
4	2.7618	1.4115	1.0211	1.0649	0.9476	0.8461	0.7603
5	2.7601	-	-	-	-	-	-
6	2.7705	1.6701	1.0217	1.1194	1.0800	0.8661	0.7901
7	2.7704	1.6621	1.0177	1.1270	1.0808	0.8472	0.7872
8	2.7689	1.6745	1.0289	1.1278	1.0872	0.8873	0.7985

Table D-27 Slurry density at 40°C for Fe^{3+}

No. of residence time	Slurry density, gram/L						
	Fe = 0 ppm	Fe = 1 ppm	Fe = 10 ppm	Fe = 20 ppm	Fe = 22 ppm	Fe = 25 ppm	Fe = 50 ppm
0	0.8074	0.7992	0.8117	0.7614	0.7892	0.8245	0.8152
1	0.9525	0.9591	0.9135	0.8446	0.8083	0.8315	0.8229
2	1.2761	1.1665	0.9980	0.9592	0.9437	0.9221	0.8332
3	-	-	-	-	-	-	-
4	1.9691	1.5213	1.0632	1.0863	1.0211	1.0076	0.8652
5	-	-	-	-	-	-	-
6	2.4591	2.0419	1.2134	1.2079	1.1019	1.0067	0.8679
7	2.4702	2.0705	1.2107	1.2009	1.1475	1.0347	0.8668
8	2.4783	2.0462	1.2143	1.2062	1.1092	1.0479	0.8672

Table D-28 Slurry density at 40°C for Zn^{2+}

No of residence time	Slurry density, gram/L						
	Zn = 0 ppm	Zn = 1 ppm	Zn = 10 ppm	Zn = 20 ppm	Zn = 22 ppm	Zn = 25 ppm	Zn = 50 ppm
0	0.8074	0.8249	0.8207	0.7994	0.8310	0.8079	0.8109
1	0.9525	1.0026	0.9274	0.9041	0.9472	0.9220	0.9505
2	1.2761	1.4231	1.2315	1.0824	0.9913	0.9754	0.9967
3	-	-	-	-	-	-	-
4	1.9691	1.7524	1.5190	1.2734	1.0067	1.0728	1.0079
5	-	-	-	-	-	-	-
6	2.4591	1.9825	1.7233	1.4045	1.1571	1.0009	1.0994
7	2.4702	1.9606	1.7641	1.4091	1.1518	1.0104	1.0902
8	2.4783	1.9807	1.7182	1.4020	1.1627	1.0063	1.0945

Table D-29 Slurry density at 40°C for SIPX

No of residence time	Slurry density, gram/L						
	SIPX = 0 ppm	SIPX = 1 ppm	SIPX = 10 ppm	SIPX = 20 ppm	SIPX = 22 ppm	SIPX = 25 ppm	SIPX = 50 ppm
0	0.8074	0.8146	0.8294	0.8102	0.7946	0.7992	0.8195
1	0.9525	0.9968	0.8530	0.8771	0.8241	0.8401	0.8180
2	1.2761	1.4568	0.8732	0.8962	0.8739	0.8916	0.8307
3	-	-	-	-	-	-	-
4	1.9691	1.7395	0.9246	0.9245	0.9135	0.9227	0.9018
5	-	-	-	-	-	-	-
6	2.4591	2.2763	0.9826	0.9863	0.9868	0.9739	0.8629
7	2.4702	2.3026	0.9980	0.9801	0.9820	0.9713	0.8635
8	2.4783	2.3261	0.9764	0.9874	0.9742	0.9767	0.8630

Table D-30 Slurry density at 40°C for Fe^{3+} + SIPX

No. of residence time	Slurry density, gram/L						
	Fe + SIPX = 0 ppm	Fe + SIPX = 1 ppm	Fe + SIPX= 10 ppm	Fe + SIPX= 20 ppm	Fe + SIPX= 22 ppm	Fe + SIPX= 25 ppm	Fe + SIPX = 50 ppm
0	0.8074	0.7892	0.8212	0.8092	0.8301	0.7900	0.8126
1	0.9525	0.8537	0.8763	0.8163	0.8392	0.8042	0.8128
2	1.2761	0.9568	0.8791	0.8585	0.8581	0.8071	0.8129
3	-	-	-	-	-	-	-
4	1.9691	1.2495	0.8962	0.9017	0.8574	0.8100	0.8421
5	-	-	-	-	-	-	0.8664
6	2.4591	1.5826	0.9123	0.9271	0.8925	0.8201	0.8678
7	2.4702	1.5802	0.9263	0.9279	0.8964	0.8107	0.8756
8	2.4783	1.5860	0.9247	0.9312	0.8931	0.8124	0.8764

Table D-31 Slurry density at 40°C for Zn^{2+} + SIPX

No of residence time	Slurry density, gram/L						
	Zn + SIPX = 0 ppm	Zn + SIPX = 1 ppm	Zn + SIPX = 10 ppm	Zn + SIPX = 20 ppm	Zn + SIPX = 22 ppm	Zn + SIPX = 25 ppm	Zn + SIPX = 50 ppm
0	0.8074	0.8107	0.8094	0.8361	0.8224	0.8096	0.7962
1	0.9525	0.9526	0.9271	0.9075	0.8506	0.8116	0.8057
2	1.2761	1.2774	0.9738	0.9527	0.9507	0.8402	0.8200
3	-	-	-	-	-	-	-
4	1.9691	1.4923	1.2679	0.9996	1.0072	0.8572	0.8179
5	-	-	-	-	-	-	-
6	2.4591	1.7295	1.3806	1.1701	1.2867	0.8887	0.8802
7	2.4702	1.7402	1.3725	1.1874	1.2775	0.8766	0.8702
8	2.4783	1.7430	1.3872	1.1902	1.2971	0.8972	0.8729

Table D-32 Slurry density at 40°C for Fe^{3+} + Zn^{2+} + SIPX

No of residence time	Slurry density, gram/L						
	Fe + Zn + SIPX = 0 ppm	Fe + Zn + SIPX = 1 ppm	Fe + Zn + SIPX= 10 ppm	Fe + Zn + SIPX= 20 ppm	Fe + Zn + SIPX= 22 ppm	Fe + Zn + SIPX= 25 ppm	Fe + Zn + SIPX= 50 ppm
0	0.8074	0.8342	0.8016	0.7698	0.7895	0.7992	0.8129
1	0.9525	0.9677	0.8172	0.8066	0.8032	0.8059	0.8160
2	1.2761	1.1629	0.8402	0.8771	0.8272	0.8187	0.8179
3	-	-	-	-	-	-	-
4	1.9691	1.3571	0.9307	0.9081	0.8514	0.8279	0.8294
5	-	-	-	-	-	-	-
6	2.4591	1.5719	0.9976	0.9409	0.8764	0.8643	0.8301
7	2.4702	1.5706	0.9901	0.9379	0.8701	0.8624	0.8342
8	2.4783	1.5783	1.0231	0.9452	0.8787	0.8639	0.8368

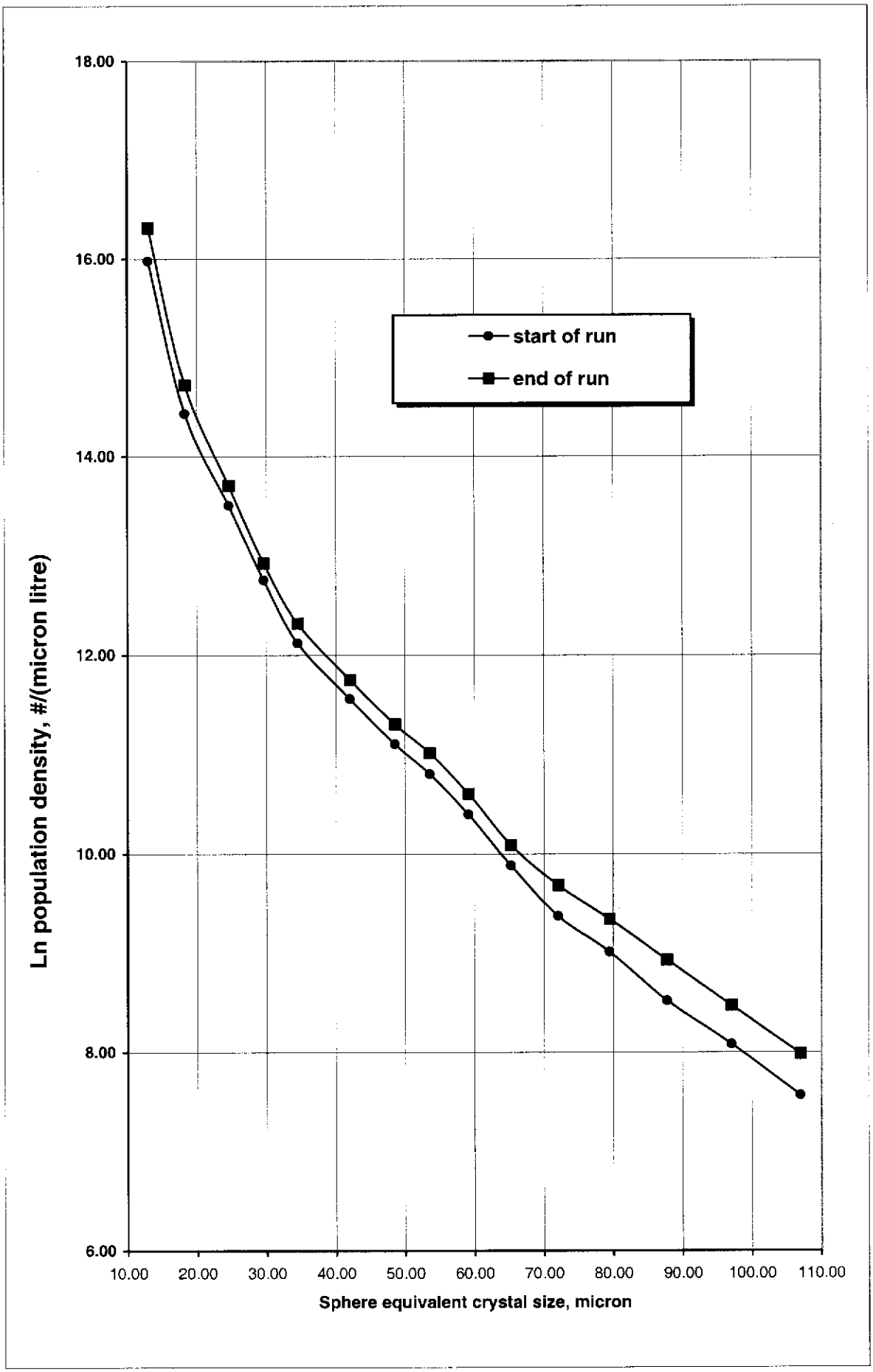

Population density plot obtained in the absence of admixtures (Fe = 0 ppm) at 25^0C

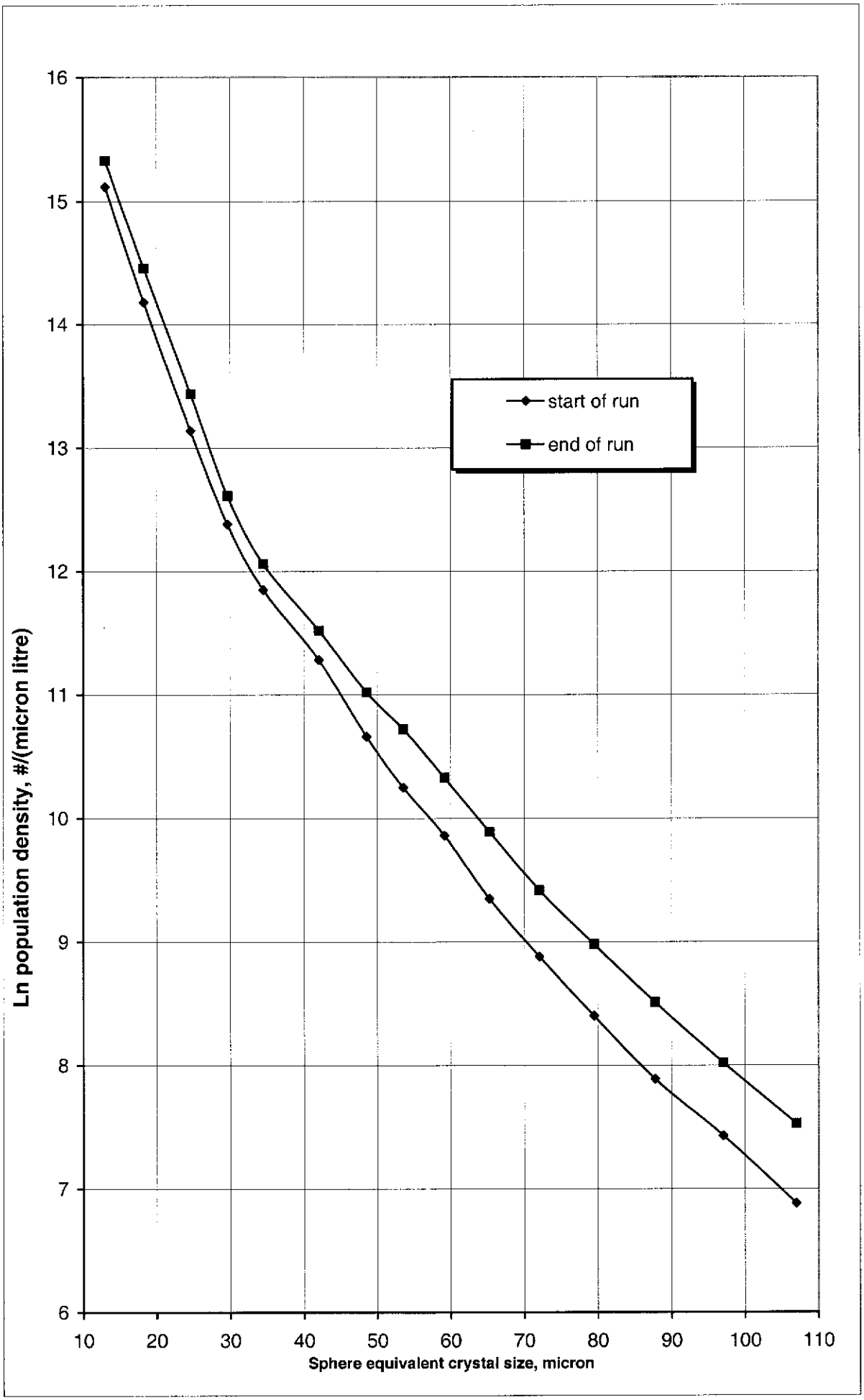

Population density plot obtained in the absence of admixtures (Fe = 0 ppm) at 40^0C

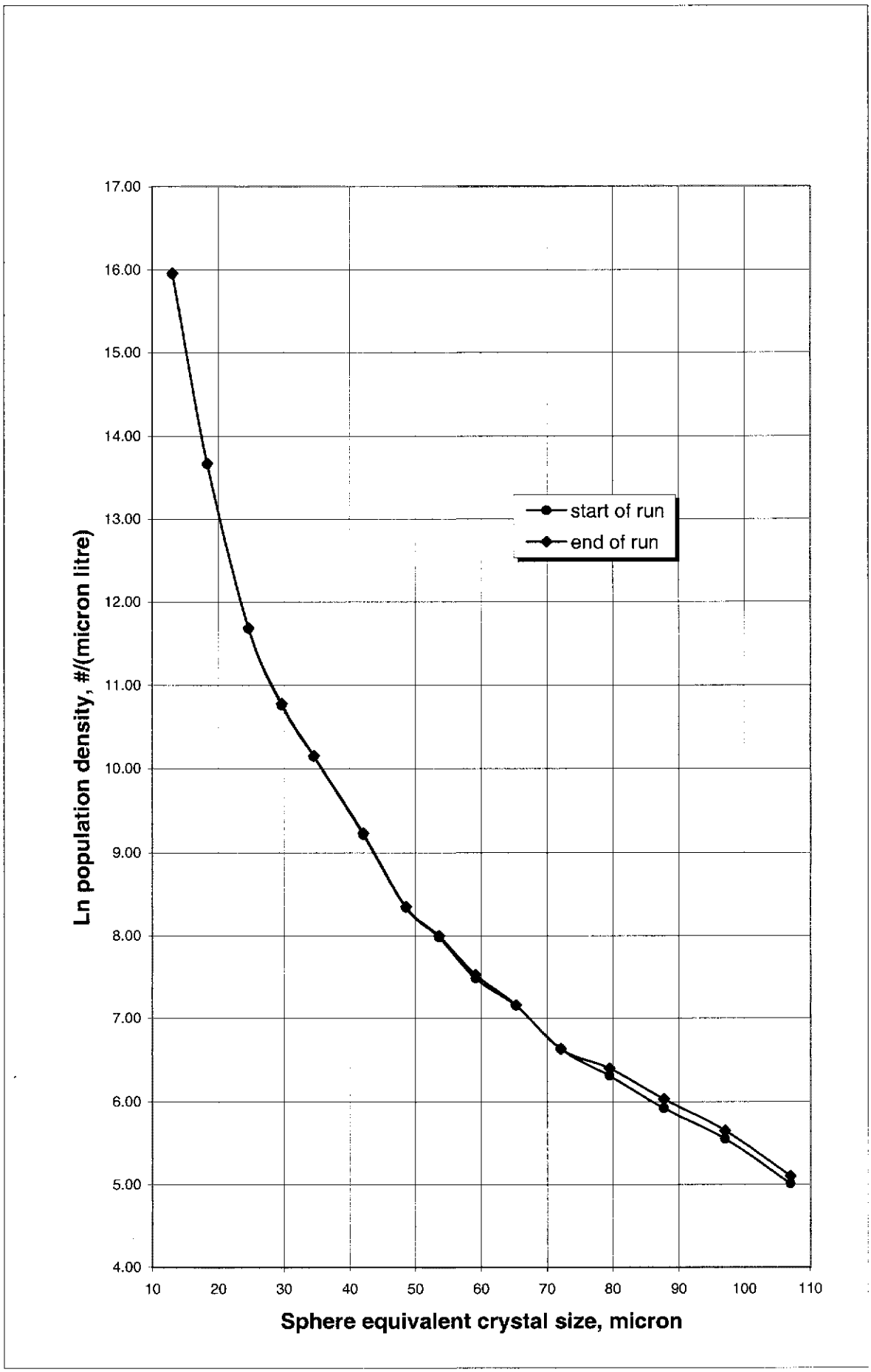

Population density plot obtained in the presence of Zn = 50 ppm at 25^0C

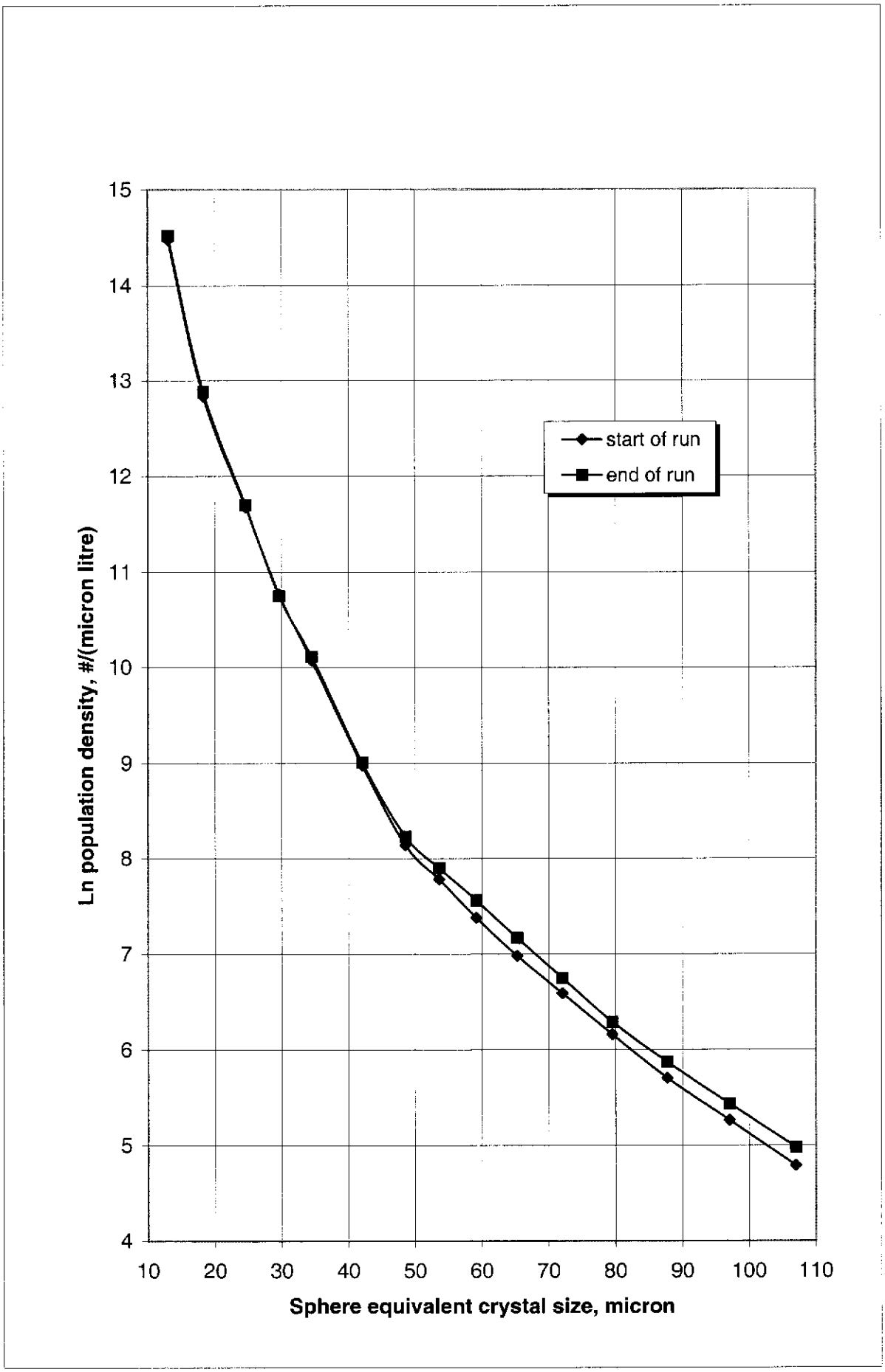

Population density plot obtained in the presence of Zn = 50 ppm at 40^0C

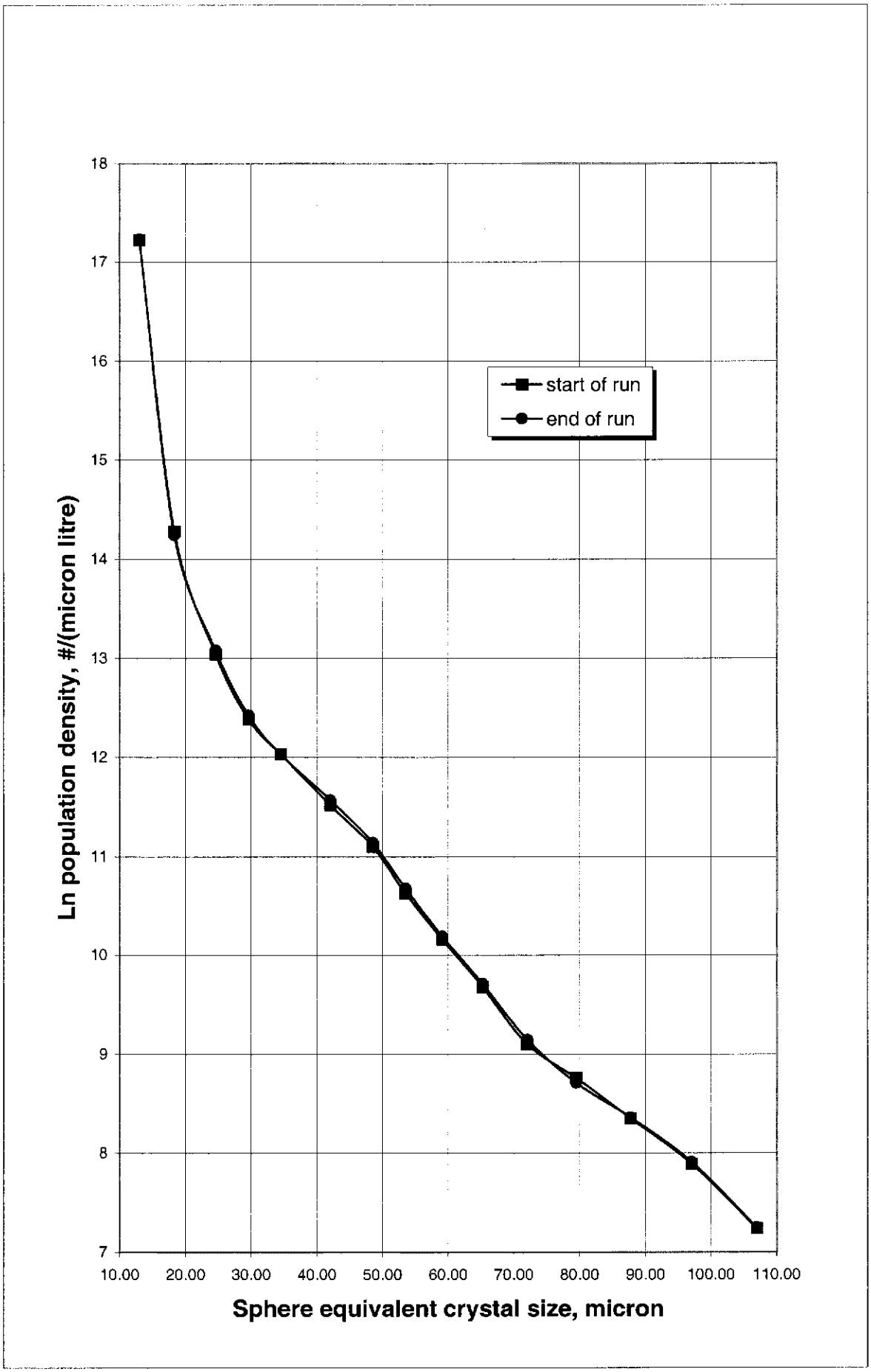

Population density plot obtained in the presence of SIPX = 50 ppm at 25^{0}C

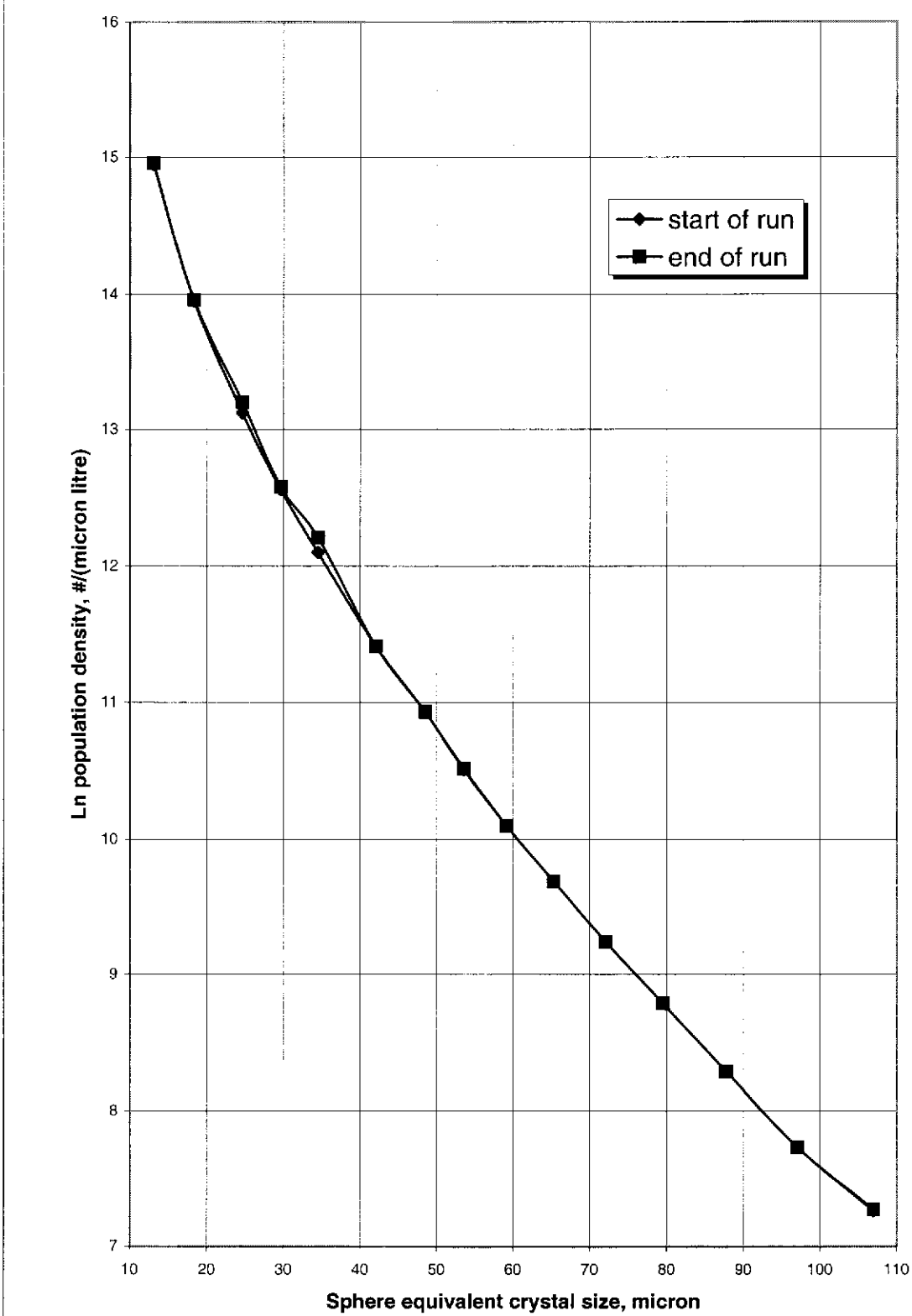

Population density plot obtained in the presence of SIPX = 50 ppm at 40^{0}C

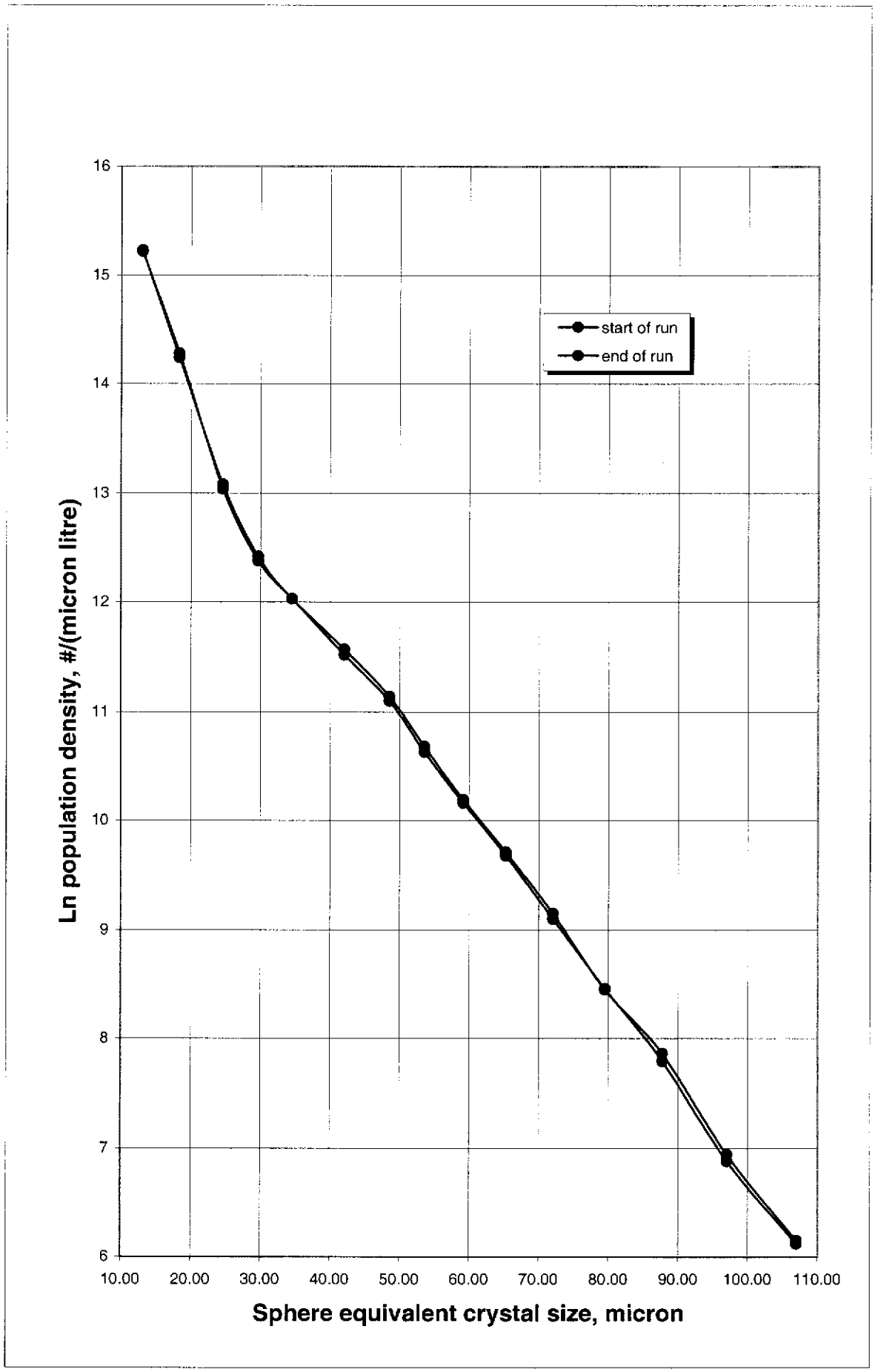

Population density plot obtained in the presence of Fe + SIPX = 50 ppm at 25^0C

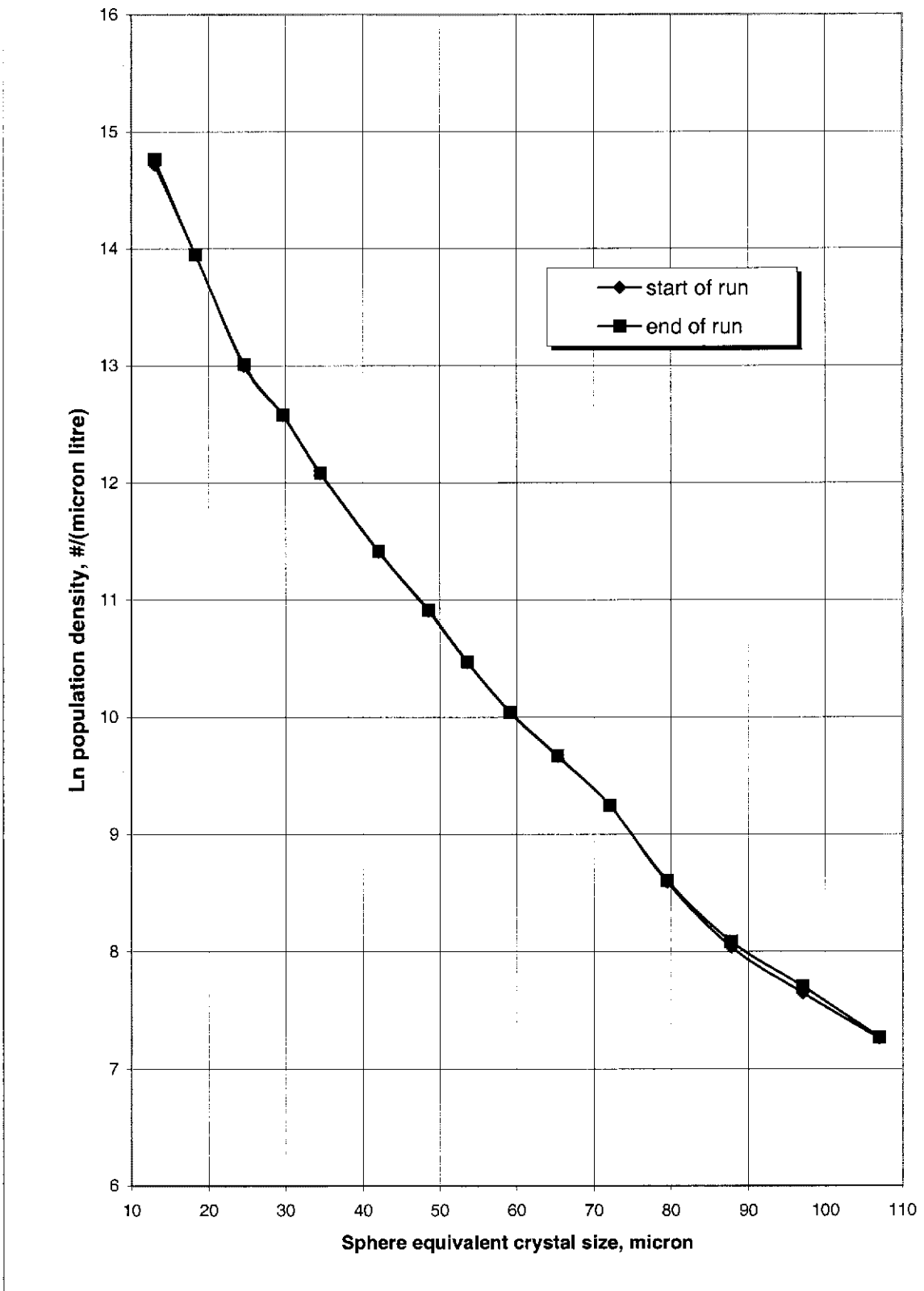

Population density plot obtained in the presence of Fe + SIPX = 50 ppm at 40^{0}C

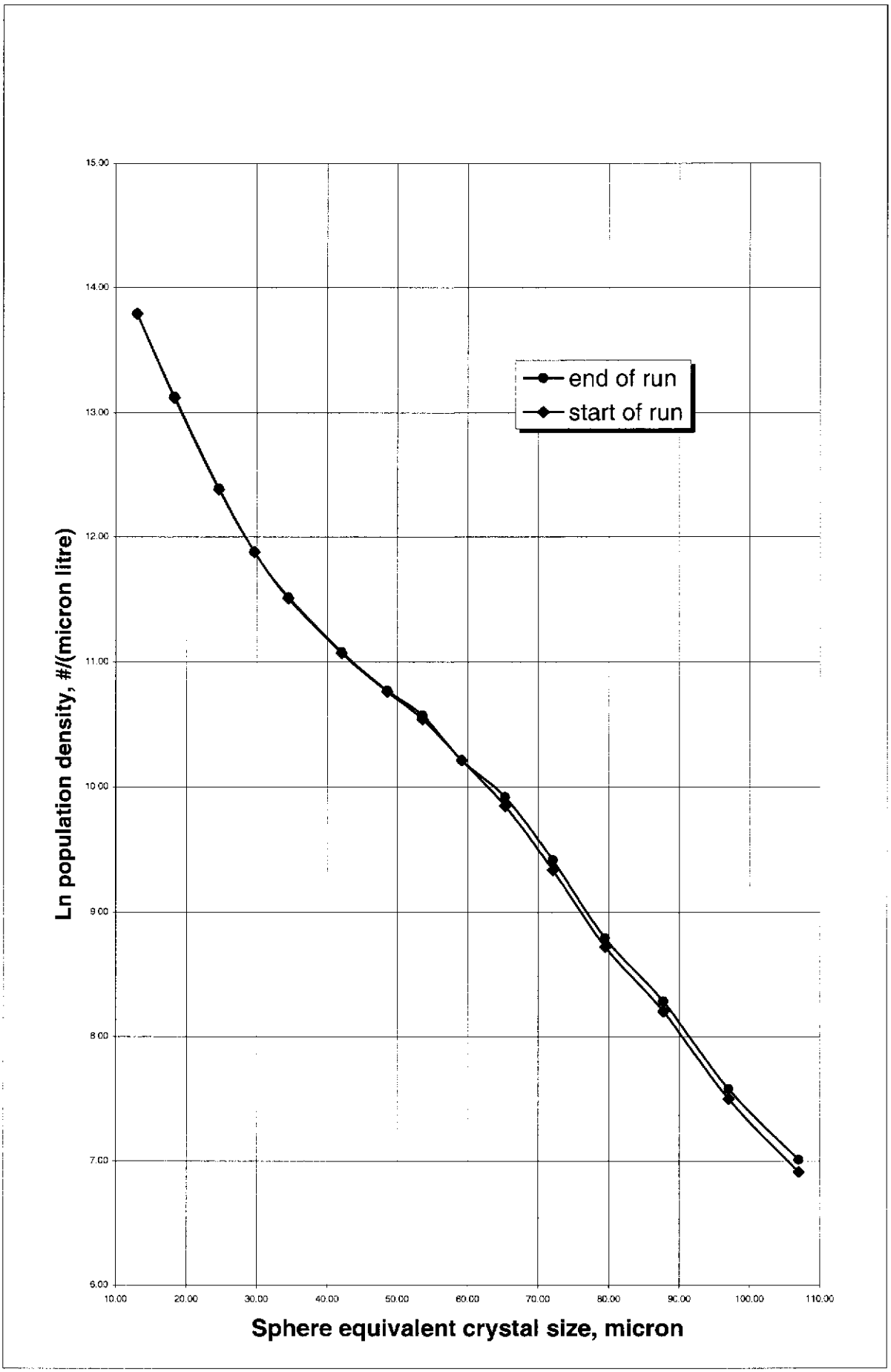

Population density plot obtained in the presence of Zn + SIPX = 50 ppm at 25^0C

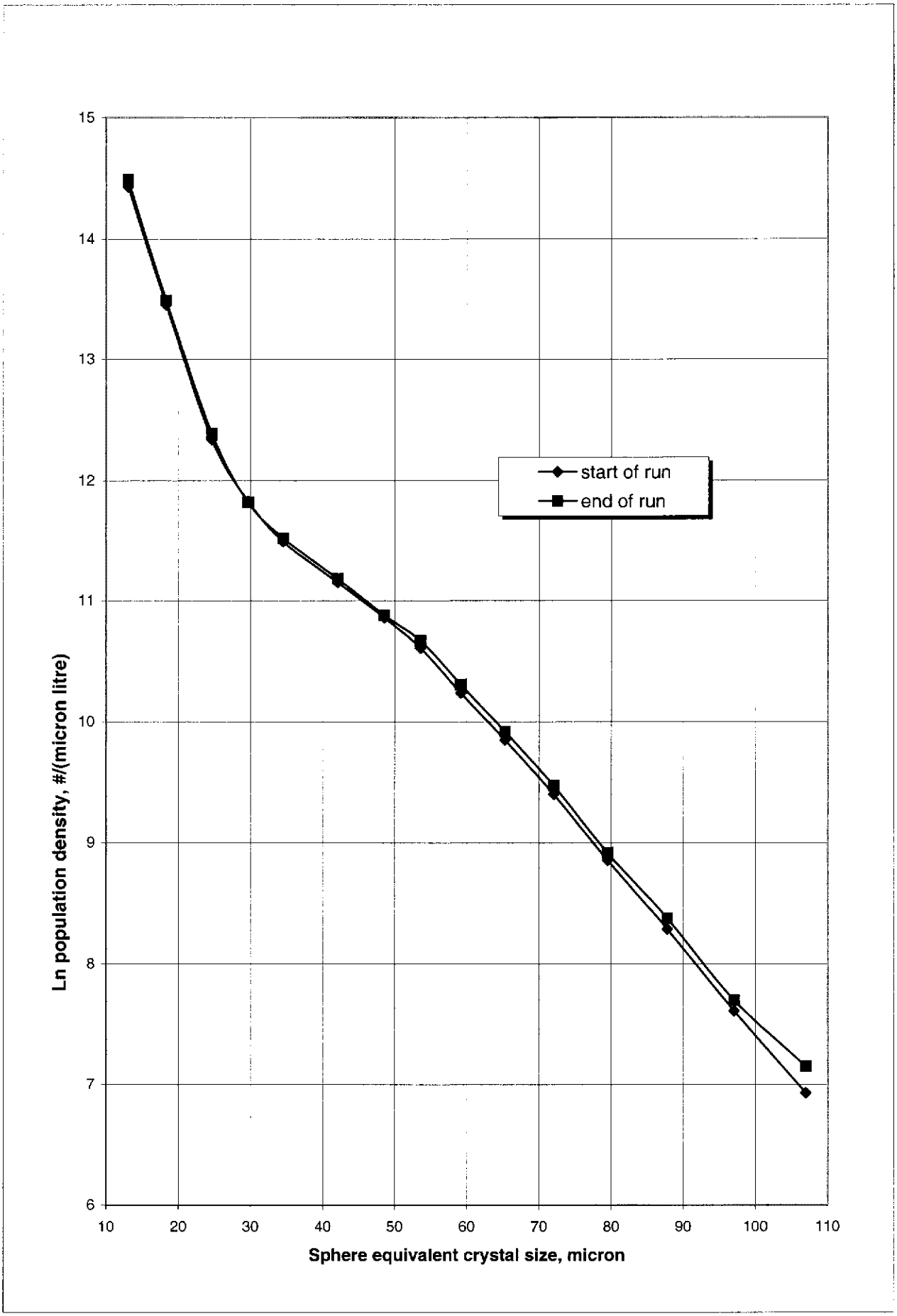

Population density plot obtained in the presence of Zn + SIPX = 50 ppm at 40^{0}C

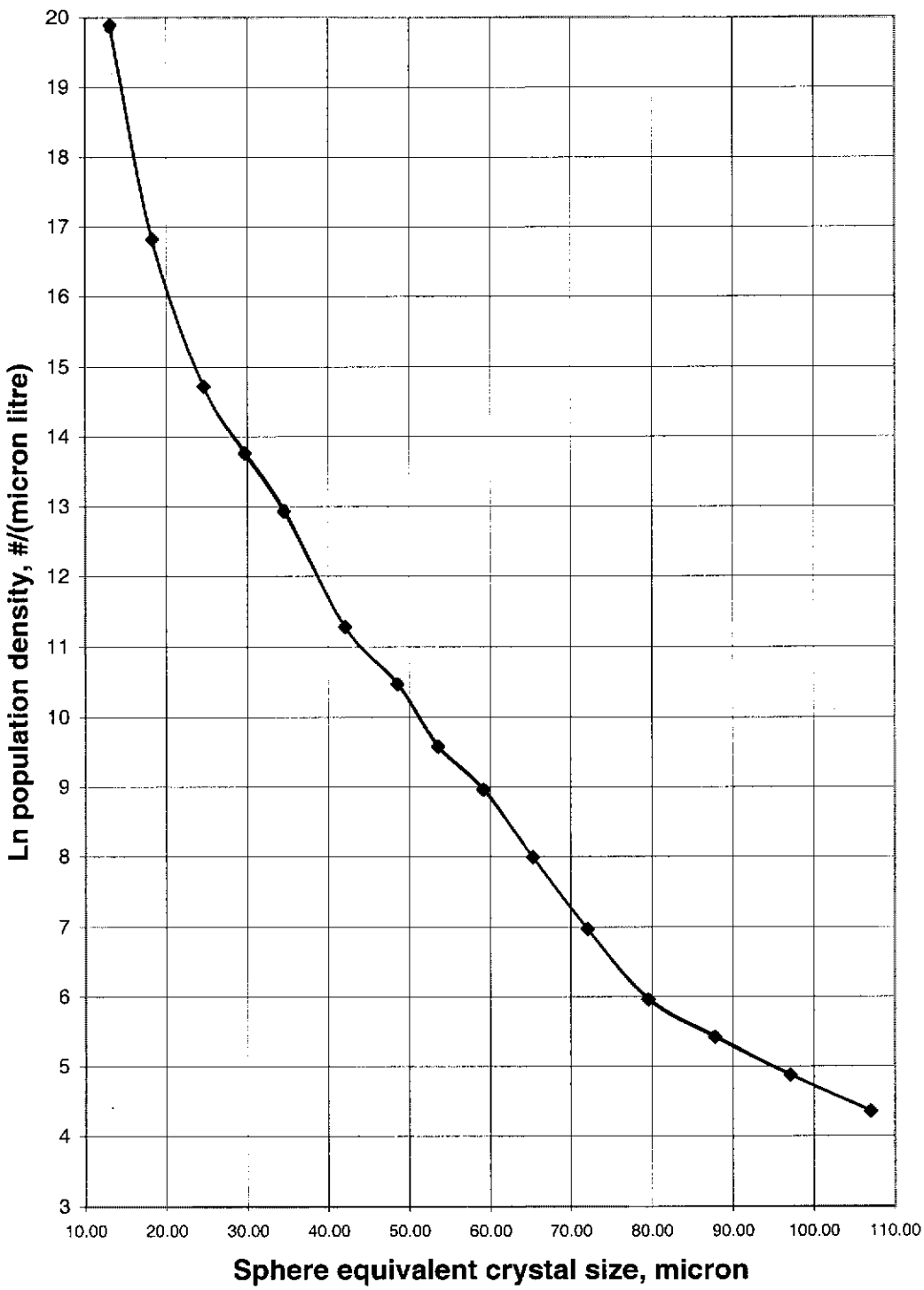

Population density plot obtained in the presence of Fe + Zn + SIPX = 50 ppm at 25^{0}C

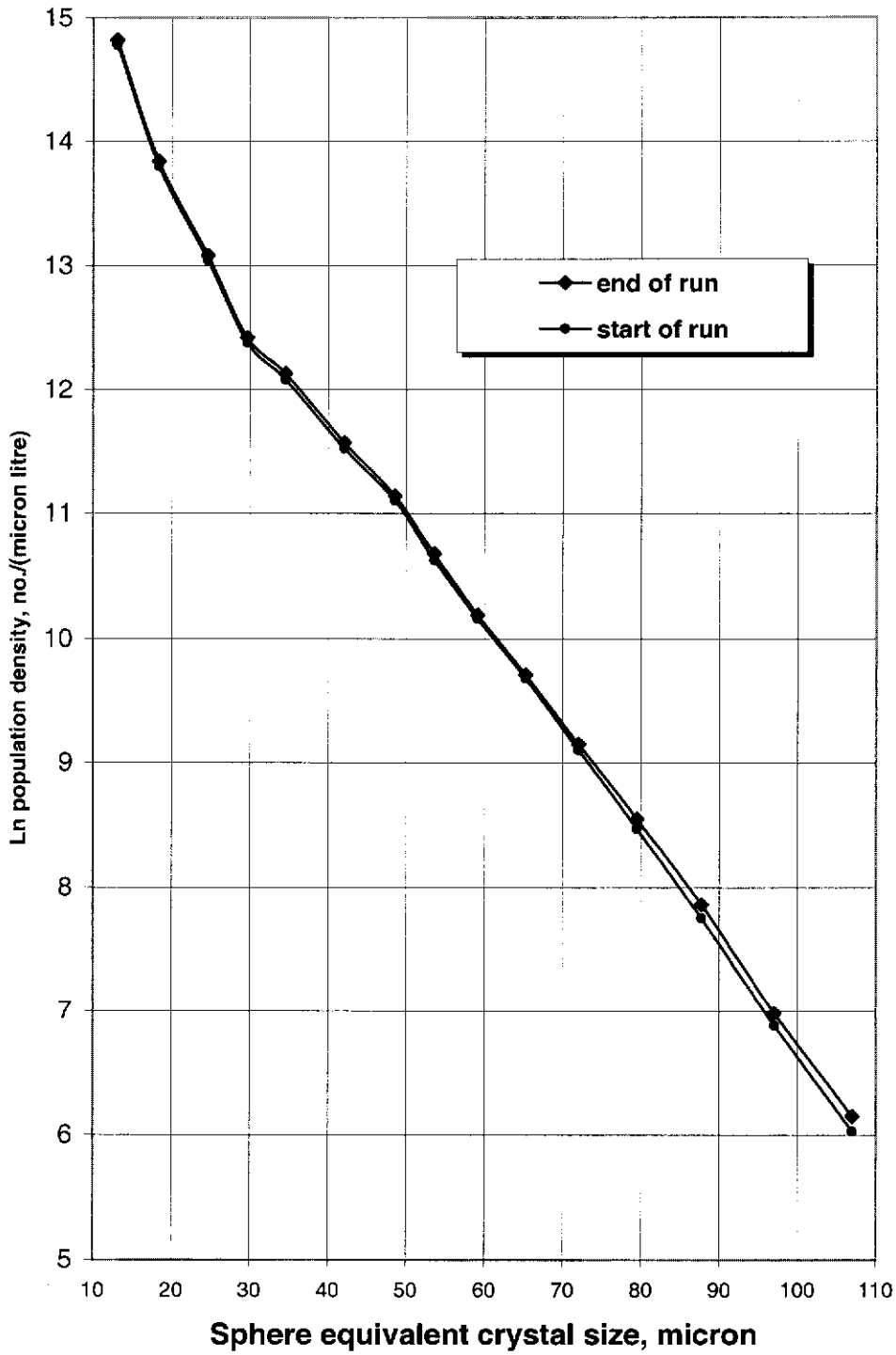

Population density plot obtained in the presence of Fe + Zn +SIPX = 50 ppm at 40^{0}C

Appendix E: Gypsum Scaling Experimental Data

Appendix E Gypsum Scaling Experiment

1. *A Sample Calculation for the Error Estimation in Preparing the Scaling Solution*

1.1. Calculation of the solutions required

Scaling experiment time = 4 hours.

Flow rate of the scaling solution = 30 ml/min.
Volume of solution needed for 4 hours = 7,200 ml.

Therefore, the volume of the Na_2SO_4 solution = 3,600 ml.
Likewise, the volume of the $CaCl_2$ solution = 3,600 ml.

For easier handling, 4,000 ml each of the two solutions (Na_2SO_4 and $CaCl_2$) were made. Thus,
volume of the Na_2SO_4 solution = 4,000 ml,
volume of the $CaCl_2$ solution = 4,000 ml.
and
The total volume to be made = 8,000 ml.

The two solutions were prepared by separate dissolution of crystals of Na_2SO_4 and $CaCl_2.2H_2O$, respectively, in distilled water. The molecular weight: Na_2SO_4 = 142.04; $CaCl_2.2H_2O$ = 172.17.

2,000 ppm of Ca^{2+} = 2,000 mg Ca^{2+} /litre.
For 8,000 litres = 2,000 x 8 mg = 16,000 mg Ca^{2+}
= 16 g Ca^{2+}.

Therefore, the $CaCl_2.2H_2O$ crystals needed = (172.17/40) x 16 grams
= 68.868 grams
= 0.4 mol.

Similarly, the Na_2SO_4 crystals needed = 0.4 mol
= 0.4 x 142.04 grams
= 56.816 grams.

1.2. Calculation of error in weighing

Error in weighing 68.868 grams of $CaCl_2.2H_2O$ = 0.0001 g
= (0.0001/68.868)
= 0.00014 %.

Error in weighing 56.816 grams of Na_2SO_4 = 0.0001 g
= (0.0001/56.816)
= 0.00018 %.

Total error in weighing = 0.00014 % + 0.00018 % = 0.00032 %.

The systematic error of the balance used was not known.

1.3. Calculation of error in solution preparation

Volume of $CaCl_2$ solution required = 4,000 ml

The solution was measured using a 2,000 ml volumetric flask with an uncertainty of 0.6 ml.

Therefore, the systematic error = 2 x (0.6/2,000) x 100 %
= 0.06 %.

For the Na_2SO_4 solution, the systematic error is the same as that for the $CaCl_2$ solution.

Therefore, the systematic error for Na_2SO_4 solution = 0.06 %.

Total error in solution preparation = 2 x 0.06 %
= 0.12 %.

Therefore, the total error in the preparation of the 2,000 ppm Ca^{2+} solution = total error in weighing + total error in solution preparation = (0.00032 + 0.12) %

= 0.12 %.

Hence, the concentration of the calculated 2,000 ppm of Ca^{2+} = 2,000 ± 0.12 %

= 2,000 ± 2.4 ppm.

The balance used for weighing might have up to 1% uncertainty (Taylor 1997) but this cannot be rigorously justified. It was decided, therefore, that the systematic error for the balance was not included. Had the systematic error for the balance been included, the 2,000 ppm Ca^{2+} solution would have uncertainty equals 2.12 %, or the solution concentration = 2,000 ± 42.4 ppm.

2. *A Sample Calculation for the Error Estimation in the Scaling Experimental Run (for 2,000 ppm of Ca^{2+} solution)*

In the experimental run, errors might arise from the pumping (= pump reliability) and the time recording.

Error in pumping = 3 % of the set flow rate.

Error in time recording = 0.5 % (Taylor 1997).

Error in weighing of the mass of the scale deposited = error due to uncertainty in the balance used = X g + 0.0001 g,
(where X = weight of the deposits, in grams).

Error from the solution preparation = 0.12 % (see sec. 1.1 above).

Error contributed by the pumping of the solution = 3 %.

Error in recording the scaling experiment time using stopwatch

= 0.5 % (Taylor 1997).

For example, weight of clean coupon = 6.3619 g.

Error in weighing the clean coupon (= the surface onto which the scale would attach)

= (0.0001/6.3619) x 100 %

= 0.00157 %.

For example, the weight of the coupon after the run = 6.3740 g.

Error in weighing of the coupon with the attached deposits (= after the run)

= (0.0001/6.3740) x 100 %

= 0.00157 %.

Therefore, the total error in weighing the mass of the deposits

= (0.00157 + 0.00157) %

= 0.00314 %.

The total error for the entire scaling experiment using 2,000 ppm of Ca^{2+} is:

1. Error due to the solution preparation	= 0.12 %
2. Error due to pumping	= 3 %
3. Error due to time recording	= 0.5 %
4. Error due to weighing of the scale	= 0.00314 %
Total error	= 3.62 %.

Appendix E-1 Gypsum scaling data for Figure 7.3 (Tables E-1 to E-5)

(Effect of Ca^{2+} concentration level on scale deposition after four hours for various piping materials in the absence of admixtures at a low flow rate of 0.4 cm/sec).

Table E-1 Scaling data at Ca^{2+} = 2,000 ppm

Type of pipe	Mass of coupons, (g)	Mass of coupons + scale, (g)	Scale formation, (kg/m^2)	Error estimate, (%)
PVC	6.3588	6.3715	0.0104	3.91
Brass	37.5078	37.5108	0.0024	3.85
Copper	39.9778	39.9792	0.0011	3.85
Stainless steel	35.9664	35.9678	0.0011	3.85

Table E - 2 Scaling data at Ca^{2+} = 3,000 ppm

Type of pipe	Mass of coupons, (g)	Mass of coupons + scale, (g)	Scale formation, (kg/m^2)	Error estimate, (%)
PVC	6.3588	6.3715	0.0104	3.91
Brass	37.9291	37.9369	0.0064	3.85
Copper	40.0536	40.0807	0.0221	3.85
Stainless steel	35.9772	35.9832	0.0049	3.85

Table E – 3 Scaling data at Ca^{2+} = 4,000 ppm

Type of pipe	Mass of coupons, (g)	Mass of coupons + scale, (g)	Scale formation, (kg/m^2)	Error estimate, (%)
PVC	6.3611	6.3947	0.0274	3.88
Brass	37.9283	37.9473	0.0155	3.82
Copper	40.0519	40.066	0.0115	3.82
Stainless steel	35.9766	36.0065	0.0244	3.82

Table E – 4 Scaling data at Ca^{2+} = 5,000 ppm

Type of pipe	Mass of coupons, (g)	Mass of coupons + scale, (g)	Scale formation, (kg/m^2)	Error estimate, (%)
PVC	6.3612	6.5284	0.1365	3.91
Brass	37.9302	38.1016	0.1399	3.85
Copper	40.0534	40.2114	0.1290	3.85
Stainless steel	35.9746	36.1302	0.1270	3.85

Table E – 5 Scaling data at Ca^{2+} = 6,000 ppm

Type of pipe	Mass of coupons, (g)	Mass of coupons + scale, (g)	Scale formation, (kg/m^2)	Error estimate, (%)
PVC	6.3566	6.6397	0.2311	3.90
Brass	37.9278	38.263	0.2736	3.85
Copper	40.0521	40.3677	0.2576	3.85
Stainless steel	35.976	36.2797	0.2479	3.85

Appendix E-2 Gypsum scaling data for Figure 7.4 (Tables E-6 to E-9)

(Effect of Fe^{3+}on gypsum scale deposited after four hours for various piping materials at a low flow rate of 0.4 cm/sec and a concentration of 2,500 ppm of Ca^{2+}).

Table E – 6 Scaling data in the absence of inhibitor

Type of pipe	Mass of coupons, (g)	Mass of coupons + scale, (g)	Scale formation, (kg/m^2)	Error estimate, (%)
PVC	6.3659	6.4115	0.0379	4.94
Brass	38.1528	38.2156	0.0512	4.89
Copper	40.1051	40.1595	0.0444	4.89
Stainless steel	35.9760	36.0413	0.0533	4.89

Table E - 7 Scaling data in the presence of 7.5 ppm of Fe^{3+}

Type of pipe	Mass of coupons, (g)	Mass of coupons + scale, (g)	Scale formation, (kg/m^2)	Error estimate, (%)
PVC	6.3642	6.3999	0.0291	6.71
Brass	38.0739	38.1053	0.0256	6.65
Copper	40.0846	40.1126	0.0228	6.65
Stainless steel	35.9756	36.0283	0.0430	6.66

Table E - 8 Scaling data in the presence of 15 ppm of Fe^{3+}

Type of pipe	Mass of coupons, (g)	Mass of coupons + scale, (g)	Scale formation, (kg/m^2)	Error estimate, (%)
PVC	6.3625	6.3812	0.0153	5.29
Brass	38.0579	38.0722	0.0117	5.24
Copper	40.0827	40.1004	0.0144	5.24
Stainless steel	35.9762	35.9870	0.0088	5.24

Table E - 9 Scaling data in the presence of 20 ppm of Fe^{3+}

Type of pipe	Mass of coupons, (g)	Mass of coupons + scale, (g)	Scale formation, (kg/m^2)	Error estimate, (%)
PVC	6.3625	6.3995	0.0302	4.94
Brass	38.0154	38.0356	0.0165	4.89
Copper	40.0755	40.0944	0.0154	4.88
Stainless steel	35.9759	35.9914	0.0126	4.89

Appendix E-3 Gypsum scaling data for Figure 7.5 (Tables E-10 to E-13)

(Effect of Fe^{3+}on gypsum scale deposited after four hours for various piping materials at a high flow rate of 1.3 cm/sec and a concentration of 2,500 ppm of Ca^{2+}).

Table E – 10 Scaling data in the absence of Fe^{3+}

Type of pipe	Mass of coupons, (g)	Mass of coupons + scale, (g)	Scale formation, (kg/m^2)	Error estimate, (%)
PVC	10.0922	10.1251	0.0499	4.51
Brass	61.3975	61.4243	0.0406	4.48
Copper	64.6659	64.7017	0.0543	4.48
Stainless steel	56.7172	56.7439	0.0405	4.48

Table E – 11 Scaling data in the presence of 7.5 ppm of Fe^{3+}

Type of pipe	Mass of coupons, (g)	Mass of coupons + scale, (g)	Scale formation, (kg/m^2)	Error estimate, (%)
PVC	10.0856	10.0984	0.0194	7.34
Brass	61.3642	61.3687	0.0068	7.31
Copper	64.6431	64.6475	0.0067	7.31
Stainless steel	55.8736	55.8786	0.0076	7.31

Table E- 12 Scaling data in the presence of 15 ppm of Fe^{3+}

Type of pipe	Mass of coupons, (g)	Mass of coupons + scale, (g)	Scale formation, (kg/m^2)	Error estimate, (%)
PVC	10.0877	10.0968	0.0138	5.93
Brass	61.3585	61.3628	0.0065	5.89
Copper	64.641	64.6468	0.0088	5.89
Stainless steel	55.8403	55.8451	0.0073	5.90

Table E – 13 Scaling data in the presence of 20 ppm of Fe^{3+}

Type of pipe	Mass of coupons, (g)	Mass of coupons + scale, (g)	Scale formation, (kg/m^2)	Error estimate, (%)
PVC	10.0874	10.0908	0.0051	5.57
Brass	61.3426	61.3463	0.0056	5.54
Copper	64.6351	64.6416	0.0098	5.54
Stainless steel	56.6047	55.6165	0.0179	5.54

Appendix E-4 Gypsum scaling data for Figure 7-6 (Tables E-14 to E-17)

(Effect of SIPX on gypsum scale deposited after four hours for various piping materials at a low flow rate of 0.4 cm/sec and a concentration of 2,500 ppm of Ca^{2+}).

Table E-14 Scaling data in the absence of SIPX.

Type of pipe	Mass of coupons, (g)	Mass of coupons + scale, (g)	Scale formation, (kg/m^2)	Error estimate, (%)
PVC	6.365	6.4115	0.0380	3.88
Brass	38.1528	38.2156	0.0513	3.82
Copper	40.1051	40.1595	0.0444	3.82
Stainless steel	35.976	36.0413	0.0533	3.82

Table E – 15 Scaling data in the presence of 5 ppm of SIPX

Type of pipe	Mass of coupons, (g)	Mass of coupons + scale, (g)	Scale formation, (kg/m^2)	Error estimate, (%)
PVC	6.3659	6.3952	0.0239	13.88
Brass	38.1414	38.1763	0.0285	13.82
Copper	40.1011	40.129	0.0228	13.82
Stainless steel	35.9763	35.9875	0.0091	13.82

Table E – 16 Scaling data in the presence of 10 ppm of SIPX.

Type of pipe	Mass of coupons, (g)	Mass of coupons + scale, (g)	Scale formation, (kg/m^2)	Error estimate, (%)
PVC	6.3629	6.3739	0.0090	8.88
Brass	38.1413	38.1462	0.0040	8.82
Copper	40.1003	40.1033	0.0024	8.82
Stainless steel	35.9757	35.9799	0.0034	8.82

Table E – 17 Scaling data in the presence of 20 ppm of SIPX.

Type of pipe	Mass of coupons, (g)	Mass of coupons + scale, (g)	Scale formation, (kg/m^2)	Error estimate, (%)
PVC	6.3627	6.3672	0.0037	6.38
Brass	38.1418	38.1431	0.0011	6.32
Copper	40.1007	40.1014	0.0006	6.32
Stainless steel	35.9756	35.976	0.0003	6.32

Appendix E-5 Gypsum scaling data for Figure 7.7 (Tables E-18 to E-21)

(Effect of SIPX on gypsum scale deposited after four hours for various piping materials at a high flow rate of 1.3 cm/sec and a concentration of 2,500 ppm of Ca^{2+}).

Table E – 18 Scaling data in the absence of SIPX.

Type of pipe	Mass of coupons, (g)	Mass of coupons + scale, (g)	Scale formation, (kg/m^2)	Error estimate, (%)
PVC	10.0922	10.1251	0.0499	4.51
Brass	61.3975	61.4243	0.0406	4.48
Copper	64.6659	64.7017	0.0543	4.48
Stainless steel	56.7172	56.7439	0.0405	4.48

Table E – 19 Scaling data in the presence of 5 ppm of SIPX.

Type of pipe	Mass of coupons, (g)	Mass of coupons + scale, (g)	Scale formation, (kg/m^2)	Error estimate, (%)
PVC	10.0926	10.113	0.0309	14.51
Brass	61.394	61.4065	0.0189	14.48
Copper	64.6642	64.6789	0.0223	14.48
Stainless steel	56.3287	56.3415	0.0194	14.48

Table E – 20 Scaling data in the presence of 10 ppm of SIPX.

Type of pipe	Mass of coupons, (g)	Mass of coupons + scale, (g)	Scale formation, (kg/m^2)	Error estimate, (%)
PVC	10.0894	10.1012	0.0179	9.51
Brass	61.3929	61.3971	0.0064	9.48
Copper	64.6633	64.667	0.0056	9.48
Stainless steel	56.3171	56.3197	0.0039	9.48

Table E – 21 Scaling data in the presence of 20 ppm of SIPX.

Type of pipe	Mass of coupons, (g)	Mass of coupons + scale, (g)	Scale formation, (kg/m^2)	Error estimate, (%)
PVC	10.0897	10.1069	0.0261	7.01
Brass	61.3946	61.3992	0.0070	6.98
Copper	64.6657	64.6699	0.0064	6.98
Stainless steel	56.3153	56.3161	0.0012	6.98

Appendix E-6 Gypsum scaling data for Figure 7-12 (Tables E-22 to E-25)

(Effect of type of piping materials on gypsum scale deposited in the absence of any admixtures at a low flow rate of 0.4 cm/sec and a concentration level of 4,000 ppm of Ca^{2+}).

Table E- 22 Scaling data after four hours of scaling time.

Type of pipe	Mass of coupons, (g)	Mass of coupons + scale, (g)	Scale formation, (kg/m^2)	Error estimate, (%)
PVC	6.3587	6.4685	0.0896	3.91
Brass	37.9293	38.0314	0.0833	3.85
Copper	40.0534	40.1371	0.0683	3.85
Stainless steel	35.9748	36.0514	0.0625	3.85

Table E – 23 Scaling data after eight hours of scaling time.

Type of pipe	Mass of coupons, (g)	Mass of coupons + scale, (g)	Scale formation, (kg/m^2)	Error estimate, (%)
PVC	6.359	6.6443	0.2329	3.96
Brass	37.9314	38.2384	0.2506	3.91
Copper	40.055	40.3237	0.2193	3.91
Stainless steel	35.9765	36.164	0.1530	3.91

Table E- 24 Scaling data after 12 hours of scaling time.

Type of pipe	Mass of coupons, (g)	Mass of coupons + scale, (g)	Scale formation, (kg/m^2)	Error estimate, (%)
PVC	6.3593	6.7476	0.3169	4.02
Brass	37.9278	38.2617	0.2725	3.97
Copper	40.0519	40.3299	0.2269	3.97
Stainless steel	35.9757	36.2784	0.2471	3.97

Table E – 25 Scaling data after 16 hours of scaling time.

Type of pipe	Mass of coupons, (g)	Mass of coupons + scale, (g)	Scale formation, (kg/m^2)	Error estimate, (%)
PVC	6.3571	7.0305	0.5496	4.08
Brass	37.9278	38.539	0.4988	4.03
Copper	40.0519	40.6359	0.4766	4.03
Stainless steel	35.9762	36.3997	0.3457	4.03

Appendix E-7 Gypsum scaling data for Figure 7-13 (Tables E-26 to E-29)

(Effect of type of piping materials on gypsum scale deposited in the absence of any admixtures at a high flow rate of 1.3 cm/sec and a concentration level of 4,000 ppm of Ca^{2+}).

Table E – 26 Scaling data after four hours of scaling time.

Type of pipe	Mass of coupons, (g)	Mass of coupons + scale, (g)	Scale formation, (kg/m^2)	Error estimate, (%)
PVC	10.085	10.1179	0.0497	4.54
Brass	61.3029	61.3276	0.0374	4.51
Copper	64.6042	64.6334	0.0443	4.51
Stainless steel	58.1467	58.168	0.0323	4.51

Table E- 27 Scaling data after eight hours of scaling time.

Type of pipe	Mass of coupons, (g)	Mass of coupons + scale, (g)	Scale formation, (kg/m^2)	Error estimate, (%)
PVC	10.0849	10.2506	0.2512	4.60
Brass	61.3046	61.4867	0.2760	4.57
Copper	64.6056	64.7767	0.2593	4.57
Stainless steel	58.1485	58.1988	0.0762	4.57

Table E- 28 Scaling data after 12 hours of scaling time.

Type of pipe	Mass of coupons, (g)	Mass of coupons + scale, (g)	Scale formation, (kg/m^2)	Error estimate, (%)
PVC	10.0844	10.1372	0.0800	4.66
Brass	61.2938	61.3473	0.0811	4.63
Copper	64.5962	64.6341	0.0574	4.63
Stainless steel	58.1483	58.1678	0.0296	4.63

Table E- 29 Scaling data after 16 hours of scaling time.

Type of pipe	Mass of coupons, (g)	Mass of coupons + scale, (g)	Scale formation, (kg/m^2)	Error estimate, (%)
PVC	10.0831	10.2541	0.2592	4.72
Brass	61.2939	61.4651	0.2595	4.69
Copper	64.5959	64.828	0.3518	4.69
Stainless steel	58.1488	58.426	0.4202	4.69

References

1. Taylor, J. R. (1997). *An Introduction to Error Analysis. The Study of Uncertainties in Physical Measurements*, University Science Books, Sausalito, California, USA.

Appendix F: Publications from the Present Study: 2001-2002

Note: For copyright reasons Appendix F has not been reproduced in full.

(Co-ordinator, ADT Project (Retrospective), Curtin University of Technology, 11/02/2004)

Headley, G., Muryanto, S. and Ang, H.M. (2001). "Effects of additives on the crystallisation rate of calcium sulphate dihydrate", *6th World Congress of Chemical Engineering. Melbourne, Australia, 23-27 September 2001.*

Murayanto, S. and Ang, H.M. (2001). "A continuous laboratory crystalliser for final year chemical engineering undergraduate projects", *ASEAN Regional Symposium on Chemical Engineering 2001, Bandung, Indonesia.*

Muryanto, S., Ang, H.M. and Parkinson, G.M. (2002). "Crystallisation kinetics of calcium sulphate dihydrate in the presence of additives", *World Engineering Congress 2002, Sarawak, Malaysia.*

Muryanto, S., Ang, H.M., Santoso, E. and Parkinson, G.M. (2002). "Gypsum scaling in isothermal flow systems", *ASEAN Regional Symposium on Chemical Engineering 2002, Kuala Lumpur, Malaysia.*

Muryanto, S., Ang, H.M., Santoso, E. and Parkinson, G.M. (2002). "Morphology of gypsum scale formed in pipes under isothermal conditions: a once-through pipe flow experiment", *Chemical Engineering Congress 2002, Manila, The Philippines.*

Muryanto, S., Ang, H.M. and Santoso, E. (2002) "A typical final year chemical engineering undergraduate laboratory project: scaling", *Journal of Chemical Engineering Education.*

Muryanto, S., Ang, H.M. and Parkinson, G.M. (2002). "Review of gypsum scaling research: effect of admixtures on gypsum crystallisation kinetics", *ASEAN Journal of Chemical Engineering.*